

# Applications of the Controlled Oxidation of Pyrroles



UNIVERSITY  
OF TASMANIA

Kieran Josef Rihak

BSc (Hons)

A thesis submitted in fulfilment of the requirements

Of the degree Doctor of Philosophy

School of Physical Sciences (Chemistry)

University of Tasmania

2017

# **Table of Contents**

<b>TABLE OF CONTENTS</b>	<b>I</b>
<b>DECLARATION</b>	<b>III</b>
<b>ACKNOWLEDGEMENTS</b>	<b>IV</b>
<b>ABSTRACT</b>	<b>V</b>
<b>ABBREVIATIONS</b>	<b>VII</b>
<b>LIST OF PUBLICATIONS</b>	<b>X</b>
<b>CHAPTER 1: TOWARDS THE SYNTHESIS OF (–)-CODONOPSINE ANALOGUES FROM PYRROLES</b>	<b>1</b>
1.1 Introduction to (–)-Codonopsine and Related Alkaloids	1
1.2 Introduction to Dearomatisation and Controlled Oxidation of Pyrroles	2
1.3 Proposed Approaches for Racemic Codonopsine Analogue Synthesis	10
1.4 Results of Racemic Work	16
1.5 Strategies for Asymmetric Syntheses	29
1.6 Results of Bicycle Approach	37
1.7 Chiral Auxiliary Approach	50
1.8 Conclusions	52
<b>CHAPTER 2: SYNTHESIS OF FLUORINATED GABA ANALOGUES THROUGH PYRROLE OXIDATION</b>	<b>55</b>
2.1 Introduction to Fluorine in Natural Products and Drugs	55
2.2 The C–F bond and How It Affects Organic Molecules' Conformations and Activity	56

<b>2.3 Fluorinated GABA Analogues: Activity and Synthesis</b>	<b>63</b>
<b>2.4 Methods for Introducing Fluorine and Deoxyfluorination</b>	<b>66</b>
<b>2.5 Proposed Approach for Synthesis of Fluorinated GABA Derivatives</b>	<b>71</b>
<b>2.6 Results</b>	<b>75</b>
<b>2.7 Conclusions</b>	<b>100</b>
 <b>CHAPTER 3: DEVELOPMENT AND APPLICATIONS OF PYRROLES AND PYRROLIDINES PREPARED FROM POLYGODIAL</b>	 <b>101</b>
<b>3.1 Introduction to Polygodial and Derivatives</b>	<b>101</b>
<b>3.2 Results and Discussion</b>	<b>105</b>
<b>3.3 Conclusions</b>	<b>126</b>
 <b>CHAPTER 4: CONCLUSIONS</b>	 <b>130</b>
 <b>CHAPTER 5: EXPERIMENTAL</b>	 <b>132</b>
<b>5.1 General Experimental</b>	<b>132</b>
<b>5.2 Chapter 1 Experimental Details</b>	<b>135</b>
<b>5.3 Chapter 2 Experimental Details</b>	<b>182</b>
<b>5.4 Chapter 3 Experimental Details</b>	<b>193</b>
 <b>CHAPTER 6: REFERENCES</b>	 <b>214</b>
 <b>APPENDICES</b>	 <b>229</b>
<b>Appendix 1: <sup>1</sup>H NMR Spectral Simulation Parameters</b>	<b>229</b>
<b>Appendix 2: X-ray Crystallography Data</b>	<b>232</b>

## **Declaration**

This thesis contains no material which has been accepted for a degree or diploma by the University or any other institution, and to the best of my knowledge contains no material previously published or written by another person, except where due acknowledgement is made in the text.

Kieran Josef Rihak,

December 2017

## **Statement of authority:**

This thesis is not to be made available for loan or copying for two years following the date this statement was signed. Following that time the thesis may be made available for loan and limited copying in accordance with the *Copyright Act 1968*

## **Acknowledgements**

There are many people who should be acknowledged for their part in helping me get through this PhD and write this god-awful book. They'll have to forgive me if I don't have the space now to sing their praises sufficiently.

First and foremost, I would like to thank my supervisors, Assoc. Prof. Jason Smith and Dr. Alex Bissember, for their guidance and advice. I owe much to Jason for his supervision and support over the last five years, and to Alex for being a quick proofreader and incurable cynic.

Of the others in our research group, I'd most like to thank my fellow travellers Krystel Woolley and Jeremy Just. They made the whole endeavour much more enjoyable, and the lab would have been a much duller and yet more disorganised place without them. Thanks also to my former senior Dr. James Howard, who even when living overseas or working at a real job was willing to offer advice and proofread drafts. And finally thanks to everyone else in the group who has helped me at some point or otherwise enriched my PhD experience.

In the Synthesis supergroup, I'd like to thank Assoc. Prof. Michael Gardiner, for his help in acquiring and processing crystal structures of my compounds. Also Dr. Curtis Ho for scoping out my crystals and being a nice guy in general.

I'd also like to thank Dr. Luke Hunter of UNSW, for valuable advice on fluorine chemistry and simulating NMR spectra of my fluorinated compounds.

I'd like to give a big acknowledgement to my close family: my mother Kate, stepfather Steve and brother Ash. They were always supportive and always had a place for me to stay when I needed to get away from the lab and decompress.

Finally, I'd like to offer endless gratitude and affection to my partner Mei Yi, who took me on at a very stressful time of life. I couldn't have found anyone more supportive or caring to help survive this.

## Abstract

The following thesis contains three parts, where the common overall goal was to develop useful applications for synthesis and modification of pyrrole heterocycles.

A range of desmethyl, *cis*-hydroxy analogues of the biologically active natural product (–)-codonopsine were prepared, using the controlled oxidation of *N*-methylpyrrole with both hypervalent iodine reagents and photooxidation as a key step. Dihydroxylation, Friedel–Crafts alkylation using aromatic nucleophiles, and reduction with LiAlH<sub>4</sub> were used to transform these  $\gamma$ -lactam intermediates to the desired analogues in mostly good overall yields. The relative stereocontrol observed in these processes was expanded to develop two approaches to asymmetric syntheses of these analogues. The use of chiral bicyclic scaffolds gave complete stereoselectivity, but the intermediates were too stable for further modification. The use of an amino acid methyl ester chiral auxiliary gave separable diastereomers, but further functionalization led to scrambling of stereocenters.

Chiral dihydroxylated bicyclic  $\gamma$ -lactam intermediates were applied to the synthesis of chiral fluorinated GABA analogues, due to their selective binding to particular GABA receptors. Direct fluorination of bicyclic diols using DeoxoFluor and DAST led to separable mixtures of mono- and difluorinated products. These proved more amenable to ring-opening of the bicyclic lactams through trapping of iminium ions than the corresponding diol-substituted bicyclic lactams, due to hyperconjugation effects of the fluorine substituents. A proof of concept preparation of a fluorohydrin analogue of GABA was successfully completed.

An approach was developed for the selective preparation of stable pyrroles and pyrrolidines from the readily available 1,4-dialdehyde natural product polygodial. A modified Paal–Knorr approach under reducing conditions made it possible to selectively produce stable pyrroles or pyrrolidines in good to excellent yields. One of the pyrroles was taken and subjected to controlled pyrrole oxidation and Friedel–Crafts alkylation to give novel analogues of the antifungal natural product (+)-Crispin A. These compounds were also

investigated as scaffolds for the preparation of chiral amines with potential applications as organocatalysts.

**Abbreviations**

2D	Two dimensional
Ac	Acetyl
Bn	Benzyl
Boc	<i>tert</i> -Butyloxycarbonyl
BuLi	Butyllithium
Bz	Benzoyl
cat.	Catalytic
°C	Degrees celsius
DABCO	1,4-Diazabicyclo[2.2.2]octane
DAST	Diethylaminosulfur trifluoride
DDQ	2,3-Dichloro-5,6-dicyano-1,4-benzoquinone
DIBAL-H	Diisobutylaluminium hydride
DMAP	Dimethylaminopyridine
DMF	Dimethylformamide
DMP	Dess–Martin periodinane
DMPU	1,2-Dimethyl-3,4,5,6-tetrahydro-2-pyrimidinone
DMSO	Dimethylsulfoxide
DNA	Deoxyribonucleic acid
dr	Diastereomeric ratio
ee	Enantiomeric excess
Eq.	Equivalents
EtOH	Ethanol



GABA	γ-Aminobutyric acid
h	Hour/s
HMBC	Heteronuclear multiple bond correlation
HRMS	High Resolution Mass Spectroscopy
HSQC	Heteronuclear single quantum correlation
IBX	2-Iodoxybenzoic acid
IR	Infrared
JRES	<i>J</i> -resolved
LED	Light Emitting Diode
<i>m</i> -CPBA	<i>meta</i> -Chloroperoxybenzoic acid
Me	Methyl
MeLi	Methyl lithium
MeOH	Methanol
min	Minute/s
MS	Mass Spectroscopy
NMO	<i>N</i> -methylmorpholine- <i>N</i> -oxide
NOE	Nuclear Overhauser effect
NOESY	Nuclear Overhauser effect spectroscopy
NFPy	<i>N</i> -Fluoropyridinium
NFSI	<i>N</i> -Fluorobenzenesulfonimide
NFSBI	<i>N</i> -Fluoro-(3,4-di- <i>tert</i> -butyl-4-methoxy)benzenesulfonamide
NMR	Nuclear Magnetic Resonance

PCC	Pyridinium chlorochromate
Ph	Phenyl
PIDA	Phenyliodine (III) diacetate
PIFA	phenyliodinebis(trifluoroacetate)
ppm	Parts per million
Py	Pyridinium
rt	Room temperature
SAR	Structure activity relationship
TBS	Tetrabutyltrimethylsilyl
TBAF	Tetra- <i>n</i> -butylammonium fluoride
TBAT	Tetrabutylammonium difluorotriphenylsilicate
TES	Triethylsilane
TFA	Trifluoroacetic acid
THF	Tetrahydrofuran
TLC	Thin layer chromatography
TMS	Trimethylsilyl
TMSCl	Trimethylsilyl chloride
TMSOTf	Trimethylsilyl trifluoromethanesulfonate
TPAP	Tetrapropylammonium perruthenate
TPP	Tetraphenylporphyrin
Ts	<i>para</i> -Toluenesulfonyl

## **List of Publications**

Howard, J. K; Rihak, K. J.; Bissember, A. C. and Smith, J. A. *Chem. Asian. J.* **2015**, *11*, 155–167

Rihak, K. J.; Bissember, A. C. and Smith, J. A *Tetrahedron* **2018**, *74*, 1167–1174

## Chapter 1: Towards the Synthesis of (–)-Codonopsine Analogues From Pyrroles

### 1.1 Introduction to (–)-Codonopsine and Related Alkaloids

Two polyhydroxylated pyrrolidine alkaloids, (–)-codonopsine and (–)-codonopsinine (**1** and **2**, Figure 1.1), have received a significant amount of attention for their biological properties. Both were originally isolated from the plant *Codonopsis clematidea* by Matkhalikova and colleagues in 1969, using samples of the plant collected in Kashka-Dar'ya Oblast in the former Uzbek Soviet Socialist Republic (modern day Qashqadaryo province in the Republic of Uzbekistan).<sup>1,2</sup> A structurally similar compound, named codonopsinol (**3**), was isolated from the same species in 2008 by Ishida and colleagues, from specimens of the plant collected in the same province.<sup>3</sup>

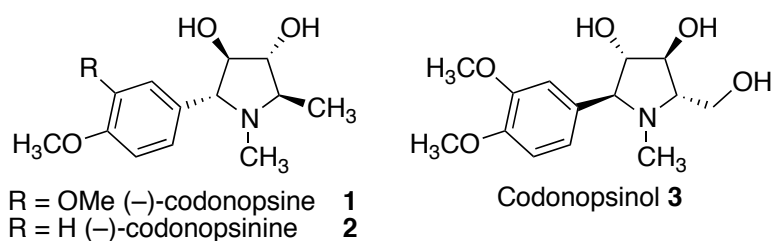


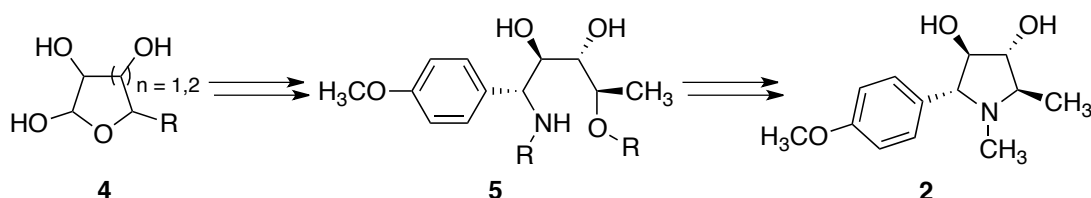
**Figure 1.1:** (–)-Codonopsine, (–)-Codonopsinine and Codonopsinol

Matkhalikova and colleagues proposed structures for (–)-codonopsine and (–)-codonopsinine based on their analysis of vicinal coupling constants in <sup>1</sup>H NMR spectra of these compounds.<sup>4–6</sup> However, their stereochemical assignments were later found to be incorrect. The actual structures of the two were determined by Kibayashi and colleagues in 1985, through a more definitive total synthesis and x-ray crystallographic analysis.<sup>7–9</sup> Additionally Tashkhodzhaev and co-workers, apparently unaware of Kibayashi's work, also established the correct structure through crystallographic analysis, in 2004.<sup>10</sup>

One study, by Matkhalikova and colleagues, proposed that codonopsine and codonopsinine have antibiotic and hypotensive effects without adversely affecting the central nervous system.<sup>11</sup> It has also reportedly been used in conjunction with a number of other plants in Uzbek traditional medicines.<sup>3</sup> However, more important to their study today is their observed effectiveness

as sugar mimics – aza-sugars that closely resemble natural sugars such that they can be used to inhibit sugar-processing enzymes. In particular, they have been reported to exhibit effectiveness in inhibiting  $\alpha$ -L-fucosidase, an enzyme found at increased concentrations in tumour and cancer cells, which has led to their structure being used as the basis for developing new potential cancer treatments.<sup>12,13</sup>

Aside from Kibayashi's structure determination work, many syntheses of codonopsine and codonopsinine have been developed over the years. Importantly, many of these have also involved the synthesis of a range of analogues of the two, allowing for compound library development and working toward the establishment of structure activity relationships (SARs). Their role as sugar mimics has informed a number of the syntheses developed, such that analogues have been prepared from similarly substituted sugars (and sugar derivatives) such as D-ribose,<sup>13</sup> L-xylose<sup>12,14</sup> and D-mannitol (Scheme 1.1).<sup>15</sup> Other approaches have been wide-ranging, although a common feature is that the pyrrolidine is most often formed through a ring-closing event of an acyclic starting material.<sup>16-21</sup> None of these syntheses to date have taken advantage of the aromatic nitrogen heterocycle pyrrole (**6**) as a starting point.



**Scheme 1.1:** Representative approach to preparing (–)-codonopsinine from sugars via acyclic intermediates

## 1.2 Introduction to Dearomatisation and Controlled Oxidation of Pyrroles

Dearomatisation of aromatic systems can be a useful tool in organic synthesis, and this strategy has been employed for both carbo- and heterocyclic systems using a variety of methods.<sup>22-24</sup> Pyrrole provides a good example of an aromatic heterocyclic moiety that can undergo substitution reactions prior to dearomatisation.<sup>25</sup> Pyrrole dearomatisation has been

dominated by reductive methods, mainly partial reduction and hydrogenation.<sup>26</sup> The Birch reduction, a dissolving-metal partial reduction approach, is a key example of these reductive methods. It has been used widely in the dearomatisation of pyrroles towards the synthesis of pyrrolidine natural product targets. This includes work by Donohoe and colleagues to prepare natural products such as 1-epiaustraline (**7**, Figure 1.2) and hyacinthacine A1 (**8**),<sup>22,27,28</sup> and also in Smith's synthesis of anisomycin (**9**),<sup>29</sup> amongst others.

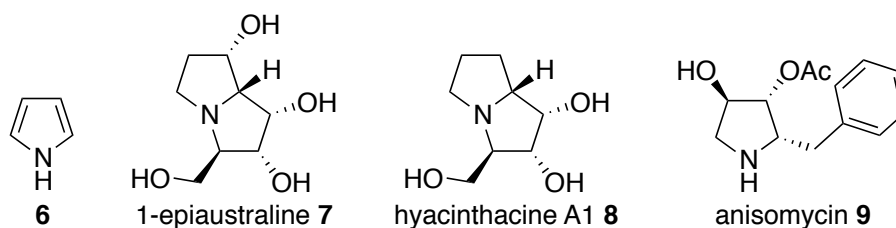
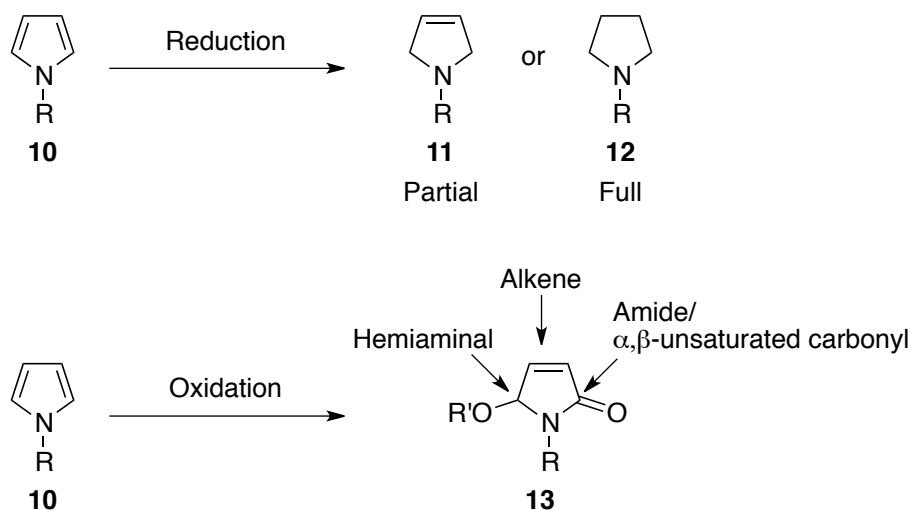


**Figure 1.2:** Pyrrole, and pyrrolidines prepared through reductive methods

An alternative to reductive dearomatisation of pyrroles would be an oxidative process. At least conceptually this could be an even more synthetically useful route. While reduction gives a pyrroline or pyrrolidine from a pyrrole, this decreases the amount of functionality available for transformation to an alkene at the most, necessitating that any other transformations be carried out on the pyrrole beforehand (Scheme 1.2). Oxidative processes, on the other hand, give highly substituted products with multiple functional handles free for further modification, such as an alkene, a hemiaminal and an amide/ $\alpha,\beta$ -unsaturated carbonyl. Such an approach could prove particularly fruitful if polyhydroxylated pyrrolidines, such as the aforementioned (–)-codonopsine and (–)-codonopsinine, were targets of interest.

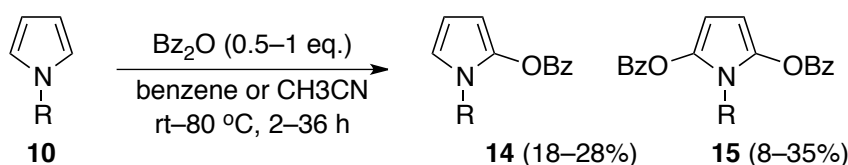
Historically and through to the present day using pyrrole oxidation in total or practical synthesis has been dismissed as not being viable, thanks largely to the perception that under acidic and oxidising conditions pyrrole polymerises uncontrollably to give pyrrole black. There is evidence to support this belief.<sup>30</sup> However, considerable work undertaken over the last hundred years investigating the viability of controlled pyrrole oxidation to provide pyrroline and pyrrolidine products, has led to the development of an array of methods

(Scheme 1.2). The results of these studies have been far from negative, as shown in a recent review of the work published by our group.<sup>31</sup>



**Scheme 1.2:** General scheme comparing reduction and oxidation of pyrroles

The earliest work on controlled pyrrole oxidation was undertaken using hydrogen peroxide in the 1920s, with major observed products being identified as 5-hydroxy-3-pyrrolin-2-one species (such as **13**), generally in low yields.<sup>32,33</sup> Since that time, this approach has been refined by a few groups, such as Bocchi's,<sup>34,35</sup> and Pichon-Santander's<sup>36</sup> and continues to be used in research working toward pyrrolidine products, with higher yields and more selective oxidations.<sup>37,38</sup> Cases where benzoyl peroxide is used as the oxidant have also been reported, which instead of oxidising to the pyrrolinone gave mixtures of 2,3 and 4-benzoyloxy-substituted pyrroles as products. For example, for a range of *N*-substituted pyrroles Aiura and colleagues reported a mixture of 2-benzoyloxy and 2,5-dibenzoyloxy products (Scheme 1.3).<sup>39,40</sup>

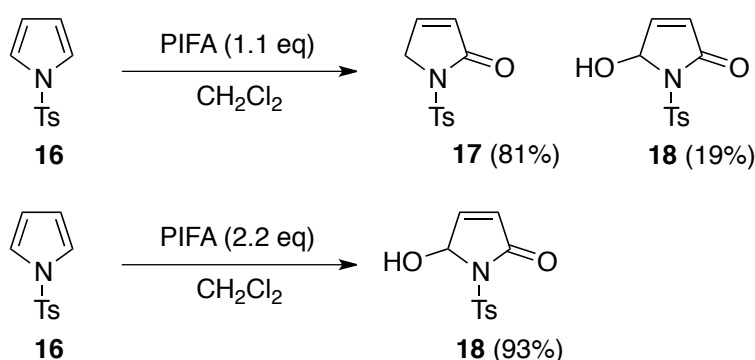


**Scheme 1.3:** Use of benzoyl peroxide to reach benzoyloxypyrroles

Other approaches to reach pyrrolinones **13** include the use of organic oxidants such as *o*-chloranil,<sup>41</sup> DDQ<sup>42,43</sup> and *m*-CPBA,<sup>44,45</sup> electrochemical oxidation,<sup>46-49</sup> inorganic oxidants such as lead tetraacetate,<sup>50-55</sup> Kao and co-workers examples with nickel peroxide and also oxone,<sup>56,57</sup> Reynolds and

colleagues use of TPAP/NMO,<sup>58</sup> and aryl iodide-catalysed peracetic acid oxidation-cyclisations.<sup>59</sup>

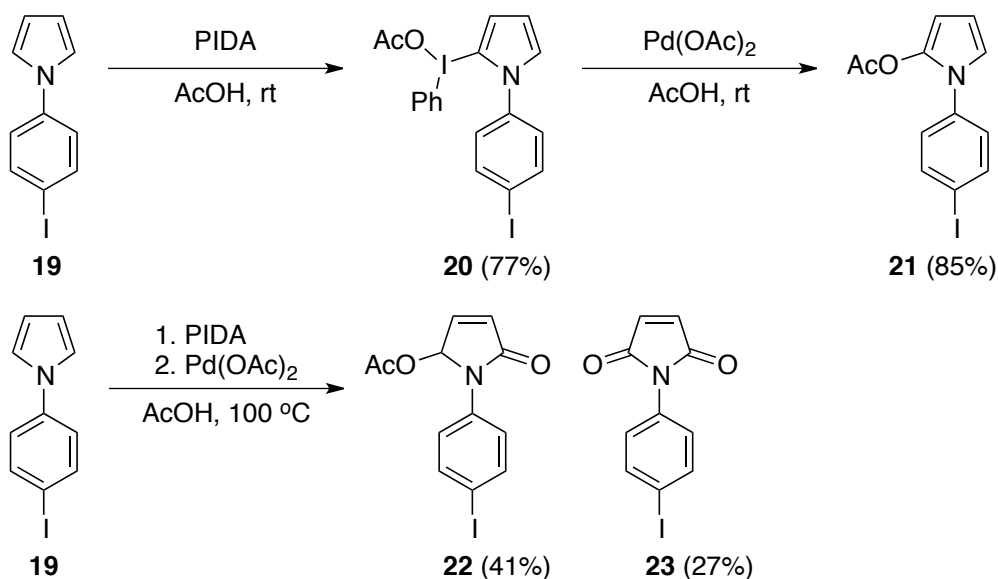
Another class of oxidant used, which is of particular interest in this work, is that of the hypervalent iodine reagents. Reports in this area have been more limited than the more traditional peroxides or even photooxidation, but a few key papers have appeared in recent years that point toward their utility in controlled oxidation of pyrroles. Alp and co-workers reported the controlled oxidation of the electron-deficient *N*-tosylpyrrole **16** using the reagent phenyliodinebis(trifluoroacetate) (PIFA, Scheme 1.4).<sup>60</sup> They observed quantitative conversion of *N*-tosylpyrrole into two  $\gamma$ -lactam species, **17** and **18**, the latter with a 5-hydroxy substituent, on treatment with 1.1 molar equivalents of the hypervalent iodine reagent. When 2.2 equivalents were used, complete conversion to **18** was achieved.



**Scheme 1.4:** Alp and colleague's oxidation of pyrroles with PIFA

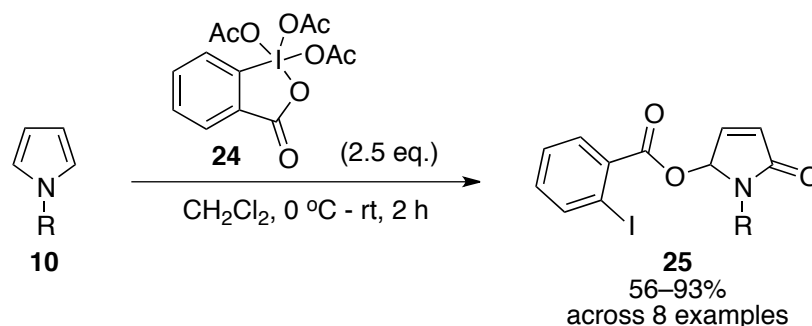
The Suna group reported similar results through their work investigating the oxidation of pyrroles by introducing acetoxy groups in the 2-position.<sup>61</sup> Using phenyliodine (III) diacetate (PIDA), they first isolated pyrrole iodonium species (such as **20**, Scheme 1.5), which were then treated with  $\text{Pd}(\text{OAc})_2$  to rearrange into the acetoxypyrroles (Such as **21**). This process could also be carried out with comparable results in one pot. When this procedure was carried out at elevated temperatures, it was observed that some pyrrole substrates converted into pyrrolinones (**22**), much like those seen in Alp's work, or maleimides (**23**), rather than the intended acetoxypyrroles.





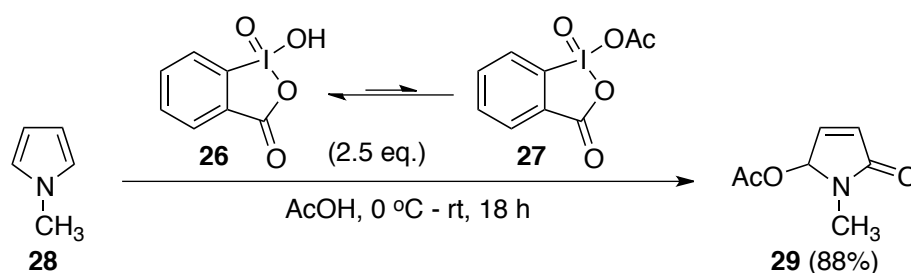
**Scheme 1.5:** Examples from Suna and co-author's work using PIDA

Work in our own group investigated this link between the use of hypervalent iodine reagents and pyrrolinone formation in more detail, and showed that Dess–Martin periodinane (DMP, **24**) was a desirable reagent for achieving this purpose on a variety of pyrrole substrates, giving pyrroline-2-ones **25** incorporating the oxidant as a 5-iodoaryloxy substituent (Scheme 1.6).<sup>62</sup> This approach was found to be widely applicable and high yielding, and furthermore was selective for oxidising pyrroles over alcohols, which historically has been DMP's main synthetic use.<sup>62–64</sup> The exact reaction mechanism for these oxidations are unknown. It is theorised to proceed either through an iodonium intermediate, as in Suna's work, followed by rearrangement to give the benzoate species; or alternatively through some kind of direct attack by the pyrrole on the oxygen of DMP, which is without precedent but would explain why none (or very little) of the 5-acetoxy product is observed under these conditions.



**Scheme 1.6:** Controlled oxidation of pyrroles using Dess–Martin periodinane

It has also been found that 2-iodoxybenzoic acid (IBX, **26**), a precursor of Dess–Martin periodinane, can be used in its place to provide the 2-acetoxy lactams, when the reaction is carried out in neat acetic acid (Scheme 1.7). This was investigated both because it would be a more atom-economical reagent, and one that is simply prepared from the inexpensive starting materials Oxone® and iodobenzoic acid.<sup>65</sup> Also, mechanistic studies suggest that the active species reacting in Dess–Martin periodinane oxidations is in fact a hydrolysed form of the reagent **27** arising from trace quantities of water present in the reaction.<sup>63</sup> It was theorised that IBX could form the same active species in the presence of acetic acid, which was borne out by NMR studies of IBX with acetic acid leading to resonances consistent with those of **27** as reported by Schreiber.<sup>63,66</sup>



**Scheme 1.7:** Use of IBX as an alternative oxidant

The amount of acetic acid used for the pyrrole oxidation reaction could be reduced by carrying out the reaction in a mixture of dichloromethane and acetic acid. However, it should be noted that as the proportion of acetic acid is reduced the yield decreases and a mixture of 5-iodoaroxyloxy and 5-acetoxy substituted products **25** and **29** are obtained. It remained a necessity to have a significant amount of acetic acid present, due both to IBX's

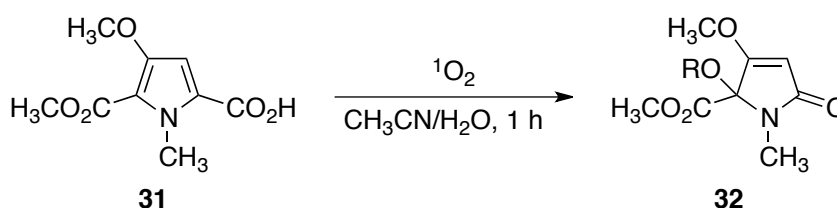
insolubility in dichloromethane and the fact that high concentrations of the acid were required to effect conversion to the active oxidant **27**.<sup>66</sup>

Another approach that has received significant attention is the use of singlet oxygen to oxidise pyrroles and other heterocycles.<sup>31,67</sup> Singlet oxygen is generated either through decomposition of a chemical reagent, or more commonly through excitation of a photoactive dye (a dye-sensitised process). Dye-sensitised reactions have become quite common in organic synthesis in general,<sup>68,69</sup> but the methods have been found to be less effective in oxidising pyrroles, giving low yields and generally a range of pyrrolidine (**13**) and maleimide (**30**) products, with other by-products such as ring-opening products occasionally observed (Scheme 1.8).<sup>70-72</sup>



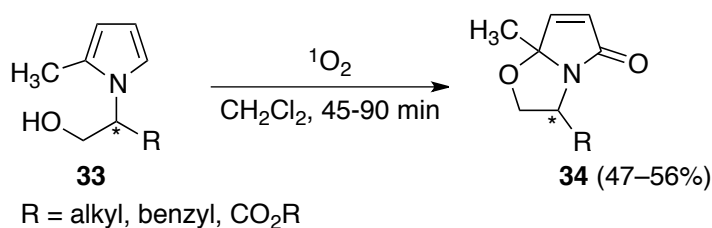
**Scheme 1.8:** General scheme for singlet oxygen oxidation of pyrroles to lactams and maleimides

An exception to this was demonstrated by Boger and Baldino, who prepared a single pyrrolidinone product regioselectively by starting with pyrrole-2-carboxylic acid **31** (Scheme 1.9). In this case, the oxidation occurs with a concomitant decarboxylation.<sup>73,74</sup>



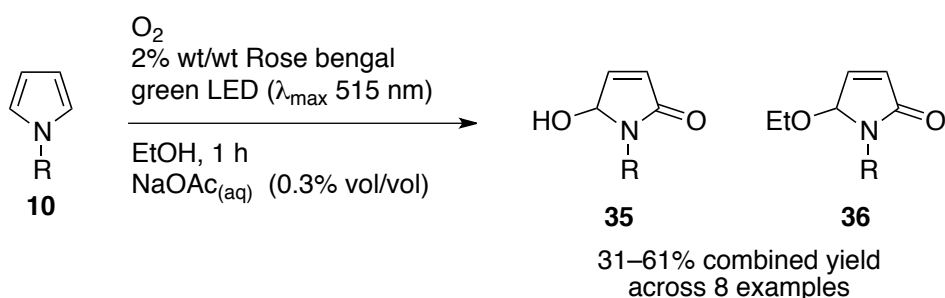
**Scheme 1.9:** Boger and Baldino's regioselective decarboxylation-photooxidation

Other research has been carried out by Demir and colleagues, who explored oxidations to give bicyclic  $\gamma$ -lactams **34**, by trapping an *N*-acyliminium intermediate (Scheme 1.10).<sup>75</sup>



**Scheme 1.10:** Demir and colleagues' photooxidation of 2-methylpyrroles to give bicyclic pyrroline-2-ones

Recent work in our group explored ways to make this process more efficient and effective, and considered the intrinsic reactivity of pyrroles in light to do so. It was proposed that the decomposition of pyrroles commonly observed was due to exposure of the pyrrole to a strong flux of UV light and heat, which most conventional lamps used for photoreactors emit in addition to the visible light needed for the oxidation to occur.<sup>76,77</sup> By using LEDs with a narrow band of visible light emission tuned to the sensitiser used (i.e. using green LEDs to excite the dye Rose bengal, in an alcoholic solvent),<sup>71,78,79</sup> undesired wavelengths of light (such as UV) were eliminated, and a range of pyrroles were oxidised in good yields on multi-gram scale (Scheme 1.11).<sup>80</sup> There was some precedence for this LED approach to photochemical reactions in the micro-batch work of Hulce and colleagues.<sup>81</sup> The reactions are also carried out in custom photoreactors constructed using cheap LED strips and lab glassware to make the process simple and low cost, thus affording a practical method for the formation of 5-hydroxypyrrolidinones as intermediates for synthesis.



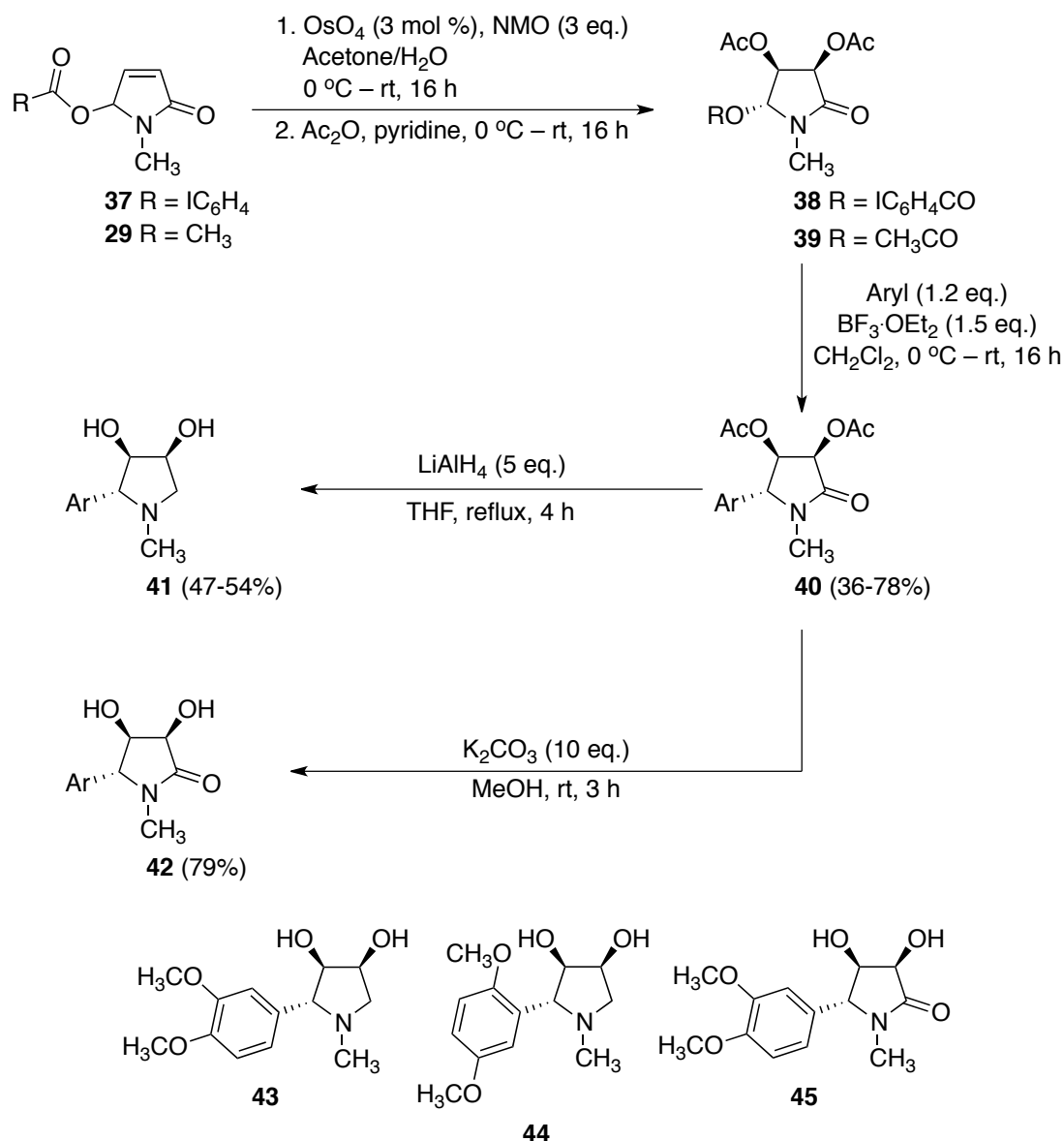
**Scheme 1.11:** Photochemical Approach to Controlled Pyrrole Oxidation

### 1.3 Proposed Approaches for Racemic Codonopsine Analogue Synthesis

#### 1.3.1 Preliminary Results of Racemic (–)-Codonopsine Analogue Synthesis

Previous work focussed on developing a synthetic route to racemic analogues of (–)-codonopsine and (–)-codonopsinine using the Dess–Martin periodinane and/or IBX oxidation of *N*-methylpyrrole **28** as the starting point.<sup>82</sup> In this work, the  $\gamma$ -lactam derived from *N*-methylpyrrole either using DMP as the oxidant (**37**) or IBX (**29**) were subjected to a range of transformations to assess their suitability to the synthesis of (–)-codonopsine analogues (Scheme 1.12).

Dihydroxylation under Upjohn conditions<sup>83</sup> of the alkene at C3–C4 of lactam **29/37** was chosen as the method for simply introducing the diol moiety into the analogues, as the [3+2]-suprafacial nature of these additions gives predictable formation of a *cis* diol.<sup>84</sup> This gave analogues that contrasted with (–)-codonopsine and (–)-codonopsinine, which have *trans*-3,4-diols. These reactions proceeded smoothly, but difficulties in purification by flash column chromatography (believed to be due to hydrolysis at C5 on silica to give a strongly polar triol species) necessitated the protection of the crude diol as the acetoxy derivative **40**, achieved by simply stirring the crude reaction mixture from the dihydroxylation in a mixture of Ac<sub>2</sub>O and pyridine. For Dess–Martin oxidation-derived lactam **37**, this protection procedure also led to an exchange of the iodoaroyloxy group at C5 with an acetoxy group, such that the 3,4-diacetoxy lactam **38** and 3,4,5-triacetoxy species **39** were the products in a combined 78% yield.



**Scheme 1.12:** Scope of preliminary work investigating codonopsine analogues

Following the dihydroxylation/protection procedure, a small range of aryl substituents were introduced at the C5 position through Friedel–Crafts alkylation, where the Lewis acid  $\text{BF}_3 \cdot \text{OEt}_2$  was used to generate an iminium ion at that position before addition of the nucleophile. Lactams **38** and **39** were used as a mixture, as both would convert to the same *N*-acyliminium intermediate when treated with a Lewis acid. It was proposed that these systems would be particularly amenable to these types of reaction due to the reported higher reactivity of *N*-acyliminium ions where the acyl functionality is endocyclic.<sup>85</sup> These reactions gave conversion to the desired aryl substituted lactams **40** in mostly good overall yields. The  $^1\text{H}$  NMR spectra showed no coupling between the protons at C4 and C5, giving only singlet and doublet

resonances for each of these respectively. This indicated that these two hydrogen atoms were in a *trans* relationship to each other. Consideration of the Karplus equation supported our prediction that relative stereocontrol would be maintained for this transformation by the acetoxy groups in C3 and C4.<sup>86</sup> A number methoxy-substituted benzene derivatives were trialled, with benzene itself proving unreactive, presumably to its being less electron-rich and hence less nucleophilic than the other electron-rich methoxyaryl substrates.

Finally, two of these substrates (those derived from 1,2-dimethoxybenzene and 1,4-dimethoxybenzene) were treated with  $\text{LiAlH}_4$  to reduce the amide at C2 to an amine and to simultaneously remove the two acetoxy protecting groups from the alcohols at C3 and C4 to yield the *cis*-diol, giving moderate to good yields of the desired products **43** and **44**. The 1,2-dimethoxybenzene derivative was also treated with  $\text{MeOH/K}_2\text{CO}_3$  to remove the acetoxy protecting groups, giving the dihydroxy lactam **45** in good yield. Further substrates were not explored due to time constraints on the project, but what was achieved indicated that this was a relatively efficient, quite mild and convenient route to racemic, *cis*-diol, desmethyl analogues of (–)-codonopsine and related compounds.

### 1.3.2 Plans for Expansion of Racemic Work

Given the success of these methods in reaching *cis*-dihydroxy analogues of codonopsine-type alkaloids, it was decided that a range of additional analogues could be synthesised to give a good representative body of work to explore their biological activity, and so develop structure activity relationships for these compounds (Figure 1.3). To this end, a range of other aryl and heterocyclic substrates were selected to be subjected to the same reaction procedure; that is, dihydroxylation/diacetoxylation, Friedel–Crafts alkylation, and then either reduction with  $\text{LiAlH}_4$  to give one class of amine *desmethyl* analogues, or deprotection of the acetoxy groups to give a selection of dihydroxy lactam analogues. The chosen list of substrates to be tested included other methoxy-substituted benzenes, most importantly methoxybenzene which can give analogues most similar to codonopsine. Also considered were some pyrrolidines featuring aromatic heterocycles at

their  $\alpha$ -positions, which could have interesting biological activities compared with the other aryls, and *N*-methylpyrrole, *N*-tosylpyrrole, furan and imidazole were chosen for this purpose.

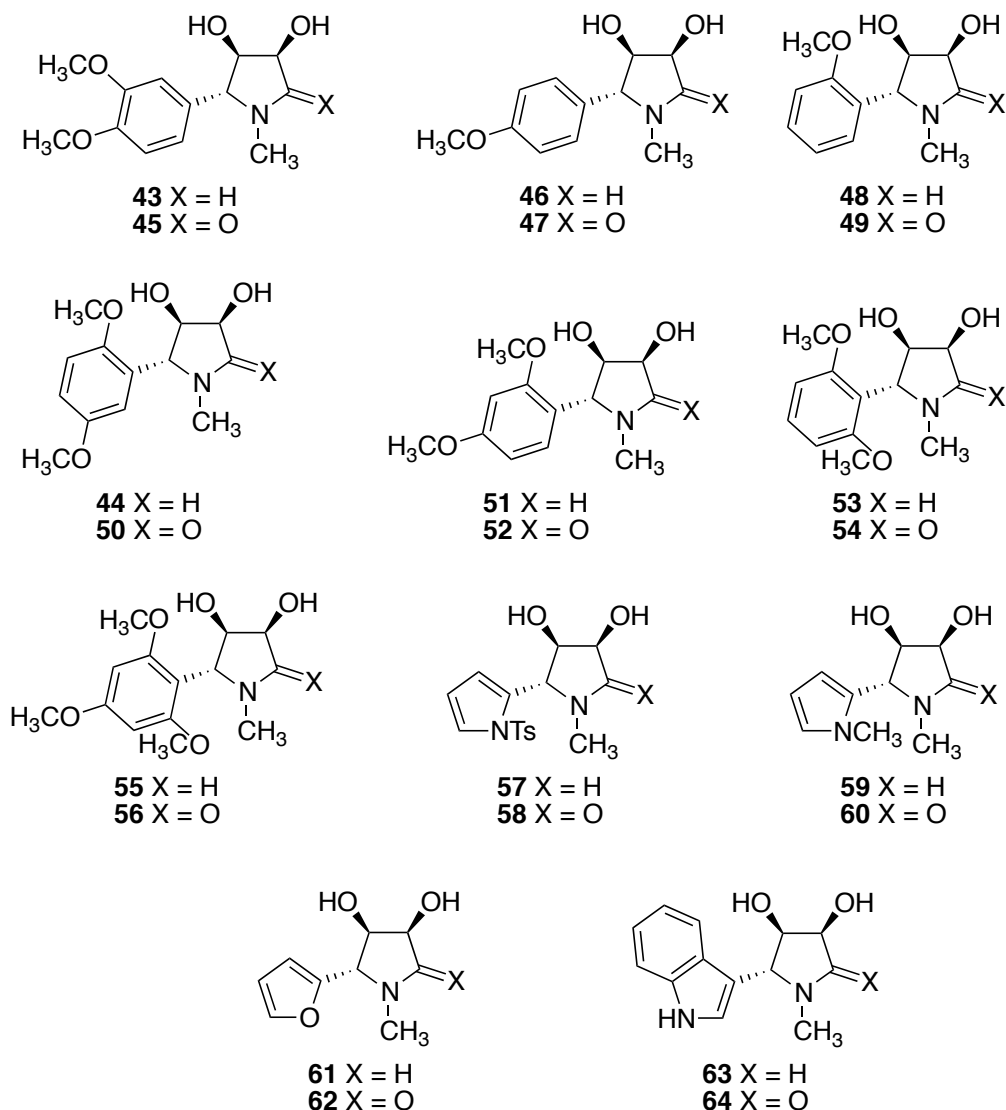


**Figure 1.3:** Proposed targets for full racemic investigation

It was also decided that one or more analogues could be pursued using purine derivatives, such as 6-methoxypurine (**65**, Figure 1.4) as the nucleophile for the Friedel–Crafts reaction. This would give structures that were very similar to aza-analogues of known biologically active nucleosides such as clofarabine (**68**).<sup>87</sup> Methods for the installation of purine derivatives into these systems have been previously reported and generally employ Lewis acids stronger than  $\text{BF}_3 \cdot \text{OEt}_2$ , such as  $\text{TiCl}_4$ .<sup>88</sup> Other similar approaches have been reported, such as Alibés and colleagues' use of tin



( $\text{SnCl}_4$ ) with added *N,O*-bis(trimethylsilyl)acetamide,<sup>89</sup> and Martínez-Montero and co-workers use of TMSOTf.<sup>87</sup>

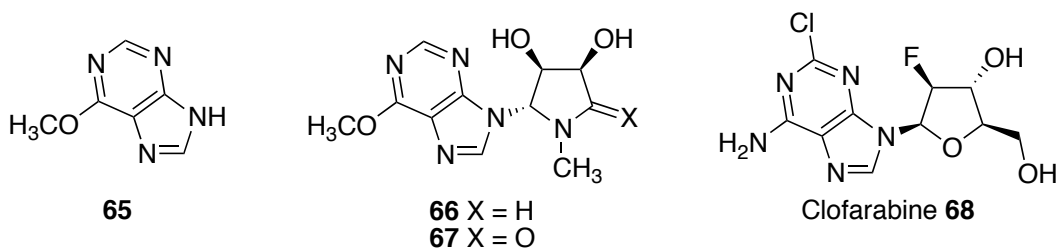
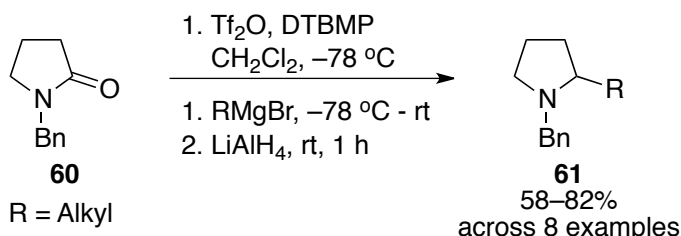


**Figure 1.4:** An example of purine targets, and a purine-containing nucleoside

In addition to reaching the desmethyl derivatives, it was also planned to utilise the lactam to introduce an alkyl group in the 2-position. Applied to the *para*-methoxybenzene derivative this would allow the synthesis of the analogue 3-*epi*-codonopsinine (**64**, Scheme 1.14).

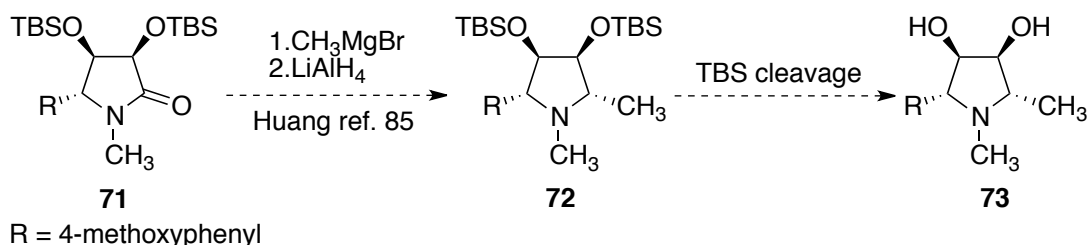
It was envisioned that this could be achieved by an additional step to the route taken for the desmethyl analogues, carrying out an alkyl addition at the amide carbonyl, followed by reduction (Scheme 1.13). Such addition-reduction procedures have been reported in the literature, and usually involve the use of either Grignard or alkyllithium reagents, with a reducing agent such as diisobutylaluminium hydride (DIBAL-H) or lithium aluminium hydride employed either to reduce the amide to a carbinolamine or to reduce the alcohol resulting from attack by the Grignard/alkyllithium on the amide carbonyl.<sup>90,91</sup> A more recent approach has been developed by Huang and colleagues, that utilises the same principal of using a Grignard reagent with  $\text{LiAlH}_4$ , but includes 2,6-di-*tert*-butylpyridine as an additive to assist the reaction.<sup>92,93</sup>



**Scheme 1.13:** Huang and colleague's approach to alkylation-reduction

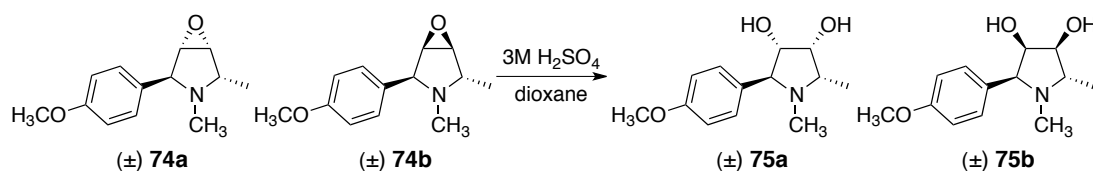
It seemed likely that the acetoxy-protecting groups used to access the other analogues would not be compatible with these reaction conditions, as

undesired side-reactions could occur. Instead, TBDMS-protected intermediate **71** would be more suitable (Scheme 1.14). This could be taken and presumably subjected to alkylation under Huang's or other conditions to give the methyl derivative **72**. Finally, the TBS protecting groups could be cleaved using TBAF to give the diol **73**.



**Scheme 1.14:** Planned route to methylated analogue

Previous work by Gourlay found an interesting result when synthesising (–)-codonopsinine *via* a different route.<sup>94</sup> In that research the final step in the synthesis was the acidic ring-opening of the epoxide of a diastereomeric mixture of **74a** and **74b**, to reach the natural *trans* diol of the natural product (Scheme 1.15). However, NMR data was found to be inconsistent with that reported by Kibayashi,<sup>9</sup> and instead seemed to support formation of *cis*-diol products **75a** and **75b**. This would be a highly unusual result, as ring-openings of epoxides in this fashion are normally expected to yield only *trans*-diol products. Thus, the full synthesis of *cis*-dihydroxy (–)-codonopsinine analogue **73** would also be invaluable in providing unambiguous NMR spectral evidence to support Gourlay's structural assignments for diols **75a** and **75b**.



**Scheme 1.15:** Gourlay's epoxide ring-opening

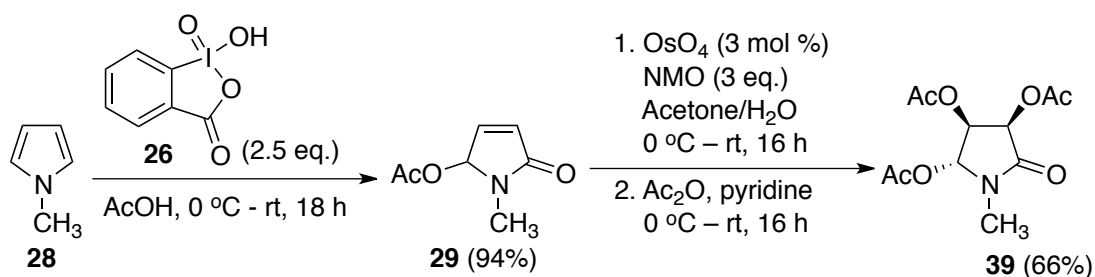
As such, it was planned to deliberately synthesise a *cis* analogue of (–)-codonopsinine *via* a pyrrole oxidation pathway, which would allow for comparison with the reported NMR data for Gourlay's product and (–)-codonopsinine to give conclusive evidence about the products formed in Gourlay's work.

With the full range of desmethyl analogues and the *epi*-codonopsinine analogue successfully prepared, a good range of substrates would have been accessed. This would provide evidence for controlled pyrrole oxidation being a useful technique for efficiently accessing biologically active natural product analogue libraries, and provide the basis for biological activity studies on these compounds.

## 1.4 Results of Racemic Work

### 1.4.1 Preparation of Racemic (–)-Codonopsine Analogues

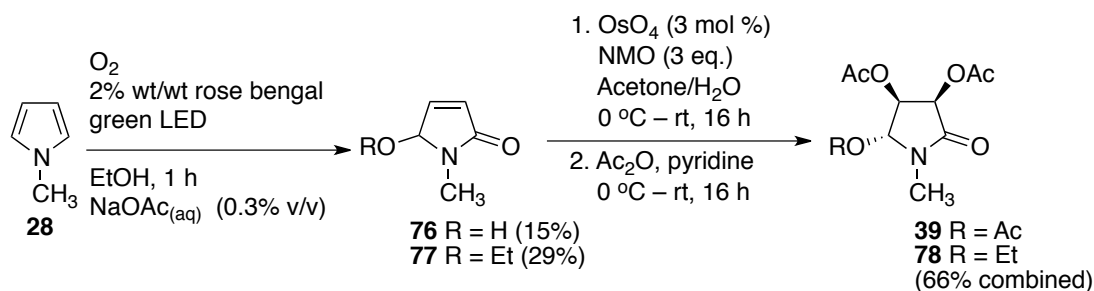
Previous work pursued the synthesis of racemic (–)-codonopsine analogues by first oxidising *N*-methylpyrrole with Dess–Martin periodinane or IBX. This expanded study began by following the procedure using IBX, to give the acetoxylactam **29** in an excellent 94% yield (Scheme 1.16). This was then subjected to dihydroxylation and acetate protection to give triacetate **39** as a single product in a 66% yield over two steps.



**Scheme 1.16:** Accessing diacetoxyl intermediates through IBX oxidation of *N*-methylpyrrole

As the low-cost and atom-economical photooxidation method and reactors became available, the production of these intermediates was switched over to this approach (Scheme 1.17). In this case, *N*-methylpyrrole was oxidised to give a mixture of 5-hydroxylactam **76** and 5-ethoxylactam **77** in a combined yield of 44%. These two products were then taken as a mixture and subjected to dihydroxylation and diacetoxylation to give what was identified as triacetoxyl derivative **39** and diacetoxyl ethoxyl derivative **78** in a 2:1 ratio, in identical yield to the IBX procedure. While these products were not separated, triacetoxyl compound **39** was identified through its <sup>1</sup>H NMR spectrum matching that obtained through the oxidation/diacetoxylation of *N*-

methylpyrrole with IBX. The second product was identified as the diacetoxo product with a 5-ethoxy substituent through the diagnostic ethyl triplet and quartet resonances at 1.23 and 4.09 ppm, respectively. The C5 methine proton of **78** was also upfield of that observed in triacetoxo derivative **39**, at 4.60 ppm rather than 6.01 ppm.



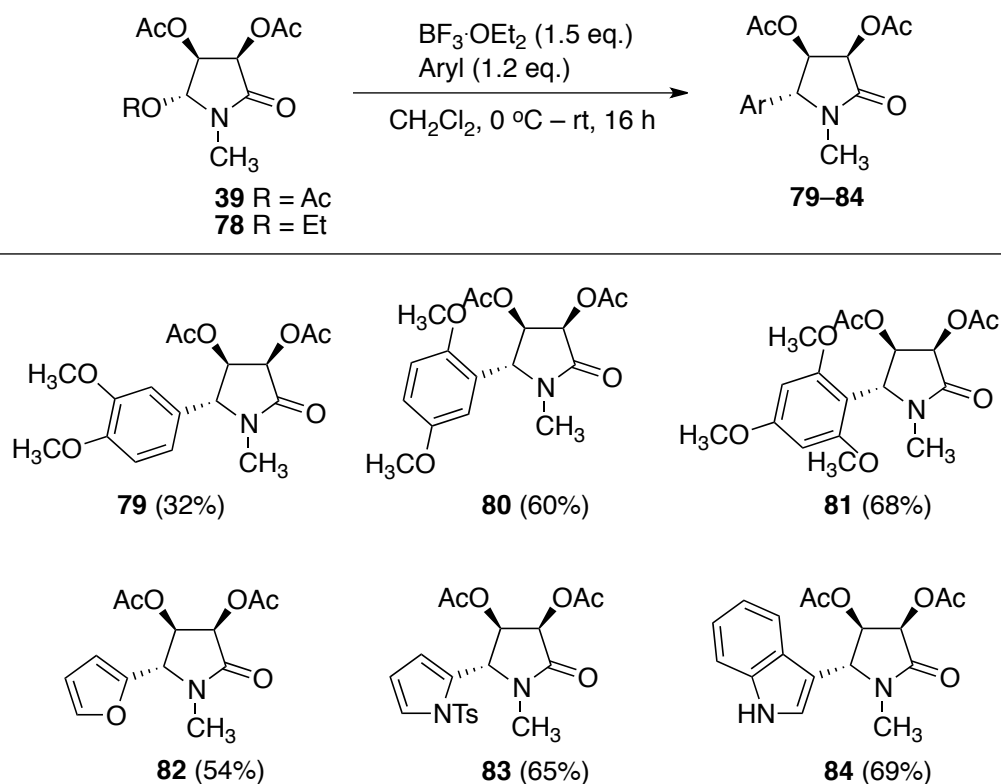
**Scheme 1.17:** Accessing diacetoxo intermediates through photooxidation of *N*-methylpyrrole

The major advantage of the photooxidation method over the IBX approach was that no stoichiometric organic oxidant was required, and the short reaction times meant that gram-quantities could be prepared simply by carrying out multiple 0.5 g scale reactions in parallel and combining crude products together for purification. By comparison, the DMP and IBX methods suffer from needing very large quantities of oxidant to be added, increasing the expense of the reactions and making the workup procedures more laborious. From a combined 8 runs of photooxidations, using a total of 4 g of *N*-methylpyrrole, a modest yield of 32% was obtained. While the yields would have been higher for a hypervalent iodine procedure, 34.5 g of IBX or 52.3 g of DMP would be required to oxidise the same amount of *N*-methylpyrrole.

The following step in the synthesis of racemic (–)-codonopsine analogues was to generate an *N*-acyliminium ion at C5 using a Lewis acid, followed by alkylation of aryl substrates. As such, both the single compound **39** and the mixture of **39** and **78** were appropriate, as the same *N*-acyliminium intermediate could be generated from both compounds.

A suite of Friedel–Crafts alkylation reactions were then performed using BF<sub>3</sub>·OEt<sub>2</sub> as the Lewis acid and the desired aromatic substituents. For the most part, these transformations were successful, giving single products in

moderate to excellent yields. (Scheme 1.18) Repeats of previously prepared compounds using veratrole (**79**) and 1,4-dimethoxybenzene (**80**) gave single regioisomers, as did furan (**82**), the less electron-rich *N*-tosylpyrrole (**83**) and indole (**84**). Success of the reactions was supported by the appearance of key aromatic  $^1\text{H}$  and  $^{13}\text{C}$  NMR spectral resonances, and a general up field (relative to triacetoxo **39**) shift of the C5 methine proton resonances to between 4.46–5.05 ppm. HRMS analysis of each of the compounds also supported their identities.

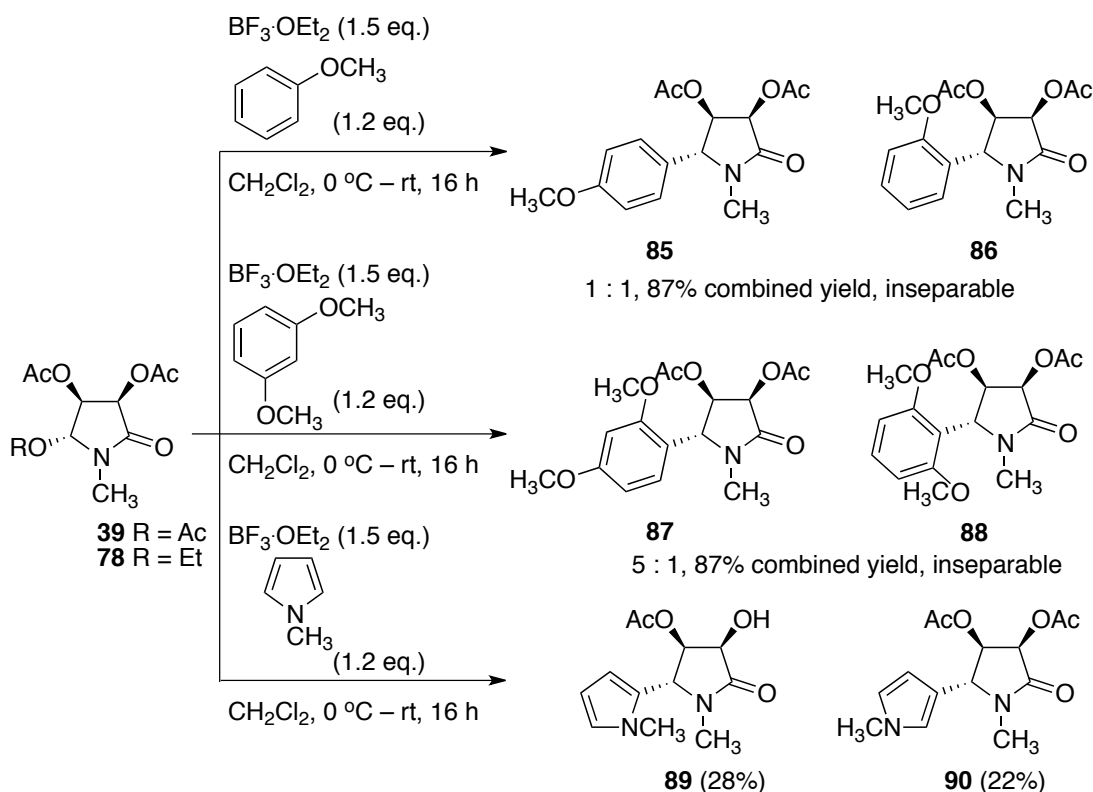


**Scheme 1.18:** Preparation of single product aryl derivatives from diacetoxo intermediates

The relative stereochemistry of the diol and the newly introduced aryl substituents was determined through analysis of the  $^1\text{H}$  NMR spectra of these compounds. The coupling constant for the methine proton in the 5-position with the hydrogen atom geminal to an alcohol in the 4-position was found to be close to or exactly 0 Hz. Thus the C5 proton resonance appeared as a singlet. The mutually coupled diol proton resonances, by contrast, appeared as doublets. For example, in the case of 1,2-dimethoxybenzene-substituted analogue **79**, the vicinal C3 and C4 methine proton resonances at

5.16 and 5.45 ppm shared a coupling of 5.6 Hz, while the methine proton resonance for C5 at 4.46 ppm showed no evidence of coupling.

Issues were encountered in the realm of regioselectivity for three of the other substrates. The 1,3-dimethoxybenzene and anisole derivatives both yielded two regioisomers for the Friedel–Crafts reaction (Scheme 1.19). Where anisole was used the reaction gave a 1:1 ratio of *ortho*-substituted product **85** and *para*-substituted product **86**, which proved to be chromatographically inseparable. Similarly, 1,3-dimethoxybenzene gave a 5:1 ratio of the 1,2,4- and 1,2,3-substituted products (**87** and **88**). These two compounds were also inseparable.



**Scheme 1.19:** Regioselectivity in Friedel–Crafts alkylations

The identities of these inseparable compounds were established through analysis of the  $^1\text{H}$  NMR spectrum of the mixture, and use of 2D NMR spectra to assign each resonance to a particular product. For example, a doublet associated with the isomer **85** at 7.06 ppm, with a coupling constant of 8.6 Hz and integrating for two hydrogen atoms was consistent with a resonance expected for a 1,4-substituted benzene. By contrast **86** featured a more complicated aromatic resonance at 7.29 ppm (a doublet of doublets of

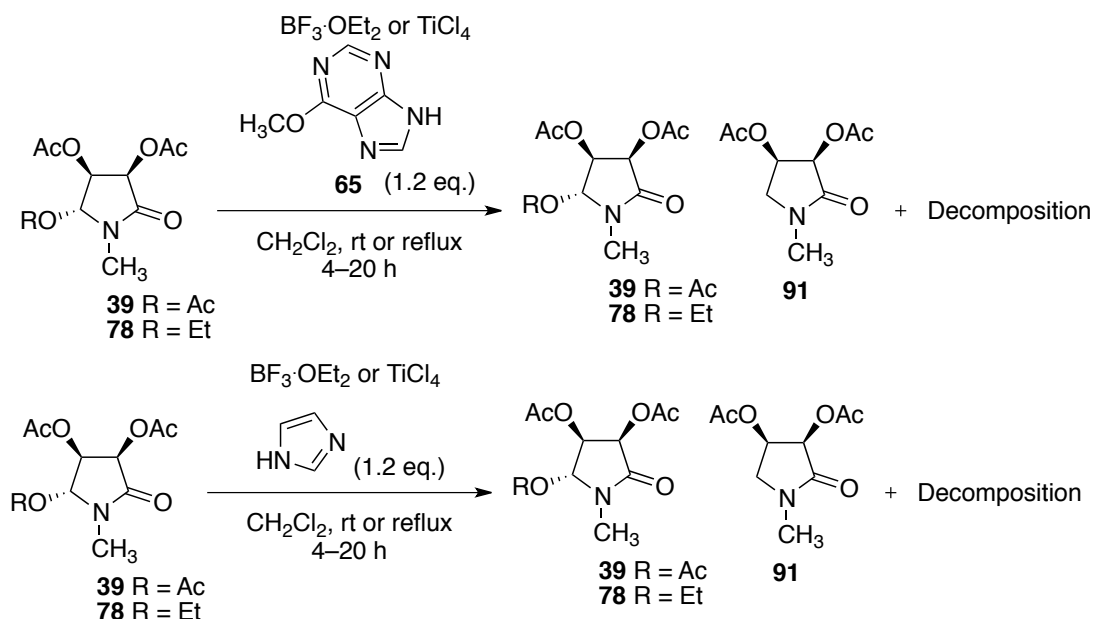
doublets) indicative of a 1,2-substituted benzene with more couplings observed between aromatic hydrogen atoms.

While the mixtures of these products could be purified by chromatography and identified by NMR analysis, it was not possible to isolate the individual products at this stage. For the 1,3-dimethoxy adduct, it was decided to end the synthesis at this step given the wide range of other compounds to prepare. However, the anisole adduct was considered important to pursue due to its similarity to the natural product and the need to reach its methyl analogue for comparison with Gourlay's work.

The use of *N*-methylpyrrole also led to the formation of two products. These were identified as products where alkylation had occurred at the C2 and C3-positions of the pyrrole, lactams **89** and **90**, in a ratio of nearly 1:1. This was surprising as *N*-methylpyrrole typically only yields 2-substituted pyrroles. The lack of selectivity for this reaction compared with the *N*-tosyl derivative can be explained by this pyrrole being more electron-rich, and thus both C2 and C3 positions are viable sites for alkylation to take place. Fortunately it was possible to separate the *N*-methyl adducts by flash column chromatography, and establish which was which through analysis of the  $^1\text{H}$  NMR spectra. For 2-substituted derivative **89**, a triplet signal at 6.07 ppm provides evidence that the proton at C4 of the pyrrole is adjacent to two other protons, supporting the proposed substitution pattern. For the 3-substituted **90**, this level of coupling of aromatic region protons is not observed.

Finally for these Friedel–Crafts alkylation investigations, it was attempted to introduce a purine derivative, 6-methoxypurine, by a similar approach (Scheme 1.20). Initial tests were carried out under roughly the same conditions as the previous experiments, starting with the triacetoxylactam and treating it with a small excess of 6-methoxypurine and an excess of  $\text{BF}_3\cdot\text{OEt}_2$  at room temperature. The reaction was monitored by TLC analysis and, when no reaction was observed after 2 hours, the mixture was heated at reflux and monitored by TLC for a further two hours before quenching.  $^1\text{H}$  NMR analysis of the crude products indicated that the only identifiable compounds were unreacted starting material, 6-methoxypurine, a compound

that appeared to be amide **91** (where the C5-acetoxy group had evidently been cleaved/reduced), and decomposition.



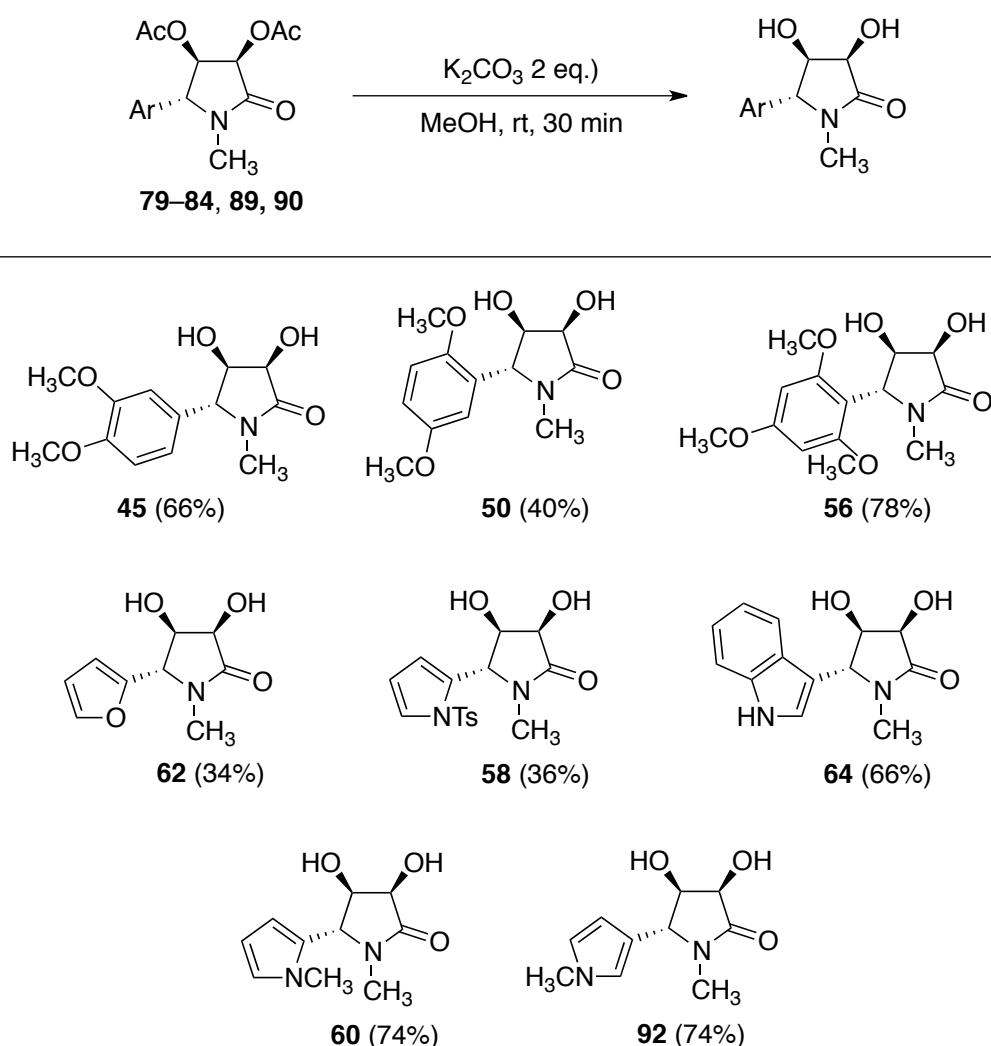
**Scheme 1.20:** Attempts at using purine and imidazole

After this first attempt more forcing conditions were trialled, with the stronger Lewis acid  $\text{TiCl}_4$ , in modest excess at room temperature or at reflux over 20 h. Unfortunately, only unreacted starting material and decomposition products were observed.

To probe whether similar substrates other than the 6-methoxypurine might be more successful, imidazole was also trialled as the aryl under a similar range of conditions (Scheme 1.18). Using  $\text{TiCl}_4$  or  $\text{BF}_3 \cdot \text{OEt}_2$  as the Lewis acid at room temperature or at reflux overnight in all cases led to mixtures of what appeared to be the reduced product **91**, starting material and mostly decomposition, with no incorporation of the imidazole. In case the desired products were forming and then decomposing,  $\text{TiCl}_4$  was used at reflux but with the reaction carefully monitored and stopped as soon as TLC analysis showed consumption of the starting materials. In this case more distinct products were observed in the  $^1\text{H}$  NMR spectrum of the crude reaction mixture, but there was again no evidence of imidazole being incorporated onto the pyrrolidine, and approximately 90% of the starting mass was lost due to decomposition.



The successfully prepared single acetoxy-protected diols **79–84** and **89–90** were all taken and subjected to deprotection, to yield the diol lactams (Scheme 1.21). Previously, this reaction was allowed to stir for several hours before removing the solvent under reduced pressure, which in a number of cases resulted in product decomposition. To overcome this problem, the amount of base and reaction times were both reduced and the reaction mixture immediately filtered through a silica plug without evaporation. This gave clean products in a much more efficient and convenient manner than the previous approach.

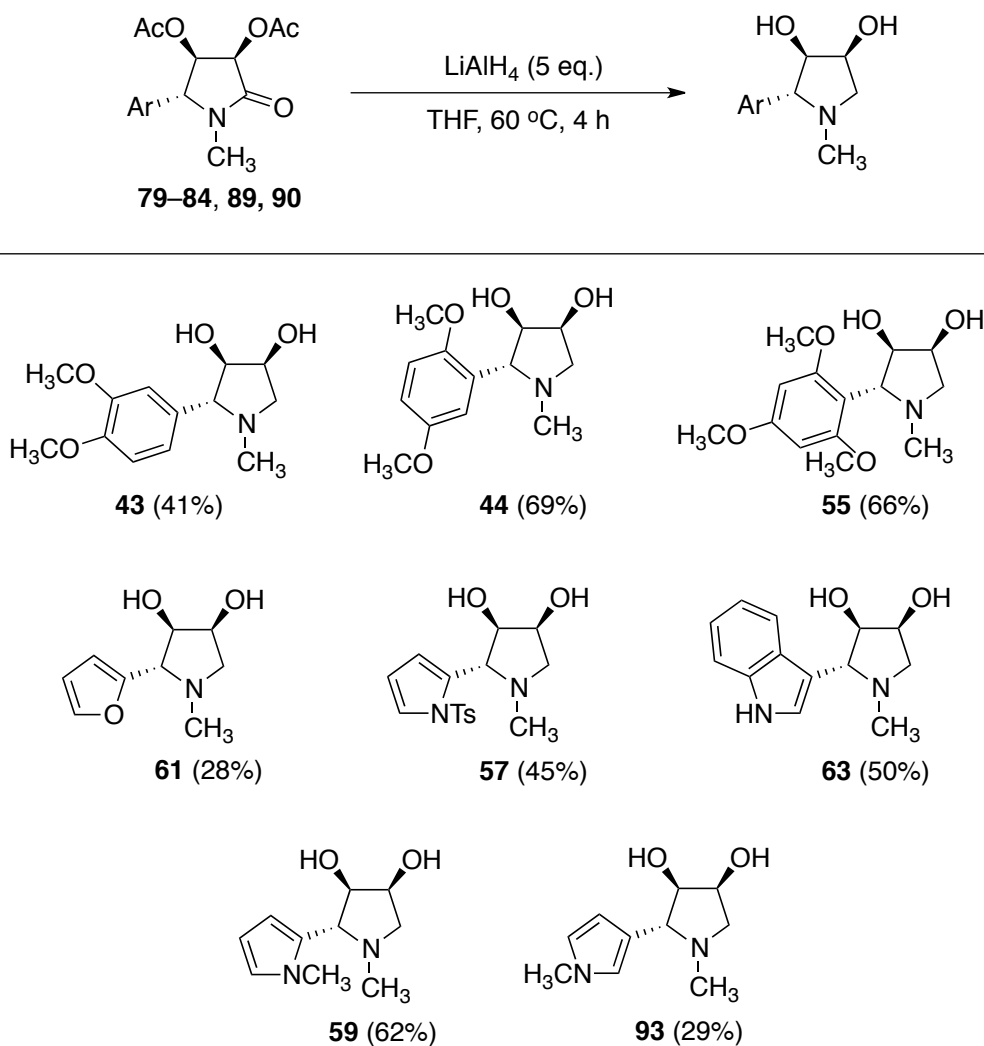


**Scheme 1.21:** Acetoxy cleavage to give (–)-codonopsine analogues

The success of these reactions was supported by the disappearance of the two acetoxy  $\text{CH}_3$  resonances in the  $^1\text{H}$  NMR spectrum and the appearance of only a single carbonyl signal for each in the  $^{13}\text{C}$  NMR spectrum. IR spectra showing only a single carbonyl stretch at about  $1690\text{ cm}^{-1}$  and a broad OH

stretch at approximately  $3300\text{ cm}^{-1}$ , and HRMS analysis provided further evidence.

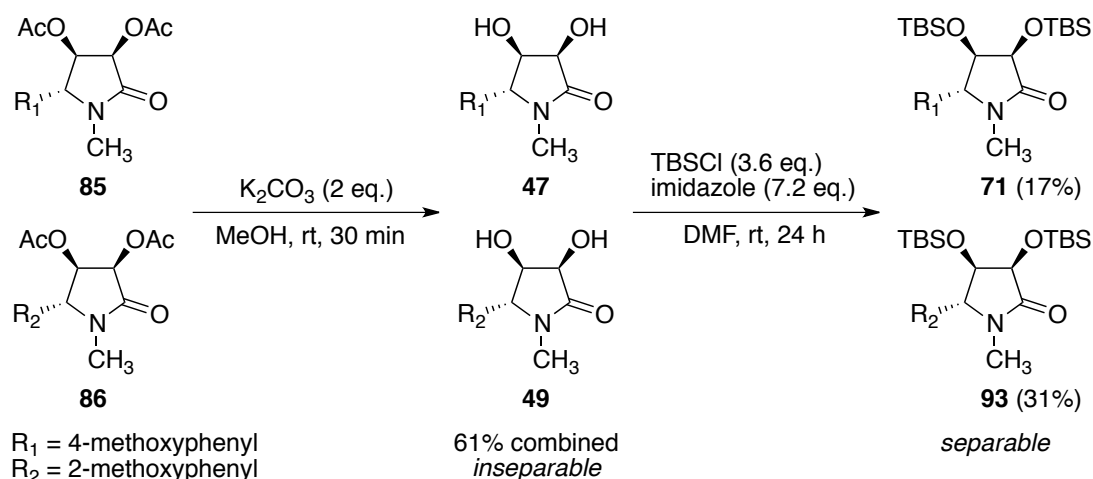
Likewise, the diacetoxo substrates were taken and subjected to reduction with  $\text{LiAlH}_4$  (Scheme 1.22). Yields were mostly reasonable and in many cases the products were obtained pure without need for any purification. The products were identified by the disappearance of any carbonyl resonances in the  $^{13}\text{C}$  NMR spectrum and IR spectra, and by the appearance of two new CH resonances in the  $^1\text{H}$  NMR spectra. These were accompanied by a noticeable up field shift of the  $^1\text{H}$  NMR resonances associated with the protons on the pyrrolidine ring. The lack of any carbonyl stretches between  $1600\text{--}1700\text{ cm}^{-1}$  and appearance of a broad OH stretch in the IR spectra provided further evidence.



**Scheme 1.22:**  $\text{LiAlH}_4$  reduction to give (–)-codonopsine analogues

It was hoped that carrying out the above described deprotection procedure on the mixed anisole derivatives **85** and **86** might lead to isomers that were separable. Unfortunately, neither the products of the acetoxy deprotection with  $K_2CO_3$  or reduction with  $LiAlH_4$  were separable by chromatography. As a primary goal for the 4-methoxyphenyl racemic analogue was to pursue alkylation/reduction of the amide, the mixture of diol lactams (**47** and **49**) produced by deacetylation with  $K_2CO_3$ , were protected as TBS groups (Scheme 1.23). Gratifyingly, the two TBS-protected ethers **71** and **93** were readily separable by flash column chromatography.

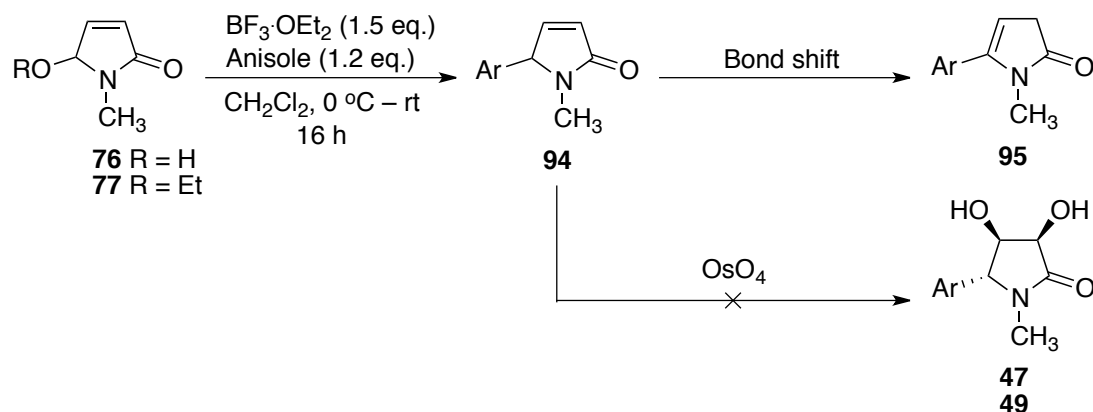
The success of the TBS-protection was verified by  $^1H$  NMR spectroscopy. Specifically, the appearance of two key peaks associated with the silyl *t*-butyl groups integrating for 9 protons between 0.85 ppm and 0.91 ppm, and four singlets integrating for 3 protons indicative of the silyl methyls between -0.09 and 0.18 ppm.



**Scheme 1.23:** TBS protection of anisole lactams

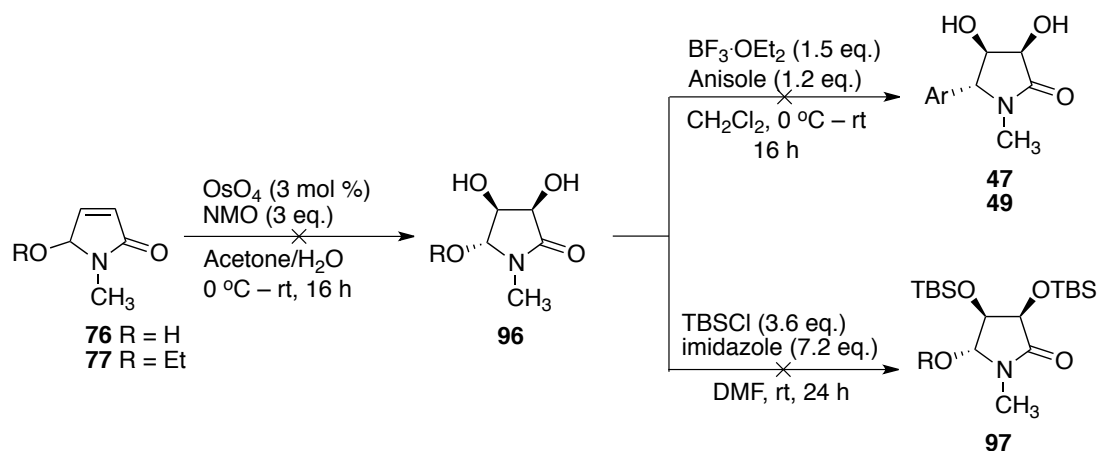
Given that compounds **71** and **93** are potential precursors for stereoisomers of (–)-codonopsinine, two routes to reduce the number of synthetic steps to reach them were attempted. First, direct Friedel–Crafts alkylation of the 5-hydroxylactam **76** and 5-ethoxylactam **77** to reach 5-aryllactam **94**, followed by dihydroxylation to give the diols **47** and **49** without the need for acetate protection and deprotection (Scheme 1.24). Unfortunately only decomposition of **94** was observed. It was theorised that a bond shift of the alkene of **94** from C3–C4 to C4–C5 occurs to give the unstable species **95**,

which rapidly decomposes. Similar reactivity has been observed in previous research by Daïch and colleagues, and by Howard.<sup>66,95</sup>



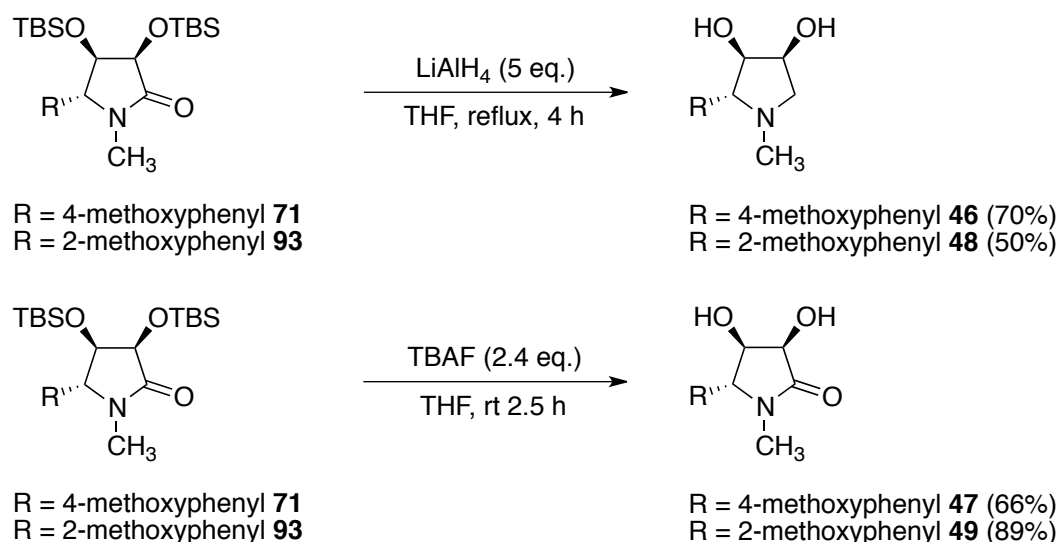
**Scheme 1.24:** Proposed decomposition pathway for aryl-substituted 3-pyrrolin-2-ones

As an alternative, the crude product of the dihydroxylation of lactams **76** and **77** was subjected to both Friedel–Crafts alkylation with anisole directly, and TBS protection, again with the intention of finding a way to avoid acetoxy protection (Scheme 1.25). Unfortunately, neither of these approaches yielded any improvement and mostly led to decomposition. The conclusion of these efforts, then, was that the most viable approach was to work through the longer route of dihydroxylation followed by acetoxy protection, alkylation, then cleavage of the acetoxy groups followed by protection of the diol as the silyl ethers.



**Scheme 1.25:** Attempts to use crude diol in synthesis of anisole derivatives

Given that the best route to the TBS-protected lactams **71** and **93** had been established, these were taken and used to generate the corresponding final racemic products of the two isomers from anisole. The pyrrolidine products, where the TBS groups were cleaved and the amide reduced, were generated by treatment with excess  $\text{LiAlH}_4$ , similarly to the acetoxy-protected intermediates, based on a literature procedure (Scheme 1.26).<sup>96</sup> This was based on evidence that the presence of adjacent  $\text{LiAlH}_4$ -reducible functional groups, in this case the amide carbonyl, facilitate the intramolecular reductive deprotection of silyl ethers of alcohols.<sup>97</sup> This yielded the desired diol products **46** and **48**. To simply cleave the silyl ether protecting groups and leave the amide functional group intact, lactams **71** and **93** were simply deprotected with TBAF, the standard approach to such transformations.<sup>98,99</sup> This gave the desired lactams **47** and **49** in good yields. These reactions completed the set of racemic desmethyl *cis*-diol codonopsine analogues to be prepared in this work.



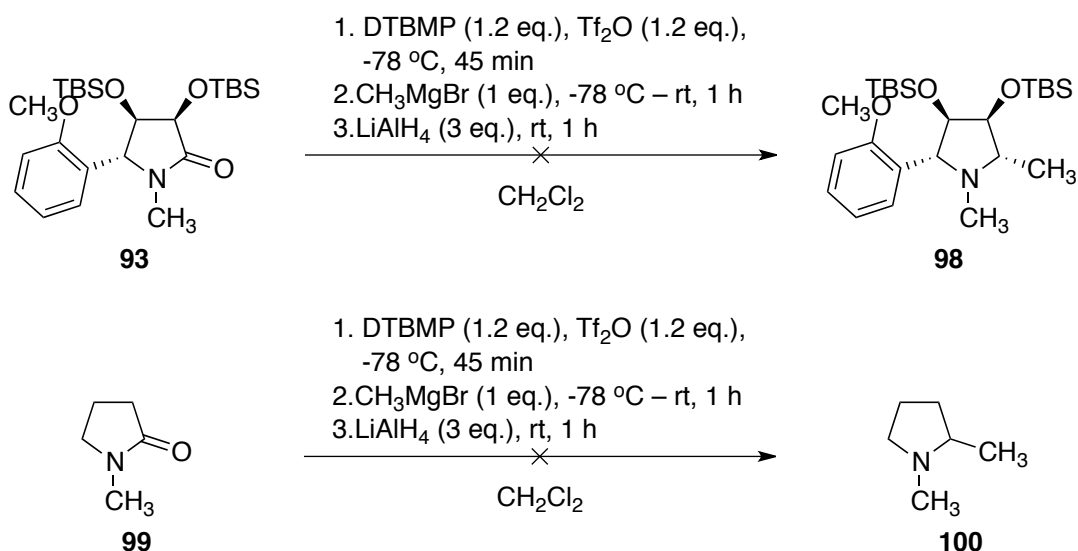
**Scheme 1.26:** Deprotection/reduction of TBS anisole substrates

#### 1.4.2 Towards Synthesis of Alkylated *cis*-diol

Finally, the possibility of using TBS-protected diol **71** as a substrate for preparing methylated (–)-codonopsinine analogues such as **63** was explored. Huang and colleagues' combined alkylation/reduction procedure for lactams was trialled first, on TBS derivative **93** (Scheme 1.27).<sup>93</sup> Despite this procedure being reported to be effective for a number of alkylmagnesium reagents, only decomposition of the starting material was observed, with no

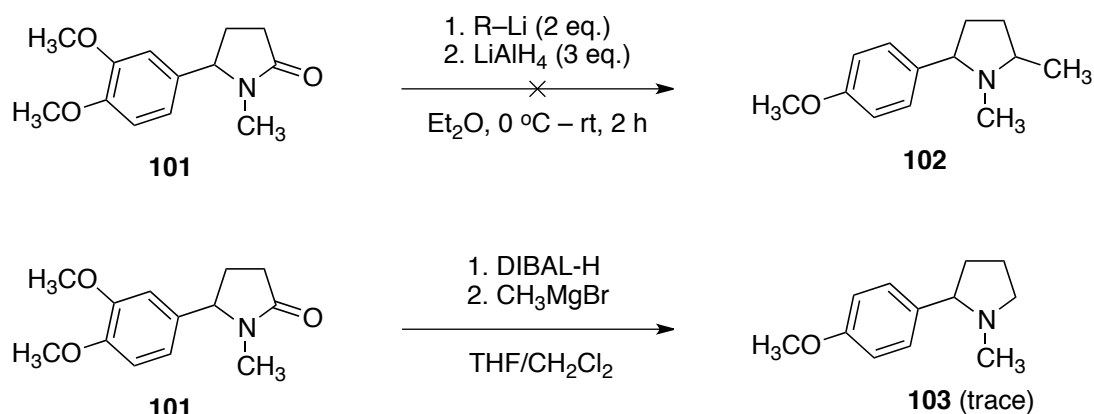
evidence of methyl incorporation to give pyrrolidine **98**. Similar results were observed for the model substrate *N*-methylpyrrolidin-2-one **99**.<sup>100</sup>

To establish whether the amide/lactam systems being used were inherently unsuitable to alkylation and reduction, the more technical approach of Huang and colleagues was shelved and simpler literature conditions trialled on the 5-arylpyrrolidinone **101** (Scheme 1.28). Initially, alkylation followed by reduction was attempted, Using both MeLi and BuLi as the alkylating agent and LiAlH<sub>4</sub> as the reducing agent, under mild conditions.<sup>90</sup> Unfortunately, mostly decomposition was observed, with the remainder being starting material and trace by-products that showed no evidence of methyl or butyl incorporation in the <sup>1</sup>H NMR spectrum.



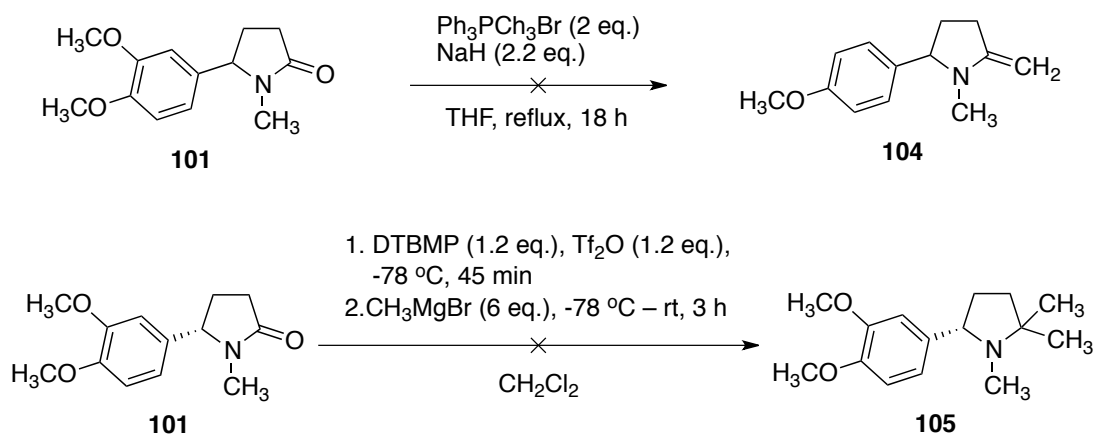
**Scheme 1.27:** Attempts at sequential alkylation/reduction

The alternative approach was also attempted, carrying out the reduction first followed by addition of the alkylating agent.<sup>91</sup> DIBAL-H was chosen as the reducing agent in this case, and a variety of conditions trialled, including varying the temperature, addition times and excess of reagents. Across all of the reactions the only identifiable products other than complete decomposition were starting material, and traces of the overreduction product **103**. This indicated that it is difficult to partially reduce the amide to the required aminol for subsequent alkylation to occur.



**Scheme 1.28:** Other attempted reduction/alkylation conditions

Two other approaches were attempted to try to generate alkylated racemic codonopsine analogues. Firstly, a Wittig procedure was trialled. While there have been some reports of these reactions working for  $\gamma$ -lactams, such conversions of amides to enamines are generally limited to cases where the conjugation of the amide bond with the lone pair of the nitrogen is weakened by strain in the molecule or competing resonances.<sup>101</sup> Unfortunately, without such effects lactam **101** proved unreactive to the Wittig reagent. These conditions were also attempted on *N*-methylpyrrolidinone **99**, with a similar lack of any reaction observed (Scheme 1.29).



**Scheme 1.29:** Final attempts at amide alkylation

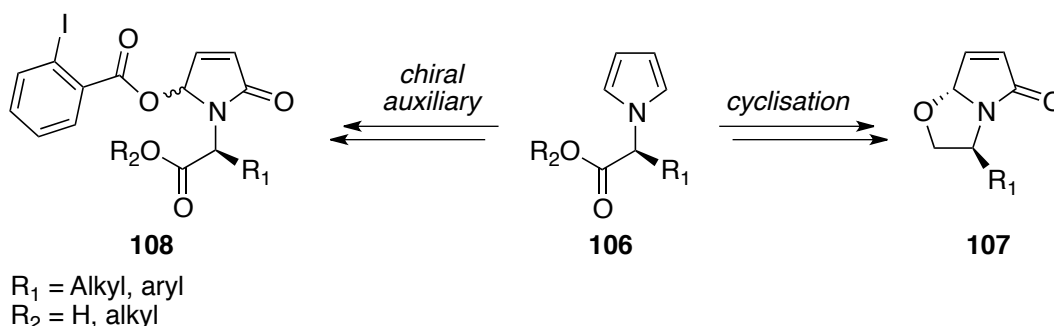
Finally, lactam **101** was subjected to Huang and colleagues dialkylation conditions, minus the added complication of carrying out a reduction step at the same time (Scheme 1.29).<sup>92</sup> While in this instance the <sup>1</sup>H NMR spectrum of the crude compound was promising, appearing to show one major product with additional singlet resonances upfield at 1–2 ppm that could indicate

addition of two methyl groups. However, the product formed proved unstable to purification and could not be isolated.

While the alkylation-reduction procedure was ultimately unsuccessful, this work did succeed in significantly expanding the scope of preliminary studies into the synthesis of racemic (–)-codonopsinine analogues. Twenty new desmethyl analogues were prepared using a variety of aromatic substituents, and variation in the functionality at the 2-position. This represents a useful library of compounds for carrying out future bioactivity assays.

### 1.5 Strategies for Asymmetric Syntheses

With the above syntheses of racemic (–)-codonopsinine analogues in mind, two pathways were envisioned for exploring the possibility of an asymmetric synthesis, where the absolute rather than just the relative stereochemistry of the products was controlled. Both of these involved the incorporation of a chiral amino acid derivative into the starting material, such as **106** (Scheme 1.30).



**Scheme 1.30:** Proposed routes to stereo-controlled lactams

The first approach was to use a chiral amino alcohol as a precursor for the pyrrole used in the synthesis. Alcohols such as (S)-(+)-2-phenylglycinol and (S)-(+)-2-phenylalaninol were considered to be viable options for this. It was proposed that the pyrroles prepared from these could be oxidised to give a diastereomeric mixture of  $\gamma$ -lactams, but that on addition of a Lewis acid to generate an *N*-acyliminium ion at C5, the proximal pendant alcohol would undergo intramolecular nucleophilic attack to form a five-membered heterocycle **107** with stereochemistry set by the amino alcohol moiety (Scheme 1.30)



Such compounds have been reported by Meyers and colleagues. They have made and used bicyclic  $\gamma$ -lactams extensively in the synthesis of chemically and biologically interesting pyrrolidine natural products and other compounds, such as (–)-rolipram (**109**, Figure 1.4), mastigophorene A (**110**) and (–)-penienone (**111**), among others.<sup>102-106</sup>

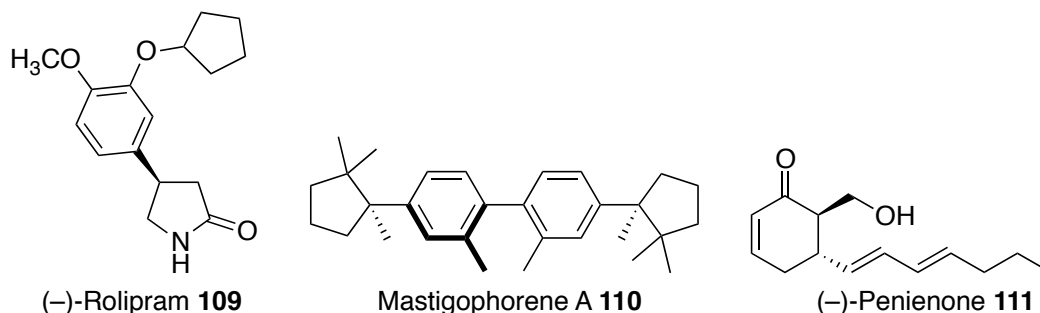
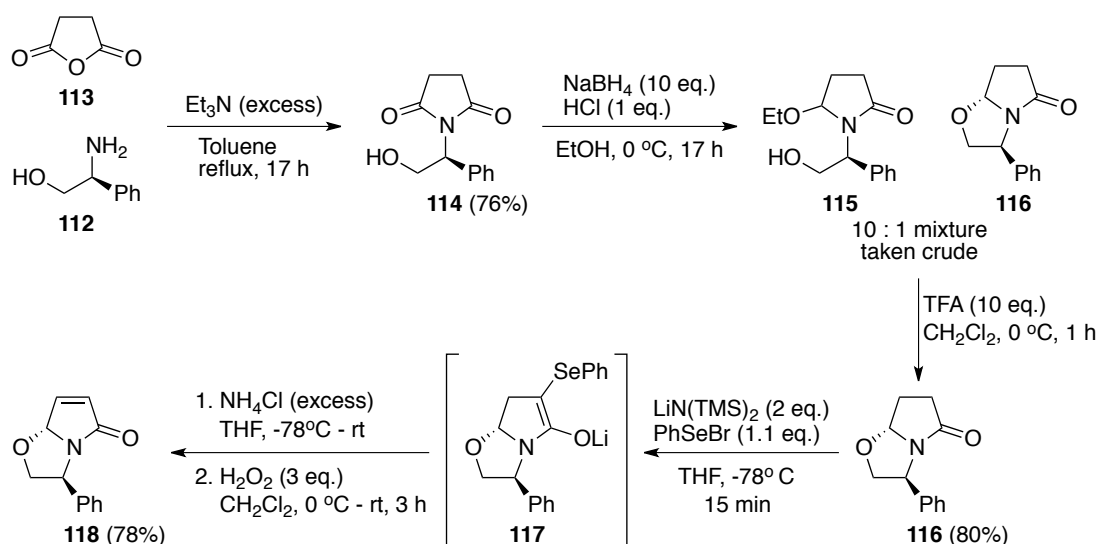


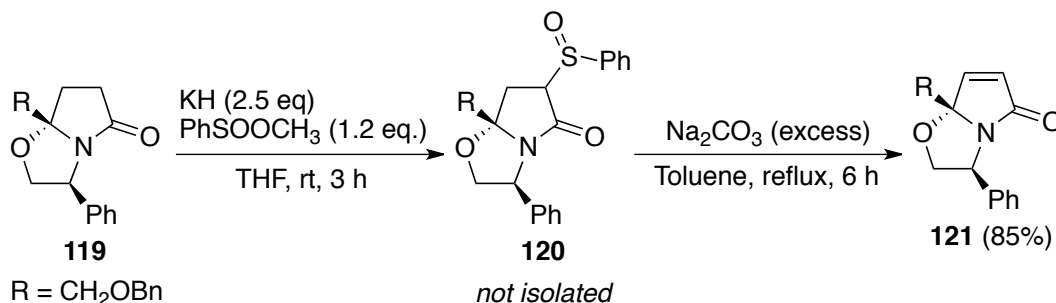
**Figure 1.4:** Examples of varied endpoints from chiral bicyclic lactams

Meyer's approach to synthesising such bicyclic intermediates involved starting with a chiral amino alcohol (*S*)-(+)-2-phenylglycinol, **112** and reacting with succinic anhydride (**113**) to give a succinimide (Scheme 1.31). The imide is then reduced with sodium borohydride before treatment with a Lewis acid to generate an iminium ion at the 5-position and allow for ring closure through attack by the alcohol functional group onto an *N*-acyliminium ion. This gave the bicyclic substrate **116** as a single enantiomer but *sans* the extra functionality of the C3-C4 double bond. Meyers and co-workers introduced this through a non-trivial and harsh selenylation-oxidation procedure, proceeding to chiral unsaturated bicyclic  $\gamma$ -lactam **118**. The procedure gave the key intermediate **118** in a 55% yield over 6 steps.



**Scheme 1.31:** Meyers' Synthesis of chiral bicyclic  $\gamma$ -lactam **118**

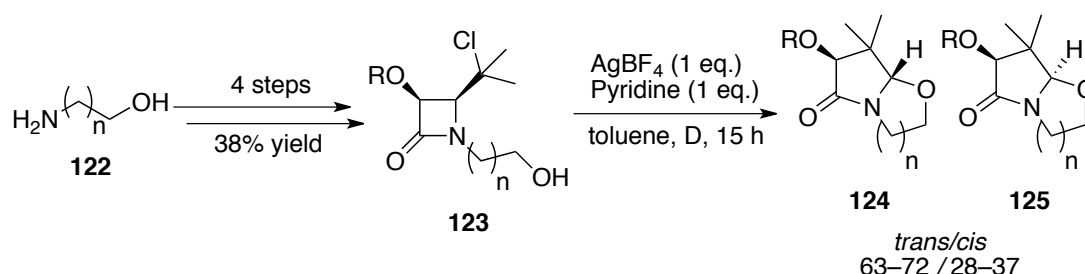
Another approach taken by Meyers and colleagues for the installation of an alkene in such bicyclic systems was to treat saturated intermediates such as **119** with methyl benzene sulfinate, followed by a period of reflux in toluene with excess base to promote elimination of the intermediate sulfoxide (Scheme 1.32).<sup>107</sup>



**Scheme 1.32:** Another of Meyers' approaches to introducing an alkene at C3-C4

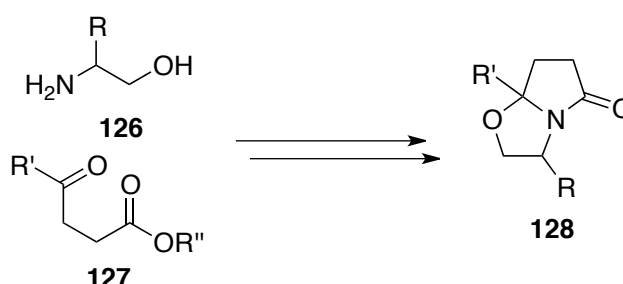
Other researchers who have prepared the same scaffold by different means include Demir and co-workers, who utilised their established pyrrole photooxidation methods to do so (Scheme 1.10).<sup>75</sup> They also used as starting materials pyrroles that incorporated chiral *N*-substituents featuring pendant hydroxyl groups (**33**). Photooxidation of the pyrrole gave the bicyclic lactams **34** in moderate yields.<sup>108</sup> However, for each chiral pyrrole used a mixture of diastereomeric products was obtained, albeit with some diastereoselectivity. They supported their stereochemical findings with a computational study which indicated that the favoured diastereomer arose because of restricted rotation of the *N*-substituents.<sup>109</sup>

Building on work by Yoshifumi<sup>110</sup> and Anaya,<sup>111</sup> De Kimpe and colleagues approached bicyclic lactams from a different angle, through the silver-mediated ring expansion of functionalised  $\beta$ -lactams (Scheme 1.33).<sup>112</sup> They synthesised a range of highly functionalised  $\beta$ -lactams **123**, with pendant alcohols as *N*-substituents, which when treated with  $\text{AgBF}_4$  and pyridine underwent ring expansion to give an iminium ion intermediate, which underwent cyclisation by nucleophilic attack of the pendant alcohol to give the bicyclic lactams **124** and **125** without stereoselectivity at the C5 position. Their approach, through requiring particular substituents to effect the ring expansion, also limited the ability to further functionalise the  $\gamma$ -lactam towards a natural product-like species.



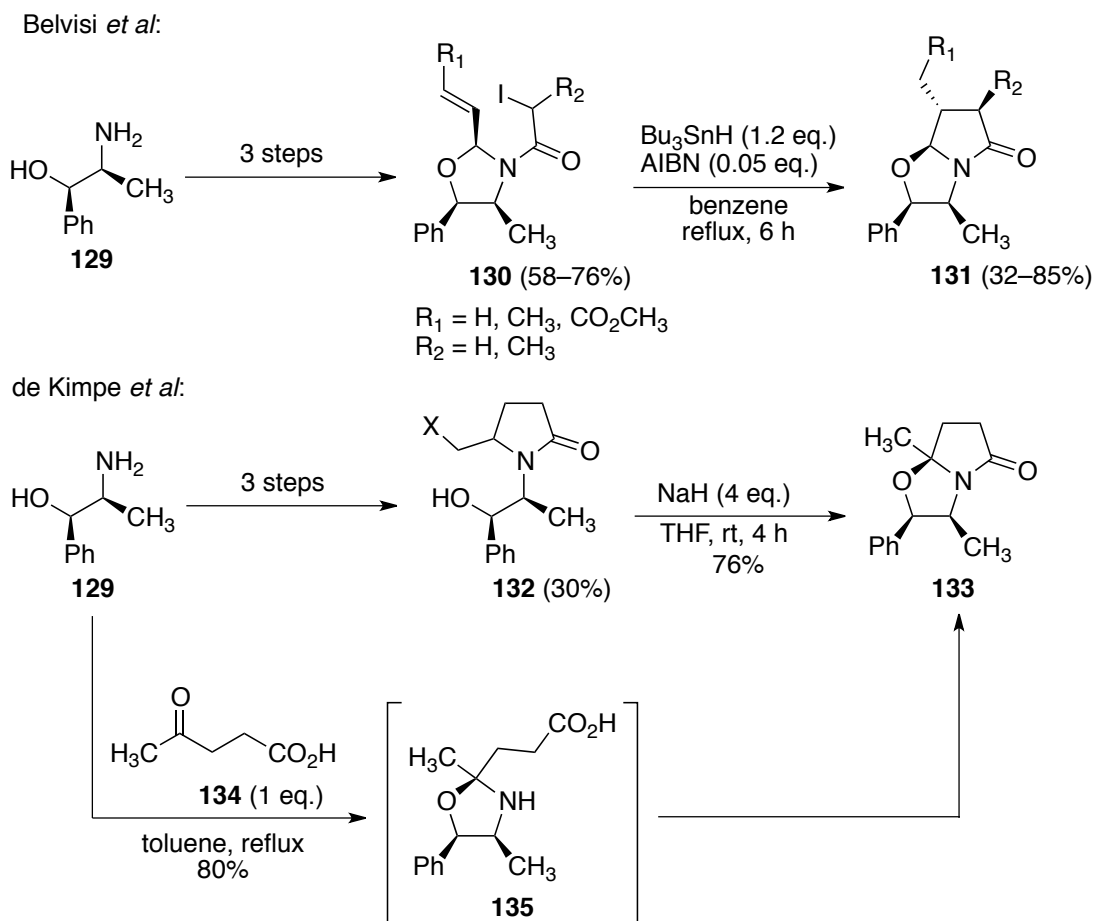
**Scheme 1.33:** de Kimpe and colleagues'  $\beta$ -lactam ring expansion

There are a number of other published examples of bicyclic  $\gamma$ -lactams in the literature. The majority utilise the cyclocondensation of a  $\beta$ -amino alcohol **126** with a  $\gamma$ -keto acid or ester **127** (Scheme 1.34).<sup>113–120</sup> While some of these take novel approaches, such as using resin-bound starting materials,<sup>121</sup> there are some common problems such as a lack of stereoselectivity, and a need to synthesise highly functionalised starting materials to give specific products. In addition, many of the lactam products observed lack the modifiable double bond at the C3–C4 position seen in bicyclic lactam **118**.



**Scheme 1.34:** General scheme of cyclocondensation reactions

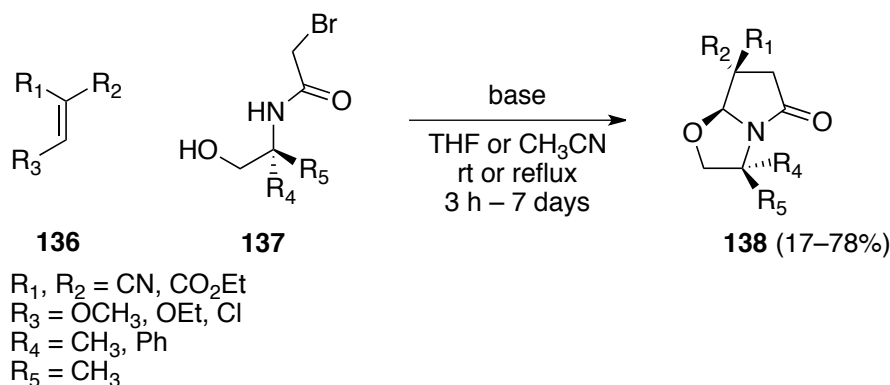
Another approach commonly taken, as is the case in both Meyers' and de Kimpe's work, is the generation of an iminium ion in a monocyclic lactam species and allowing ring closure through intramolecular attack of a pendant alcohol or other nucleophile.<sup>122-126</sup> In these cases the iminium is usually generated through treatment of a partially reduced maleimide or succinimide with a Lewis acid.



There have been some other novel approaches taken to forming these kinds of molecules, normally with particular built in functionality and reduced scope for post-formation manipulation. Belvisi and de Kimpe both developed approaches starting from (1*R*,2*S*)-norephedrine (**129**, Scheme 1.35). Belvisi's approach involved the cyclisation of an iodoamide intermediate **130**.<sup>127</sup> De Kimpe and colleagues formed bicyclic lactams both through the NaH deprotonation of 5-halomethyl pyrrolidinones **132** to generate an alkene which is attacked by the pendant alcohol, and also in a one pot condensation

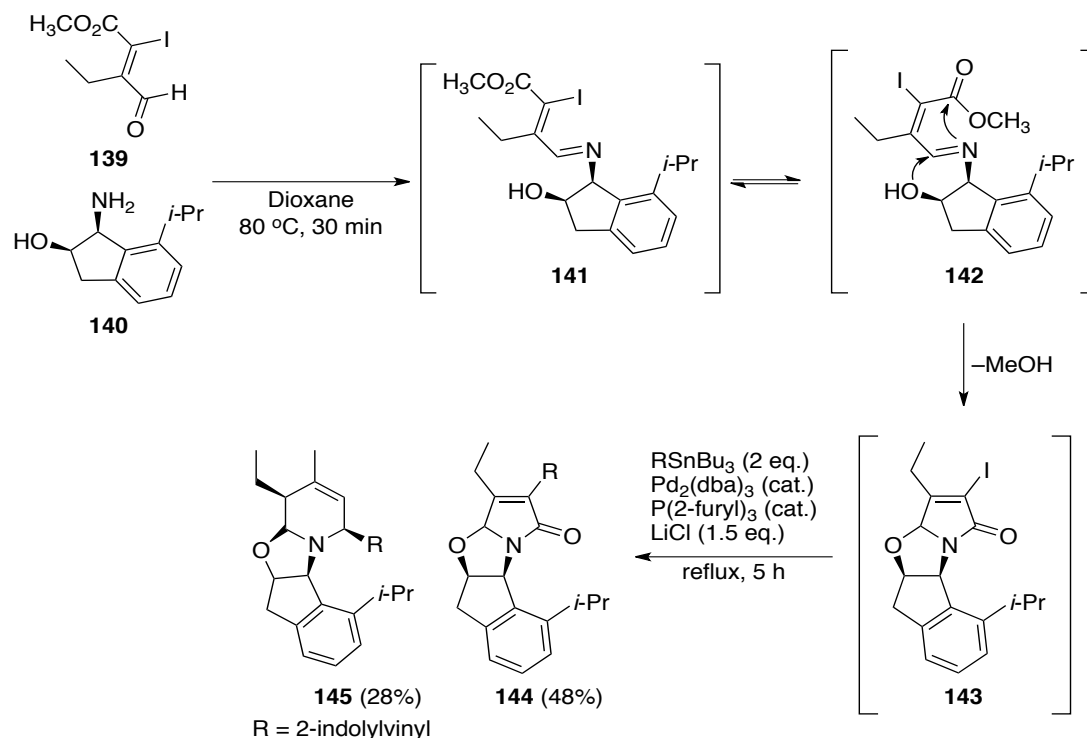
reaction of the (1*R*,2*S*)-norephedrine with levulinic acid **134**, through intermediate oxazoline **135**.<sup>128</sup>

Le Goff and colleagues developed a domino process with commercially available electron-deficient Michael acceptors and specifically prepared acyclic amides **137** (Scheme 1.36).<sup>129</sup>



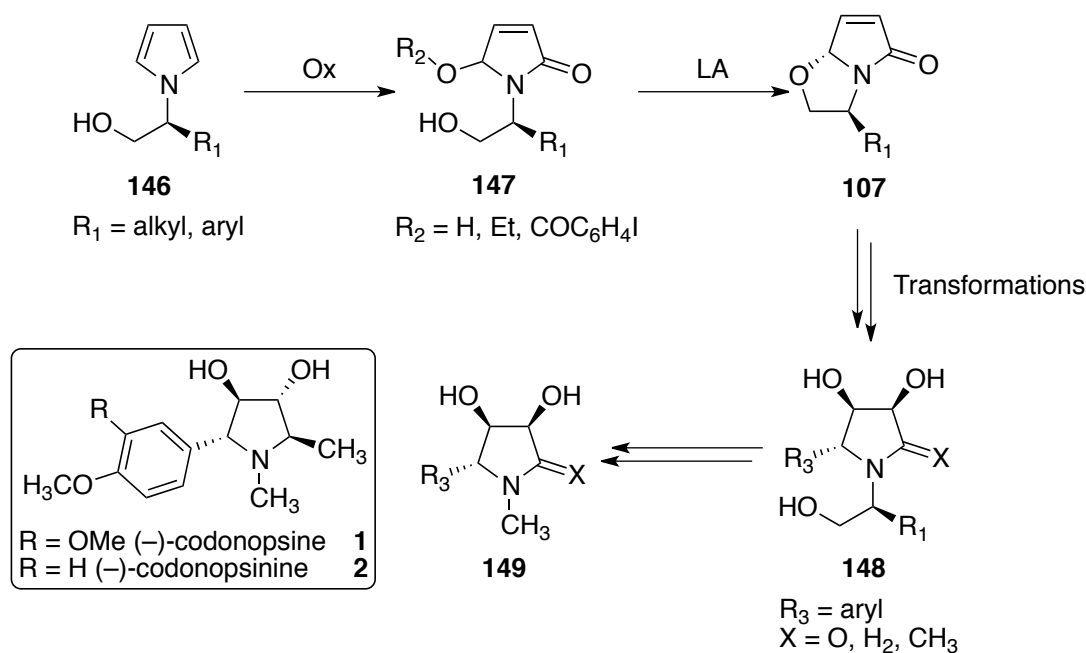
**Scheme 1.36:** Le Goff's Domino process

Katsumura and colleagues developed a one-pot asymmetric aza-electrocyclisation of vinyl iodide **139** and aminoindanol **140** followed by Stille coupling, which yielded a complex polycyclic  $\gamma$ -lactam **144** in addition to a  $\delta$ -lactam **145** (Scheme 1.37).<sup>130</sup>



**Scheme 1.37:** Katsumura's one pot aza-electrocyclisation with Stille coupling

The planned route to chiral bicyclic  $\gamma$ -lactams in this work shared some similarities with Meyers and colleagues' work, using a chiral amino alcohol as a starting point, and taking the iminium generation route to form the second ring in the bicycle (Scheme 1.38). However, it was instead proposed to form a pyrrole, **146**, from the amino alcohol, rather than a succinimide, through a mild variation on the Clauson–Kaas pyrrole synthesis developed in the Smith group.<sup>131</sup>

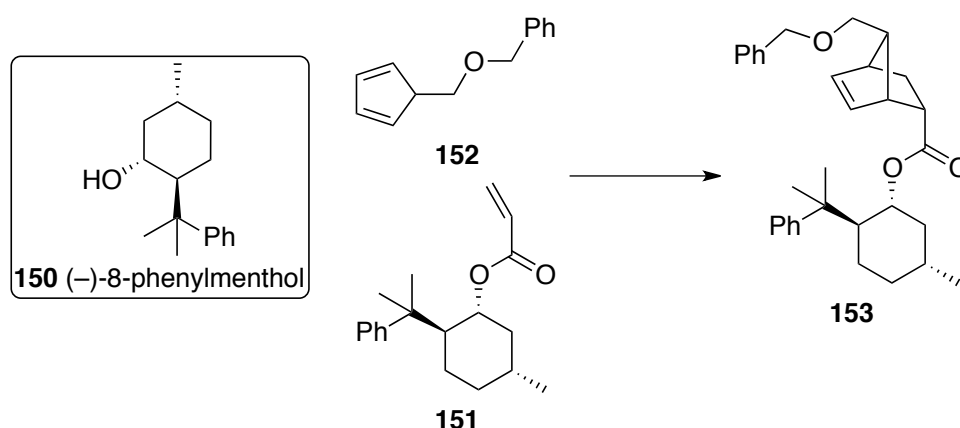


**Scheme 1.38:** Planned route to chiral bicyclic  $\gamma$ -lactams

This species could then be oxidised to give the corresponding monocyclic  $\gamma$ -lactam **147**, using either hypervalent iodine oxidation or photochemical oxidation.<sup>62,80</sup> This  $\gamma$ -lactam intermediate could then be treated with a Lewis acid such as  $\text{BF}_3 \cdot \text{OEt}_2$ , or a Brønsted acid such as TFA, to give a bicyclic lactam **107** via an *N*-acyliminium intermediate, with the stereochemistry set for the ether substituent in the 5-position by the chiral *N*-substituent. This intermediate could then be modified in much the same way as the previously discussed racemic compounds, through dihydroxylation and Friedel–Crafts alkylation to give chiral intermediates such as **148**. Finally, the *N*-substituent could be cleaved through hydrogenation or other means and the nitrogen methylated to give (–)-codonopsine analogues **149**.

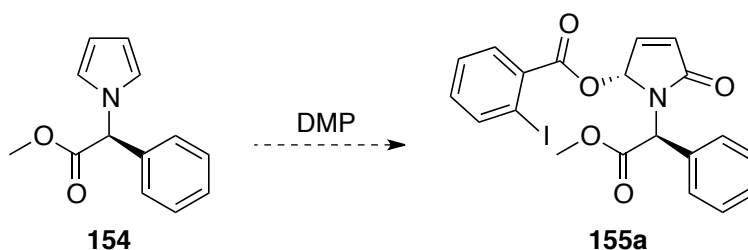
The second proposed approach to reach such analogues was one inspired by the use of chiral auxiliaries in asymmetric organic synthesis (Scheme

1.15). Probably the best known and one of the most widely used of these is (–)-8-phenylmenthol (**150**, Scheme 1.39).<sup>132</sup> These chiral auxiliaries can direct the face of certain chemical transformations by placing a bulky chiral group in the way, as in the case of Corey’s use of (–)-8-phenylmenthol in a facially selective Diels–Alder reaction involving the auxiliary-substituted dienophile **151** and cyclopentadiene derivative **152** (Scheme 1.33).<sup>132</sup>



**Scheme 1.39:** 8-phenylmenthol/action of a chiral auxiliary

The approach to be taken in this work was not to use 8-phenylmenthol itself, but to synthesise a pyrrole starting material that incorporated a bulky chiral *N*-substituent that might achieve a similar effect (Scheme 1.40). Thus, it was planned to use (*S*)-(+)-2-phenylglycine methyl ester as the basis for pyrrole **154**, which would provide a relatively bulky chiral group. It was hypothesised that on treatment with Dess–Martin periodinane, oxidation to yield the 2-iodoaryloxy moiety at C5 would favour one face over the other to give only one of the two possible diastereomeric products, such as **155a**.



**Scheme 1.40:** Plan for using chiral auxiliary to control oxidation stereochemistry

While chiral *N*-benzylamines are not reported to be highly efficient chiral auxiliaries, they are readily removed<sup>133</sup> and in the event of diastereomers forming these could be separated. This would allow for stereoselective

transformations to be carried out around the lactam ring without the need to form a chiral bicyclic lactam first. This would potentially offer a shorter synthetic route to the same chiral (–)-codonopsine analogues.

## 1.6 Results of Bicycle Approach

### 1.6.1 Bicycle Syntheses

The first step for both the bicycle and the chiral auxiliary approaches to these asymmetric syntheses was the preparation of the starting pyrroles from the corresponding chiral amine or amino acid derivatives (Figure 1.5). For the bicycle approach, pyrroles **156** and **157** were prepared from the corresponding (S)-(+)-2-phenylglycinol and (S)-(+)-2-phenylalaninol in near quantitative yield, through a modified Clauson–Kaas procedure in a buffered biphasic mixture.<sup>131</sup> The pyrrole derived from L-phenylglycine methyl ester hydrochloride, **154**, was prepared similarly, to be used in the chiral auxiliary pathway. Finally, another less bulky pyrrole was prepared to test the limits of the chiral auxiliary approach, from (R)-1-phenylethylamine (**158**). This was attempted as an on-water reaction, based on work by McErlean and colleagues.<sup>134,135</sup> While this made the reaction operationally simpler, the yields were lower than would be achieved by the method of Smith and co-workers.

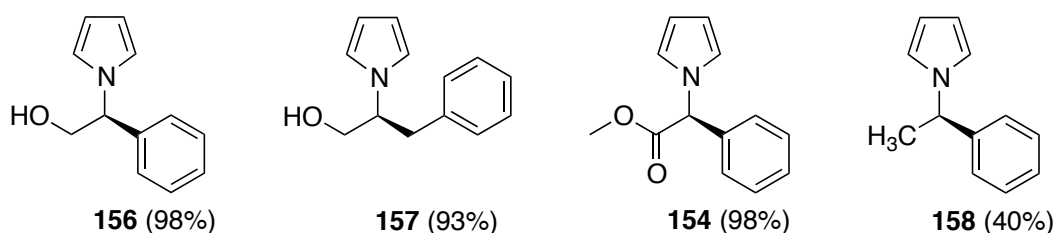
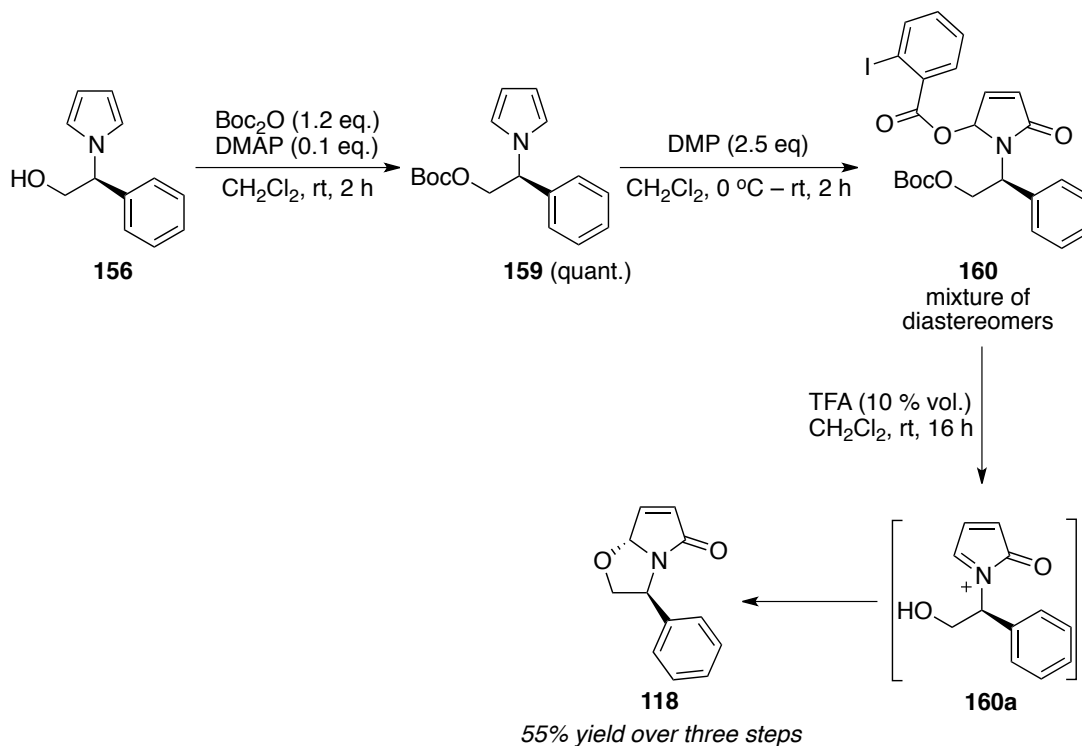


**Figure 1.5:** Pyrroles prepared for this work

The first transformation of this pyrrole was to protect the alcohol **156** with a Boc group to give pyrrole **159** (Scheme 1.41). While, as stated above, DMP has been shown to selectively target pyrroles over alcohols,<sup>62</sup> the alcohol oxidation is still very facile and it was deemed prudent to prevent this unwanted side reaction occurring from the outset. After the reaction was observed to be complete by TLC, the solvent was removed and a <sup>1</sup>H NMR spectrum of the crude mixture analysed to ensure that the Boc group had



been incorporated, through the appearance of a singlet peak integrating for 9 protons in the  $^1\text{H}$  NMR spectrum. Protected pyrrole **159** was then subjected to the oxidation step without purification.



**Scheme 1.41:** The synthesis of chiral bicycle **118**

Oxidation of pyrrole **159** was carried out under the previously developed conditions using Dess–Martin periodinane. It was found that this reaction was sluggish if the dichloromethane solvent was too dry. Consequently, the addition of one or two drops of water to the reaction mixture helped the oxidation to proceed smoothly to completion in 2 h, consistent with previous observations.<sup>66</sup> The  $^1\text{H}$  NMR spectrum of crude **160** was observed to be quite complicated, indicative of the formation of a mixture of diastereomers at C5 of the  $\gamma$ -lactam. The crude mixture was subjected to the next step to avoid an unnecessary purification.

The crude mixture of  $\gamma$ -lactams **160** was treated with trifluoroacetic acid (TFA, 10% v/v) overnight. The intention in this step was to carry out three reactions in three stages in one pot: first the acid-promoted cleavage of the Boc protecting group from the alcohol, secondly Brønsted acid generation of an iminium ion at C5 of the lactam (to give iminium **160a**), and finally cyclisation by nucleophilic attack of the oxygen in the alcohol. Pleasingly, this

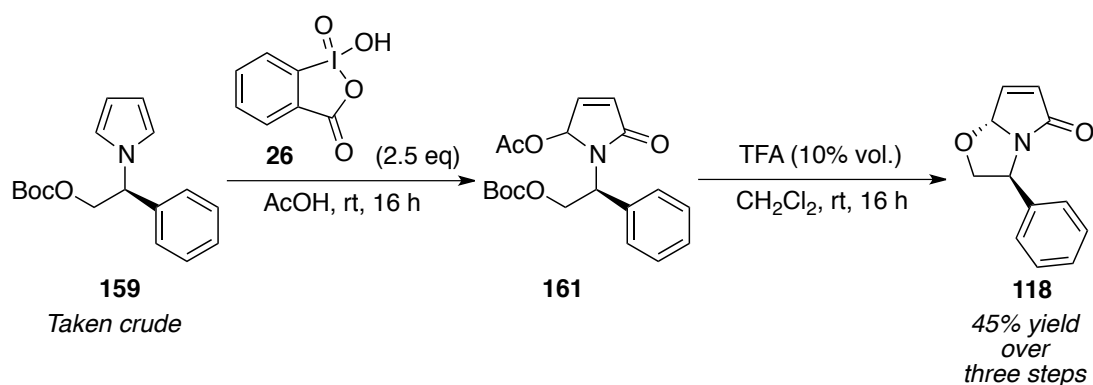
gave a single product, which was identified as the desired bicyclic  $\gamma$ -lactam **118** as a single enantiomer. Key indicators of success in the NMR spectra were the alkene peaks in the  $^1\text{H}$  NMR spectrum at 6.29 ppm and 7.21 ppm, and the now individually resolved diastereotopic proton resonances of the phenylethanol fragment, adjacent the newly formed ether at 4.10 ppm and 4.75 ppm, identified by their mutual couplings and coupling with the adjacent methine proton. The appearance of a single carbonyl in the  $^{13}\text{C}$  NMR spectrum at 176.8 ppm supported the conclusion that the elimination of the iodoaroyloxy sidechain of lactam **160** had occurred.

All characterisation data were in agreement with those reported by Meyers. The  $^1\text{H}$  and  $^{13}\text{C}$  NMR resonances' chemical shifts were within 0.03 and 0.2 ppm of the reported values, respectively. The observed optical rotation of  $+104^\circ$  was also close to the reported value of  $+116^\circ$ , accounting for a large difference in concentration between the two samples. Furthermore, x-ray crystal structures of derivatives of bicycle **118** supported the structural and absolute stereochemical assignment (*vide infra*). The overall yield for these reactions, essentially five reactions in three steps, was 55%, which is comparable to that reported for Meyers and co-workers' approach, but obtained using much milder and less rigorous methods.<sup>102</sup>

As all of the reactions in this sequence were carried out using dichloromethane as the solvent, a one-pot approach was attempted where each reagent was added sequentially after TLC analysis showed completion of the preceding step. This approach initially appeared quite successful, giving yields comparable to the stepwise approach, when carried out on a small scale. However, it was observed that the results were not reproducible on larger scales. Not carrying out the reductive workup procedure after the oxidation step hindered the progress of the TFA ring-closing step such that there was only partial conversion of the lactam **160** after 16 h, with little change even if further TFA was added. In this instance the reaction would need to be worked up and treated with TFA a second time to achieve full conversion. Thus, the best method adopted was to carry out the Boc protection and oxidation in one pot, followed by working up the reaction, then

treating the crude intermediate  $\gamma$ -lactams with TFA to give the key intermediate **118**.

Alternative oxidants were also explored to compare results. IBX was used in place of DMP to give similar results (Scheme 1.42). In this case, the reactions had to be carried out in a stepwise fashion from the outset, as it was necessary to oxidise the pyrrole in acetic acid rather than dichloromethane. An additional difficulty imposed by using this oxidant is that all of the acetic acid used as solvent was neutralised with a base on workup, which also removed the 2-iodobenzoic acid by-product. For large-scale reactions, this can be a slow and arduous exercise. However, the IBX procedure does give comparable yields of bicyclic  $\gamma$ -lactam **118** to the DMP process, albeit over a significantly longer reaction time.



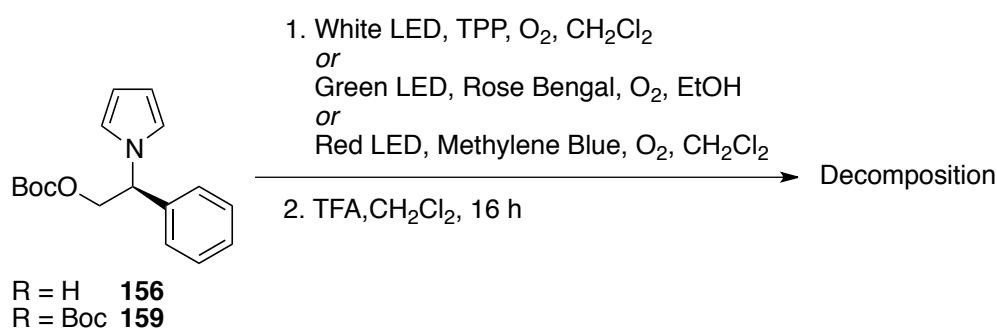
**Scheme 1.42:** IBX as an alternative oxidant

It was hoped that photooxidation could also be used to reach bicyclic lactam **118** in a more economical manner. Pyrrole **156** was subjected to photooxidation conditions previously developed, using a photoreactor with red LEDs and methylene blue as the sensitiser (Scheme 1.43).<sup>80</sup> As with the hypervalent iodine route, the crude residue was treated with TFA immediately. Unfortunately, this gave complete decomposition of the starting material. The Boc-protected pyrrole **159** was subjected to the same photooxidation conditions. In this case, the desired bicyclic lactam **118** was isolated, but only in trace quantities compared with the near total decomposition of the starting material.

Pyrrole **159** was also subjected to two other sets of photooxidation conditions, to determine whether the results could be improved. (Scheme

1.43) Our established conditions for using green LEDs with Rose bengal as the sensitiser, which worked well for a variety of pyrroles previously,<sup>80</sup> also gave no sign of the desired lactam following treatment with TFA, and the <sup>1</sup>H NMR of the crude reaction mixture of the oxidation prior to TFA treatment showed essentially complete decomposition by that stage. A white LED photoreactor was also used, with tetraphenylporphyrin (TPP) as the sensitiser, which was closest to the white light used in Demir's work in this area.<sup>75</sup> Unfortunately, this also led only to decomposition.

It was clear from these reactions that these particular pyrroles were not amenable to photooxidation. It is possible that the benzylic methine hydrogen may be involved in causing the decomposition, although these photooxidation conditions were appropriate for *N*-benzylpyrrole itself. Therefore it was concluded that preparation of the desired bicyclic lactam was best pursued by hypervalent iodine reagent oxidation.



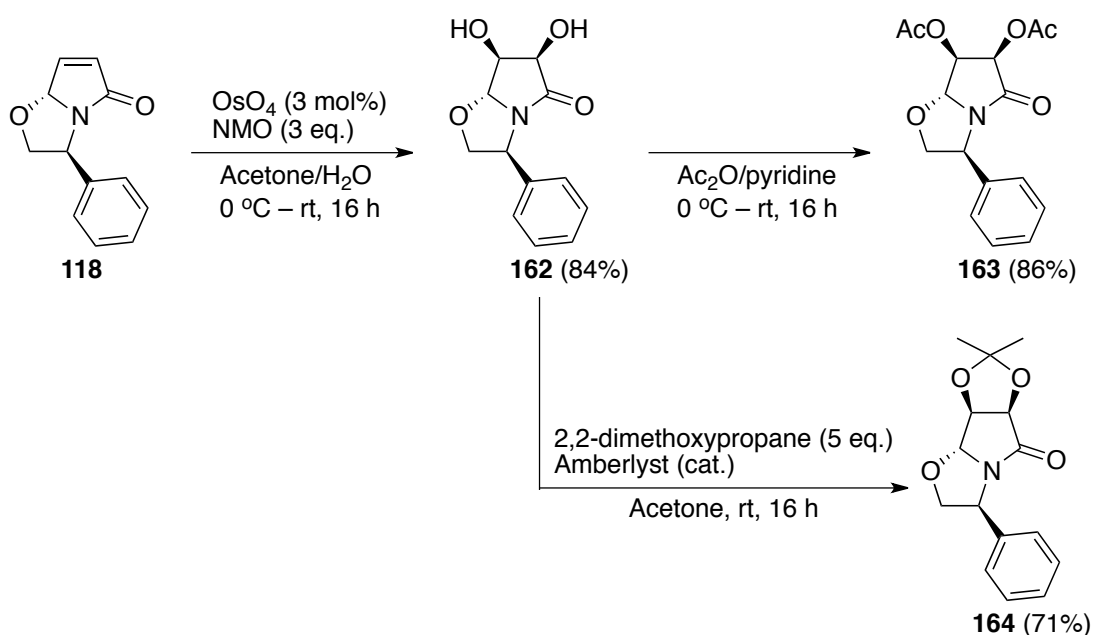
**Scheme 1.43:** Attempted photooxidation conditions

### 1.6.2 Reactivity of the Chiral Bicyclic Lactam **118**

With the chiral bicyclic lactam **118** in hand, the first transformation carried out towards the synthesis of chiral (–)-codonopsine analogues was a dihydroxylation under Upjohn conditions, which gave an 84% yield of the desired diol **162** (Scheme 1.44). Unlike in the racemic syntheses, this diol was isolable and amenable to purification. The diol did prove to be highly polar, however, and insoluble in common organic solvents other than DMSO at higher concentrations. The formation of the diol was supported by the appearance of two doublet peaks in the <sup>1</sup>H NMR spectrum in DMSO-d<sub>6</sub> at 5.51 and 5.95 ppm representative of the hydroxyl protons coupling to the adjacent methines. Furthermore, these proton resonances did not display

HSQC correlations to carbon atoms. The fact that only a single product was isolated from this reaction indicated that the chiral C5 substituent was indeed controlling the facial selectivity of the dihydroxylation reaction, and thus most likely forming a diol with a *trans* relationship to that substituent.

Diol **162** was then protected as a diacetate, under the same conditions as described for the racemic intermediates, which gave **163** in a yield of 86%. A significant reduction in polarity was observed, and the appearance of two  $^1\text{H}$  and  $^{13}\text{C}$  NMR resonances consistent with the introduction of two acetate esters supported the formation of the desired product.



**Scheme 1.44:** Dihydroxylation and protection of bicyclic **108**

Diacetoxylactam **163** was particularly important for establishing that the stereochemistry of the ether at C5 would bias transformations at other positions on the ring to give single stereoisomers. Initially the exact relative stereochemistry was uncertain, as the coupling constant observed between the lactam ring protons at C4 and C5 was 2.9 Hz (Figure 1.6). While this is considerably less than the coupling between the C3 and C4 protons of 6.8 Hz, in a system where the C4 and C5 protons had a fixed dihedral angle of about  $90^\circ$ , the coupling constant should be close to 0 Hz, if the coupling followed what would be expected from the basic Karplus relationship.<sup>86</sup> Indeed, in the racemic work discussed in section 1.3.1 this was observed to be the case.

The observed couplings for strained five-membered rings such as **163** could be expected to vary greatly from the idealised unstrained open chain case of the original Karplus relationship, and the many substituents on the ring would likewise play some role in affecting the couplings observed.

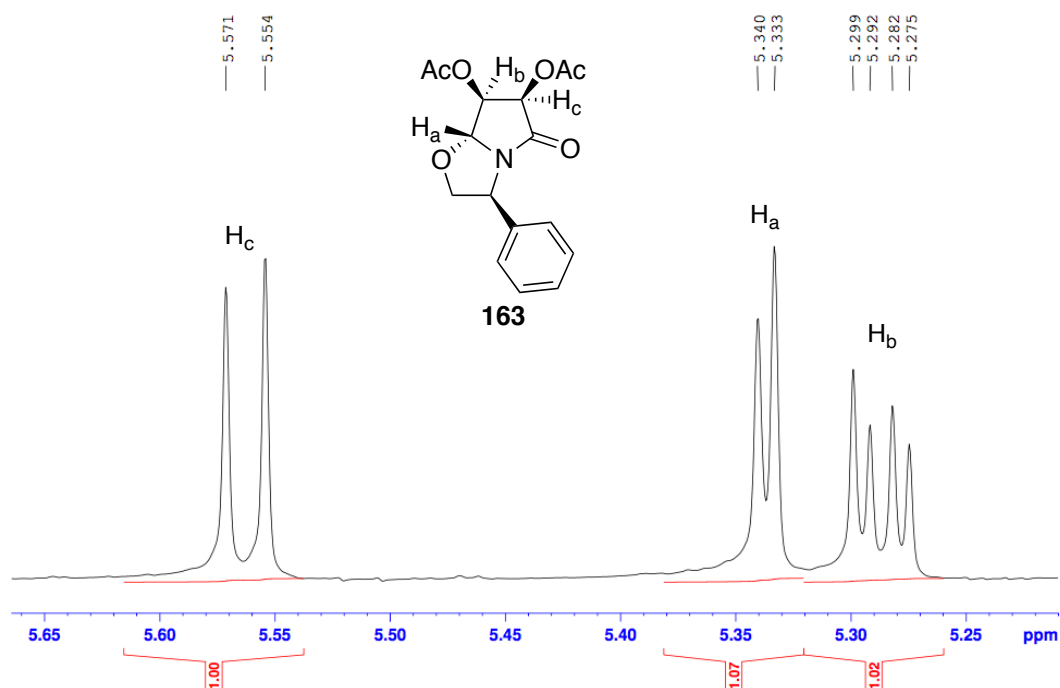


**Figure 1.6:** Observed coupling constants for bicyclic compound **163**

Fortunately it was possible to crystallise this species and acquire an X-ray crystal structure (Figure 1.7). The crystal structure of lactam **163** showed that the hydrogen at H5 was *trans* to that at C4, therefore supporting the conclusion that the face of addition was controlled by the C5 substituent. This analysis also allowed us to measure the dihedral angles between the C3, C4 and C5 hydrogen atoms. These were  $23.6^\circ$  for the dihedral angle between the C3 and C4 protons, and  $95.8^\circ$  between the C4 and C5 protons, the latter value being very close to what was initially expected, which demonstrated that in this system such dihedral angles do not have the same magnitude effect on the coupling constants as might be expected in a less rigid and small ring system.

Diol **162** was also protected as the acetal **164**, which was produced in a 71% yield after stirring with 2,2-dimethoxypropane and catalytic amberlyst acidic resin (Scheme 1.44). The identity of the product was supported by the

appearance of two singlet peaks integrating for 3 protons at 1.42 and 1.56 ppm in the  $^1\text{H}$  NMR spectrum indicative of the incorporation of acetone as an acetal.

With the stereochemistry assigned, diacetoxo **163** was treated with a Lewis acid and an arene to effect a Friedel–Crafts alkylation reaction (Scheme 1.45). However, under the previously developed conditions with  $\text{BF}_3\cdot\text{OEt}_2$  and 1,2-dimethoxybenzene no reaction was observed after 16 h. This somewhat surprising result has been attributed to the high stability of the ether at C5, leading to a lack of *N*-acyliminium ion formation.

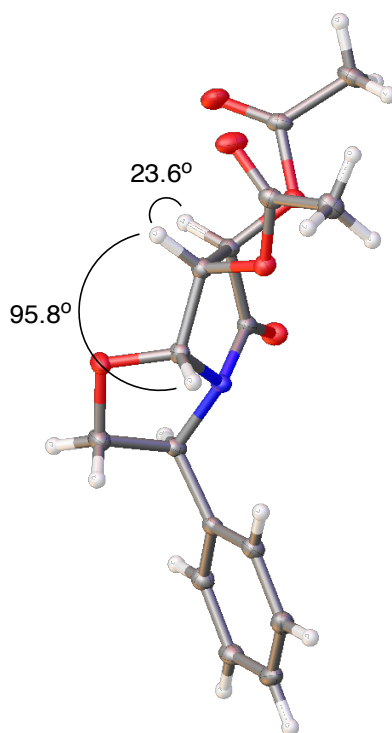
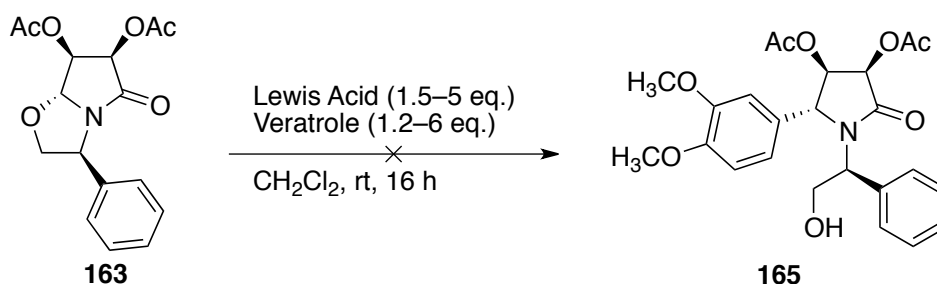


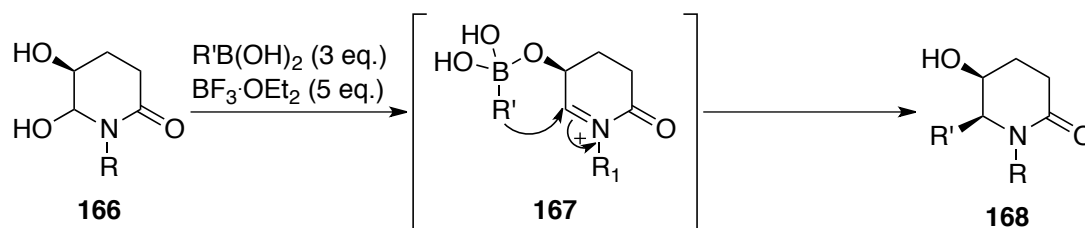
**Figure 1.7:** X-ray crystal structure of bicycle **163**

Trialling different Lewis acids such as  $\text{TiCl}_4$  did not improve the outcome, even when added in great excess (Scheme 1.45). TMSOTf was also used, under the same conditions as the  $\text{BF}_3\cdot\text{OEt}_2$ , in the hopes that the alcohol would be trapped *in situ* as the trimethylsilyl ether, but this also failed to promote any reaction.



**Scheme 1.45:** Conditions for attempted Friedel–Crafts alkylation of lactam **135**

Other attempted approaches included a Petasis borono-Mannich reaction *via* cyclic *N*-acyliminium ions, based on work by Batey and Pyne using vinyl or arylboronic acids or boronate esters with *N*-acyliminium ions generated by Lewis acids from cyclic amides with a 1,2-diol **166** (Scheme 1.46).<sup>136–138</sup> In the case where the diol was not derivatised, these are theorised to proceed through the formation of a boron ester, such as **167**, with the C3 alcohol adjacent to the iminium site, followed by intramolecular attack of the boron R-group. This generally directs the stereoselectivity of the reaction to give a *cis* relationship between the alcohol and the R-group introduced, as for  $\delta$ -lactam **168**. However, Pyne and colleagues observed that in the instance where the C3 alcohol is protected as a benzyl ether the reactions still proceed but give a majority *trans* product. They also noted that the reactions were usually only successful for very electron-rich boronic acids (such as methoxyphenyl derivatives), and that five-membered cyclic amides were usually less successful than their six-membered analogues.

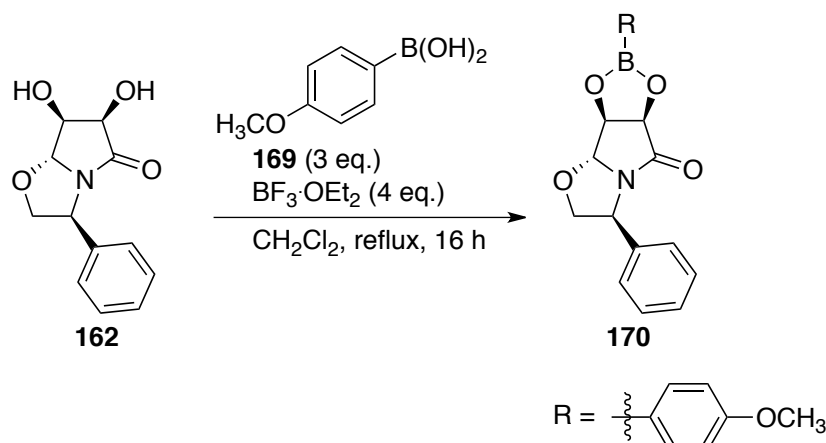


**Scheme 1.46:** Mechanism for Pyne and colleagues's Borono-Mannich reactions

Unfortunately, when the acetoxy bicycle **163** was treated with *para*-methoxyphenylboronic acid (**169**) and  $\text{BF}_3 \cdot \text{OEt}_2$  under Batey and Pyne's conditions, stirring in dichloromethane at room temperature, no reaction was observed. As Pyne hypothesised that the reaction can proceed through a

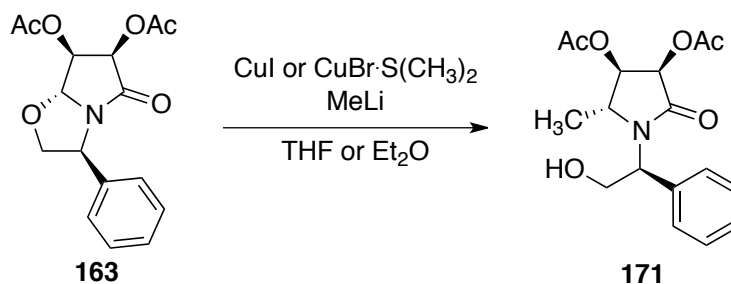


boronate ester intermediate such as **167**, the reaction was repeated using diol **162**, where such an intermediate could form (Scheme 1.47). In this case, the substrate was converted into a new product, which initially looked promising by  $^1\text{H}$  NMR analysis through the addition of resonances consistent with a 1,4-disubstituted aryl group and a methoxy peak at around 3.8 ppm. However, closer analysis by HSQC and HMBC experiments indicated that this aryl moiety was not incorporated into the main lactam portion of the molecule, and TLC analysis indicated that the compound was far less polar than would be expected for the desired triol product. Pyne and colleagues observed that in some cases with cyclic amides with 2,3-diols a boronate diester was the main product. Therefore, it was proposed that a similar process had occurred here, with the boron reacting with the diol exclusively, giving boronate diester **170**.



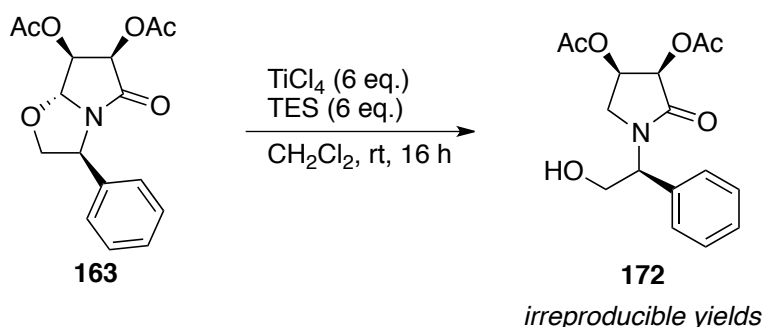
**Scheme 1.47:** Deduced result of attempted Petasis borono-Mannich reaction

A variety of cuprate reaction conditions were also trialled to attempt to introduce a methyl group in the 5-position of bicyclic lactam **163**, on the assumption that the aryl moiety could be introduced at a later stage through the amide functional group. Unfortunately at a range of temperatures, using  $\text{CuI}$  and  $\text{CuBrMe}_2\text{S}$  as copper sources, in THF or  $\text{Et}_2\text{O}$  as solvent, and even including  $\text{TMSCl}$  as an additive to trap the pendant alcohol, either no reaction or decomposition of the starting materials was observed (Scheme 1.48).



**Scheme 1.48:** Attempted cuprate conditions of diacetoxylactam **163**

To probe whether any reactivity at the C5 position was possible, diacetoxylactam **163** was treated with a large excess of  $\text{TiCl}_4$  as the Lewis acid and triethylsilane as the nucleophile. It was hoped that a less hindered hydride nucleophile would have readier access to the iminium ion than a bulkier aryl. If this were successful, it might still be possible to reach codonopsine analogues through Grignard-type chemistry on the amide to introduce the aryl group at C2. However, even under the most forcing conditions, and long reaction times, results were unsatisfactory. While in a first test some of the desired ring-opened species was obtained (**172**, Scheme 1.42), these yields were inconsistent, and irreproducible, with reactions returning mostly starting material and decomposition products. This result is not without precedent, as Meyers' and colleagues found in their synthesis of (–)-rolipram that reactions of bicyclic lactams with C3 or C4 oxygen substituents proceeded poorly under similar conditions, and concluded that they were not compatible with this methodology.<sup>103</sup>



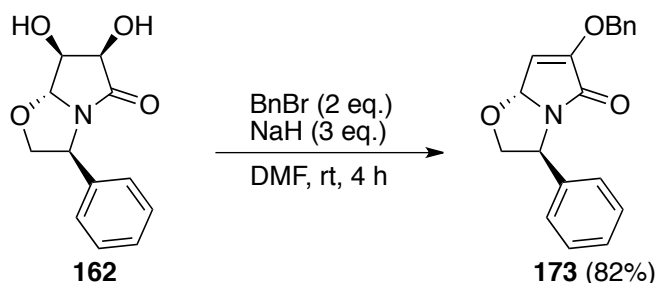
**Scheme 1.49:** Conditions for ring-opening diacetoxylactam **163**

Attempts were made to remove the *N*-substituent of **172**, using what material was available from the inconsistent reactions carried out. Standard hydrogenation conditions using a  $\text{Pd(OH)}_2$  catalyst in EtOH gave no reaction.

An oxidative debenzylation approach developed by Moriyama and Togo, which utilised KBr with Oxone<sup>®</sup>, was also unsuccessful.<sup>139</sup>

These studies led us to conclude that the bicyclic lactam **118**, while a robust platform for stereoselective functionalization of C3 and C4, is too stable to form the *N*-acyliminium intermediate required to reach (–)-codonopsine analogues with absolute stereochemical control. It was decided that the use of a chiral auxiliary that did not form a stable bicyclic system might ultimately prove a better solution.

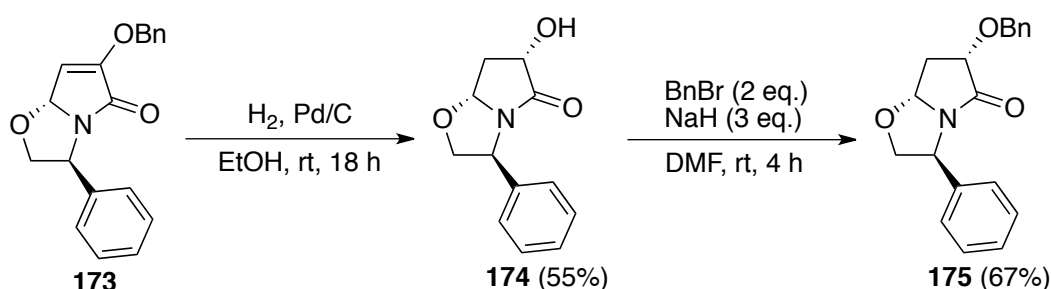
Some further transformations carried out using the bicyclic diol **162** were of interest. As an alternative to the acetoxy or acetal protecting groups, protection of the diol as a benzyl ether was also attempted (Scheme 1.50). The protection was carried out under standard conditions, using NaH and benzyl bromide. However, rather than giving the expected dibenzylated product, alkene **173** was isolated in a high yield. At first it was unclear what had happened in the reaction, as the <sup>1</sup>H and <sup>13</sup>C NMR spectra only indicated one benzyl group being present, with no evidence of another unprotected alcohol as might be expected. Furthermore, the <sup>1</sup>H NMR spectrum indicated that there were only two protons on the pyrrolidine portion of the molecule, through the appearance of doublets at 5.56 ppm and 5.88 ppm. Through HRMS and IR analysis it was postulated that elimination of the alcohol β to the carbonyl had occurred. This structure was supported by acquisition of an X-ray crystal structure, which also provided unambiguous support for the stereochemical configuration of the bicycle (Figure 1.8).



**Scheme 1.50:** Benzyl protection and elimination of diol **162**

Further to this, benzyl ether **173** was hydrogenated to give alcohol **174** (Scheme 1.51). This transformation was expected to be facially selective to yield an alcohol with the opposite stereochemical orientation at C3 to that

seen in diol **162**, resulting in a *syn* relationship between the H3 and H5 protons. This proved successful, with the expected alcohol **174** isolated in a 55% yield. The loss of the benzyl group was supported by disappearance of the benzyl CH<sub>2</sub> signal at 5.03 ppm and a multiplet integrating for 5 protons in the aromatic region of 7.26–7.45 ppm of the <sup>1</sup>H NMR spectrum, and the appearance of a broad OH stretch at 3335 cm<sup>-1</sup> in the IR spectrum. The hydrogenation of the alkene was supported by the appearance of the two diastereotopic protons of H4 in the <sup>1</sup>H NMR spectrum as a doublet of doublet of doublets at 2.05 ppm and a multiplet at 2.96–3.05 ppm.



**Scheme 1.51:** Further transformations of the benzyl derivative **173**

Alcohol **174** was protected once again as the benzyl derivative, giving benzyl ether **175** in a yield of 67%. It was possible to crystallise benzyl ether **175** and acquire an X-ray crystal structure of it (Figure 1.8), which supported our proposed inversion of the C3 stereochemistry through the elimination-hydrogenation reactions. Therefore we have demonstrated that a hydroxyl group has been introduced at C3 in both possible orientations.

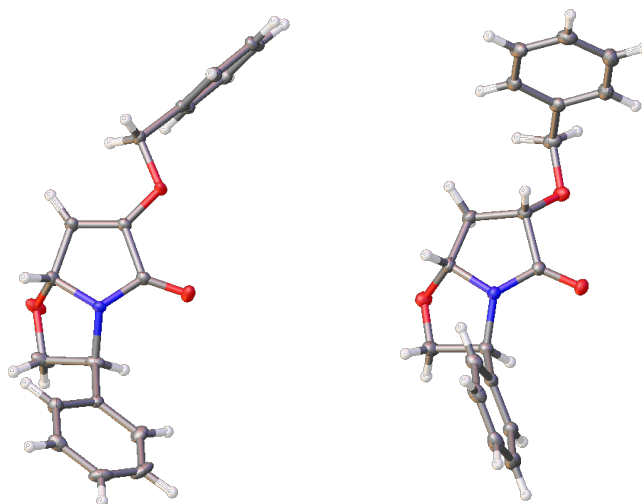
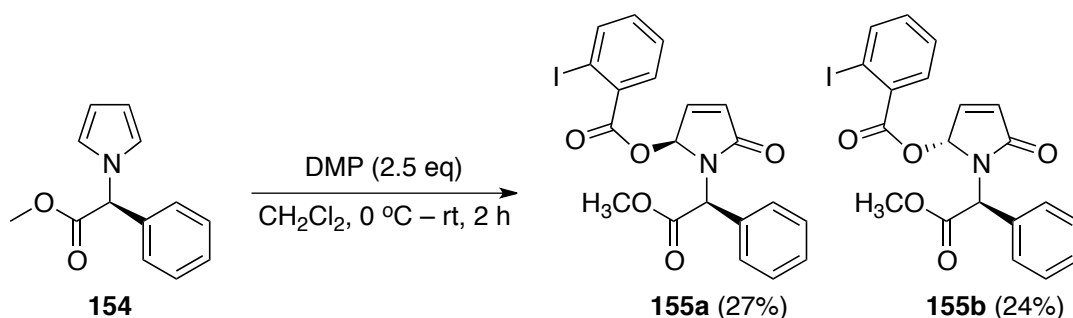


**Figure 1.8:** X-ray crystal structures of benzyl-protected biocycles **173** and **175**

## 1.7 Chiral Auxiliary Approach

The chosen pyrrole substrate for testing this approach was then prepared from *S*-(+)-2-phenylglycine methyl ester hydrochloride, **154**. Oxidation of this pyrrole under the standard Dess–Martin periodinane conditions did not, however, yield a single diastereomeric product. Instead two distinct products were obtained in a 1:1 ratio, which were believed to be the two possible diastereomeric products of the oxidation reaction, epimeric at the 5-position, lactams **155a** and **155b** (Scheme 1.52). The two diastereomers were separable by flash column chromatography, and their independent identities were supported by full  $^1\text{H}$  and  $^{13}\text{C}$  NMR analysis; through their having identical molecular masses as supported by HRMS analysis, and through the acquisition of an X-ray crystal structure of both compounds to determine the relative stereochemistry (Figure 1.9).



**Scheme 1.52:** Synthesis of chromatographically separable chiral lactams

This was not the ideal result, as there was no bias in facial selectivity in the pyrrole oxidation as a result of having the chiral moiety included in the pyrrole. However, it was a success in that the two diastereomers could be isolated. As such, it was believed that these individual diastereomers could be taken and subjected to the same transformations as in the racemic work, to give both enantiomeric series of codonopsine-like compounds starting from a single enantiomer of pyrrole **154**.

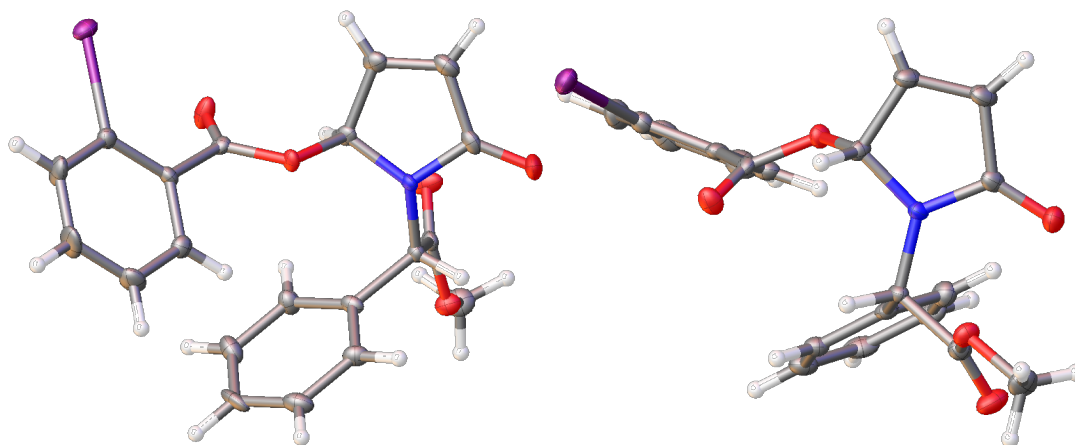
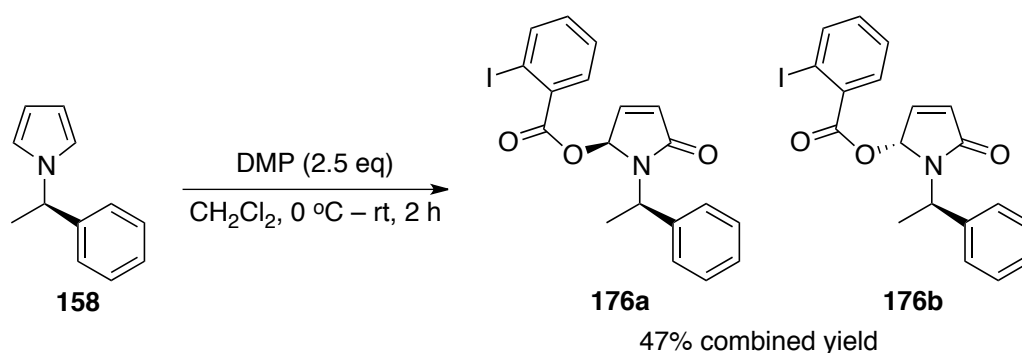


**Figure 1.9:** X-ray structures of the diastereomers **155a** (left) and **155b** (right)

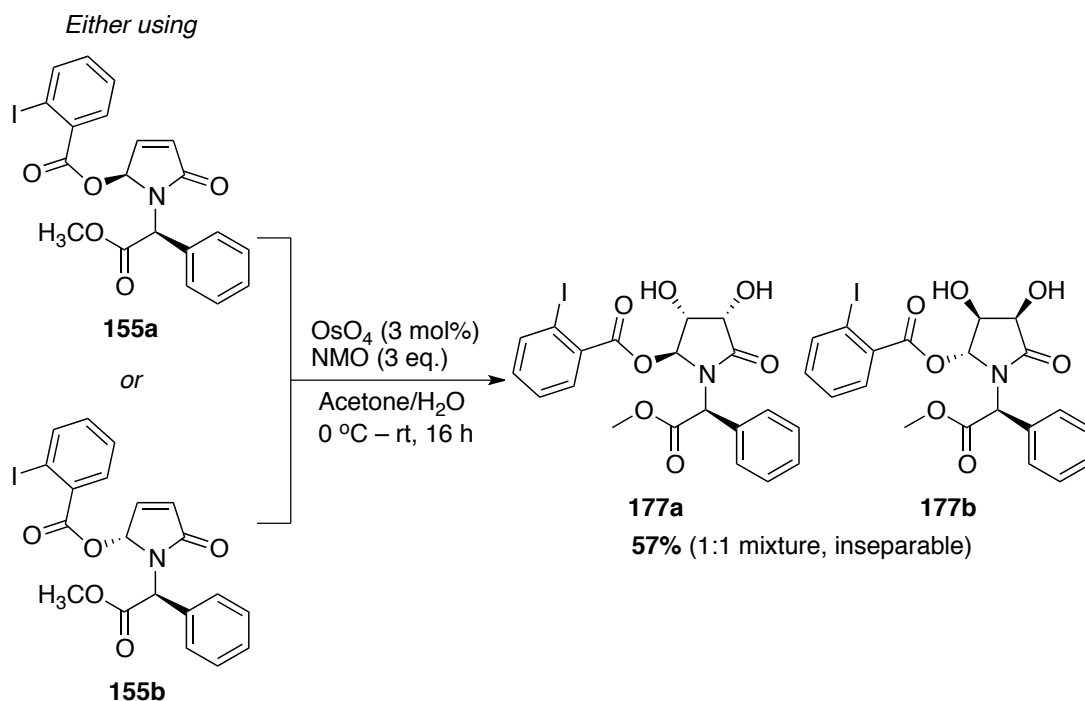
Given that this oxidation did not give facial selectivity, but did give separable products, it was decided to take a less sterically hindered pyrrole and oxidise that to see whether any pyrrole with a chiral *N*-substituent would give separable diastereomers. To this end pyrrole **158** was oxidised under the same conditions as **154** (Scheme 1.53). This again gave what appeared to be two possible diastereomers. However, in this case the products were not separable by chromatography, and only a mixture of the two could be isolated, in a 47% combined yield. This indicated that the auxiliary from phenylglycine methyl ester was indeed necessary to give separable oxidation products.



**Scheme 1.53:** Oxidation of the pyrrole **158**

The individual diastereomers **155a** and **155b** were each taken and separately subjected to dihydroxylation under Upjohn conditions (Scheme 1.54). Unusually, both of these reactions led to a mixture of products rather than each giving a single diastereomeric dihydroxylated product – i.e. **177a** for **155a** and **177b** for **155b**, respectively. In fact, both led to what appeared

to be a 1:1 mixture of **177a** and **177b**, based on NMR analysis. This indicates under these scrambling of the C5 substituent occurred, such that it was unable to direct the outcome of the dihydroxylation to give a single diastereomer as the product. Also unfortunately, the mixture of products obtained were not chromatographically separable like their predecessors **155a** and **155b**.



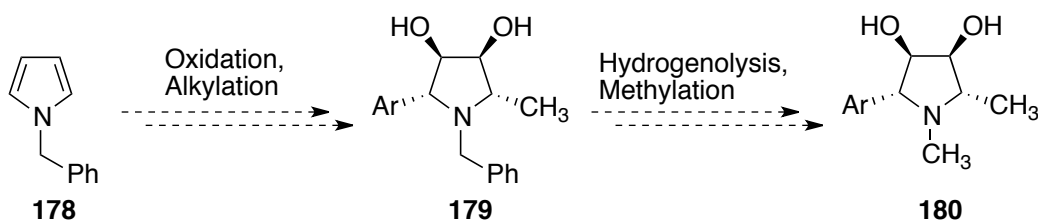
**Scheme 1.53:** Scrambling through dihydroxylation

This result seemed to eliminate the possibility of using this particular auxiliary inspired approach to obtain chiral codonopsine analogues. While attempts could have been made to carry out the transformations in a different order to remove the risk of epimerisation, experience with the racemic species indicated that the aryl intermediates with alkenes still in place at C3-C4 are too unstable to be subjected to dihydroxylation. And in any case, as the chiral *N*-substituent cannot control the stereochemistry at C5, carrying out further transformations here without functionalising the alkene first would lead to further mixtures of possibly inseparable diastereomers.

## 1.8 Conclusions

In conclusion, the scope of previous racemic work was successfully expanded to produce a range of (–)-codonopsine and (–)-codonopsinine

analogues. Unfortunately, it was not possible to develop a route to 2-methyl substituted analogues closer to the natural products. An alternative route to be explored in future work would involve the use of a different pyrrole starting material, such as *N*-benzylpyrrole **178** (Scheme 1.54). In Huang and colleagues' work with amide alkylation and reduction they only used *N*-benzylpyrrolidinones, so a lactam with this *N*-protecting group could be more amenable to that transformation.<sup>93</sup>



**Scheme 1.54:** Proposed alternative racemic pyrrole route

An advantage of the *N*-benzyl substituent is that it can be simply cleaved by hydrogenation and the free amine methylated. Also, it would be fruitful to consider methods for introducing a *trans* diol at the C3-C4 alkene of the  $\gamma$ -lactams rather than a *cis* diol, to give analogues that more closely mimic the stereochemistry of the natural product. Biological testing of this full suite of analogues would be valuable for establishing their activity in assays compared with (–)-codonopsine and (–)-codonopsinine.

A new synthesis was developed for a key chiral bicyclic lactam **118**. This incorporated pyrrole synthesis and oxidation chemistry previously developed in the Smith group, and proved to be a milder and more efficient approach than many of those previously reported, with good overall yields and excellent stereochemical control. The reactivity of bicyclic lactam **118** was investigated with a view to carrying out asymmetric total syntheses of (–)-codonopsine and (–)-codonopsinine, although it proved too stable to transformations at the ether C5 position for this to be viable. However, it remains a valuable intermediate, and was used successfully in the synthesis of fluorinated natural product analogues (See Chapter 2)

A chiral auxiliary approach was also explored for the asymmetric synthesis of (–)-codonopsine and (–)-codonopsinine analogues, utilising bulky chiral *N*-substituents. This led to separable mixtures of diastereomeric  $\gamma$ -lactams.



These ultimately were also not suitable to this application due to scrambling of the stereochemical configuration of the C5 ester in subsequent steps. Further studies could involve investigating transformations to these intermediates that do not involve ablation of stereochemistry by iminium formation.

## Chapter 2: Synthesis of Fluorinated GABA Analogues through Pyrrole Oxidation

### 2.1 Introduction to Fluorine in Natural Products and Drugs

Organic natural products containing fluorine are rare. In fact, only five have been reliably reported (Figure 2.1).<sup>140</sup> There have been few other reports<sup>141</sup> and in some cases the compounds have been either of suspect natural origin,<sup>142,143</sup> or have been disproven through synthetic studies and proper interpretation of spectroscopic data.<sup>144,145</sup>

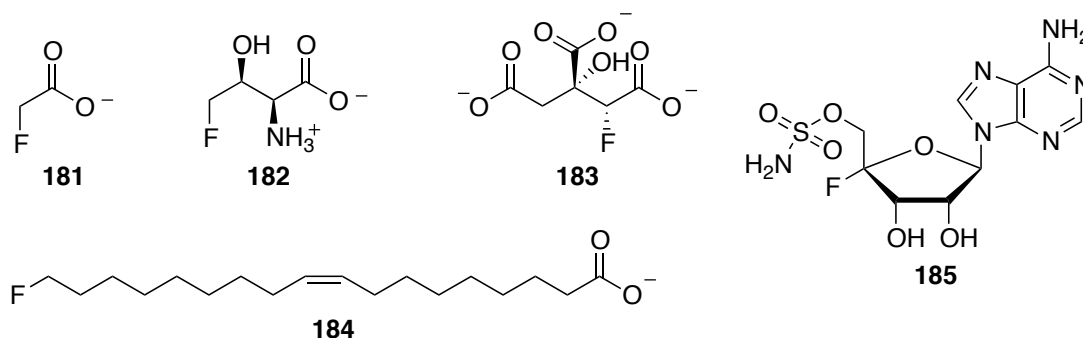


**Figure 2.1** Reported fluorine-containing natural products

Despite this relative lack of fluorinated natural products, fluorinated analogues of known natural compounds have become popular and effective drug molecule targets.<sup>146-148</sup> In 2007 fluorine-containing molecules made up an estimated 20% of all pharmaceuticals,<sup>149</sup> and by 1990 up to 30% of all agrochemicals.<sup>150</sup> Fluorine containing drugs are also among some of the best known and most widely used, including the antidepressant Prozac (fluoxetine, **186**),<sup>151,152</sup> the cholesterol-controlling drug Lipitor (atorvastatin, **187**),<sup>153</sup> and many prospective anti-cancer agents.<sup>149</sup>

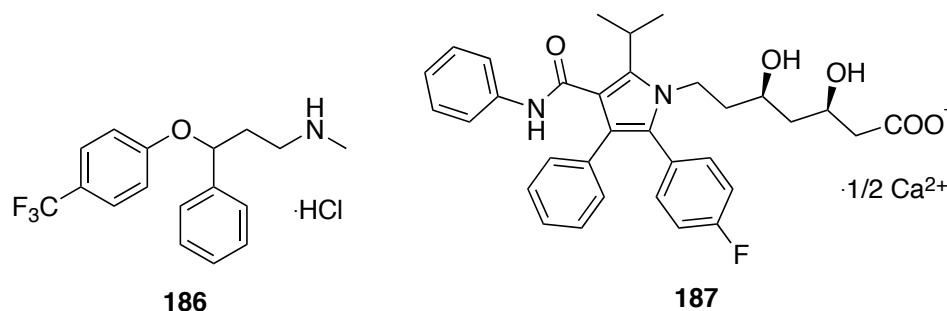


**Figure 2.2** Common fluorine-containing drugs Prozac (**186**) and Lipitor (**187**)

Introduction of fluorine into potential drug molecules can have significant effects on their activity, which is generally tied to their ability to bind to certain receptors effectively. Fluorine can enable this kind of increased activity through a number of effects it has on molecules it is added to.

## 2.2 The C–F bond and How It Affects Organic Molecules' Conformations and Activity

Fluorine has a number of characteristics that affect how it bonds with carbon atoms in organic molecules, and what effect these bonds can have on the molecule's activity, reactivity and conformation.<sup>154</sup> Firstly, fluorine is a highly electronegative element, the most electronegative by the Pauling scale.<sup>155</sup> It has a high nuclear charge, with 9 protons in its nucleus, and a relatively small number of electrons without occupancy in higher orbitals (only up to the  $2p$  orbital). As a result the electrons are all tightly held closer to the positive nucleus, which gives fluorine a relatively small atomic radius of 1.47 Å (in between hydrogen with 1.2 Å and oxygen with 1.52 Å).<sup>156</sup>

This high electronegativity has an impact on the nature of C–F bonds. The tendency of fluorine to attract electron density means that C–F bonds have a highly polar character, with a significant  $\delta^-$  at the fluorine. The effect of this is to give the bonds an almost, or at least partially, ionic character, such as an electrostatic attraction between  $\delta^+$  and  $\delta^-$  rather than a simple covalent sharing of electrons.<sup>154</sup> This ionic character increases with the addition of more fluorine atoms to a single carbon centre. This makes the bond both shorter (1.35 Å, in between the C–H length of 1.09 Å and the C–O length of 1.43 Å) and very strong.<sup>156</sup> As such, it is also of itself quite unreactive.

The atomic radius, bond length and stability of the C–F bond have made it something of a go-to hydrogen substitute for drug molecules in medicinal chemistry. However, the highly polar character of the bond compared with C–H bonds makes it more like the C–O bonds of alcohols, and the electronegativity and other characteristics of fluorine can have a range of other effects on organic molecules to affect activity and the binding of a potential drug molecule to a receptor. The study of relationships between different functional groups' size, conformation and packing, and

interchangeability within drug molecules, is called bioisosterism.<sup>157,158</sup> It has been studied in great depth for fluorine containing functional groups, such as finding alkyl moieties that are best substituted by trifluoromethane groups,<sup>159,160</sup> fluorine substituting for hydroxyl or methyl groups,<sup>161,162</sup> fluorovinyl groups being used as analogues for peptide bonds,<sup>163-165</sup> and difluorotoluene being used as an analogue for the DNA base thymine,<sup>166</sup> among others.<sup>167-169</sup>

The electron-withdrawing character of fluorine can have a significant effect on the bioactivity and bioavailability of fluorine-containing drug molecules. Exchanging hydrogen with fluorine has generally been observed to produce more lipophilic molecules.<sup>170,171</sup> This occurs through increasing the acidity of neighbouring functional groups and thus lowering the pKa of the molecule as a whole.<sup>172</sup> This increases the logD value and hence the lipophilicity, that can lead to a more favourable partition of the drug between the polar aqueous media of the cell and the less polar receptor site.<sup>170,173,174</sup> This is not a hard and fast rule of course,<sup>175</sup> but some predictive rules have been developed to calculate the theoretical pKa of drug molecules based on the introduction of fluorine near to heteroatom functionalities.<sup>172</sup> This effect has been well-studied for fluorine being introduced near amines, where increasing the number of fluorine atoms has been shown to decrease the basicity.<sup>172,176</sup> Indeed, enough adjacent fluorine atoms can leave an amine deprotonated as physiological pH.<sup>173</sup> The effect has likewise been seen in increasing the acidity of nearby carboxylic acids, alcohols and phenols.

The presence of a C–F bond gives rise to intermolecular and intramolecular interactions that can play a major role in determining the conformation of a molecule. This is of particular importance in drug design, where molecular conformation can bias a molecule towards binding or not binding to a desired receptor.

One conformational effect of inclusion of fluorine is widening of the H–C–H bond angles of sp<sup>3</sup> carbon atoms it is attached to, an effect that increases with two fluorine atoms present.<sup>154</sup> This is possibly due to its withdrawal of electron density through the C–F bond into the fluorine's p<sup>2</sup> orbital, which

gives the carbon atom more of an  $sp^2$  character and widens the H–C–H bond angle. The change in angle is not especially large, being only on the order of  $0.8^\circ$  in  $CH_3F$ , but this can lead to significant conformational disorder in long-chain molecules such as fluorinated fatty acids.

The substantial ionic character of the C–F bond gives rise to a large dipole moment, which would be expected to promote electrostatic (dipole-dipole and charge-dipole) intermolecular and intramolecular interactions. Indeed, hydrogen bonding is observed with alcohols, although fluorine's low proton affinity makes these interactions weaker and less favourable than traditional hydrogen bonds.<sup>171,177</sup>

There are also many cases where dipole-dipole interactions between C–F bonds and the C=O bonds of peptide amides have been observed.<sup>146,161</sup> These interactions occur in an orthognonal arrangement, with the F of the C–F bond directed towards the C of the amide carbonyl (Figure 2.3). While these interactions are much weaker than hydrogen bonds,<sup>178</sup> Müller and colleague's extensive analysis of various fluorinated inhibitors (mainly Thrombin inhibitors, with fluorophenyl substituents), show that incorporation of fluorine to give these interactions can have significant effects on the conformation of the drug molecule (twisting or changing shape to fit to peptide amides) and lead to great increases in potency.<sup>171,179</sup> This effect is also observed for aliphatic C–F containing molecules and trifluormethyl groups.<sup>180</sup>

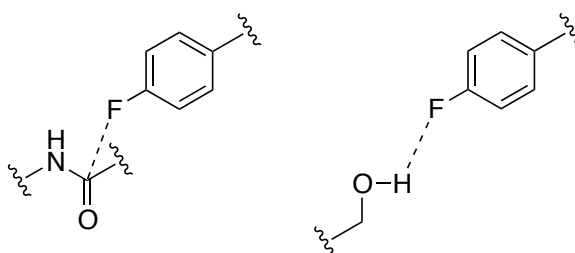
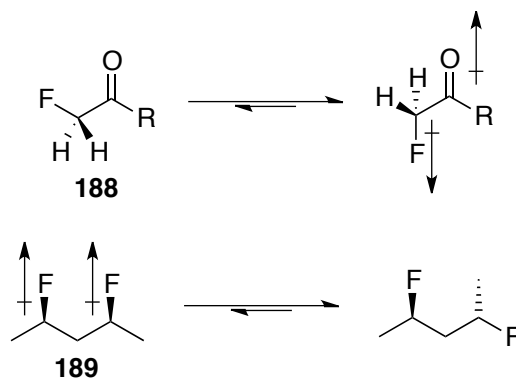


**Figure 2.3:** C–F intermolecular dipole-dipole interaction

These dipolar interactions can also occur intramolecularly, with significant conformational outcomes. A well-documented example of this is where a fluorine atom is introduced  $\alpha$  to a carbonyl group. In this case the two dipoles repel each other and the molecule will twist such that they are antiparallel to

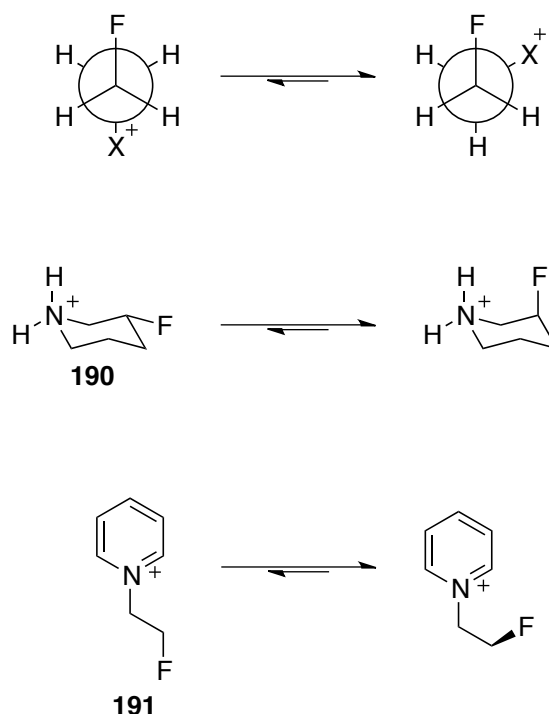
one another (Scheme 2.1). The effect decreases with a decreasing dipole moment of the carbonyl, with amides showing the most pronounced twisting, and aldehydes the least.<sup>181-184</sup> 1,3-Difluoroalkanes exhibit similar behaviour, with the dipoles of the C–F bonds forcing the fluorine atoms to avoid parallel alignment.<sup>185,186</sup>



**Scheme 2.1:** Intramolecular dipole-dipole effects of fluorine substitution

Substitution of fluorine onto aromatic rings greatly increases the positive polarisation of *ortho* hydrogen atoms, strengthening their interactions with N and O atoms and C–H--- $\pi$  interactions. This also affects the electronics of the aromatic ring, which can be seen in the case of hexafluorobenzene which, compared to benzene, has a large positive rather than negative quadrupole.<sup>187</sup> These changes in electronics can affect the interactions of rings such that they  $\pi$ -stack in a face to face fashion, edge to face, or even eliminate interactions that occur in fluorine-free cases, depending on the number and pattern of fluorine atoms introduced.<sup>188,189</sup>

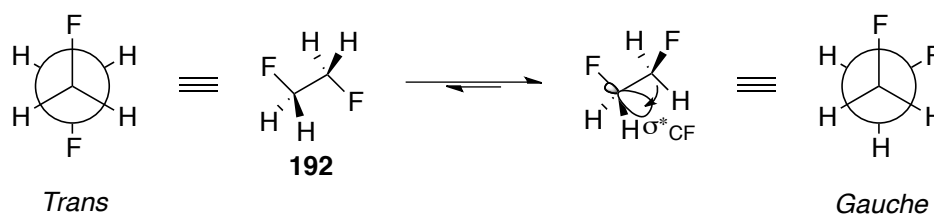
Charge-dipole interactions, where the dipole of the C–F bond interacts favourably with a formally charged heteroatom, are stronger than dipole-dipole interactions. As intramolecular interactions they can have significant impacts on conformation. In cases where the fluorine and charged atom are vicinal, a *gauche* conformation will be adopted in preference (Scheme 2.2).<sup>190-192</sup> The effect is seen in a variety of species, such as increasing the puckering of azetidinium rings,<sup>192</sup> influencing the orientation of substituents of six-membered heterocycles (such as **190**),<sup>190</sup> and even the orientation of fluorine atoms pendant to charged heterocycles (such as **191**).<sup>192</sup>



**Scheme 2.2:** Effects of charge-dipole interactions on molecular conformation

The other case where *gauche* conformers are preferred is in 1,2-difluoro compounds. While it might be expected, as is the case for 1,3-difluorinated species, that the two electronegative fluorine atoms would repel each other, another important feature of the C–F bond, called hyperconjugation, makes the opposite true.

Difluoroethane (**192**, Scheme 2.3) provides a simple and well-studied example of this effect. The C–F bonds in this molecule feature a relatively low energy  $\sigma_{\text{C-F}}^*$  antibonding orbital, that is directed parallel to the bond and away from the fluorine. In the *gauche* conformation, the antibonding orbital of each C–F bond is aligned to have good overlap with and receive electron density from a vicinal C–H bond. This would normally be expected to weaken a bond and destabilise a molecule, but for a C–F bond the lengthening of the bond and reduction in its covalent character actually enhances its ionic character and strengthens the bond between the increasingly  $\delta^-$  fluorine and  $\delta^+$  carbon.<sup>154</sup> In the alternative *trans*-conformer, while dipole-dipole interactions are minimised, neither of the  $\sigma_{\text{C-F}}^*$  antibonding orbitals are aligned to receive electron density from a C–H bond. This makes this conformer only metastable, and not the equilibrium conformation.



**Scheme 2.3:** Hyperconjugation of 1,2-difluoroethane **192**

This effect was first reported by Wolfe and colleagues in the 1970s,<sup>193</sup> and there have been many investigations since attempting to explain it or prove what interactions are responsible for *gauche* preference. A number of computational studies have probed the extent to which hyperconjugation could play a role, through selectively analysing model difluoroethane where certain interactions are excluded. Brunck and colleagues found that the *trans* conformer was preferred when hyperconjugation interactions were excluded.<sup>194</sup> Rablen and coworkers examined cases where a silyl group was in place rather than a vicinal fluorine, and found that while the *trans* conformer should have been greatly favoured in this case it was only marginally so due to hyperconjugation interactions.<sup>195</sup>

Goodman and colleagues went further in probing a range of contributing interactions individually.<sup>196</sup> This included relaxation effects, hyperconjugation with geminal substituents, and the “bent bond” alternative theory put forward by Wiberg and colleagues, where the electrostatic pull of F in the C–F bonds reduces the electron density of the C–C bond in the *trans* but not in the *gauche*-conformer.<sup>197,198</sup> They found that of the possible interactions, relaxation effects and intramolecular hyperconjugation played the greatest role, while bent bond effects and others accounted for only a fraction of the stability of the *gauche*-conformer.<sup>196</sup>

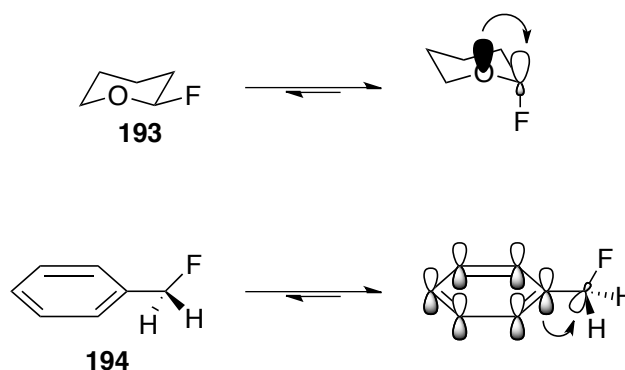
It is also worth noting that the dihedral angle of the *gauche* conformer in difluoroethane is not the ideal 60 ° that might be expected to allow maximum overlap for hyperconjugation. Many experimental and computational analyses have shown that the angle is between 71–72 °, which is believed to be due to the effects of dipolar repulsion.<sup>196</sup>

The  $\sigma_{\text{C-F}}^*$  antibonding orbital can accept electron density from neighbouring aligned electron-rich bonds, such as C–H bonds or  $\pi$  bonds, and also lone



pairs of electronegative heteroatoms like O and N, or nucleophiles, with more electronegative substituents giving a stronger effect.<sup>191,197,199-203</sup>

2-Fluoropyran derivative **193** is a good example of hyperconjugation through donation from a lone pair of an oxygen atom, which favours an axial rather than equatorial orientation for the fluorine (Scheme 2.4).<sup>203</sup> Benzyl fluoride **194** demonstrates an example of fluorine favouring an orientation where the antibonding orbital is aligned to accept electron density from a  $\pi$  system.<sup>200</sup>



**Scheme 2.4:** Other examples of hyperconjugation effects on conformation

Hyperconjugation can also be used to explain the preferred conformations of 1,3-difluorinated systems, such as for the 1,3-difluoropropane mentioned above.<sup>185,186</sup> When the fluorine atoms are out of alignment with the right orientation (**195 A**, Figure 2.4), both antibonding orbitals are being fed electron density by a C–H orbital. In **B** they are not aligned, but there is only one interaction, reducing the stability of this conformer. In **C** there are no interactions, and in **D**, while there is one hyperconjugation interaction, there is also F–F repulsion, which makes this the least stable conformer.

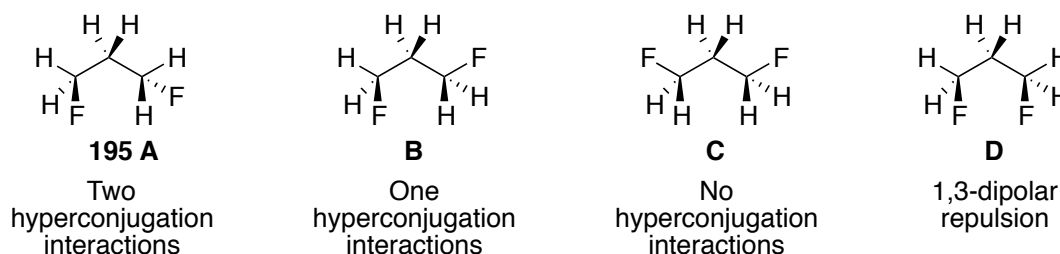


**Figure 2.4:** Hyperconjugation to explain 1,3-dipolar repulsion

Combinations of the *gauche* effect for vicinal fluorines and the 1,3-dipolar repulsion effect have an influence on the conformation of extended

multivincinal fluorinated molecules, which have been investigated in depth by O'Hagan and colleagues, amongst others. In extended systems vicinal fluorines will arrange such that they are *gauche* while 1,3-fluorines will be effectively *anti*.<sup>186</sup>

### 2.3 Fluorinated GABA Analogues: Activity and Synthesis

$\gamma$ -Aminobutyric acid (GABA, **196**, Figure 2.5) serves as a major neurotransmitter molecule, and its binding to certain receptors is necessary for a number of actions such as the opening of ion channels and activation of enzymes.<sup>204</sup> GABA binds to three main types of receptors in the body, known as GABA<sub>A</sub>, GABA<sub>B</sub> and GABA<sub>C</sub> receptors, each of which has its own subtypes.<sup>205-210</sup> GABA<sub>A</sub> and GABA<sub>C</sub> receptors are ligand gated ion channels, and GABA<sub>B</sub> receptors are G-protein-coupled receptors, that rely on a secondary messenger system to mediate their effects.<sup>205</sup> The signalling mediated by GABA receptors can differ greatly in different regions of the brain, different types of cells, and even cells in different locations.<sup>208</sup> For example, GABA<sub>A</sub> type receptors can be involved in the symptoms of schizophrenia,<sup>211</sup> and elsewhere in sensorimotor information processing.<sup>212</sup> This makes an understanding of how GABA binds specifically to different receptor types and subtypes, and what effects these can have, very important.

As such, the preparation of compounds that enhance, activate or diminish the activity of GABA at specific receptor types/subtypes is of significant interest for understanding its biological role and developing therapeutic medications for a number of GABA receptor linked medical conditions. There are many and varied structures of drugs and strategies used to inhibit GABA receptors at present, from small molecules to proteins.<sup>207,213,214</sup> The fact that GABA itself engages with all of these receptors indicates that a good understanding of how its conformation changes to suit receptor shape and functionality would be useful for more targeted drug design.

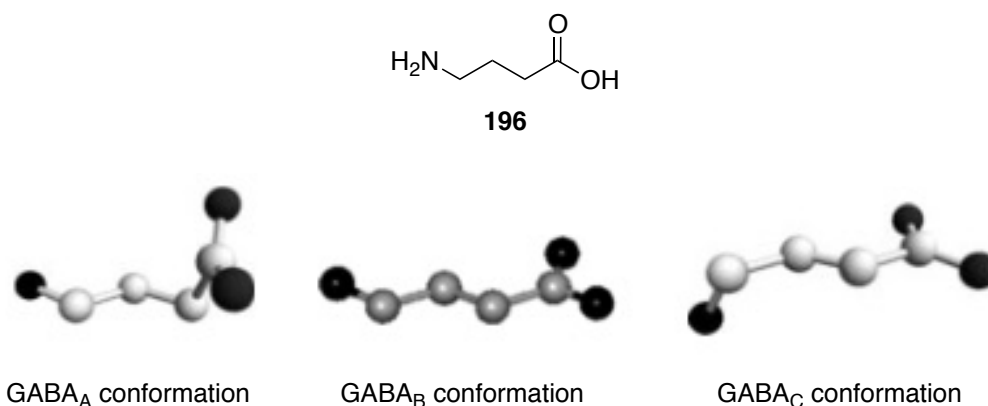


**Figure 2.5:** GABA and its proposed conformations in different receptors

A considerable amount of research has focussed on characterising the GABA receptor binding pockets, initially using other related ligand-gated ion channel protein crystal structures and computer modelling.<sup>215-218</sup> In 2013 a high resolution crystal structure was obtained of GABA<sub>B</sub> both alone and co-crystallised with GABA and an antagonist.<sup>219</sup> The structure of the receptor itself altered significantly between the three cases, suggesting agonist-binding triggers a conformational change necessary for channel activation. This showed that in GABA<sub>B</sub>, GABA adopts an extended zigzag conformation (Figure 2.5) to establish an interaction between the carboxylic acid group and a tyrosine residue in the binding pocket.<sup>219</sup> Though less definitive, testing of many conformationally restricted GABA analogues has given a consensus on the conformation of GABA in GABA<sub>A</sub> and GABA<sub>C</sub> receptors as well, identifying them as having a more extended geometry than in GABA<sub>B</sub>.<sup>220</sup>

The groups of O'Hagan and Hunter have taken significant interest in investigating the use of fluorinated analogues of GABA as potential agonists and antagonists.<sup>221-223</sup> Due to hyperconjugation effects in their vicinal polyfluorinated backbones, and also the charge-dipole effects of fluorine adjacent to the charged C–N<sup>+</sup> bonds, these species can adopt very particular and well-defined conformations while having a minimal impact on the size and sterics of GABA, which can be used to determine the conformation of GABA best suited to the binding pockets of different GABA receptors.<sup>154,224</sup>

Hunter and O'Hagan have prepared a range of mono and difluorinated GABA analogues, examined their lowest energy conformations and tested them for binding affinity with GABA<sub>A</sub>, GABA<sub>B</sub> and GABA<sub>C</sub> receptors (Figure 2.6).<sup>225</sup> In

the monofluorinated analogues **197** and **198**, the conformation is set mainly by the  $F\cdots N^+$  attraction, but in **199–202**, hyperconjugation effects lead the C–F bonds to adopt a *gauche* conformation.<sup>226</sup>

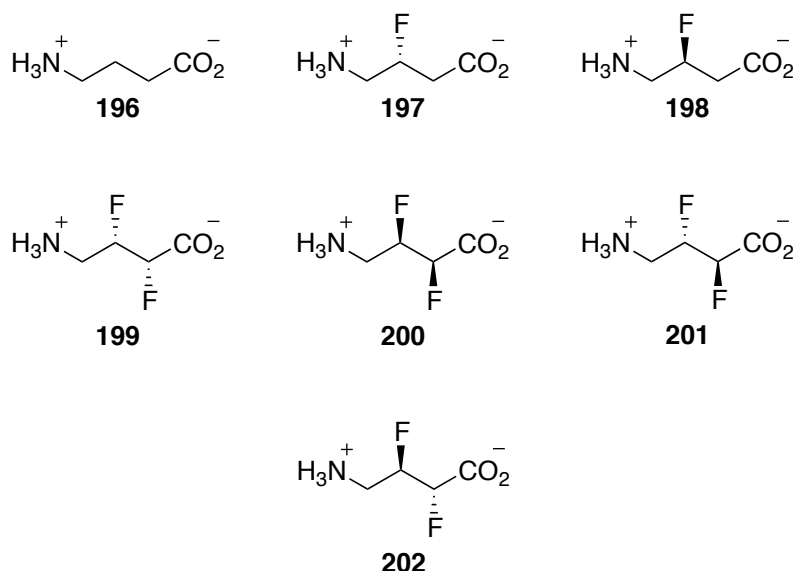


**Figure 2.6:** GABA, and a variety of fluorinated derivatives used by Hunter and colleagues

Analogues **199–202** were first tested against the  $GABA_B$  receptor for benchmarking, as the binding mode of GABA is well established for this receptor (Table 2.1). Following this, the full range of fluorinated compounds were tested against the  $GABA_A$  and  $GABA_C$  receptors. *Syn*-difluorinated analogues **199** and **200** showed agonist activity against  $GABA_B$ , due to their extended zigzag conformations most closely matching that of GABA in the receptor. Monofluorinated compounds **197** and **198** have an extended conformation, and showed agonist activity in both the  $GABA_A$  and  $GABA_C$  receptors.<sup>227</sup> With their similar bent conformations, the *anti*-difluorinated analogues **201** and **202** showed weak agonistic activity for  $GABA_B$  but weak antagonistic activity for the other two receptors.<sup>223,225</sup>

These studies gave the researchers a good idea of the binding geometries of each of the fluorinated analogues, and helped to support the models of GABA binding geometries developed for the  $GABA_A$  and  $GABA_C$  receptors.

**Table 2.1:** Summary of activity of fluorinated GABA analogues for GABA<sub>A</sub>, GABA<sub>B</sub> and GABA<sub>C</sub> receptors

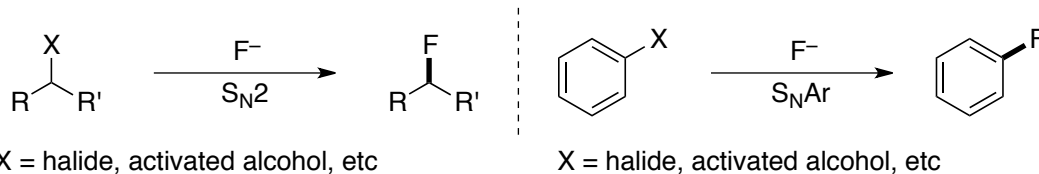
Compound	GABA <sub>A</sub> Activity	GABA <sub>B</sub> Activity	GABA <sub>C</sub> Activity
<b>196</b>	Agonist	Agonist	Agonist
<b>197</b>	Weak agonist	N/A	Agonist
<b>198</b>	Weak agonist	N/A	Agonist
<b>199</b>	nil	nil	Agonist
<b>200</b>	nil	Agonist	Antagonist
<b>201</b>	Weak antagonist	Weak agonist	Weak antagonist
<b>202</b>	Weak antagonist	Weak agonist	Weak antagonist

## 2.4 Methods for Introducing Fluorine and Deoxyfluorination

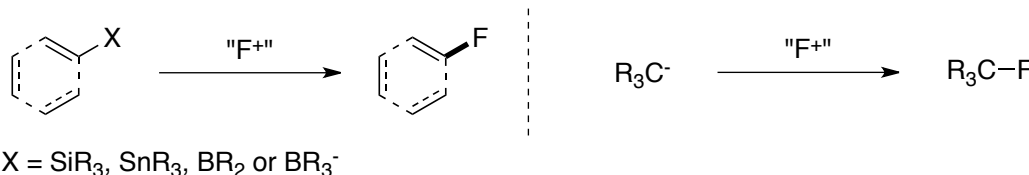
### 2.4.1 General Approach to Fluorination of Organic Molecules

There are three main routes utilised for introducing fluorine to organic scaffolds: nucleophilic, electrophilic and radical fluorination (Scheme 2.5).<sup>228</sup> In nucleophilic fluorination, the substrate behaves as an electrophile while an F<sup>-</sup> source acts as a nucleophile. In these reactions, a suitable leaving group on the substrate is replaced with fluoride in what is generally an S<sub>N</sub>2 reaction, with inversion of stereochemistry at the site of substitution (Scheme 2.5). A particular example of these nucleophilic reactions is where an alcohol is substituted is called deoxyfluorination, discussed in in section 2.4.2.

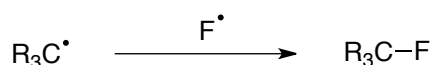
Nucleophilic:



Electrophilic:



Radical:

**Scheme 2.5** General schemes for fluorination reactions

The more traditional reagents in nucleophilic fluorination include complexes of HF, such as HF/pyridine, tetrabutylammonium fluoride (TBAF) and tetrabutylammonium difluorotriphenylsilicate (TBAT). Hypervalent iodine and bromine reagents have also been reported, such as IPyBF<sub>4</sub>, *para*-iodotoluene difluoride and *para*-trifluoromethylphenylbromine difluoride (**203**, **204**, and **205**, Figure 2.7).<sup>229-231</sup> A number of more recently developed reagents aim to improve on issues associated with these, such as poor air stability and hygroscopicity. For example, to circumvent the issue of TBAF's hygroscopicity, which can lead to unwanted side reactions of hydroxide, Sun and colleagues developed an approach for preparing and then using anhydrous TBAF *in situ*, through a fluoride shuttling approach starting from KF. They tested this successfully on a range of alkyl halides, nitro groups and activated alcohols.<sup>232,233</sup> Kim and co-workers developed an alternative approach to circumvent TBAF's hygroscopicity, by synthesising a non-hygroscopic reagent, TBAF (*t*-BuOH)<sub>4</sub>, that also performed well in substituting bromides, tosylates, mesylates and silyl ethers.<sup>234</sup>

In a similar vein, Hammond and colleagues sought to develop new versions of the more established hydrogen-bonded HF complexes to give stable and selective reagents, which gave rise to a DMPU/HF complex (**206**, Figure 2.7). This proved to be useful for the selective mono or difluorination of alkynes.<sup>235</sup>

Hara and co-workers developed an alternative to the older reagent  $\text{IF}_5$ , by mixing it with a 50:50 mix of pyridine:HF to produce  $\text{IF}_5$ -pyridine-HF.<sup>236</sup> This reduced issues of rearrangements and overfluorination for a number of fluorinations of  $\alpha$ -(aryltio)carbonyl compounds, and desulfurisation/difluorination, in good to excellent yields. An obvious disadvantage is the use of significant amounts of HF in preparation of the reagent, although the reagent itself is more stable than  $\text{IF}_5$ . They found similar results working with  $\text{BrF}_3$ - $\text{KHF}_2$ .<sup>237</sup>

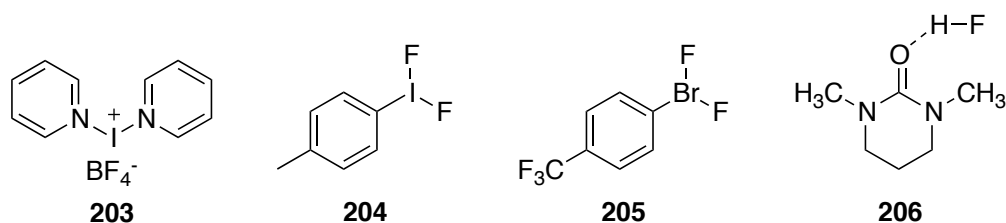


**Figure 2.7:** Some nucleophilic fluorination reagents

In electrophilic fluorination the roles are reversed, with the reagent designed to act as an equivalent for  $\text{F}^+$  (Scheme 2.5). The substrate is most often an electron rich system such as an alkene, alkyne or arene; although it can also be a carbon site with a nucleophilic labile substituent such as  $\text{C-Si}$ ,  $\text{C-B}$  or  $\text{C-Sn}$ .<sup>238</sup> The most common reagents deployed are those with  $\text{N-F}$  bonds, such as NFPy salts (**207**),<sup>239</sup> NFSI (**208**),<sup>240</sup> and the popular reagents Selectfluor<sup>®</sup> (**209**) and Accufluor<sup>™</sup> (**210**, Figure 2.8).<sup>241-244</sup> Newer reagents again tend to build on their predecessors, such as in Yasui and colleagues development of NFSBI (**211**), a sterically demanding variant of NFSI that allowed for modest improvement in the enantioselectivity of fluorination reactions.<sup>245</sup> Zhu and co-workers achieved better results through preparation of a chiral NFSI analogue.<sup>246</sup>

Likewise, Wolstenhulme and colleagues developed a chiral  $\text{F}^+$  source based on Selectfluor<sup>®</sup>, with a DABCO-based dication skeleton (**213**), which proved effective in fluorocyclisation of alkenes.<sup>247</sup>

Other researchers have looked into adding chiral metal complex catalysts to improve the enantioselectivity of fluorination.<sup>248</sup> Geary and colleagues synthesised an interesting iodane species, a fluorinated hypervalent iodine reagent used for electrophilic fluorination (**212**).<sup>249</sup>

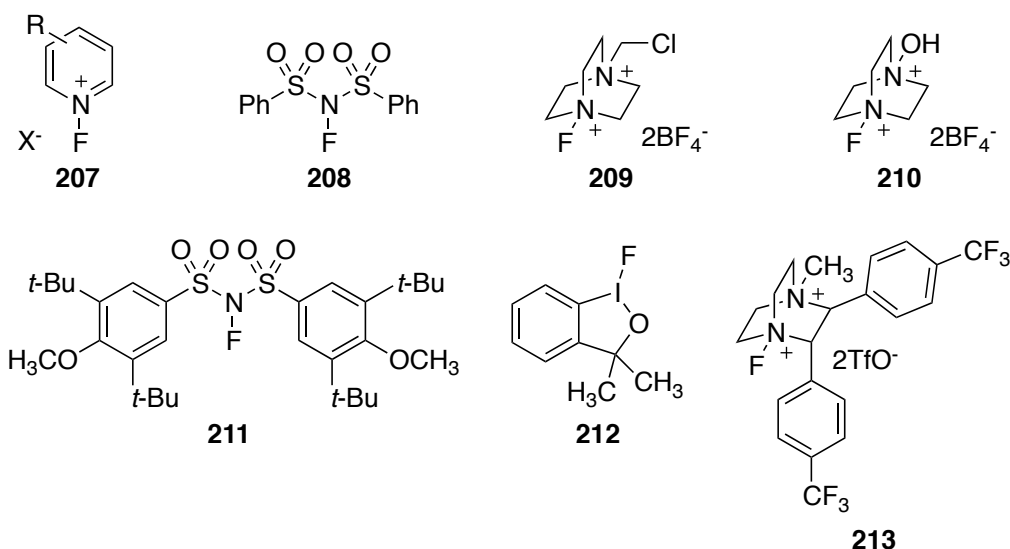
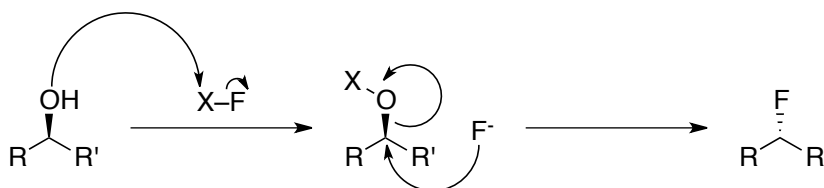


**Figure 2.8:** Common and newer electrophilic fluorination reagents

Cases of radical fluorination are rarer, but do exist. The standard approach in these cases is to use a carbon-centred radical as the substrate, and then a source of molecular fluorine (Scheme 2.5).<sup>250</sup> Early examples of the fluorine sources used were fluorine itself, hypofluorite sources, or XeF<sub>2</sub>.<sup>251-253</sup> More recently N–F electrophilic fluorine reagents have also proven to be good sources,<sup>254-256</sup> along with a couple of recent reports of using fluorinated solvents.<sup>257,258</sup>

#### 2.4.2 Reagents and Methods for Deoxyfluorination

Deoxyfluorination is a particular case of nucleophilic fluorination, although it has developed its own particular subset of popular reagents. In general terms, deoxyfluorination proceeds *via* nucleophilic attack of the alcohol on to the electrophilic reagent, which converts the alcohol into a good leaving group and generates F<sup>-</sup> (Scheme 2.6). The F<sup>-</sup> then normally undergoes S<sub>N</sub>2 substitution of the activated alcohol to give fluorination with inversion of stereochemistry.



**Scheme 2.6:** General scheme for deoxyfluorination



Two of the most well-established and popular of the reagents used for deoxyfluorination are diethylaminosulfur trifluoride (DAST, **214**, Figure 2.9) and Deoxo-Fluor<sup>®</sup> (bis-(2-methoxyethyl)aminosulfur trifluoride, **215**).<sup>259-261</sup> Deoxo-Fluor<sup>®</sup> is generally superior to DAST in that it is tolerant of higher reaction temperatures, where DAST decomposes to explosive species. Other reagents have been developed based on the structure of these two, notably the reagents XtalFluor-E<sup>®</sup> (**216**) and XtalFluor-M<sup>®</sup> (**217**).<sup>262-264</sup> These are stable crystalline solids, and showed good activity in the fluorination of primary alcohols and secondary alcohols, and the difluorination of ketones. They did however show a tendency to form elimination by-products, a problem in common with both DAST and Deoxo-Fluor<sup>®</sup>. More recently developed reagents such as PyFluor (**219**) claim to reduce or remove this complication entirely.<sup>265</sup>

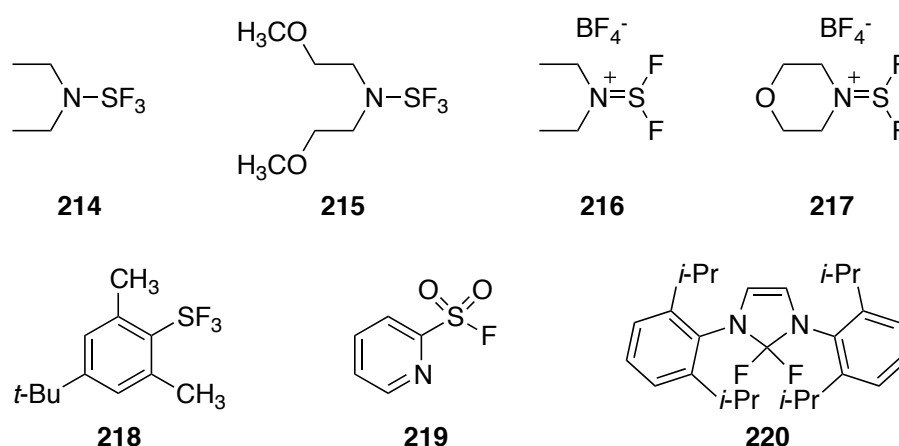


**Figure 2.9:** Deoxyfluorination reagents

Alternative reagents include Fluolead<sup>™</sup> (**218**). Developed by Umemoto and colleagues, it is an arylsulfur trifluoride reagent that is crystalline, relatively inert to aqueous hydrolysis, and thermally very stable.<sup>266</sup> It can be applied to the deoxyfluorination of a range of alcohols, and also difluorination of ketones. When vicinal diols were reacted with one molar equivalent of the reagent, one alcohol was substituted for fluorine, while the other was converted to a sulfinic ester.<sup>266</sup> The same group also developed arylsulfur tetrafluoride reagents, which can be converted to the arylsulfur trifluorides *in situ* and showed good reactivity in fluorination across a variety of substrates.<sup>267</sup>

Finally, Ritter and colleagues have developed the fluorination reagent PhenoFluor™ (**220**), prepared from a chloroimidazolium salt.<sup>268,269</sup> This reagent showed excellent reactivity compared to the other popular reagents, such as DAST and Deoxo-Fluor®, for the deoxyfluorination of phenols. It was also proven to be very selective in deoxyfluorination of alkyl alcohols, including in late stage transformations of complex natural product analogues.<sup>270</sup>

## 2.5 Proposed Approach for Synthesis of Fluorinated GABA Derivatives

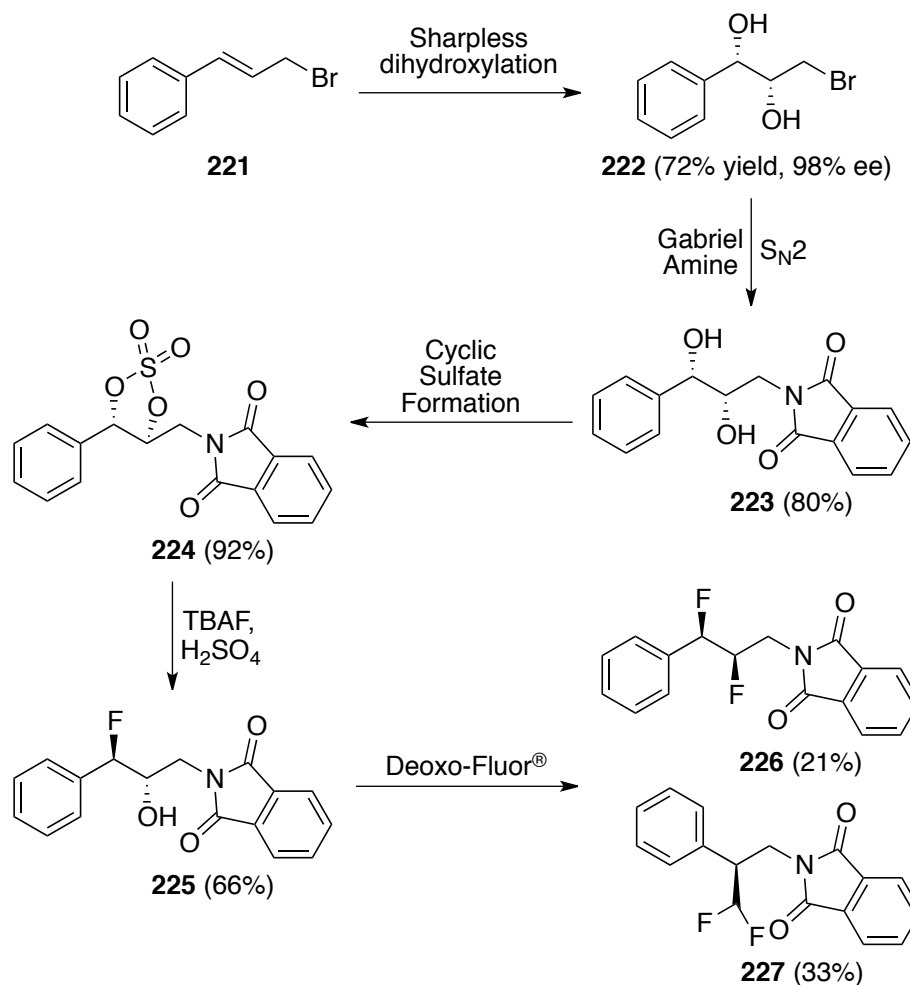
### 2.5.1 Hunter and Colleagues' Synthesis of Fluorinated GABA analogues

Hunter and colleagues have already developed a synthesis of difluorinated derivatives of GABA, with two routes that both utilise cinnamyl bromide (**221**) as the starting point, and making use of methodology developed by O'Hagan and colleagues (Scheme 2.7).<sup>227,271-273</sup>

Cinnamyl bromide **221** was subjected to a Sharpless asymmetric dihydroxylation,<sup>274</sup> to give diol **222** in high yield and excellent enantiomeric excess. The protected amine **223** was then formed by reaction with potassium phthalimide in high yield. This gave the intermediate **223** that would be used for both pathways. For the first pathway, this diol was converted to the corresponding cyclic sulphate **224** by treatment with thionyl chloride, followed by oxidation with sodium periodate and ruthenium chloride.<sup>275</sup> The first fluorination was then carried out by treatment with TBAF followed by sulphuric acid, which gave fluorination with inversion of stereochemistry at the C2 position and removal of the sulphate, to furnish fluorohydrin **225** in a good yield.

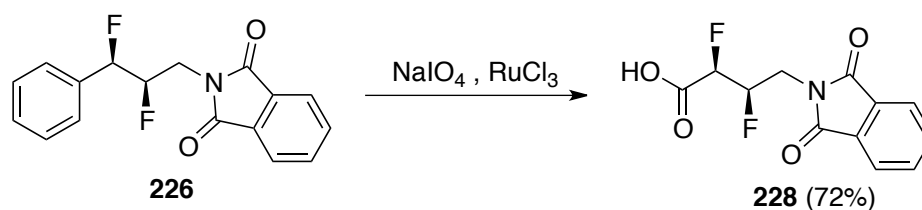
Next, the key step of the second fluorination was carried out using Deoxo-Fluor®.<sup>261</sup> Unfortunately, while the difluorinated species **226** was obtained in a yield of 22%, the major product (in 33% yield) was branched difluorinated species **227**, believed to arise from neighbouring group participation and migration of the phenyl group. A workaround was attempted where TMS

morpholine was added to suppress the rearrangement pathway, but this led to the formation of several elimination products.<sup>276 277</sup>



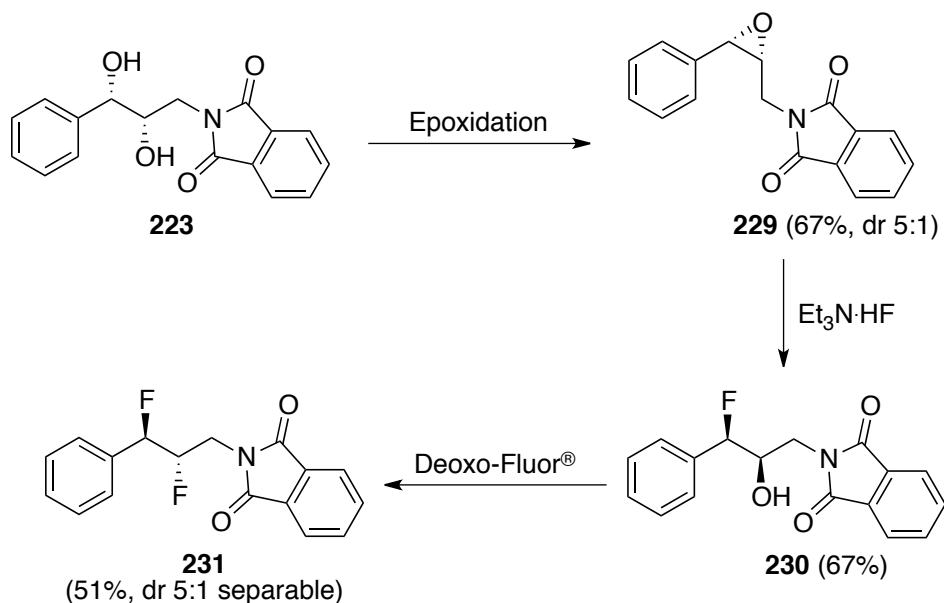
**Scheme 2.7:** Hunter's synthesis of *syn*-difluoroGABA

Following this step, the desired difluorinated species **226** was treated with sodium periodate and ruthenium chloride, which oxidised the phenyl group to the carboxylic acid **228**, giving a good yield of the *syn*-difluoro GABA analogue with the phthalimide protecting group still in place.<sup>278</sup> This was then deprotected and incorporated into short peptides.



**Scheme 2.8:** Oxidation of the phenyl group to reach the amino acid

To reach the *anti* difluorinated analogue, diol **223** was converted to the epoxide **229** with a dr of 5:1, using an approach developed by Nilewski and colleagues (Scheme 2.9).<sup>279</sup> This was opened with triethylamine hydrofluoride to give the *syn* fluorohydrin **230**.<sup>280</sup> This was then treated with Deoxo-Fluor<sup>®</sup> to give the *anti*-difluorinated compound **231** with a much smaller proportion of the side reaction/rearrangement, in a reasonable yield of 51%. This was then taken through the same oxidation procedure to give the carboxylic acid.



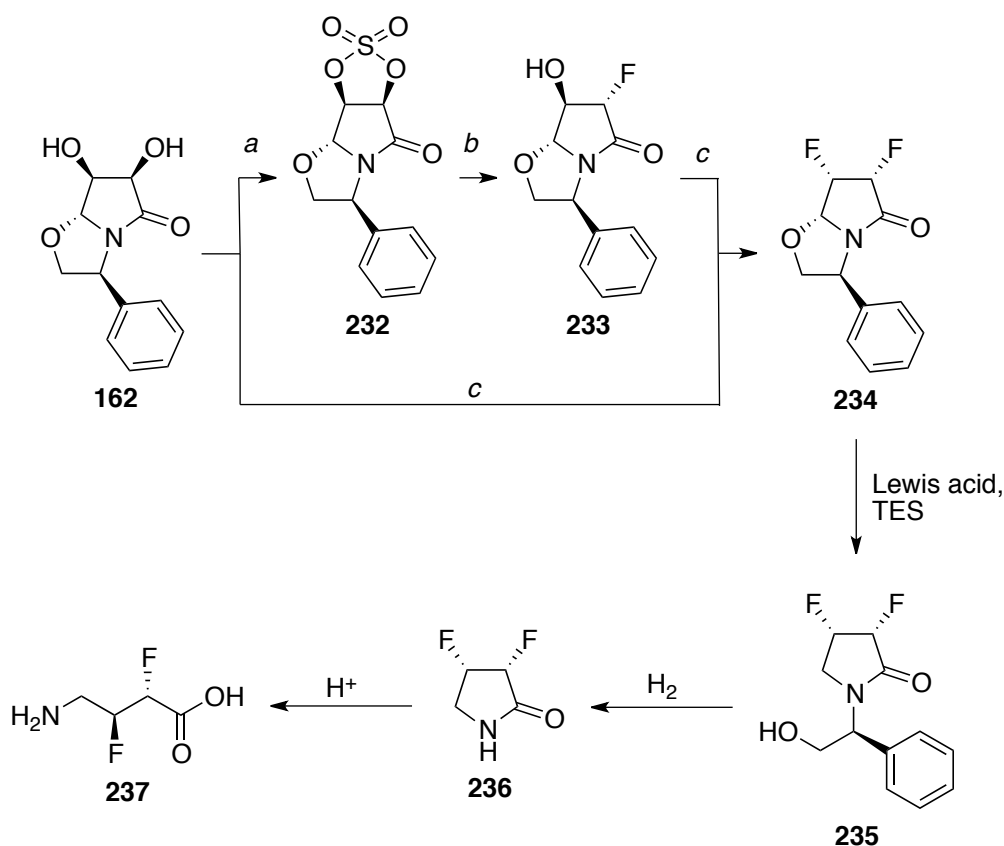
**Scheme 2.9:** Variations to give the *trans*-difluoro GABA analogue

With Hunter and co-workers' synthesis in mind, an approach to the synthesis of fluorinated GABA derivatives was developed that would hopefully circumvent issues of unwanted rearrangement products in the fluorination process and hence allow easier access to these fluorinated GABA analogues.

### 2.5.2 Proposed Approach to Fluorinated GABA Analogues

The proposed starting point for this synthesis was the bicyclic heterocycle **162**, prepared originally for the synthesis of chiral (–)-codonopsinine analogues (Scheme 2.10). The planned route involved first fluorinating this diol, which could be carried out in one of two ways. Hunter's protocol could be followed of first preparing a cyclic sulphate, such as **232**, and then the first fluorination could be performed by treating this with TBAF to yield fluorohydrin **233**. Deoxyfluorination could then be carried out on the

remaining alcohol using Deoxo-Fluor<sup>®</sup> or a related fluorination compound, such as DAST, to give the difluorinated bicyclic species **234**. Alternatively, direct fluorination of the diol *via* dexoyfluorination could be explored, to determine whether a single difluorinated product, or a useful mixture of mono and difluorinated products could be obtained. This would allow fluorinated derivatives to be accessed while circumventing a three-step procedure.



**Scheme 2.10:** Planned route/s to fluorinated GABA analogues. a. SOCl<sub>2</sub>, NaIO<sub>4</sub>, RuCl<sub>3</sub> b. TBAF c. Deoxo-Fluor<sup>®</sup>

It was hypothesised that the fluorinated derivative/s of the diol would be affected by hyperconjugation effects of the C–F bonds, weakening the C–O bond of the endocyclic ether linkage, compared to the very stable diol diacetate derivative **163** discussed in Chapter 1. This should allow for easier ring-opening with a Lewis acid, such as BF<sub>3</sub>·OEt<sub>2</sub> or TiCl<sub>4</sub>, and trapping of the iminium ion thus generated with triethylsilane. This would give the monocyclic fluorinated lactam **235**.

From lactam **235**, the following step would be cleavage of the chiral *N*-phenylethanol group, either by hydrogenolysis<sup>281,282</sup> or possibly a dissolving

metal reduction to give amide **236**.<sup>103,283,284</sup> Given this had proved difficult in the earlier work, it was not clear whether these compounds might behave differently due to hyperconjugation effects from the fluorine leading to a more facile cleavage of the phenylethanol fragment.

Finally, difluorinated lactam **236** could be subjected to acid-mediated ring-opening to generate the open chain fluorinated GABA analogue **237**.<sup>285</sup> This should lead to fluoro-GABA analogues for which the stereochemistry of the substituents has been set by the bicyclic precursor. The bicyclic intermediate would not be prone to rearrange to form a species like **227**, which ought to lead to a more efficient and straightforward synthetic pathway overall. It would also highlight an application for the chiral bicyclic intermediates. Furthermore, a range of different analogues could be prepared, depending on the chosen approach to fluorination and the prior transformations carried out on the bicyclic diol (Figure 2.10). For example, intermediate fluorohydrin **233**, if isolated, could provide the monofluorinated analogue **238**. Also, It might be possible to investigate using the alcohol **174**, prepared through elimination and hydrogenation of diol **162** (from Chapter 1), to reach monofluorinated analogues such as **239** or **240**.

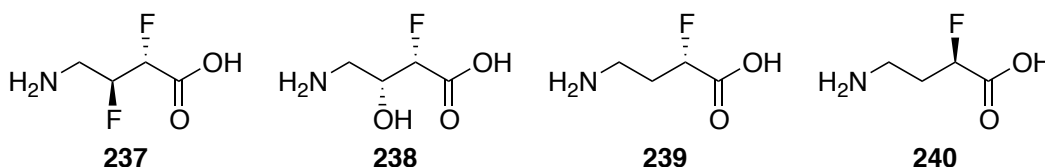


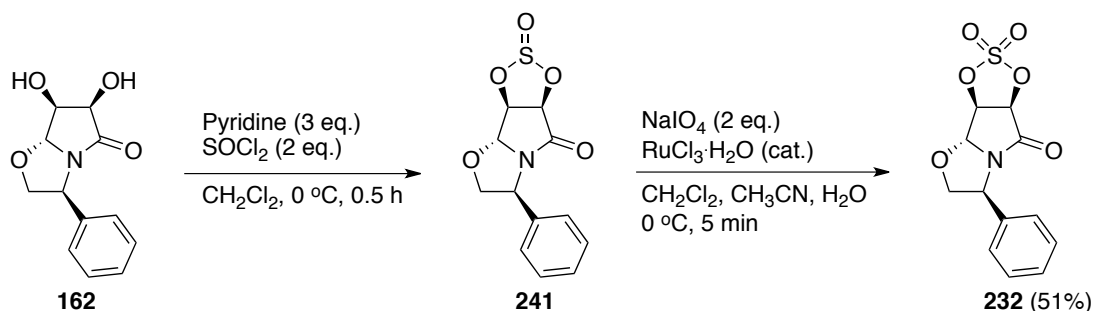
**Figure 2.10:** Potential fluorinated GABA targets for this work

## 2.6 Results

### 2.6.1: Fluorination of the Diol

The fluorination of diol **162** was focused on first. To begin with, applying Hunter's method for fluorination of acyclic vicinal diols was explored, which meant that the diol **162** needed to first be converted to the cyclic sulphate derivative **232** (Scheme 2.11). This involved first preparing the cyclic sulphite **241** through treatment of **134** with thionyl chloride and pyridine, which was immediately subjected to oxidation with ruthenium chloride and sodium

periodate. This provided the desired cyclic sulphate **232** in a yield of 51% over two steps.



**Scheme 2.11:** Formation of the cyclic sulphate ester **232**

The <sup>1</sup>H NMR spectrum for this compound supported the structure in that it featured resonances consistent with the bicyclic diol with no evidence of broad OH peaks. The compound was much less polar than the starting diol and soluble in chloroform, supporting the conversion. There were obviously no resonances in the <sup>1</sup>H or <sup>13</sup>C NMR spectra to confirm the presence of the cyclic sulphate. However, the crystalline solid compound was recrystallised by slow evaporation and the structure supported by X-ray crystallographic analysis (Figure 2.11). The result was also supported by HRMS analysis.

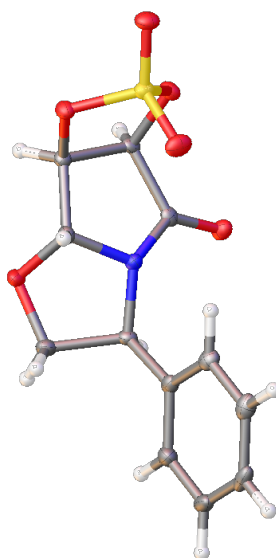
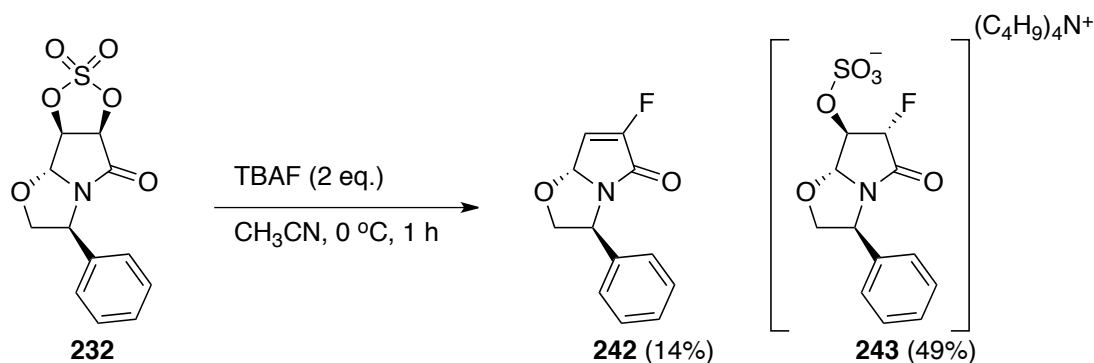


**Figure 2.11:** X-ray crystal structure of cyclic sulphate **232**

The following step was treatment of **232** with TBAF, which theoretically should open the cyclic sulphate and give a single deoxyfluorination to yield a fluorohydrin species such as **233**. In this case, the reaction led to a mixture of

two major products, both of which by  $^{19}\text{F}$  NMR contained a single fluorine atom (Scheme 2.12). The first, minor product was identified as the fluoroalkene **242**, which seems to have arisen through ring-opening with fluoride to the desired fluorohydrin followed by elimination. The second product was tentatively identified as the tetrabutylammonium salt of the desired monofluorinated product, **243**, in a 49% yield.



**Scheme 2.12:** Ring-opening fluorination of cyclic sulphate **232**

Key indicators of the identity of fluoroalkene **242** were derived through analysing the  $^1\text{H}$  NMR spectrum of this compound, mainly through the loss of two aliphatic CH resonances and appearance of a single alkenyl CH signal: a doublet of doublets at 5.71 ppm. The coupling constants of this signal were of 6 Hz and 2 Hz (Figure 2.12). The 6 Hz coupling constant is consistent with the 2–20 Hz range expected for an alkenyl proton adjacent to an alkenyl fluorine atom. The smaller 2 Hz coupling is shared with another doublet of doublets further downfield, at 6.75 ppm. This was assigned as the methine proton at C5, which does not exhibit a vicinal coupling with the fluorine atom at C3. It is possible that this signal's further 1 Hz coupling is shared with the fluorine, but that this coupling was not resolved in the  $^{19}\text{F}$  NMR spectrum.



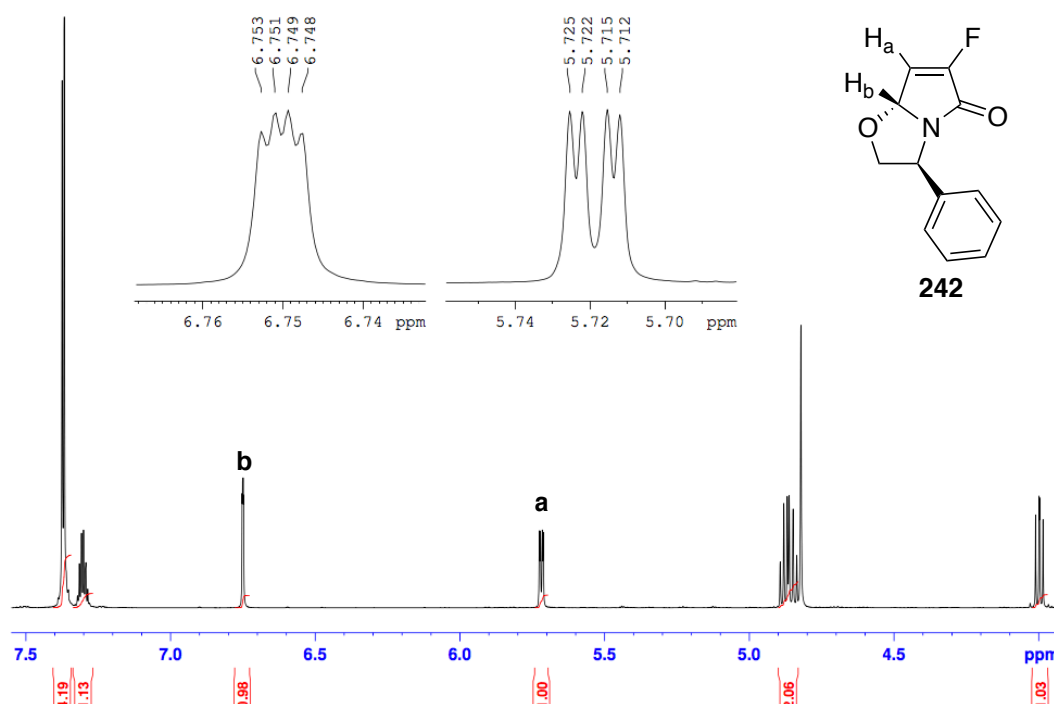


Figure 2.12:  $^1\text{H}$  NMR spectrum of fluoroalkene **242** showing key resonances

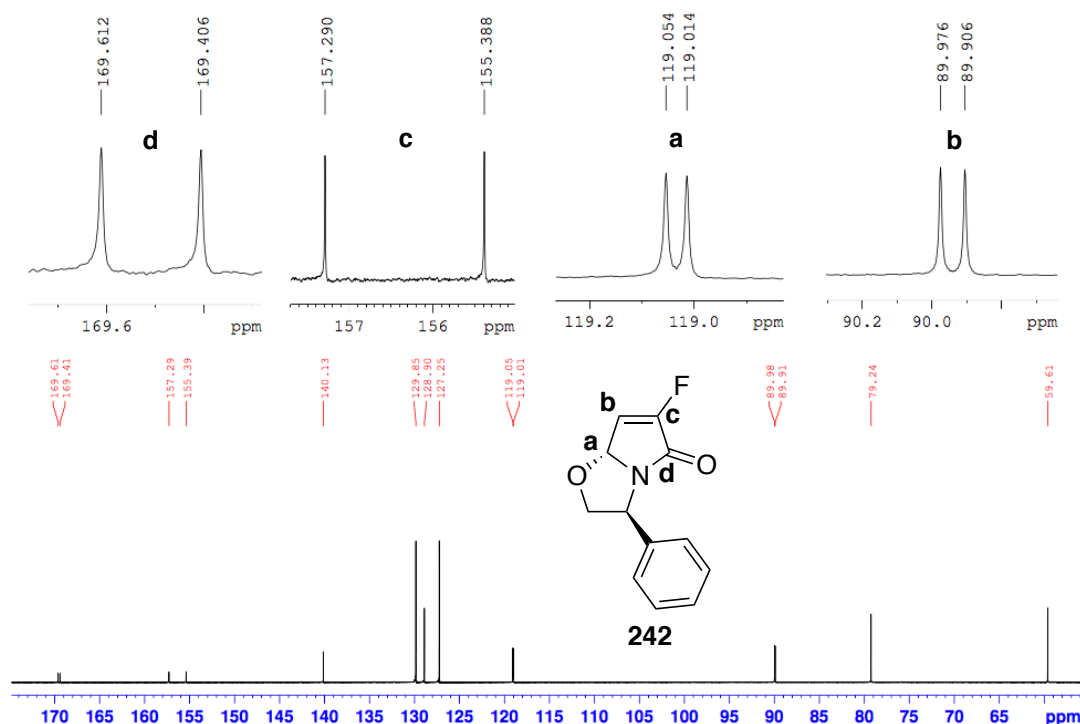
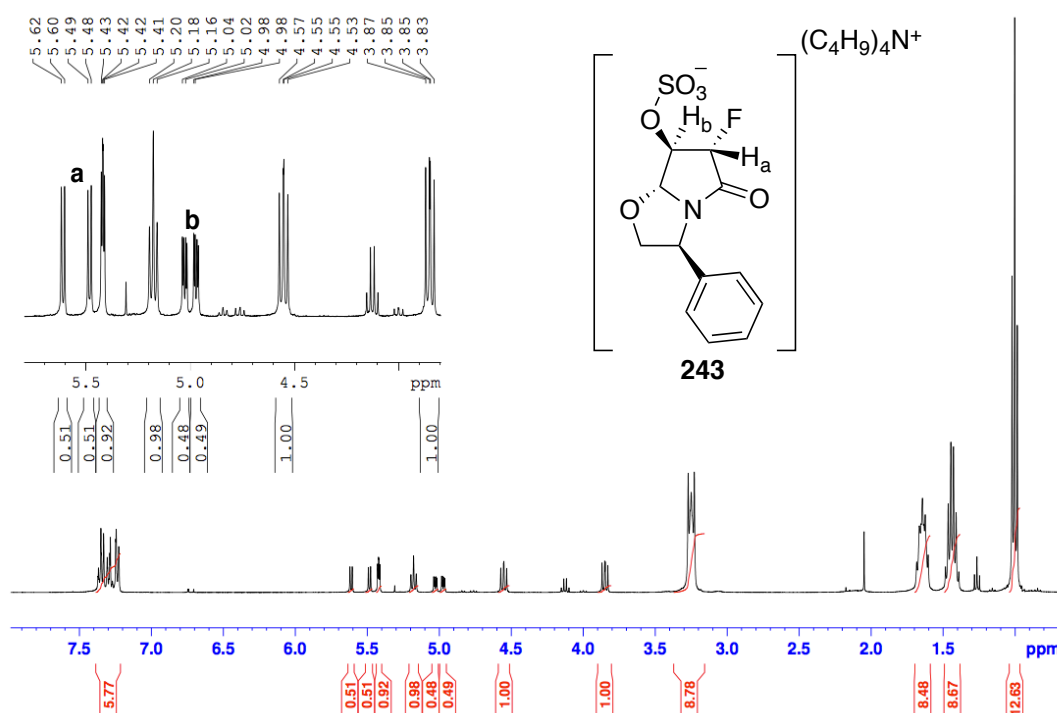


Figure 2.13:  $^{13}\text{C}$  NMR spectrum for fluoroalkene **242**

Importantly for this structural assignment, the  $^{13}\text{C}$  NMR spectrum showed splitting of three resonances associated with the lactam ring: the amide carbonyl signal at 169.5 ppm, the alkene signal at 89.9 ppm, the aminol carbon atom at 119.0 ppm, and a very large 286 Hz coupling for the fluoralkene carbon atom at 156.3 ppm. Also,  $^{19}\text{F}$  NMR spectrum of the

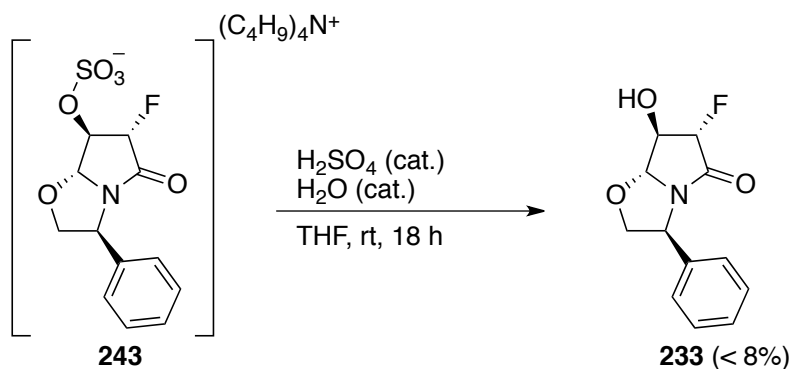
compound showed only a single peak at  $-134.48$  ppm, a doublet with a resolved coupling constant of 6 Hz, which corresponds with the 6 Hz coupling observed in the  $^1\text{H}$  NMR spectrum. Furthermore, the mass spectrometry data for the compound was consistent with what would be expected for this fluoroalkene compound's mass and molecular formula.

Tetrabutylammonium salt **243** was tentatively assigned only from its  $^1\text{H}$  NMR spectrum, as the product was reacted further to support its identity (Figure 2.14). The  $^1\text{H}$  NMR spectrum featured two resonances with very diagnostic couplings: a doublet of doublets at 5.55 ppm, and a doublet of doublets at 5.00 ppm. The first of these had a coupling constant of 51 Hz, indicative of a geminal coupling with a fluorine atom. The latter had a coupling constant of 22 Hz, which is consistent with a vicinal H–F coupling. These indicate that a single deoxyfluorination did occur, most likely at the alcohol adjacent to the amide, as there is only one 22 Hz coupling, where two would be expected if deoxyfluorination had occurred at the C4 alcohol (one for the C3 and one for the C5 methine protons). Furthermore, a triplet at 1.00 ppm integrating for roughly 12 H and multiplets between 1.38 and 3.29 ppm each integrating for roughly 8 H indicate that this is a tetrabutylammonium group. These resonances did not disappear after purification of the compound by chromatography and this was the major reason for assignment of this structure as a sulfonate salt.



**Figure 2.14:**  $^1\text{H}$  NMR spectrum of tetrabutylammonium salt **243**

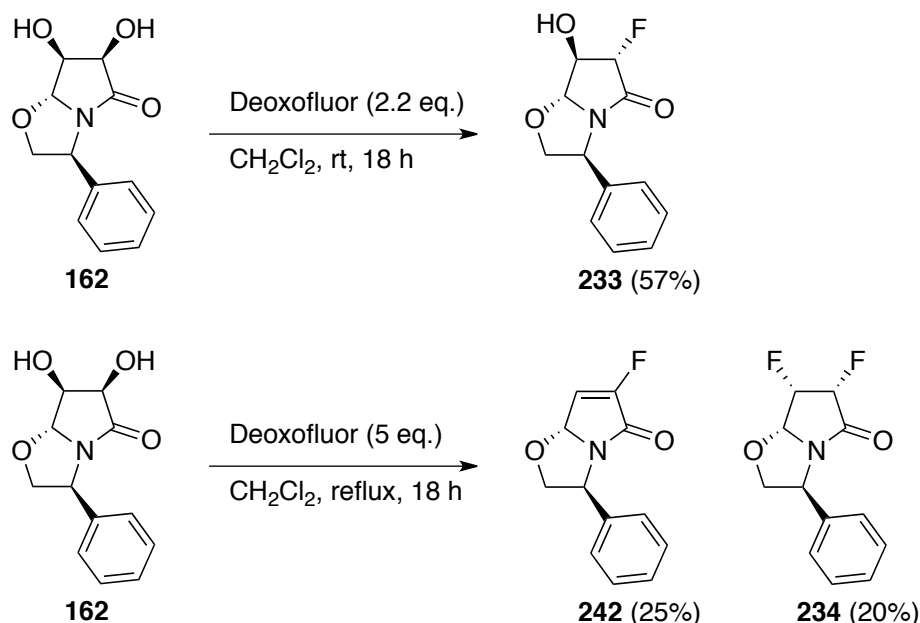
To provide evidence for this characterisation, intermediate **243** was treated with acid, to determine whether it could be simply converted to fluorohydrin **233** (Scheme 2.13). When a small sample of the salt was taken and stirred in THF with 37  $\mu\text{L}$  of conc.  $\text{H}_2\text{SO}_4$  and a drop of water (20  $\mu\text{L}$ ), for 18 h, a single product was obtained, identified as the fluorohydrin **233** (*vide infra*). However, the yield of the product was quite low, at less than 8%. The remainder of the material appeared to be lost to decomposition.



**Scheme 2.13:** Acid treatment of the tetrabutylammonium salt **243**

While this was successful in reaching the desired fluorohydrin intermediate **233**, the mixture of products and low overall yield for what became a four-step process was far from ideal. This led us to investigate the direct

deoxyfluorination of the diol **162**, to see whether this might be a more efficient approach. Thus, diol **162** was reacted with 2.2 molar equivalents of Deoxofluor® at reflux overnight (Scheme 2.14). This gave almost exclusively the fluorohydrin **233**, in a yield of 57%, representing a significant improvement over the previous approach. There were also trace amounts of the fluoroalkene **242** and the difluorinated species **234** present, which were easily separable by flash column chromatography.



**Scheme 2.14:** Deoxofluor® fluorination of diol **162**

The crude reaction mixture of **233** was heated at reflux with a greater excess of Deoxofluor® (10 molar equivalents) to try to form the difluorinated product. All of the fluorohydrin was converted into a mixture of the fluoroalkene and difluorinated species, in a ratio of roughly 1 : 0.7. Similar results could be obtained by heating the diol **162** at reflux with 5 molar equivalents of Deoxofluor®, giving exclusively the fluoroalkene **242** and difluorinated product **234** in yields of 25% and 20% respectively. These results demonstrated that Deoxofluor® could be used directly on the diol **162** to give moderate yields of three desirable fluorinated species for further derivatisation towards fluorinated GABA analogues.

The structure and stereochemistry of fluorohydrin **233** was assigned through analysis of the NMR spectra and other data. Firstly, the  $^1\text{H}$  NMR spectrum featured resonances similar to those present in that of the salt **243**, with a doublet of doublets at 5.35 ppm integrating for a single proton, with a 52 Hz coupling indicative of a geminal fluorine substituent (Figure 2.15). Another signal at 4.49, a doublet of doublets of doublets, had a 20 Hz coupling, consistent with it being vicinal to the fluorine atom. As this exhibited an extra coupling compared with the 5.53 signal, it was most likely that this was the proton at C4, between the ether methine and fluoro methine protons, and the mutual couplings of 7.8 Hz (between the C3 and C4 protons) and 3.3 Hz (between the C4 and C5 protons) support this.

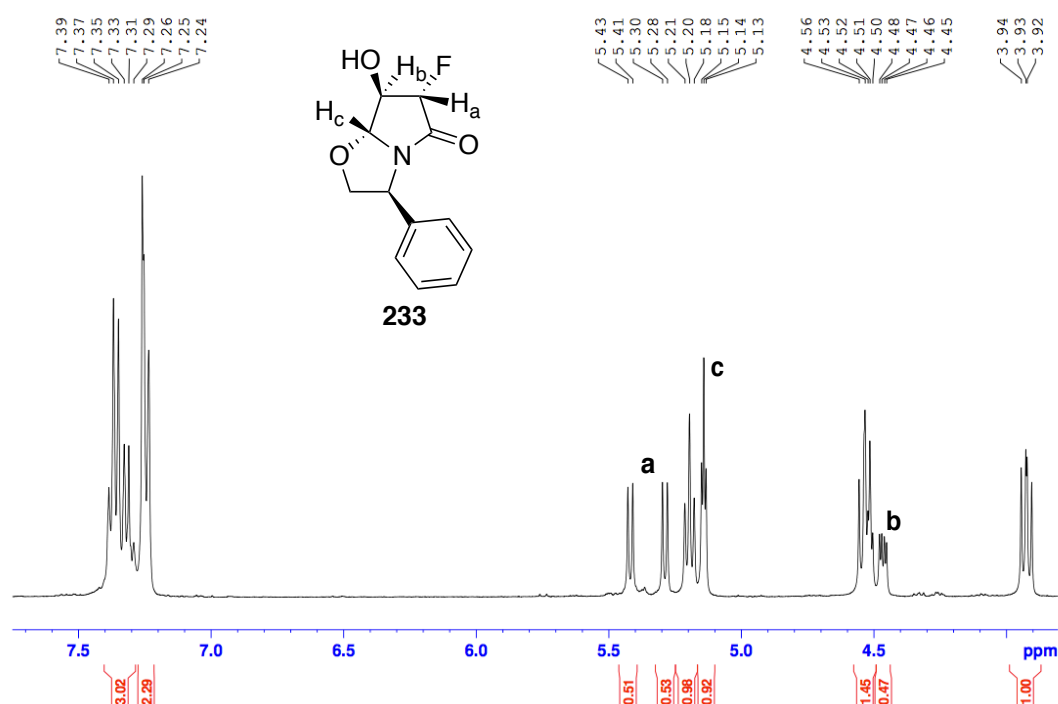


**Figure 2.15:**  $^1\text{H}$  NMR of fluorohydrin **233**

Furthermore, in the  $^{19}\text{F}$  NMR spectrum, a signal is observed at  $-198.3$  ppm, as a doublet of doublets of doublets, with 5.2, 20.7 and 3.6 Hz couplings (Figure 2.16). This is consistent with a geminal coupling at C3, vicinal at C4 and a more distant coupling at C5. The C5  $^1\text{H}$  signal at 5.14 ppm appears to be a triplet, likely due to the two very similar couplings observed with the CH proton (3.3 Hz) and the F atom (3.6 Hz). Finally, the  $^{13}\text{C}$  NMR spectrum showed splitting of resonances associated with the lactam ring carbon atoms, similar to fluoroalkene **242**. Notable were the 24.1 Hz coupling of the

amide carbon at 168.8 ppm and the 196.9 Hz coupling of the fluorine-substituted C3 carbon at 95.2 ppm. Also the 9.4 Hz coupling of the carbon at 93.1 ppm and the 20.0 Hz coupling of the carbon at 78.7 ppm, which supported the presence of a single fluorine atom on the lactam ring.

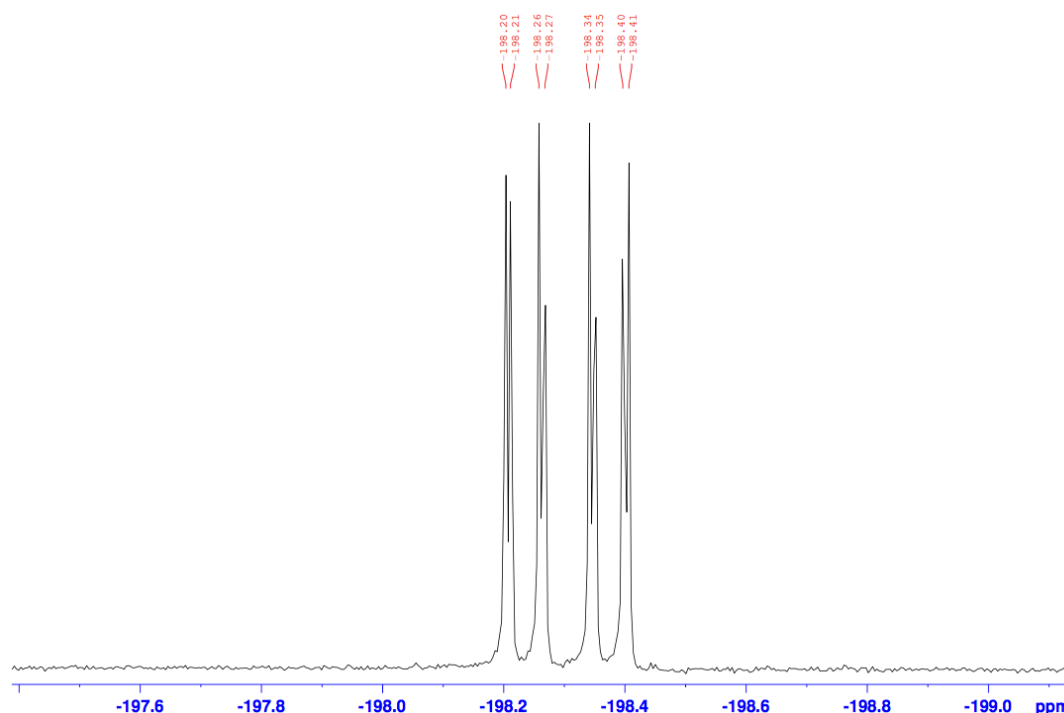


**Figure 2.16:**  $^{19}\text{F}$  NMR spectrum of fluorohydrin **233**

Given that half of the key vicinal  $^1\text{H}$  signal at 4.49 ppm was obscured by one of the resonances associated with the phenylethanol portion of the molecule, the  $^1\text{H}$  NMR spectrum of **233** was simulated using the Bruker Topspin software's Simulation & Iteration of 1D spectra tool (or DAISY), to provide support for the assignment of chemical shifts and coupling constants. The resonances associated with the aryl substituent were omitted, as they were not necessary for clarification. Thus, 8 atoms were added to make up the fragment being simulated, 7 being the protons to be simulated and another being the fluorine atom, and each assigned as the correct type of nucleus (Appendix 1). Each was given its  $^1\text{H}$  chemical shift, as gleaned from the empirical spectrum, or its approximate  $^{19}\text{F}$  chemical shift in the case of the fluorine. Exact fluorine chemical shifts were not strictly necessary, as only the  $^1\text{H}$  NMR spectrum was being simulated. The couplings between each proton and fluorine were entered into the table of the Scalars tab. Finally, the

lineshape was optimised through the Lineshapes tab, by increasing the global linewidth until the peaks had a more realistic shape. This gave a simulated spectrum that agreed well with the experimental spectrum, supporting the chemical shift and coupling constant assignments (Figure 2.17)

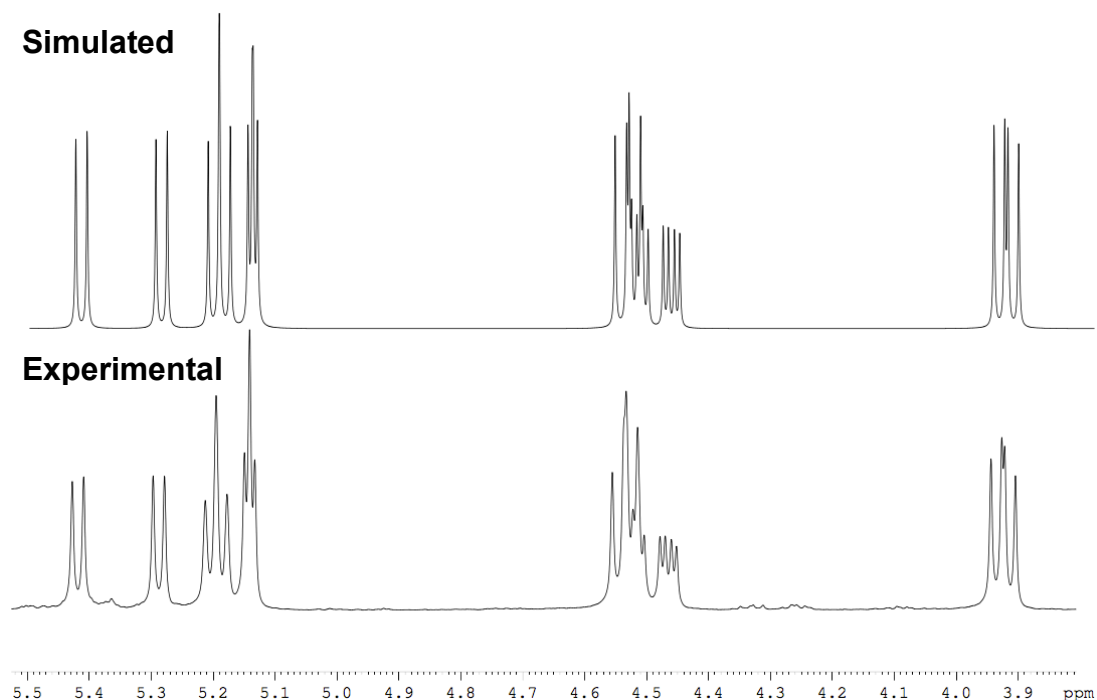


**Figure 2.17:** Comparison of real and simulated spectra for fluorohydrin **233**

To further support this characterisation, fluorohydrin **233** was recrystallised and an X-ray crystal structure obtained (Figure 2.18). This validated our structural and stereochemical assignments, showing deoxyfluorination at the C3 alcohol with the expected inversion of stereochemistry, to give a *trans*-relationship with the remaining alcohol.

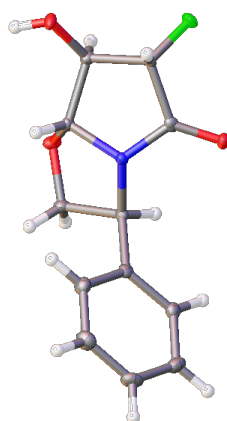


**Figure 2.18:** X-ray crystal structure of fluorohydrin **233**

The final fluorinated product, the difluorinated bicyclic lactam **234**, had its structure and stereochemistry assigned through a similar process. Issues were encountered in analysing the  $^1\text{H}$  NMR spectrum as the additional fluorine atom gave a complex spectrum with all of the lactam protons having an additional large coupling constant, such that many of the resonances were overlapping in the region from 5.26–5.50 ppm (Figure 2.19). Analysis of the  $^{19}\text{F}$ ,  $^{13}\text{C}$  and 2D NMR spectra provided support for assignments in the  $^1\text{H}$  NMR spectrum, aided by the significant and multiple coupling constants observed in these spectra.

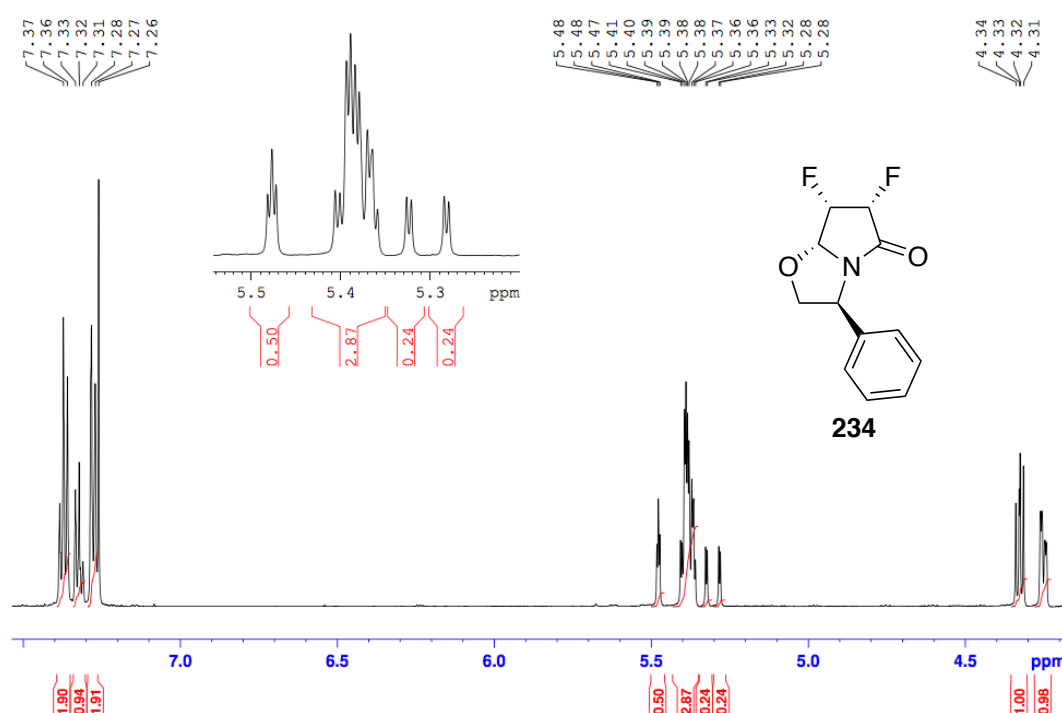


**Figure 2.19:**  $^1\text{H}$  NMR spectrum of lactam **234**

The evidence that two fluorine atoms were present was borne out by analysis of the  $^{19}\text{F}$  NMR spectrum, which featured two resonances, one at  $-215.89$  ppm, a doublet of doublets with 47.8 and 5.6 Hz couplings; and the other at  $-221.79$  ppm, a doublet of doublets of doublets of doublets with couplings of 55.7, 25.2, 14.1 and 5.6 Hz (Figure 2.20). It was presumed that the latter signal is that at C4, and is exhibiting coupling with both its geminal proton, two vicinal protons and the vicinal fluorine. The other fluorine at  $-215.89$  ppm only seems to have an observable coupling with its geminal proton and vicinal fluorine at C4, which may be associated with the dihedral angle between the *trans* oriented hydrogen and fluorine atoms.



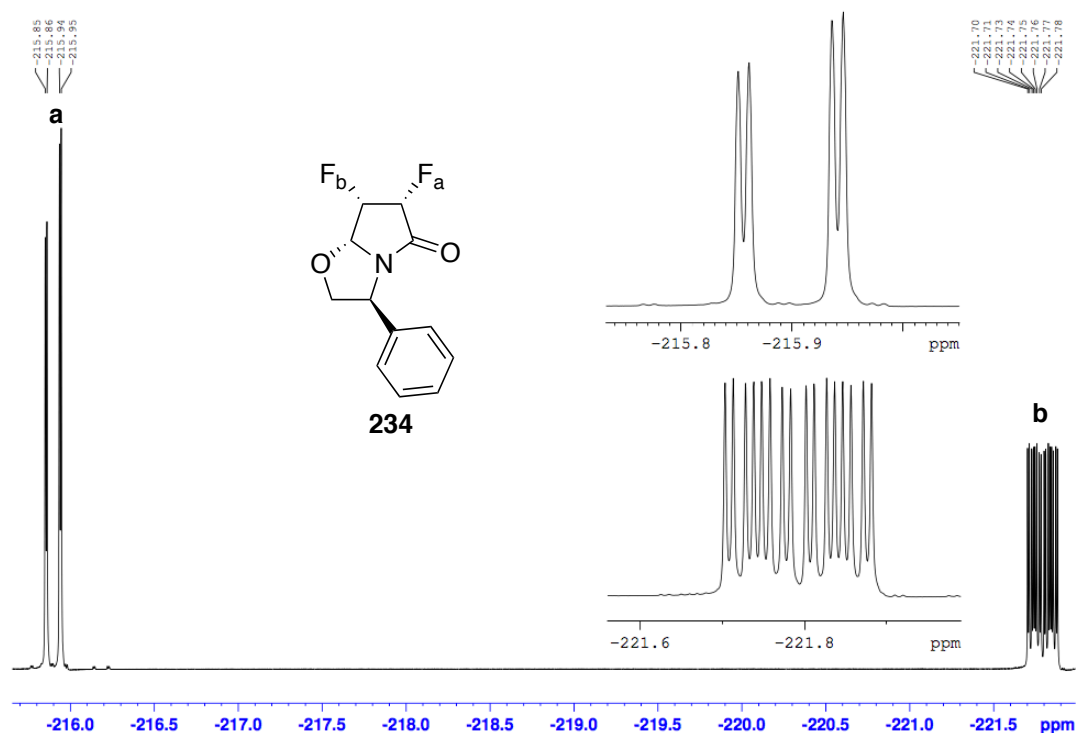
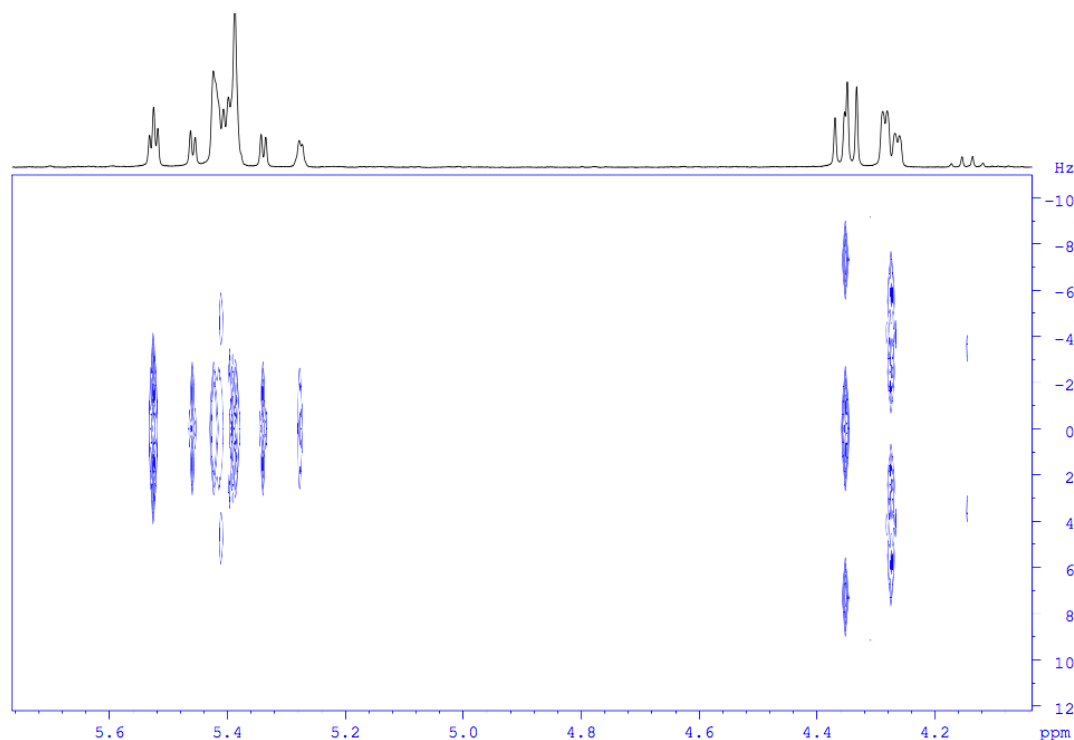


**Figure 2.20:**  $^{19}\text{F}$  NMR Spectrum of lactam **234**

Assuming a geminal fluorine atom gives a coupling constant in the  $^1\text{H}$  NMR spectrum of roughly 50 Hz and a vicinal fluorine atom gives a coupling constant of approximately 20 Hz, it is reasonable to expect that the signal for the C3 proton would be made up of four doublets each integrating for of 0.25 H spread over a wide area. Similarly, the protons at C4 and C5 would have multiple fluorine couplings, resulting in the greatly overlapped region between of the  $^1\text{H}$  NMR spectrum.

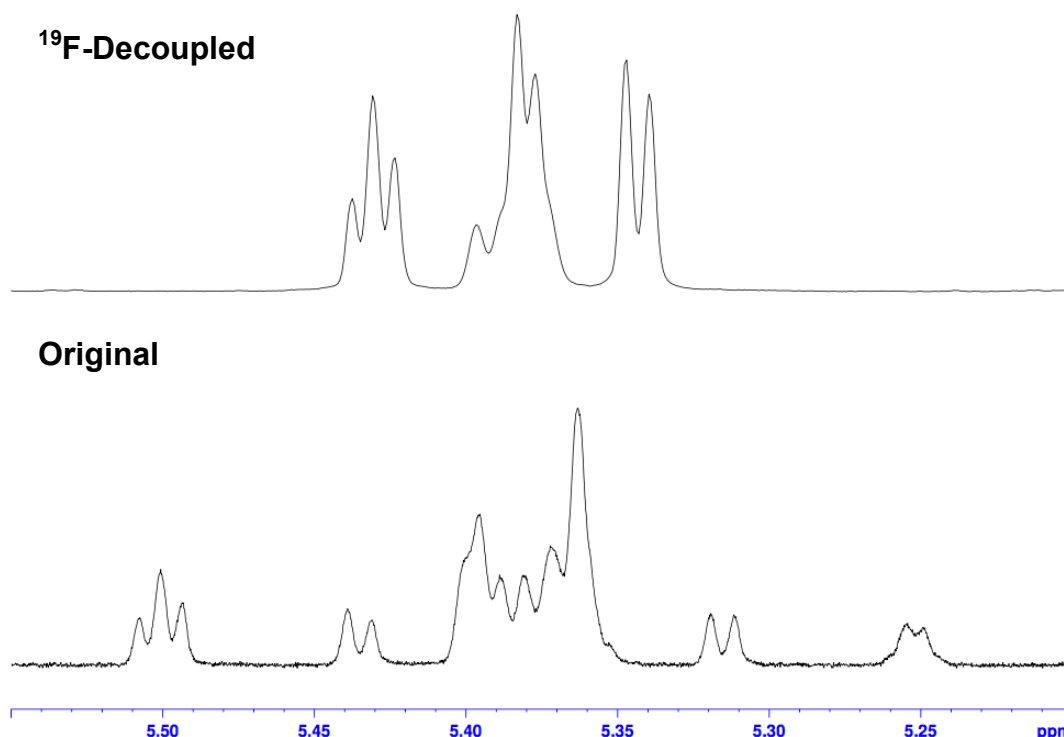
To provide evidence to support this structural assignment, specific  $^1\text{H}$  based NMR experiments were run of compound **234**. First, a J-Resolved (or JRES) spectrum of the compound was obtained, which separates the chemical shift and scalar couplings of resonances and projects these onto two axes (Figure 2.21). This breaks down in the 2D space the number of actual resonances present under a given multiplet or apparent resonance (Figure 2.21).<sup>286</sup> The experiment carried out only removed the homonuclear ( $^1\text{H}$ - $^1\text{H}$ ) couplings, which left the region of 5.26-5.50 ppm still hard to resolve. The resonances at 4.25 and 4.32 ppm, for example, which represent the phenylethanol portion of the molecule and thus have no fluorine coupling, have their shift and coupling neatly separated to give one line of resonances each in the x-

dimension and four peaks each in the y-dimension, matching up with their doublet of doublet 1D resonances. Under the fluorine-affected region, there are still at least six overlapping resonances, although it does indicate that the region has fewer individual resonances than might have been determined from the  $^1\text{H}$  NMR spectrum alone.



**Figure 2.21:** JRES spectrum of difluorinated compound **234**

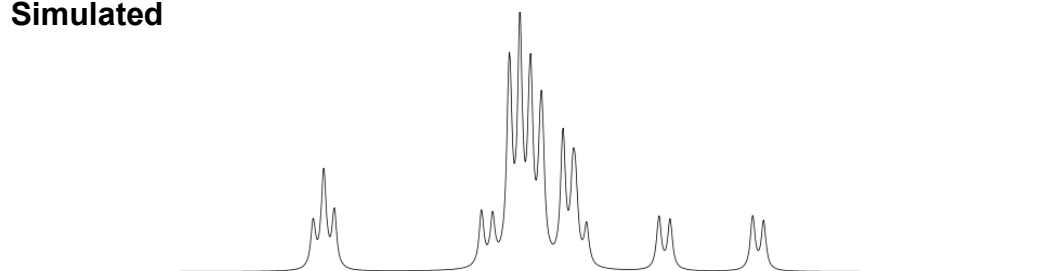
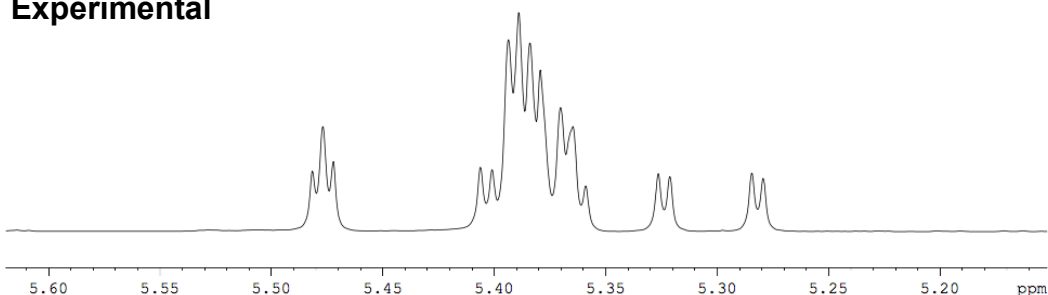
Secondly, a  $^{19}\text{F}$ -decoupled  $^1\text{H}$  NMR spectrum was obtained (Figure 2.22). This proved more effective than the JRES spectrum, simplifying the region into essentially three peaks, where only the  $^1\text{H}$ – $^1\text{H}$  coupling was observed. The resolution was not ideal, but it supported the theory that there were only three or four distinct resonances there, and approximately the chemical shift of each.



**Figure 2.22:**  $^{19}\text{F}$ -decoupled  $^1\text{H}$  NMR spectrum of **234**

The  $^1\text{H}$  NMR spectrum of this compound was also simulated in DAISY, and then compared with the experimental spectrum. Unlike in the case of the fluorohydrin **233**, for difluorinated compound **234** it was necessary to develop an accurate simulation to be able to correctly assign each of the chemical shifts and couplings when reporting the  $^1\text{H}$  NMR spectra. The process was much the same as for **233**, with the number of resonances set first, with best first estimates of their chemical shifts and coupling magnitudes based on the data obtained from the  $^1\text{H}$  and  $^{19}\text{F}$  NMR spectra (Appendix 1). These values were adjusted until the spectrum matched the experimentally obtained spectrum, and the lineshape broadened to show that the assigned coupling constants were reasonable for that spectrum.

Thus, the assignments for this difluorinated compound **234** were derived through the simulation process. This excludes those that were unambiguous – the phenyl multiplets at 7.25–7.29 ppm, 7.30–7.34 ppm and 7.35–7.39 ppm. This allowed for full assignment of the lactam protons, and the agreement between the simulated and experimental spectra supported the structural assignment for the compound.

**Simulated****Experimental**

**Figure 2.23:** Simulated and Experimental spectra of **234**

To provide further support for our assignment, this fluorinated lactam was also recrystallised successfully and an X-ray crystal obtained. This unambiguously established deoxyfluorination had proceeded with inversion of stereochemistry at both sites to give a *cis*-difluorinated bicyclic  $\gamma$ -lactam (Figure 2.24). This demonstrated the utility of this approach for controlling the stereochemistry of fluorination, as the ether substituent can be used to set the stereochemical configuration of the diol in **162**, but does not have any influence on the following fluorination step.

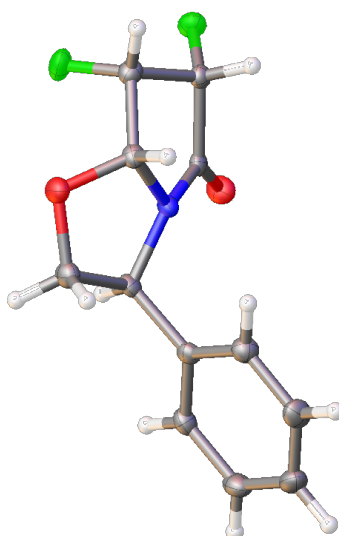
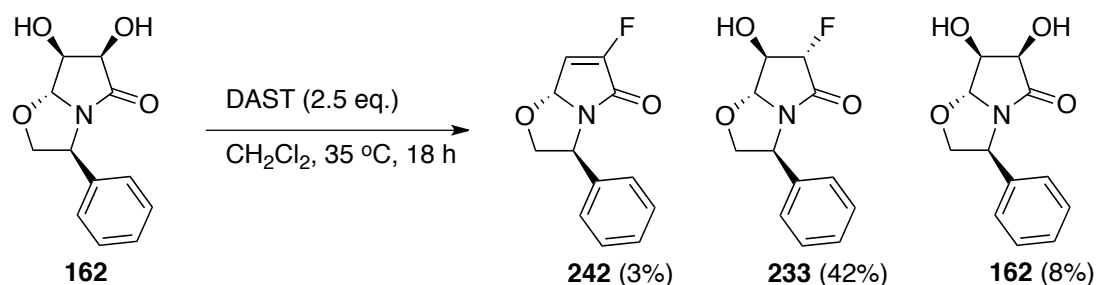


**Figure 2.24:** X-ray crystal structure of difluorinated bicyclic lactam **234**

Given the expense in using large quantities of Deoxofluor<sup>®</sup> to prepare fluorinated derivatives, the reagent DAST was trialled as a potentially more economical alternative. Due to the explosive nature of its decomposition products, these reactions were not carried out above 35 °C.<sup>260</sup> They gave similar overall yields to the Deoxofluor<sup>®</sup> procedure, but there were some noticeable drawbacks. Firstly, a proportion of the elimination product **242** was always present, and the reactions did not proceed to completion (Scheme 2.15). When the reactions were carried out for periods of time longer than 18 hours (up to two days), in the hopes of consuming all of the starting material, the proportion of elimination product increased, while some starting material still remained.



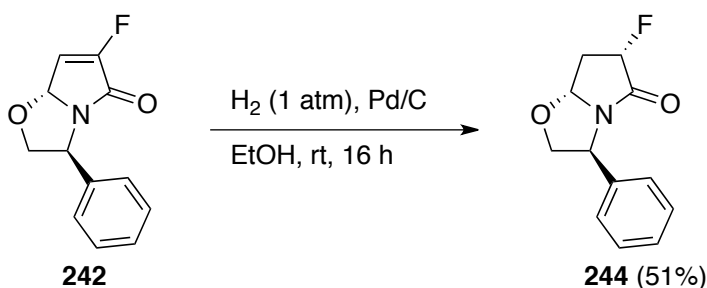
**Scheme 2.15:** Results of DAST fluorination

However, the results were sufficient that it was surmised that scaling up would give usable quantities of both the fluorohydrin and the fluoroalkene, both of interest for preparing a variety of fluorinated GABA analogues. Unfortunately, on increasing the scale above 100-200 mg of diol, a number of unidentified decomposition and by-products were observed, the proportion of which increased with increasing reaction scale. This limited the ability to prepare large quantities of the fluorinated intermediates to carrying out a number of smaller-scale reactions and combining the products for purification. This approach yielded sufficient fluorohydrin **233** for carrying out investigations of the subsequent steps towards synthesising fluorinated GABA analogues. A smaller quantity of the fluoroalkene **242** was isolated, which allowed for some investigation towards reaching monofluorinated GABA analogues (Section 2.6.2)

### 2.6.2 Routes To Monofluorinated Analogues

Investigations of fluorination pathways were carried out, to demonstrate the possibility of using the diol **162** as the starting point for a wide variety of fluorinated GABA analogues. As the above methods led to a fluoroalkene, fluorohydrin and difluoro species, it was seen as desirable to have efficient pathways to monofluorinated analogues.

To achieve this from the fluoroalkene **242**, it was clear that simple hydrogenation would likely be the most efficient route to give a monofluorinated species with a stereogenic centre at C3. We expected that this reaction should give a single product, with addition of hydrogen determined by the ether substituent at C5, forcing it to occur on the opposite face. As such, the fluoroalkene **242** was hydrogenated under a balloon of H<sub>2</sub> overnight, which gave the desired product **244** as a single stereoisomer in a reasonable 51% yield (Scheme 2.16).



**Scheme 2.16:** Hydrogenation of fluoroalkene **242**

The success of this reaction was obvious in the NMR spectra for **244**. Specifically, in the <sup>1</sup>H NMR, the fine <sup>19</sup>F–<sup>1</sup>H couplings observed in the fluoroalkene were replaced by a doublet of triplets for the C3 proton at 5.41 ppm, with the typical geminal coupling of 52.3 Hz, and a coupling with vicinal protons of 8.4 Hz (Figure 2.25). The vicinal <sup>19</sup>F–<sup>1</sup>H couplings were visible in the upfield resonances at 2.28 ppm, which could be rationalised as a dddd with a clear vicinal fluorine coupling of 26 Hz. The other vicinal signal was identified as a complex multiplet from 3.06–3.13 ppm, which clearly by the spread and shape was influenced by the fluorine and a number of adjacent protons, but the exact coupling constants were difficult to determine.

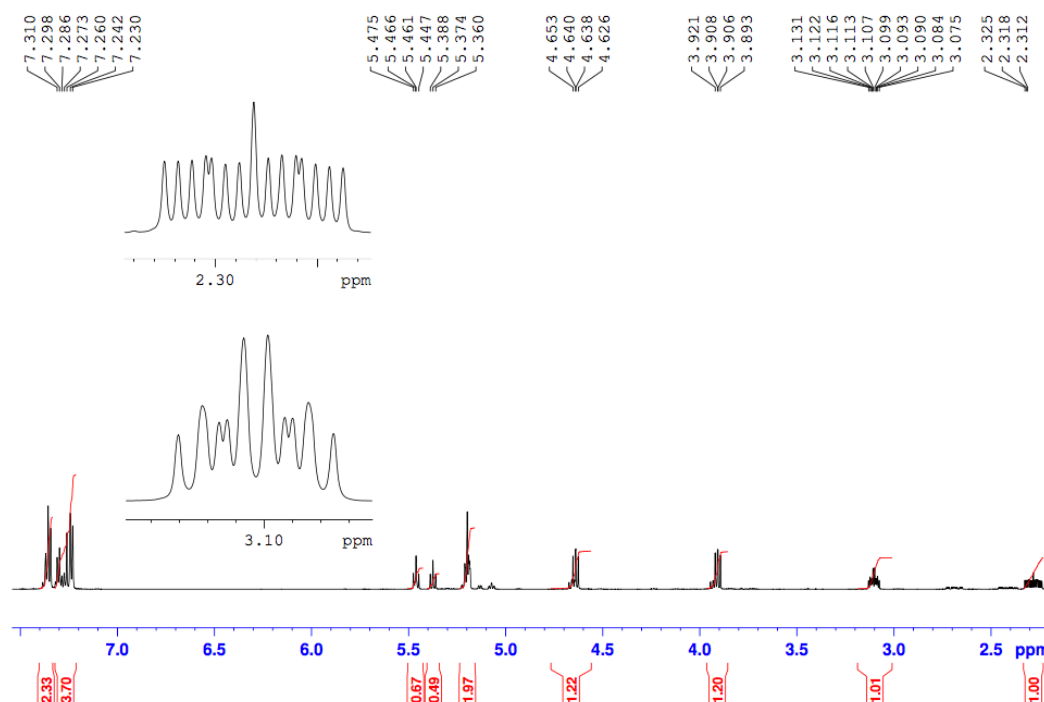
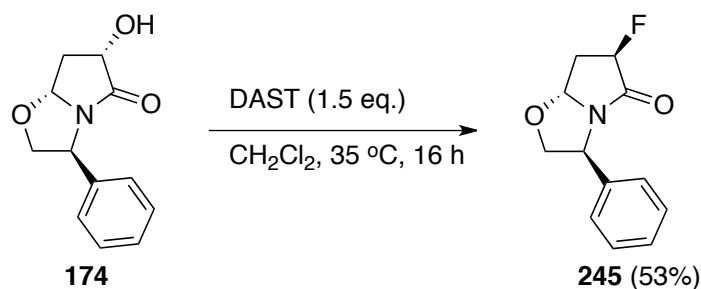


**Figure 2.25:**  $^1\text{H}$  NMR spectrum of hydrogenation product **244**

We theorised that the monofluorinated bicyclic lactam **245** with the opposite stereochemistry at the C3 C–F bond could be prepared by direct deoxyfluorination of the alcohol **174**, synthesised earlier in Chapter 1. This species was treated with an excess of DAST, heated to 35 °C for 16 h (Scheme 2.17). After this time, the majority of the alcohol had converted through to the fluorinated product **245**, in a yield of 53%. However, even after this extended reaction time a reasonable portion of the starting material remained (13% was recovered), highlighting how DAST can be a less effective deoxyfluorination reagent in these systems. Fortunately, all of the unreacted starting material was recovered, and while some decomposition took place no elimination products were observed for this mono-deoxyfluorination.



**Scheme 2.17:** DAST fluorination of alcohol **174**

This mono-fluorinated compound (**245**) was also distinguishable from the diastereomer **244** by NMR spectroscopic analysis. The chemical shifts and coupling constants observed in the  $^1\text{H}$  NMR spectrum were similar to those observed for **244**, but with distinct splitting patterns as a result of the differing fluorine orientation. For example the C3 proton at 5.17 ppm, appeared more as a doublet of doublets of doublets for **245** than the doublet of triplets observed in **244**. The complex resonances at 2.40 ppm and 2.68 ppm were also quite different from those observed in **244**, due to changes of stereochemistry of the C3 centre. The two  $^{19}\text{F}$  NMR spectra likewise both featured a single resonance at approximately the same chemical shift, but for compound **244** appeared as a doublet of doublets of triplets while for the stereoisomer **245** appeared as a doublet of doublets of doublets. These assignments were supported by the  $^{13}\text{C}$  and 2D NMR spectra, and HRMS analysis.

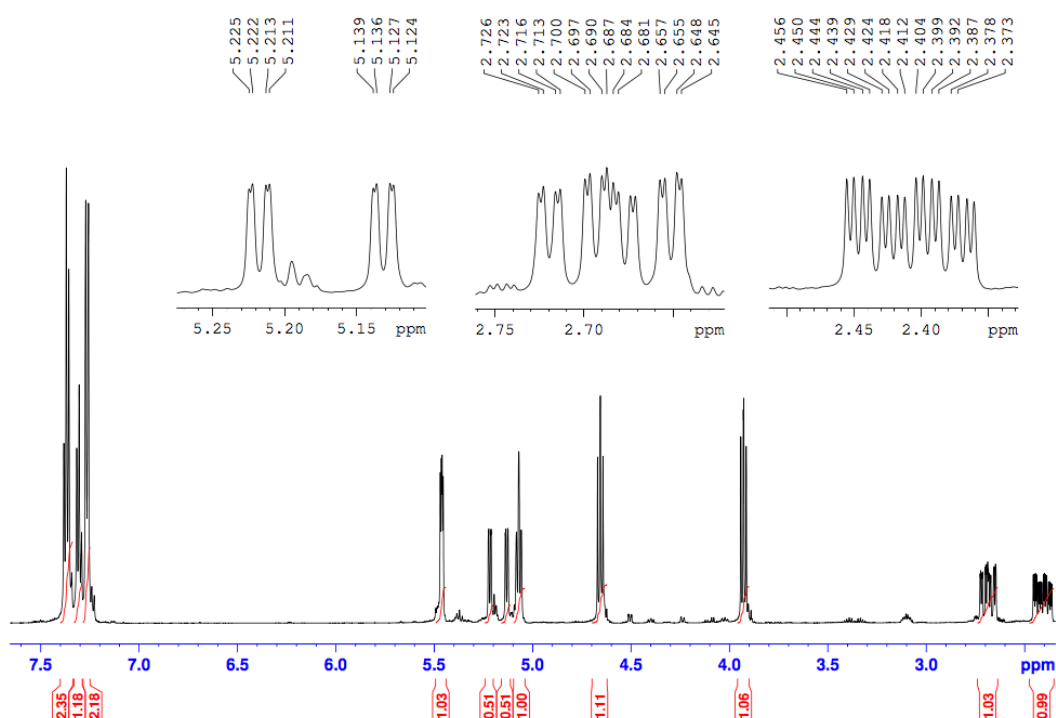
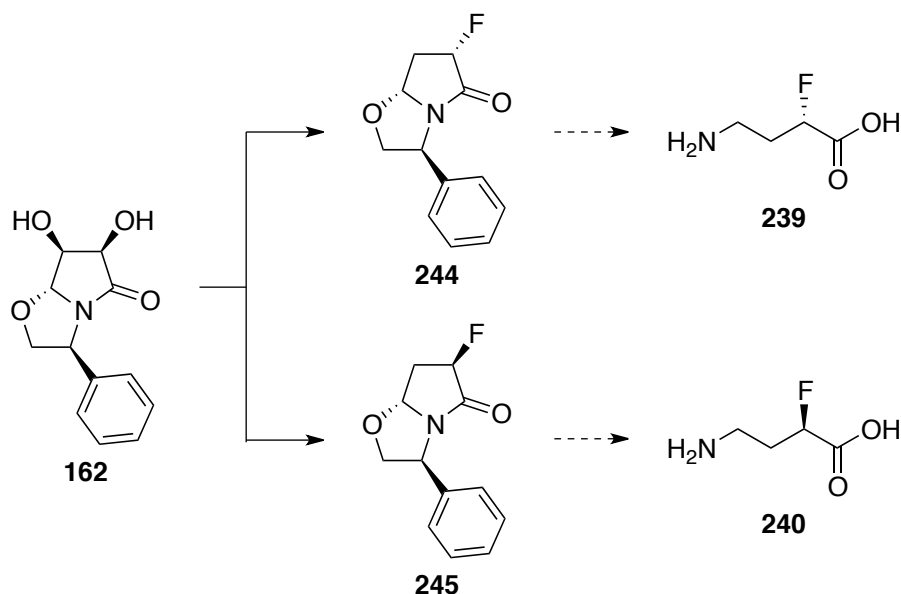


**Figure 2.26:**  $^1\text{H}$  NMR spectrum of fluorinated bicyclic lactam **245**

These results are significant because they demonstrate that not only is it possible to form a variety of fluorinated GABA precursors using the diol **162**, but it is possible to reach both enantiomeric forms of 2-fluoro- $\gamma$ -aminobutyric acid *via* a common intermediate (Scheme 2.18). This has established straightforward routes to reach intermediates for two monofluorinated, one



fluorohydrin, and one difluorinated GABA analogue, using the oxidation of chiral pyrroles as a starting point. In theory, this gives access to four different stereodefined analogues, with the potential to reach others by exploiting alternative fluorination or hydroxylation techniques starting from the diol **162**, or the bicycle **118**. Given bicyclic lactam **118**'s ability to control stereochemistry of reactions at the alkene, there are many possibilities for potential analogues beyond those prepared here.



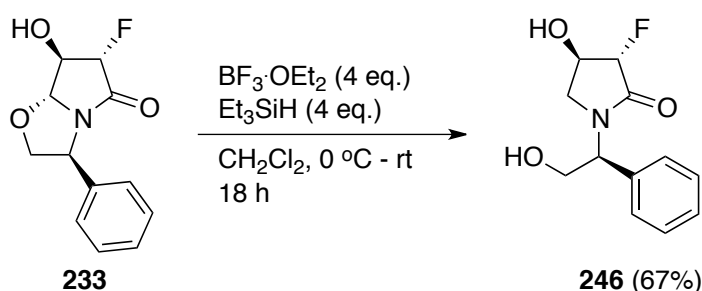
**Scheme 2.18:** Two enantiomers of GABA from a common intermediate

### 2.6.3: Further Transformations Towards Fluorinated GABA Analogues

Once the stereo-controlled synthesis of a range of fluorinated bicycles had been established, it was necessary to investigate their deprotection to yield fluorinated GABA analogues. The most accessible of these, fluorohydrin **233**, was employed as the test substrate. As stated in section 2.5.2, the aim was to first open the ring formed by the ether linkage of the phenylethanol portion, followed by cleavage of the chiral *N*-phenylethanol substituent and subsequent acidic or basic ring-opening of the lactam to give the open chain fluorinated GABA analogue.

The first step investigated was the ring opening at the ether group of C5 of the lactam. As discussed above, in the case where there was no fluorine present in the molecule (i.e. diacetoxo compound **163**), cleaving this bond through generation of an iminium ion was very difficult. However, it was

anticipated that the presence of fluorine at C3 of the lactam would act through hyperconjugation effects to weaken the C–O bond at C5 and hence facilitate ring opening. The influence of the fluorine atom on the C5 position was indicated by the  $^{13}\text{C}$  NMR spectrum of fluorohydrin **233**, through a 9.4 Hz C–F coupling of the resonance at 95.2 ppm. Gratifyingly, this did indeed prove to be the case. When fluorohydrin **233** was treated with an excess of  $\text{BF}_3\cdot\text{OEt}_2$  and TES, a reasonable yield of the ring-opened lactam **246** was formed (Scheme 2.19).



**Scheme 2.19:** Ring opening of fluorohydrin **233**

The structure was supported by an increase in the number of resonances in the  $^1\text{H}$  NMR spectrum, specifically by the appearance of two resonances: a doublet of doublets of doublets at 2.94 ppm and a doublet of doublets at 3.79 ppm, representative of the methylene protons at C5 of the lactam. HRMS analysis gave a result consistent with an increase equivalent of two hydrogen atoms from the bicyclic fluorohydrin **233**. The compound was also recrystallised and an X-ray crystal structure obtained, supporting the reduction (Figure 2.27).

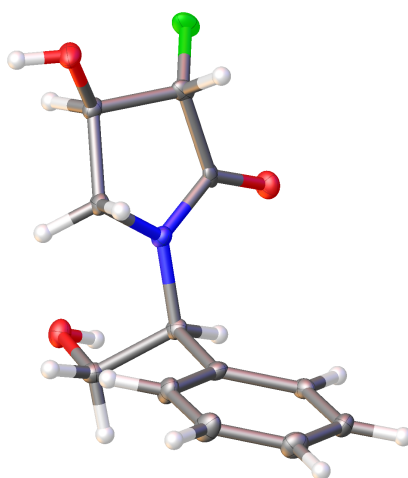
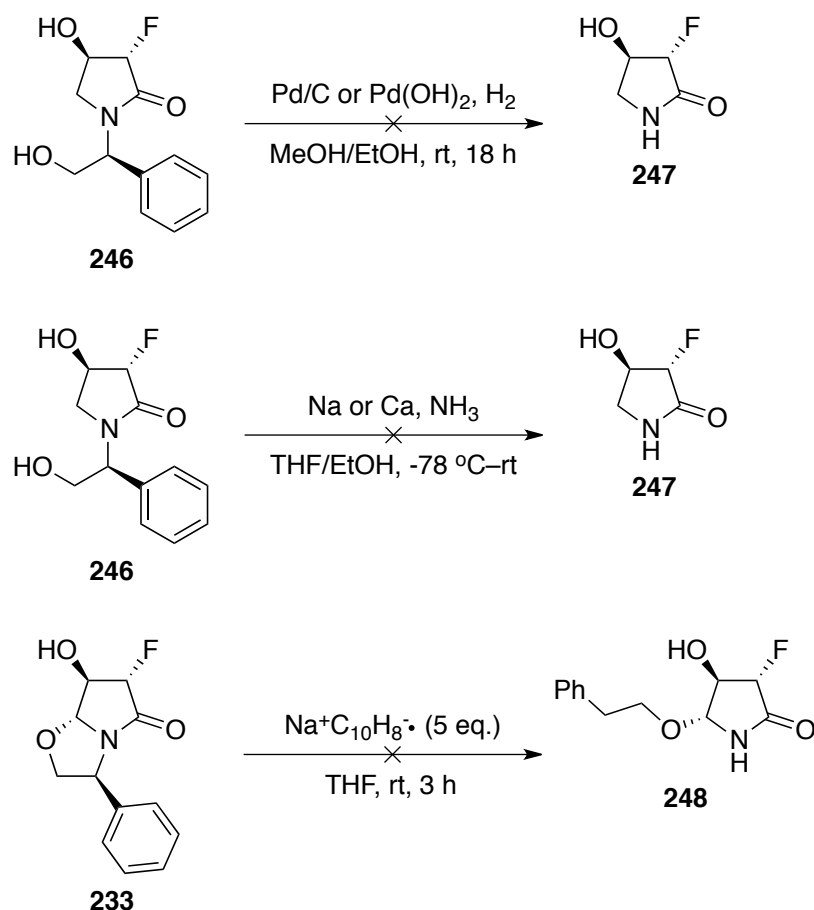


**Figure 2.27:** X-ray crystal structure of the ring-opened fluorohydrin **246**

The next step was to remove the *N*-phenylethanol substituent, prior to the final ring-opening. Given that this should behave similarly to an *N*-benzyl group, the first attempts were hydrogenolysis. However, use of both Pd/C and Pd(OH)<sub>2</sub>, provided no reaction even after extended reaction times. There are many examples in the literature of the cleavage of these groups from pyrrolidines but not for pyrrolidinones. Evidently the amide affects the reactivity, and the introduction of an adjacent fluorine atom had no impact on this.

Based on Meyers' work, a dissolving metal reduction was also attempted (Scheme 2.20).<sup>103</sup> Ammonia was condensed into a cold solution of the fluorohydrin **246** containing sodium or calcium metal and allowed to warm slowly to room temperature. In neither case was the desired product obtained, with only decomposition of the starting material observed.



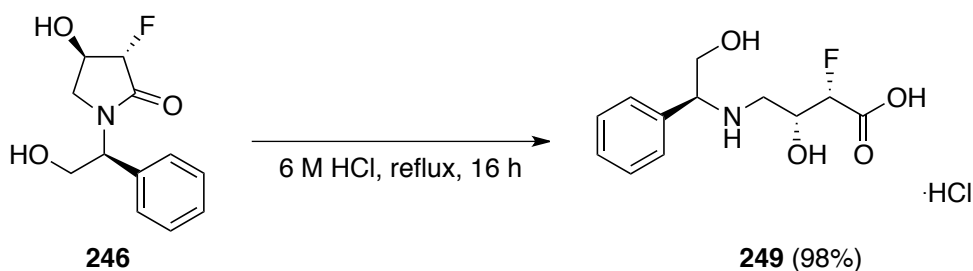
**Scheme 2.20:** Attempts to remove *N*-substituent of fluorohydrin **246**

Another approach was attempted on the closed bicycle **233**, treating the fluorohydrin with sodium naphthalenide in an attempt to cleave the benzyl

group and open the oxazolidine ring (Scheme 2.20).<sup>287</sup> Unfortunately in this case also no reaction was observed.

As these efforts to remove the *N*-substituent from the pyrrolidinone proved fruitless, it was decided to change tack and instead investigate opening the pyrrolidinone to give an acyclic species first. It was believed that this would remove the difficulties associated with cleaving the *N*-substituent from a cyclic amide and make hydrogenolysis a viable approach again.

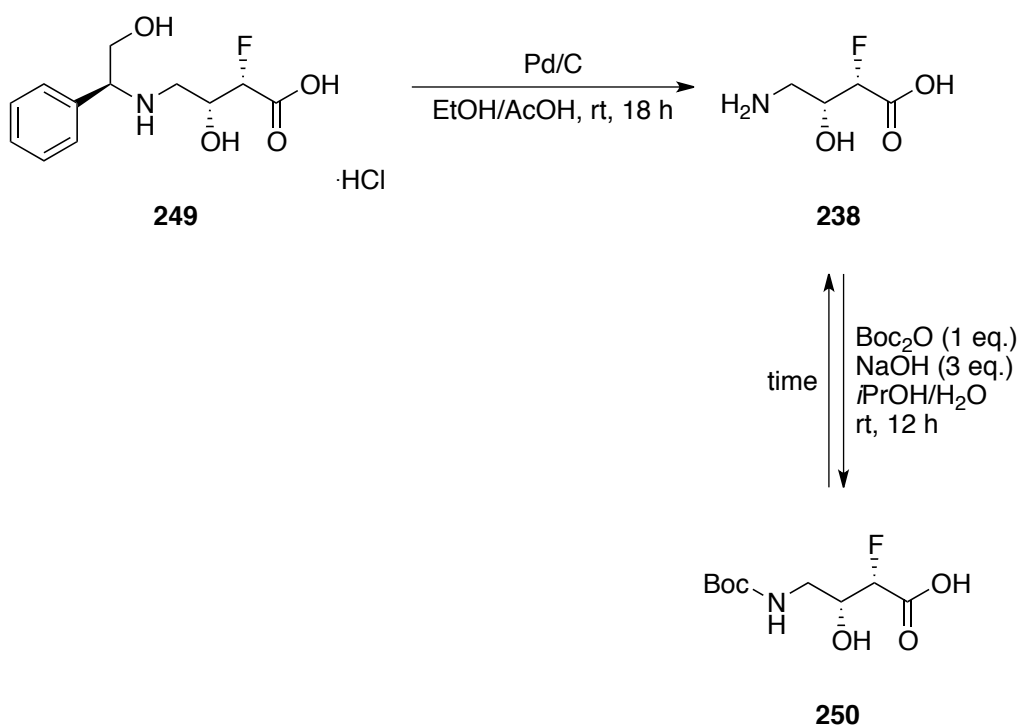
The ring-opening of fluorohydrin **246** was carried out by simply stirring in hydrochloric acid for several hours (Scheme 2.21). This gave the desired acyclic compound **249** as the hydrochloride salt in near-quantitative yield. The <sup>1</sup>H and <sup>13</sup>C NMR spectra were consistent with what would be expected for this transformation. A doublet at 5.01 ppm with a 47.7 Hz coupling in the <sup>1</sup>H NMR spectrum represented the proton geminal to the fluorine atom and adjacent to the carboxylic acid. Changes in the <sup>1</sup>H and <sup>13</sup>C NMR spectra were noticeable but not major, however other spectroscopic techniques supported the outcome. In the IR spectrum, the carbonyl stretch of the acid appears at 1730 cm<sup>-1</sup>, compared with the carbonyl stretch in lactam **246** at 1690 cm<sup>-1</sup>. HRMS analysis gave an exact mass consistent with the, protonated amino acid.



**Scheme 2.21:** Acidic ring-opening of pyrrolidinone **246**

The final step towards the synthesis of fluorinated GABA analogues was to identify a method to cleave the *N*-substituent to give the free amino acid. Hydrogenolysis was again tried, this time with more success. First attempts examined using both Pd/C and Pd(OH)<sub>2</sub> as catalysts, under both 1 atm of hydrogen and at elevated pressures on a shaker-hydrogenator. Results ranged from no reaction to decomposition in most cases. Importantly, when the reaction was carried out with acetic acid present, the <sup>1</sup>H NMR spectrum

of the crude reaction mixture gave clear signs of the phenylethanol fragment disappearing with the remaining resonances staying much the same as those in the precursor. Therefore the product was tentatively assigned as **238** (Scheme 2.22). Difficulties were encountered in attempting to purify this compound, as it proved to be (unsurprisingly) insoluble in organic solvents and highly polar, and the small amount of product obtained did not prove amenable to recrystallization by dissolving in hot MeOH or vapour diffusion methods.



**Scheme 2.22:** Attempts to reach a characterisable GABA analogue

With a view to providing further evidence that these reactions could be successful, the presumed amino acid **238** was treated with Boc<sub>2</sub>O in the hopes of giving an *N*-protected species **250** that might be more easily purified and characterised. The <sup>1</sup>H NMR spectrum of the crude reaction mixture appeared promising, with a singlet peak integrating for 9 protons appearing at 1.38 ppm. However, after 24 h another compound started to appear in the <sup>1</sup>H NMR spectrum, and over the course of several days increased in quantity until there was nearly a 1:1 ratio of it with the desired product. The chemical shifts of this second compound matched those of the amino acid **238**. This led to the conclusion that the Boc-protected product was deprotecting itself. As the other key functionality in the molecule is a

carboxylic acid with an adjacent fluorine atom, similar to TFA, it was theorised that the carboxylic acid of this molecule was acidic enough to slowly promote cleavage of the Boc group. Addition of 2 drops of trifluoroacetic acid to the NMR sample (in D<sub>2</sub>O) led to complete reversion within 12 hours, supporting this theory.

While this result was not helpful for reaching a pure Boc-protected analogue, it did provide further support for the observation that the *N*-phenylethanol fragment had been successfully removed *via* the hydrogenation procedure. Additionally, it was possible through analysis of the HSQC NMR spectrum to assign the <sup>1</sup>H and <sup>13</sup>C NMR resonances of amino acid **238**, which showed that there were four proton resonances for the carbon backbone and four carbon atoms in the molecule, each coupled with the fluorine atom. This was consistent with the expected structure. HRMS analysis of the sample also indicated that the desired amino acid had been formed.

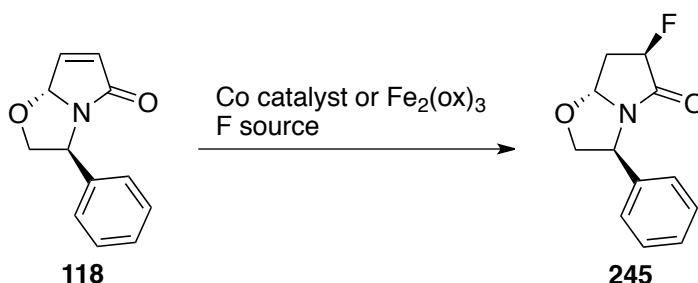
Hunter and colleagues observed that for *syn*-difluorinated GABA analogues the  $\alpha$ H- $\beta$ H,  $\alpha$ F- $\beta$ H and also the  $\beta$ H- $\gamma$ H NMR coupling constants were either relatively high or low, which implied a rigid zigzag conformation.<sup>223</sup> In the *anti*-difluorinated analogues the coupling constants tended to be closer to each other. For the fluorohydrin analogue **238**, the  $\beta$ H- $\gamma$ H coupling constants were determined to be 2.9 and 9.2 Hz, a more pronounced difference than that observed even in the *syn*-difluorinated analogues prepared by Hunter. However, the key  $\alpha$ F- $\beta$ H coupling constant was determined to be 24 Hz, in the middle of the range observed in Hunter's difluorinated analogues, and the  $\alpha$ H- $\beta$ H coupling constant of 1.7 HZ was closer to those observed in the *anti*-difluorinated compounds. This indicated that for the fluorohydrin analogue **238** NMR spectroscopic data alone is not sufficient to establish the conformation. As such, preparation of an analogue of **238** stable to crystallisation would be valuable for defining the conformation through an X-ray crystal structure. Alternatively, computational methods could be explored to determine the lowest energy conformers for this compound.

## 2.7 Conclusions

A route to a range of fluorinated bicycles starting from bicyclic diol **162** has been established, giving the potential for preparing a variety of fluorinated GABA analogues varying in substitution pattern and stereochemistry. Spectroscopic evidence was acquired to support that the novel fluorinated GABA analogue **238** had been successfully reached as a proof of concept for this synthesis, but due to time constraints this procedure could not be repeated on a larger scale and the product isolated as desired. For future work, this synthesis would be repeated and then applied to the other fluorinated bicyclic lactams prepared, to give a full suite of monofluorinated and difluorinated GABA analogues. NMR spectroscopic analysis, X-ray crystallography and computational modelling could then be used to determine the new analogues' conformations and compare them with the known compounds.

This would be assisted by further development of the approach to reaching the key fluorinated intermediates to make it more scalable, or by performing the reactions in parallel. Potential availability of new deoxyfluorinating reagents such as PyFluor, or their preparation, could also make this step in the synthesis proceed more selectively.<sup>265</sup>

Finally, alternative methods for introducing fluorine to the bicycle **118** could be explored. Direct hydrofluorination of the alkene might be a convenient approach at least for reaching monofluorinated analogues without the need to go through intermediate diol **162** (Scheme 2.23).<sup>288,289</sup>



**Scheme 2.23:** Potential direct hydrofluorination route to fluorinated analogues

## Chapter 3: Development and Applications of Pyrroles and Pyrrolidines Prepared from Polygodial

### 3.1 Introduction to Polygodial and Derivatives

#### 3.1.1 Source and isolation of polygodial

Polygodial (**251**, Figure 3.1) is a bicyclic sesquiterpenoid natural product isolated from the leaves of *Tasmannia lanceolata* in Tasmania and south-eastern Australia,<sup>290</sup> and from varieties of *Winteraceae*,<sup>291</sup> *Polygonaceae*<sup>292</sup> and *Canellaceae*.<sup>293</sup> It has also been isolated from some varieties of marine sponges and molluscs.<sup>294,295</sup> It is a chiral molecule with three contiguous stereogenic centres, and a 1,4-dialdehyde system made up of an allylic and a pseudo-neopentyl aldehyde. Moreover, its carbon backbone features in the structure of many other natural products.

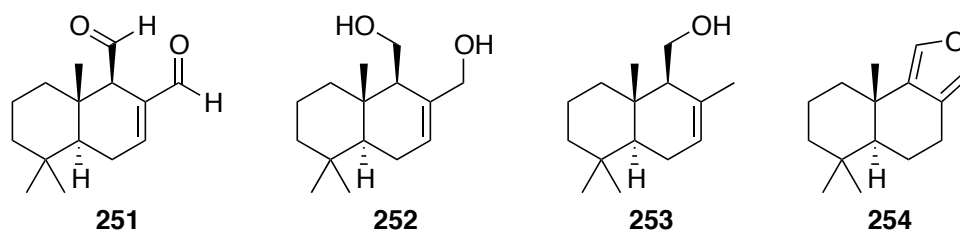


**Figure 3.1:** Polygodial (**251**), drimendiol (**252**), (–)-drimenol (**253**) and euryfuran (**254**)

Recent work has established a versatile and efficient method of pressurised hot water extraction (PHWE) of natural products from plant material using a household espresso machine.<sup>296</sup> This was applied to the extraction of polygodial from dried leaves of *T. lanceolata* bred to have high polygodial content, such that it was possible to isolate the compound in high purity and gram quantities in a matter of hours.<sup>297</sup> Further to this, polygodial was used as a starting point to rapidly prepare some structurally similar natural products: drimendiol (**252**), (–)-drimenol (**253**) and euryfuran (**254**).<sup>298–300</sup> This methodology showed that it was viable to isolate polygodial from plants and employ it as a complex chiral scaffold for the synthesis of natural products and their derivatives, which remain of significant interest in drug design.<sup>301</sup>

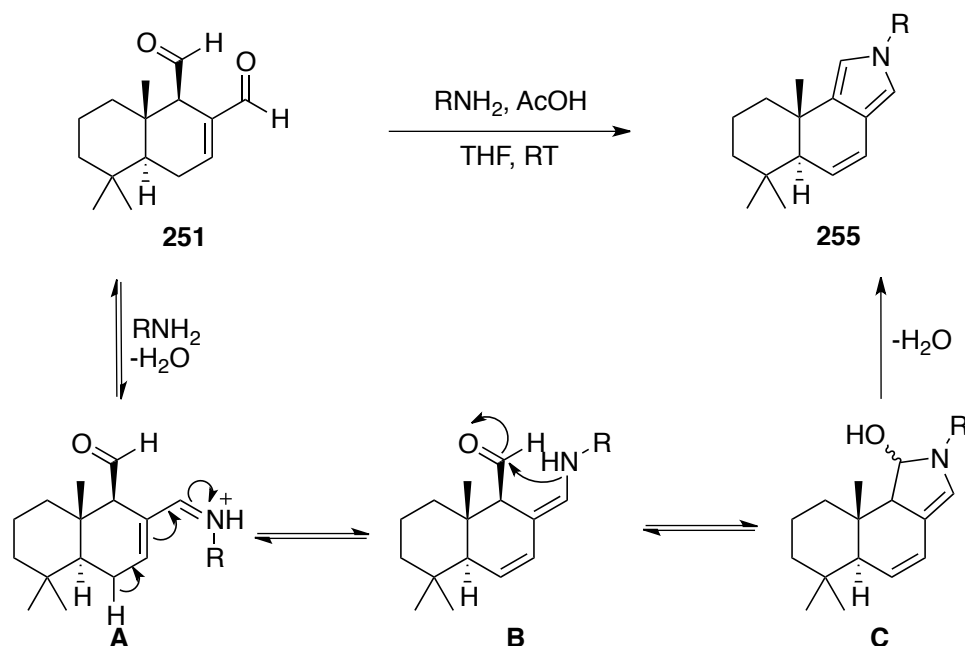


### 3.1.2 Biological Activity and Mechanism

Polygodial is reported to have a diverse range of biological activities and applications, including antifouling activity,<sup>302</sup> activity as a deterrent or anti-feedant for insects,<sup>295,303,304</sup> antibacterial and antiparasitic activity,<sup>305-307</sup> anti-fungal activity,<sup>308-310</sup> anti-allergic and anti-inflammatory activity.<sup>311</sup> It also has vanilloid and antinociceptive activity, giving similar responses to capsaicin.<sup>312-317</sup>

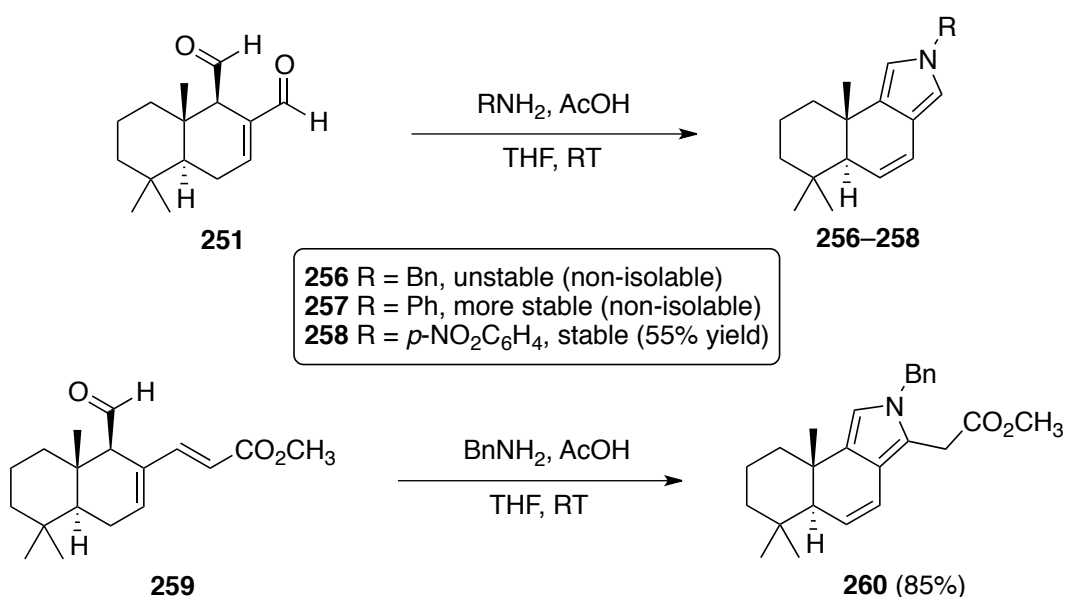
Its biological activity has been theorised to involve the 1,4-dialdehyde undergoing Paal–Knorr-type reactions with an amine group, such as that of lysine in cells, to form pyrroles.<sup>318</sup> This hypothesis was given some support in early investigations where <sup>1</sup>H NMR monitoring experiments suggested the formation of a pyrrole-like product when polygodial and methylamine were reacted under pseudo-biological conditions.<sup>319,320</sup> However, the unsaturated pyrrole product of this reaction was not isolable.

Recent work by Kornienko and colleagues aimed to build on this research and show that a modified Paal–Knorr reaction of polygodial with amines could yield pyrrole products similar to those understood to be involved in the biological activity.<sup>321</sup> TLC analysis suggested polygodial reacted with benzylamine in the presence of an acid catalyst, but that any pyrrole products formed swiftly decomposed and were not isolable. This was consistent with previous reports.<sup>319,320</sup> They proposed a mechanism for the reaction where the endocyclic double bond present in polygodial shifts as the aromatic ring is formed, and that this product is unstable and likely decomposes *via* some oxidative pathway (Scheme 3.1). However, they were able to form more stable pyrroles using electron- deficient amines such as aniline and 4-nitroaniline, which supported their hypothesis of the double bond shifting (Scheme 3.2).



**Scheme 3.1:** Mechanism for pyrrole formation and alkene shift in Kornienko's work

They also had success in forming pyrroles from derivatised polygodial.<sup>322</sup> In these cases they carried out Wittig reactions on the allylic aldehyde with a range of ylides, and then the pyrrole formation by conjugate addition and imine formation. In these cases, the pyrrole products formed were more stable to isolation, although only one of the Wittig precursors was tested in anti-cancer studies to gauge their potential effectiveness (Scheme 3.2).

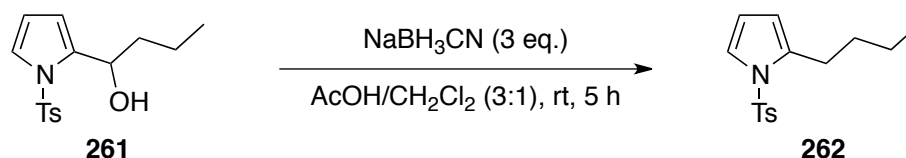


**Scheme 3.2:** Examples of polygodial-derived pyrroles synthesised by Kornienko and colleagues

### 3.1.3 Goals and Strategy

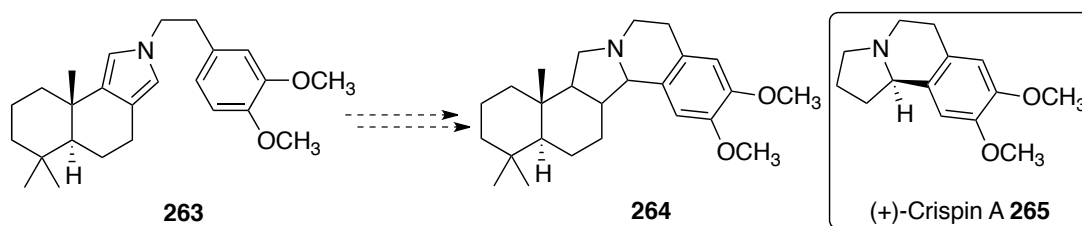
The goals for this project were twofold: firstly, to develop an approach to synthesising stable *N*-alkylpyrroles and pyrrolidine species from polygodial. Secondly, to take these molecules to form novel natural product analogues, thus further illustrating the potential for polygodial to be used as an advanced scaffold in the synthesis of valuable biologically active compounds.

For the first goal, the intention was to optimise the pyrrole formation reaction conditions developed by Kornienko and colleagues to remove the double bond that seems to impart such instability to any *N*-alkylpyrroles formed. Previous experience in the group of synthesis and reduction of pyrroles led us to postulate that an approach combining pyrrole synthesis with reduction of any unstable intermediates could be a viable option. Prior work in the Smith group demonstrated that unstable  $\alpha$ -hydroxypyrroles could be reduced to stable alkyl derivatives by employing sodium cyanoborohydride in acetic acid (Scheme 3.3).<sup>29,323</sup> We envisioned using similar conditions for the pyrrole formation reaction to trap and reduce unstable intermediates/pyrroles.



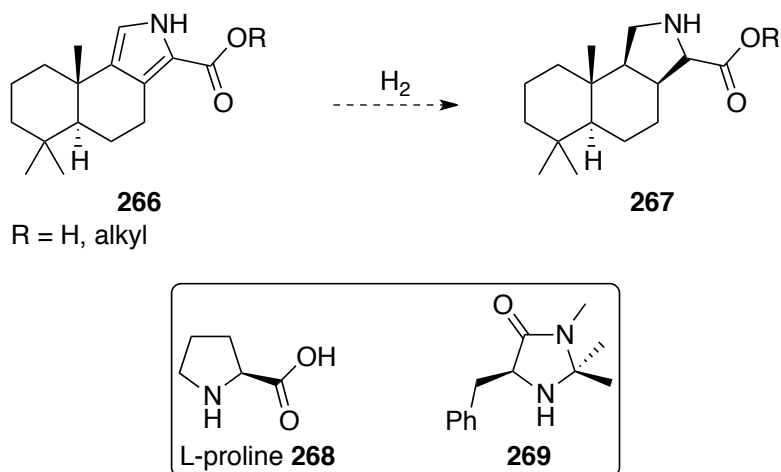
**Scheme 3.3:** Example of sodium cyanoborohydride reduction of an  $\alpha$ -hydroxypyrrole

Assuming this was successful, we had a number of additional goals for applications for these polygodial-derived pyrroles. Firstly, oxidation of these pyrroles by our established methods would provide rapid access to highly functionalised chiral intermediates.<sup>62</sup> It would be interesting to observe the regioselectivity and stereoselectivity (if any) that would be observed under such conditions, i.e. what impact the stereogenic centres in the polygodial backbone would have on transformations to the adjacent pyrrole. This would make it possible to access novel analogues of a range of natural products, such as (+)-crispin A (**265**, Scheme 3.4), an antifungal natural product.<sup>324</sup> An *N*-dimethoxyphenethyl substituted pyrrole derivative such as pyrrole **263** was seen as a viable starting point for this synthesis (Scheme 3.4)



**Scheme 3.4:** Proposed starting material for (+)-crispin A analogue target

Synthesis of an *N*-H pyrrole derivative would also be of interest as a starting point for accessing chiral secondary amines. Through hydrogenation of substituted pyrroles such as **266**, chiral pyrrolidines **267** could be reached. These could provide interesting substrates for asymmetric organocatalysis (Scheme 3.5). For example, as a replacement for L-proline (**268**) in Hajos–Parrish reactions,<sup>325</sup> Aldol additions<sup>326–329</sup> or Mannich reactions.<sup>330–334</sup> They could also potentially serve as substitutes for McMillan’s catalyst (**269**) in Diels–Alder and other cycloaddition reactions.<sup>335,336</sup>



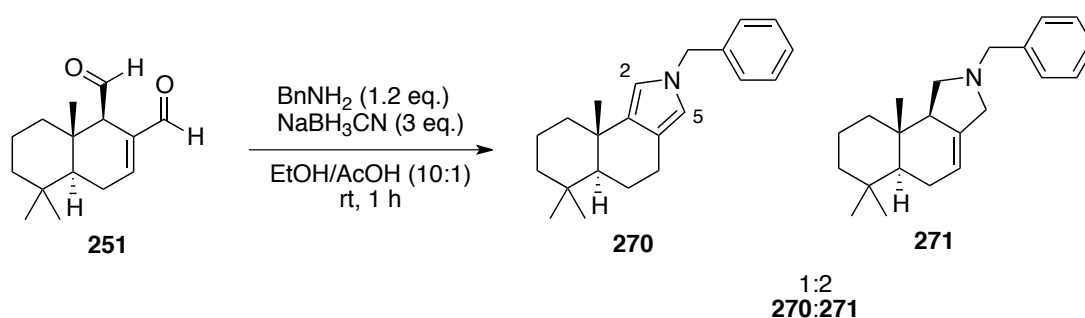
**Scheme 3.5:** Potential applications for *N*-H pyrroles prepared from polygodial

## 3.2 Results and Discussion

### 3.2.1 Development of Selective Pyrrole/Pyrrolidine Syntheses

In line with our goals outlined above, a simple strategy was devised for a test reaction where polygodial, benzylamine and a reducing agent (sodium cyanoborohydride) would all be mixed in a solution of 10:1 ethanol:acetic acid, under an inert atmosphere, and stirred until TLC analysis indicated complete consumption of the polygodial (Scheme 3.6).

This approach led to the formation of two different products, that were isolated by flash column chromatography. One featured resonances in the  $^1\text{H}$  NMR spectrum at 6.31 (a singlet) and 6.37 ppm (a doublet with very fine coupling of 2.2 Hz), and no evidence of any remaining alkene (Figure 3.2). This was consistent with the formation of a pyrrole, where the C5 proton was potentially demonstrating some weak coupling with the nearest polygodial backbone methylene proton. This indicated successful formation of the *N*-benzylpyrrole **270**, with the destabilising alkene removed through reduction, and was supported by subsequent HRMS analysis.



**Scheme 3.6:** First test of pyrrole formation reaction

The second product isolated featured no  $^1\text{H}$  NMR resonances indicative of a pyrrole, but did include similar resonances indicating incorporation of the benzylamine, and a singlet at 5.37 ppm characteristic of the alkene in polygodial still being present (Figure 3.2). With HRMS analysis supporting this it was identified as the *N*-benzylpyrrolidine **271**, which is likely formed through a competitive reductive amination mechanism (*vide infra*). The stereochemical configuration at the pyrrolidine position C3 was assigned as *R*, based on the assumption that the stereochemistry of the pseudo-neopentylaldehyde in polygodial would not be altered through the reductive amination. The ratio of pyrrole:pyrrolidine was 1:2, indicating that the pyrrolidine reductive amination pathway is favoured when all of the reagents are added to the reaction at the same time.

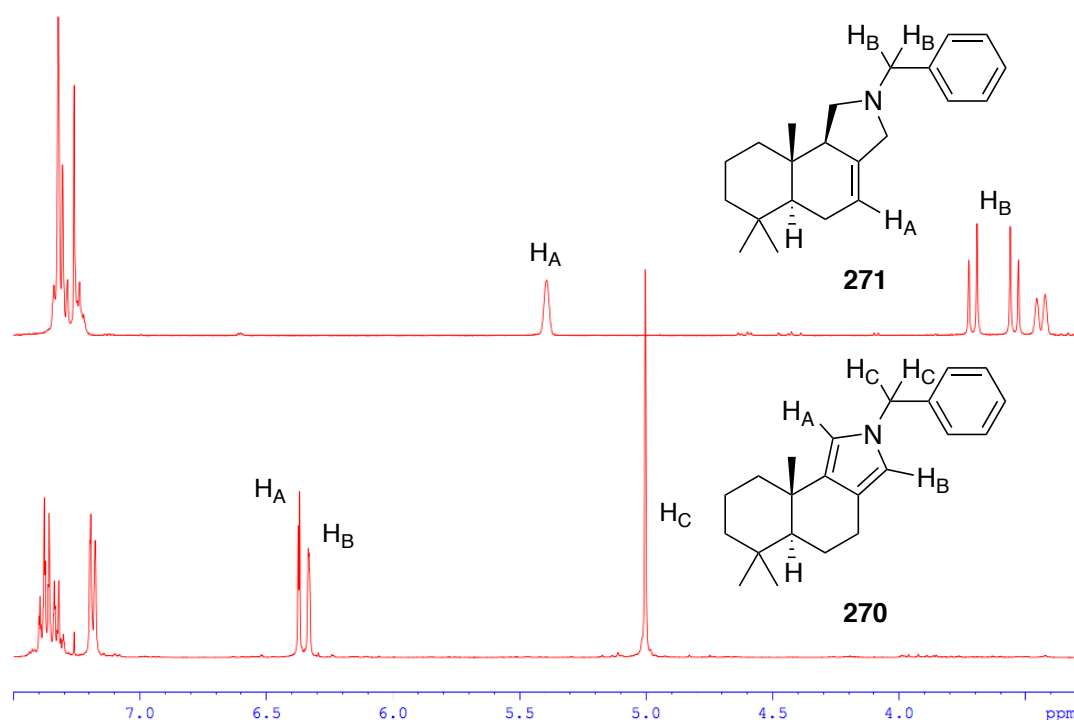
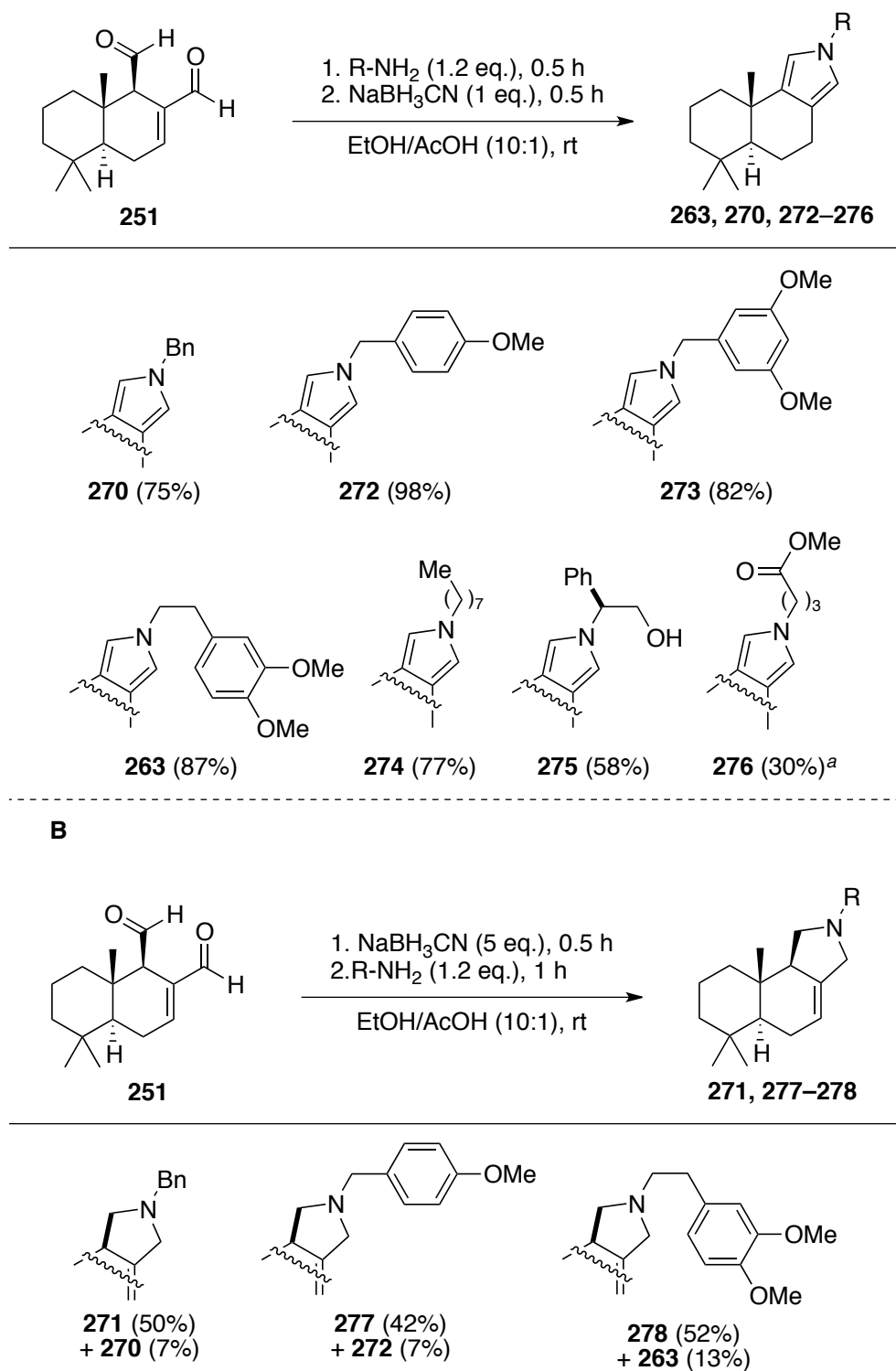


**Figure 3.2:** Key peaks in the pyrrole and pyrrolidine NMR spectra

To see whether the reaction conditions could be altered to favour pyrrole formation over the double reductive amination, the reaction was repeated where the amine was added first and the sodium cyanoborohydride only added once TLC analysis indicated complete consumption of the polygodial, which occurred within 30 minutes (Scheme 3.7). In this way, all of the polygodial may react to form a pyrrole derivative before reduction occurs, and as such there would be no imine present to be reduced by the sodium cyanoborohydride. This precludes any formation of the pyrrolidine product **271**, with the reaction giving only the desired pyrrole **270** in a 75% yield. The reaction was repeated with reduced amounts of sodium cyanoborohydride, and it was found to proceed smoothly with just 1 molar equivalent added.

This approach was shown to be applicable across a range of alkylamines, giving good to excellent yields of the desired pyrroles (Scheme 3.7). Difficulties were only encountered in the preparation of the GABA methyl ester derivative, for which GABA methyl ester hydrochloride was used as the amine starting material. In this case pyrrole **276** was not observed under the conditions described above. As the only difference was the use of an HCl salt, buffering the system with 2 eq. of sodium acetate was attempted. In this

way it was possible to reach pyrrole **276**, albeit in a lower yield than those observed for the other alkylamines. When NaOH was used to buffer the system similar results were obtained.



**Scheme 3.7:** Pyrrole and Pyrrolidine Syntheses. <sup>a</sup>The reaction was performed using  $\gamma$ -aminobutyric acid methyl ester hydrochloride and NaOAc (2.4 eq.).

Given the success in biasing the reaction to give only pyrrole products, the opposite was then attempted to give only the reductive amination pyrrolidine products (Scheme 3.7). This was investigated by first stirring polygodial with an excess of sodium cyanoborohydride then slowly adding benzylamine, as a dilute solution in EtOH, dropwise through a dropping funnel. Tests with increasing excesses of sodium cyanoborohydride, and increasingly dilute solutions of the benzylamine, led to a ratio of about 8:1 pyrrolidine (**271**):pyrrole (**270**), using 5 eq. of sodium cyanoborohydride and a dilute solution of the amine added drop-wise over 15 minutes. This did not exclusively provide one product, but did ensure that the pyrrolidine was the major product. Given the straightforward chromatographic separation of the two products, it represented an efficient approach to directly access the pyrrolidine substrates. These conditions were also applied to two of the other amines, 2,4-dimethoxyphenylethylamine and 4-methoxybenzylamine. The overall yields were comparable, with the ratio of pyrrolidine:pyrrole between 5:1 and 8:1.

NOESY NMR analysis of the phenethylamine derivative **278** was used to provide support for the assignment of the stereocentre at C3 of the pyrrolidine as *R*-configured. First the C3 methine proton was identified as being the broad signal at 2.36–2.42 in the  $^1\text{H}$  NMR spectrum, and the vicinal methyl substituent identified as the singlet integrating for 3 protons at 0.77 ppm. This assignment was supported by these resonances having mutual couplings in the HMBC NMR spectrum. While these two groups were within three bonds of each other, in the NOESY spectrum there was no observable NOE correlation (Figure 3.3), providing evidence that the methine proton at C3 of the pyrrolidine is oriented away from the vicinal methyl group.



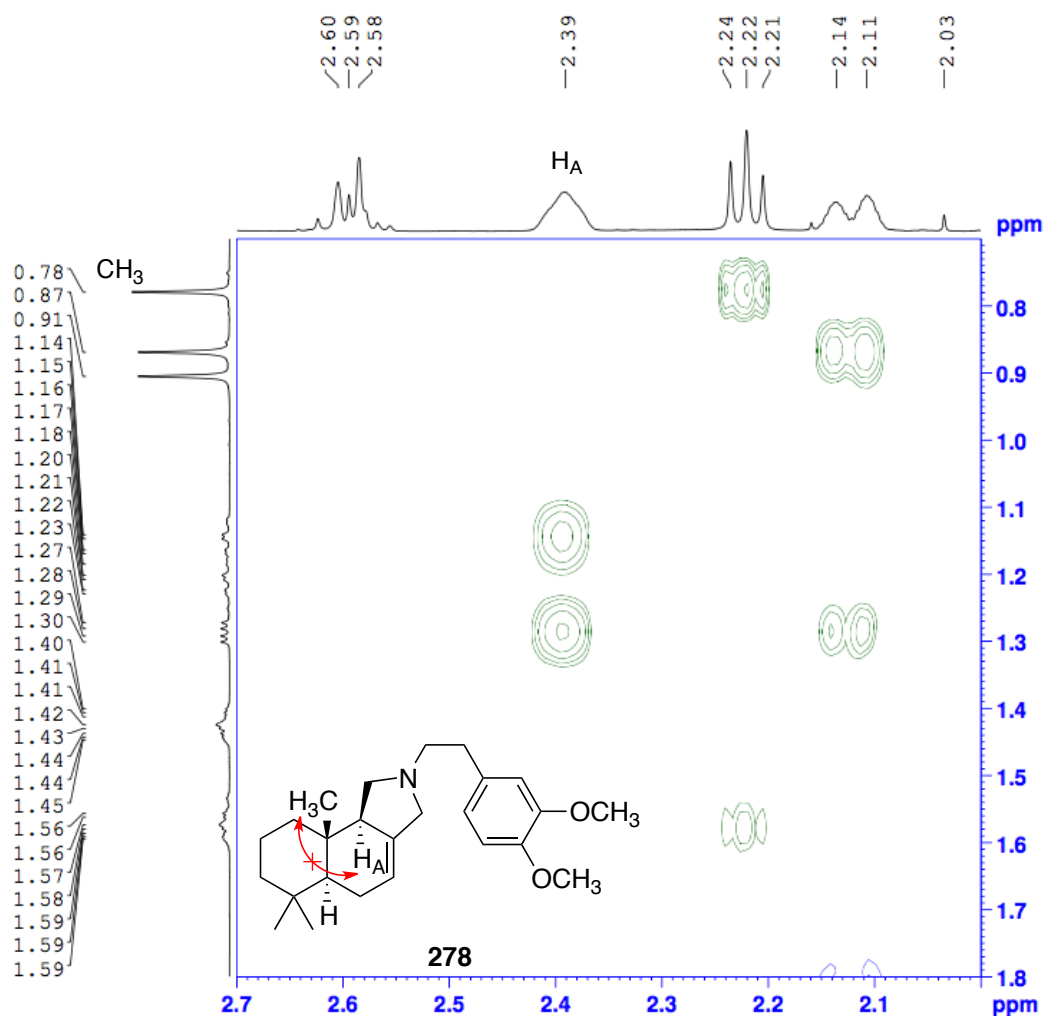


**Figure 3.3:** NOESY spectrum showing absence of a C3 methine and methyl correlation

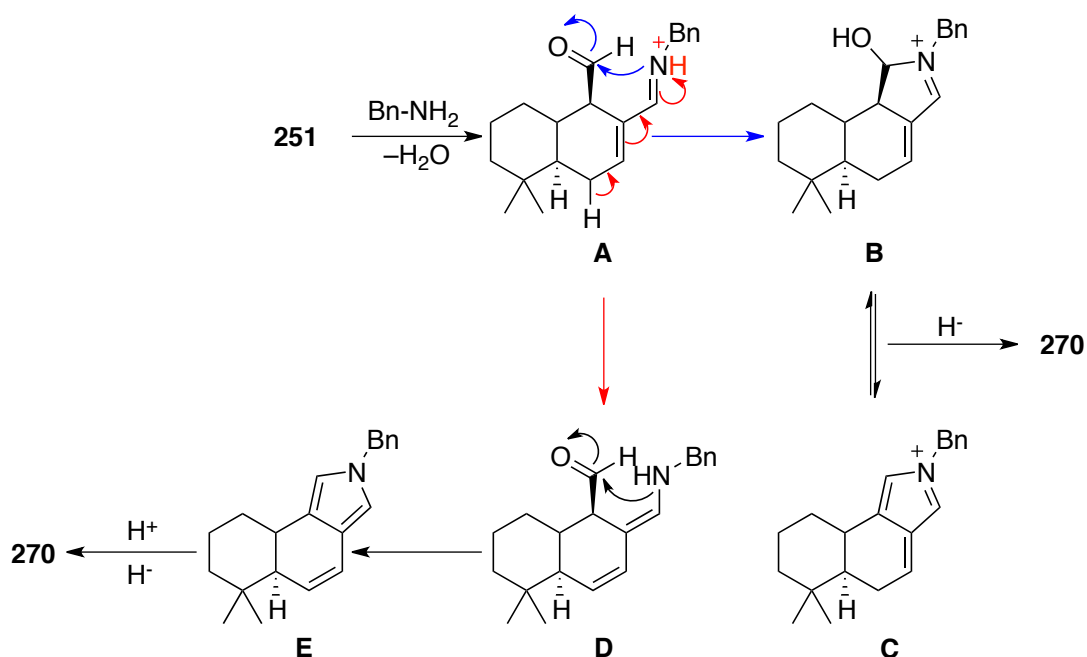
### 3.2.2 Mechanistic Discussion for Pyrrole/Pyrrolidine Formation

From the above empirical observations we suggest that these reactions proceed first through condensation of the amine and the unsaturated aldehyde to give the imine species **A** (Scheme 3.8). The pyrrolidine product is favoured when sodium cyanoborohydride is present at the time of amine addition. This implies that in this case the sodium cyanoborohydride reduces imine **A** on its formation to give an amine, which can undergo an intramolecular reductive amination with the remaining aldehyde to give pyrrolidine **271** (Scheme 3.9). However, when the reducing agent is not added until after polygodial and the amine have been allowed to stir together for 30 minutes, the pyrrole is formed exclusively. In the absence of sodium cyanoborohydride, then, this intermediate imine **A** must react further in order

to preclude any reduction of the imine that would lead to pyrrolidine products. There are a number of possible mechanistic pathways for this to occur.

It is proposed that this may proceed through intramolecular attack of the pseudo-neopentyl aldehyde by the imine of **A** to form the cyclic iminium species **B**. This could in turn convert or interconvert with the iminium **C**, through elimination of water. In either case, pyrrole product **270** would be reached through elimination and reduction of the iminium by addition of sodium cyanoborohydride, followed by a proton shift to remove the exocyclic alkene and generate the aromatic system.

An alternative pathway to give enamine **D**, following a mechanism more like Kornienko's where the double bond shifts following formation of the first imine, might also be possible. In this case the enamine **D** would undergo a condensation with the aldehyde to form pyrrole **270**. Under these acidic reaction conditions the alkene can be protonated and then reduced by the sodium cyanoborohydride.

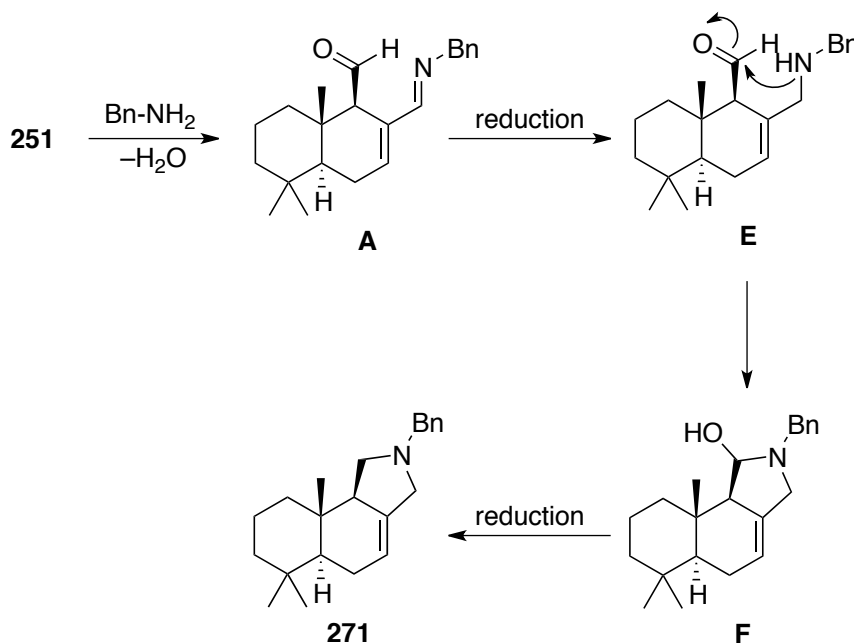


**Scheme 3.8:** Proposed mechanisms for pyrrole formation

There are of course other alternative pathways to reach the pyrrole, involving a variety of possible cyclic intermediates, such as  $\alpha$ -hydroxypyrroles, but these could all be reduced under the described reaction conditions to give the same pyrrole product **270**. The important common feature of all,

however, is the transformation following the first amination to preclude pyrrolidine formation. Thus, whether one or more of these possible pathways is being followed the end result is the same.

To provide evidence for this rapid reaction of imine **A** in the absence of a reducing agent, a  $^1\text{H}$  NMR experiment was conducted where a sample of polygodial and benzylamine in methanol- $d_4$  with a drop of acetic acid was monitored by NMR spectroscopy (solvent-suppressed for acetic acid), before and after the addition of the amine. It was observed that only a few minutes after addition of the amine the spectrum became quite complicated, but notably that any trace of the aldehyde peaks associated with polygodial at 9.46 and 9.53 ppm had completely disappeared. This implied that not only had the conjugated aldehyde reacted to form an imine, but that this had proceeded to react with the second aldehyde to form another intermediate or intermediates.



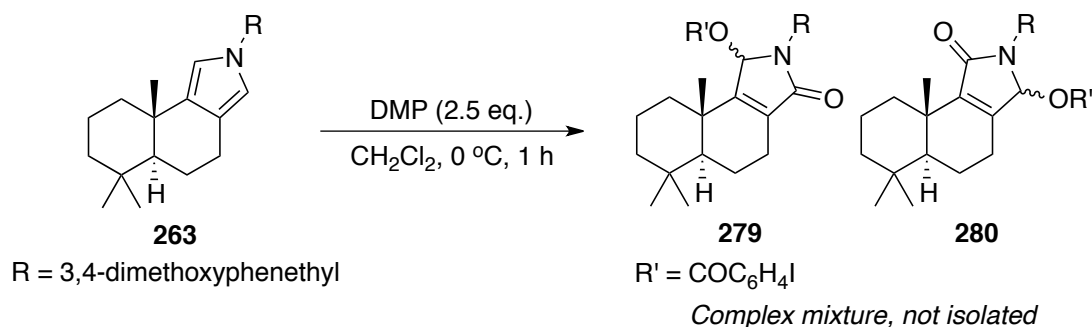
**Scheme 3.9:** Proposed mechanism for pyrrolidine formation

The pyrrolidine product was favoured when sodium cyanoborohydride was present at the time of amine addition, which implies that in this case the sodium cyanoborohydride reduces imine **A** on formation to give amine **E**, that can undergo an intramolecular reductive amination with the remaining aldehyde to give pyrrolidine **271** (Scheme 3.9). Clearly, through the experimental results, this imine reduction is a very facile reaction that

dominates when all three reagents are mixed at the same time. However, the persistence of the pyrrole formation even in the presence of an excess of reducing agent, and the NMR evidence of it swiftly converting the 1,4-dialdehyde to other intermediates, shows that this too is a highly competitive reaction pathway.

### 3.2.3 Application to (+)-Crispin A Analogues

With the ability to form stable pyrroles and pyrrolidines from polygodial established, it was decided to apply these novel scaffolds for further synthetic manipulations. To synthesise analogues of (+)-crispin A (**265**), *N*-dimethoxyphenethylpyrrole **263** was taken as the starting point. It was theorised that this could be oxidised using our Dess–Martin periodinane approach to give a mixture of regio- and stereoisomeric  $\gamma$ -lactams,<sup>62</sup> that could be further manipulated to reach analogues of natural products. This offered potential for two regioisomers to form, lactams **279** and **280**, and two diastereomers of each regioisomer, where the stereochemical configuration of the pendant iodoaryl ester is either *R* or *S* (Scheme 3.10). The ratio of different regio- and stereoisomers at this point would be interesting from the point of view of observing how much the existing stereochemistry of the polygodial backbone can influence the formation of a new stereogenic centre.

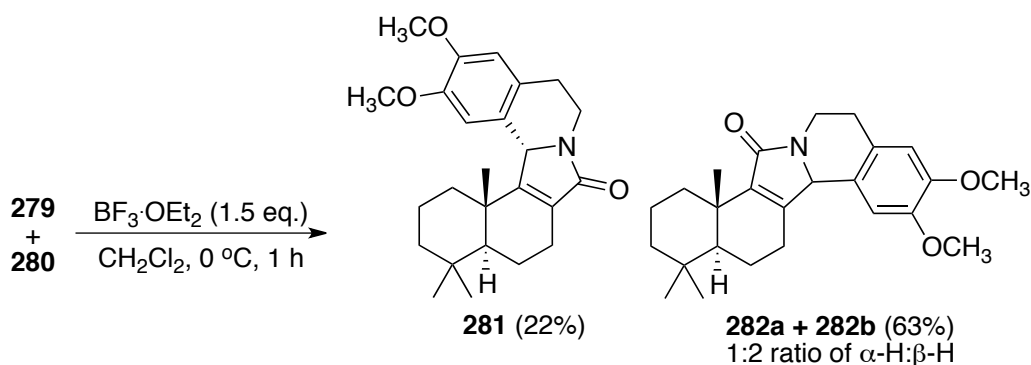


**Scheme 3.10:** Possible stereochemical outcomes of oxidation of pyrrole **212**

As expected, when the pyrrole **263** was taken and submitted to Dess–Martin oxidation for 1 h, a complicated mixture of products was obtained. However, the <sup>1</sup>H NMR spectrum did suggest that all of pyrrole **263** had been consumed, due to the absence of the resonances at 6.21 and 6.22 ppm.

Additionally, the appearance of a number of new resonances above 8 ppm indicated the incorporation of the iodoaroyloxy moiety.

As the overall aim was to access (+)-crispin A analogues, rather than probe the crude oxidation mixture too closely, the cyclisation step was carried out on the complex mixture. To that end it was taken up in dry  $\text{CH}_2\text{Cl}_2$  and treated with 1.5 molar equivalents of  $\text{BF}_3\cdot\text{OEt}_2$  for 1 h. The intention of the reaction was to generate an iminium ion by elimination of the iodoaroyloxy ester and allow intramolecular Friedel–Crafts alkylation with the pendant 3,4-dimethoxyphenethyl group to occur (Scheme 3.11). This furnished a mixture of novel pentacyclic compounds, identified as  $\gamma$ -lactam **281**, isolated as a single diastereomer, and its isomers **282a** and **282b**, an inseparable ~2:1 mixture of diastereomers.



**Scheme 3.11:** Results of  $\text{BF}_3\cdot\text{OEt}_2$  cyclisation

The identity of these was supported by the appearance of a likely C2 methine signal in the  $^1\text{H}$  NMR of  $\gamma$ -lactam **281** at 5.28 ppm, and  $^{13}\text{C}$  resonances at 172.8 ppm, representative of the amide, and eight resonances between 112.3 and 163.2 ppm, consistent with the six dimethoxyphenethyl aryl carbon atoms and the two alkene carbon atoms of the lactam. The structure of lactam **281** was also supported by IR spectroscopy, with the presence of an amide stretch at  $1682\text{ cm}^{-1}$ , and lack of any likely ester stretch, indicating the iminium formation and Friedel–Crafts alkylation reaction had proceeded. HRMS analysis also gave an exact mass consistent with the assigned structure.

The stereochemistry of  $\gamma$ -lactam **281** was assigned through analysis of the HMBC and NOESY 2D NMR spectra. The HMBC spectrum allowed for the

assignment of the singlet at 5.28 ppm as the C2 methine proton in the lactam ( $H_A$ ), and the singlet at 1.16 as the angular methyl substituent, through shared HMBC correlations for these two  $^1H$  NMR resonances (Figure 3.4).

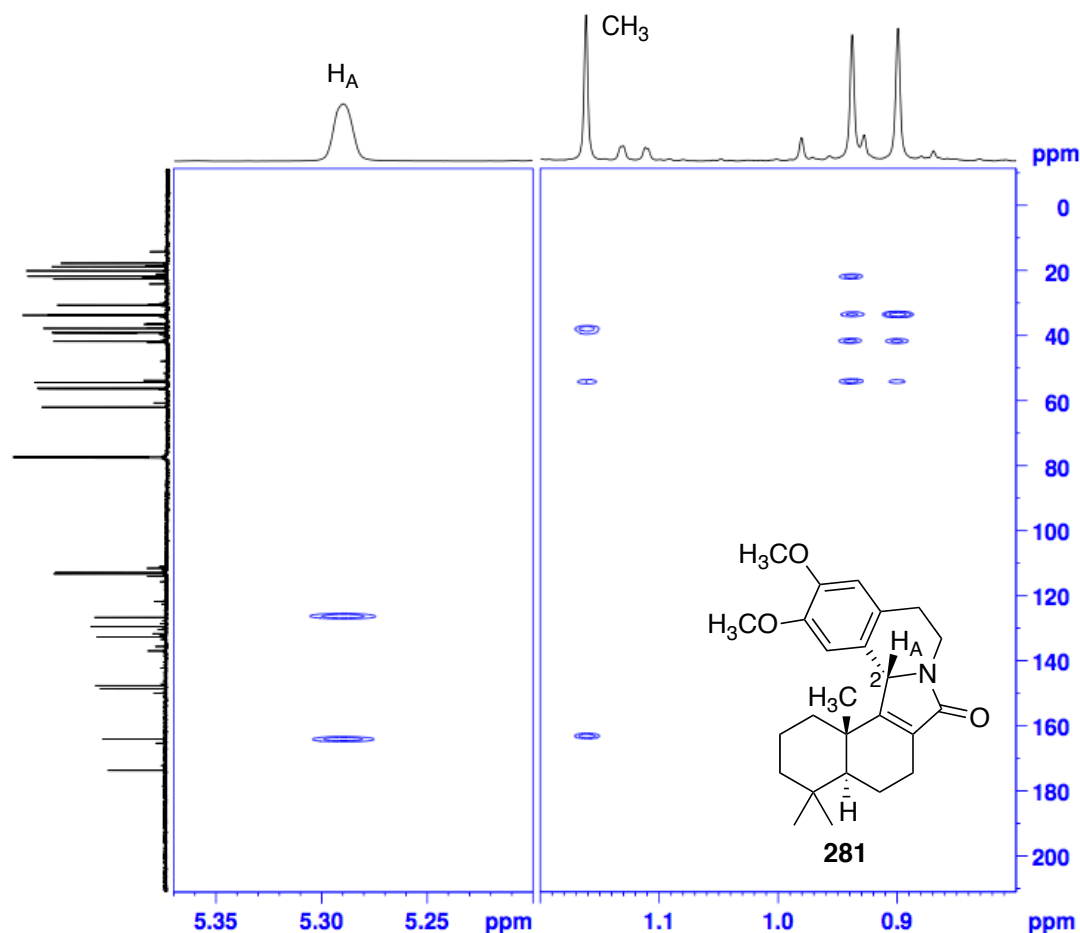


**Figure 3.4:** Expansions of pyrrolinone **281** HMBC showing shared correlations

With these resonances established, it was possible to observe in the NOESY spectrum that there is a weak correlation between these two resonances, which indicated that they were on the same face of the molecule (Figure 3.5). This provides evidence that the Friedel–Crafts reaction likely proceeds with stereoselectivity to this product due to the steric hindrance of the proximal angular methyl group which directs the reaction from the  $\alpha$ -face of the molecule.

The mixed diastereomers, **282a** and **282b**, were identified through analysis of their combined  $^1H$  and  $^{13}C$  NMR spectra. The  $^1H$  NMR spectrum featured similar arrangements of  $^1H$  resonances to lactam **281**, with two sets of backbone methyl group resonances between 0.87 and 1.06 ppm observed,

consistent with a mixture of diastereomers. The 2:1 ratio of products is proposed to arise from the  $\beta$ -face of the lactam opposite the angular methyl group being less hindered at C5, leading alkylation to occur predominantly on that face. The higher combined yield of these products compared with compound **281** could arise from it being more favourable for intermediate oxidised species **280** to form in the oxidation step, where the bulky iodoaroyloxy group is in a less sterically hindered environment.

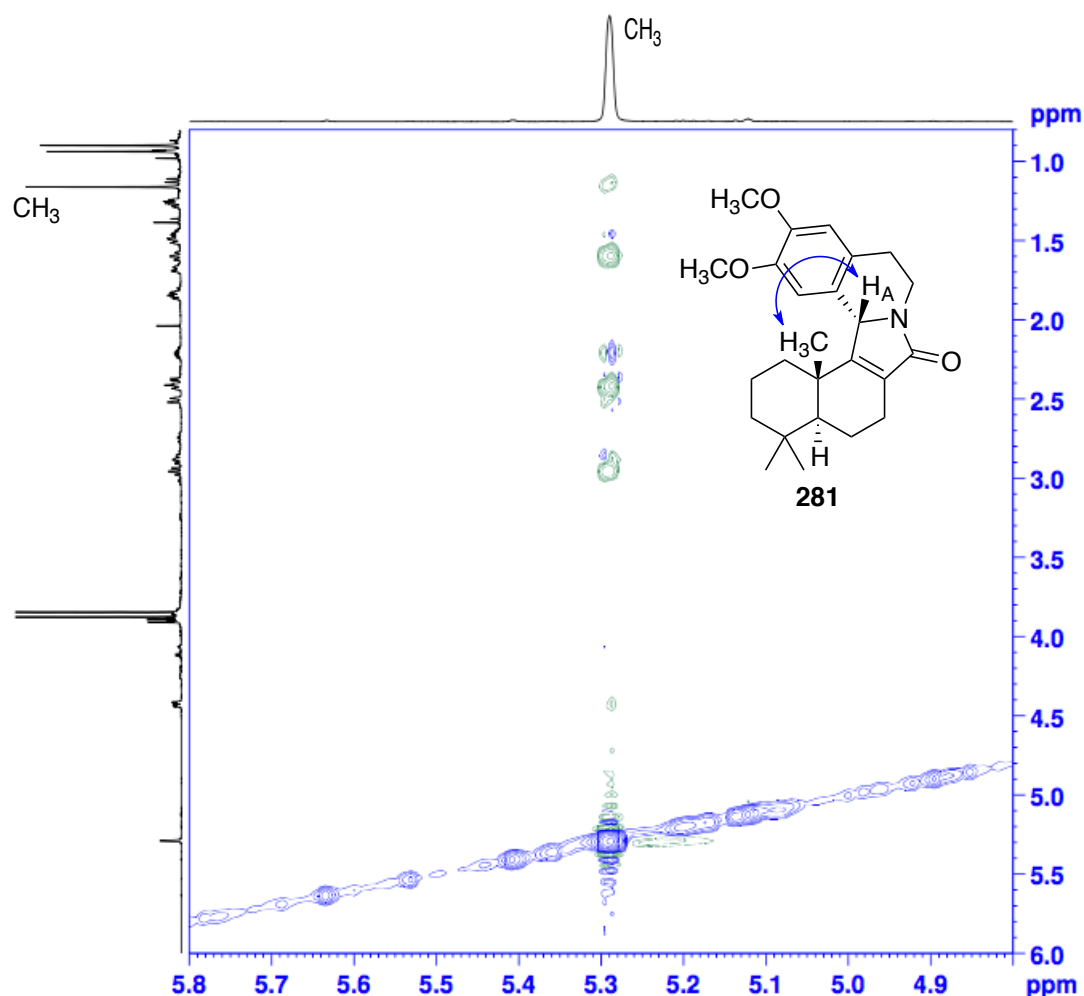
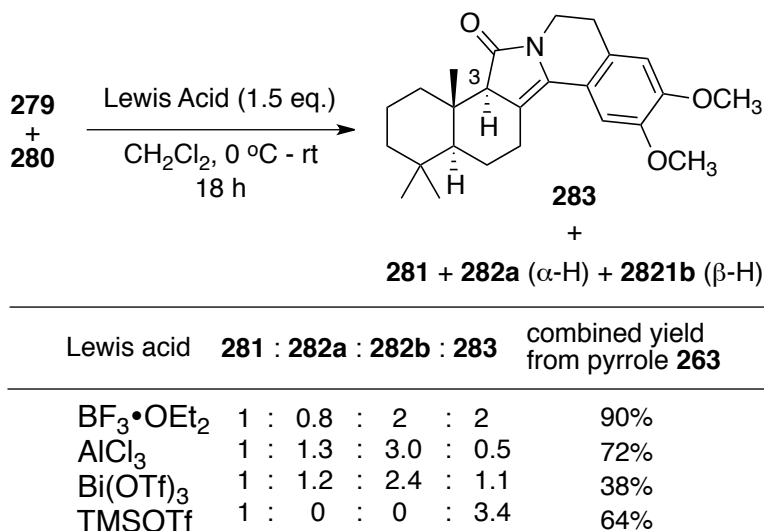


**Figure 3.5:** Expansion of NOESY spectrum for compound **281**, showing weak correlation between C2 proton and proximal methyl protons

Interestingly, when the reaction was repeated for 18 h rather than 1 h, a fourth product was obtained, identified as the 4-pyrrolin-2-one isomer **283** (Scheme 3.12). This was hypothesised to result from the double bond in the two diastereomers **282a** and **282b** shifting from C3–C4 to C4–C5, a phenomenon previously observed when attempting the intermolecular Friedel–Crafts alkylations of racemic  $\gamma$ -lactams with electron-rich aryls. In this

case, however, the bond-shifted product was not as prone to immediate decomposition as those acyclic derivatives and was stable enough to purify and analyse to determine the structure of the molecule.



**Scheme 3.12:** Products of overnight Friedel–Crafts reactions

The structure was supported by <sup>1</sup>H NMR spectroscopy. In contrast to the other three isomers formed in the reaction there was no methine peak near 5 ppm to indicate the presence of a C5 methine proton. There was, however, a resonance at 2.64 ppm, likely that of the methine proton in the C3 position at the junction of the lactam and polygodial backbone. Furthermore, there were still alkene resonances present alongside the aromatic resonances between 109.6–148.7 ppm. Additionally, the IR and MS analysis agreed that it was a similar compound to lactam **281** and the diastereomers **282**, with an identical molecular weight.

The stereochemistry of the methine proton at C3, adjacent to the amide, was assigned by the analysis of the NOESY NMR spectrum of the compound (Figure 3.6). The <sup>1</sup>H NMR resonance for the methine proton at C3 was established as the singlet at 2.64 ppm (H<sub>A</sub>), and the angular methyl group established as the singlet at 0.80 ppm, through the HSQC and HMBC NMR spectra. In the NOESY spectrum, no correlation was observed between these two resonances, which supported the *trans* relationship at these substituents.



To investigate whether the choice of Lewis acid used could influence the ratio of these products, perhaps to favour formation of a single diastereomer of **282**, or push the isomerisation to 4-pyrrolin-2-one **283**, the overnight conditions were repeated with a selection of Lewis acids (Scheme 3.8). Some results remained constant: As the oxidation reaction and hence its regioselectivity would not be affected by a change of Lewis acid, the ratio of lactam **281** to the mixture of other isomers remained 1:~4 in all cases. Likewise the ratio of diastereomers **282a** to **282b** were nearly constant at approximately 2:1. This is understandable in that the oxidation step rather than the alkylation step sets the ratio of lactam **281** to other products. Also, assuming both diastereomers of **282** are equally prone to the alkene shift, their relative abundance should not differ drastically for different reaction conditions. So the use of different Lewis acids did little in general to favour one or the other of these isomers.

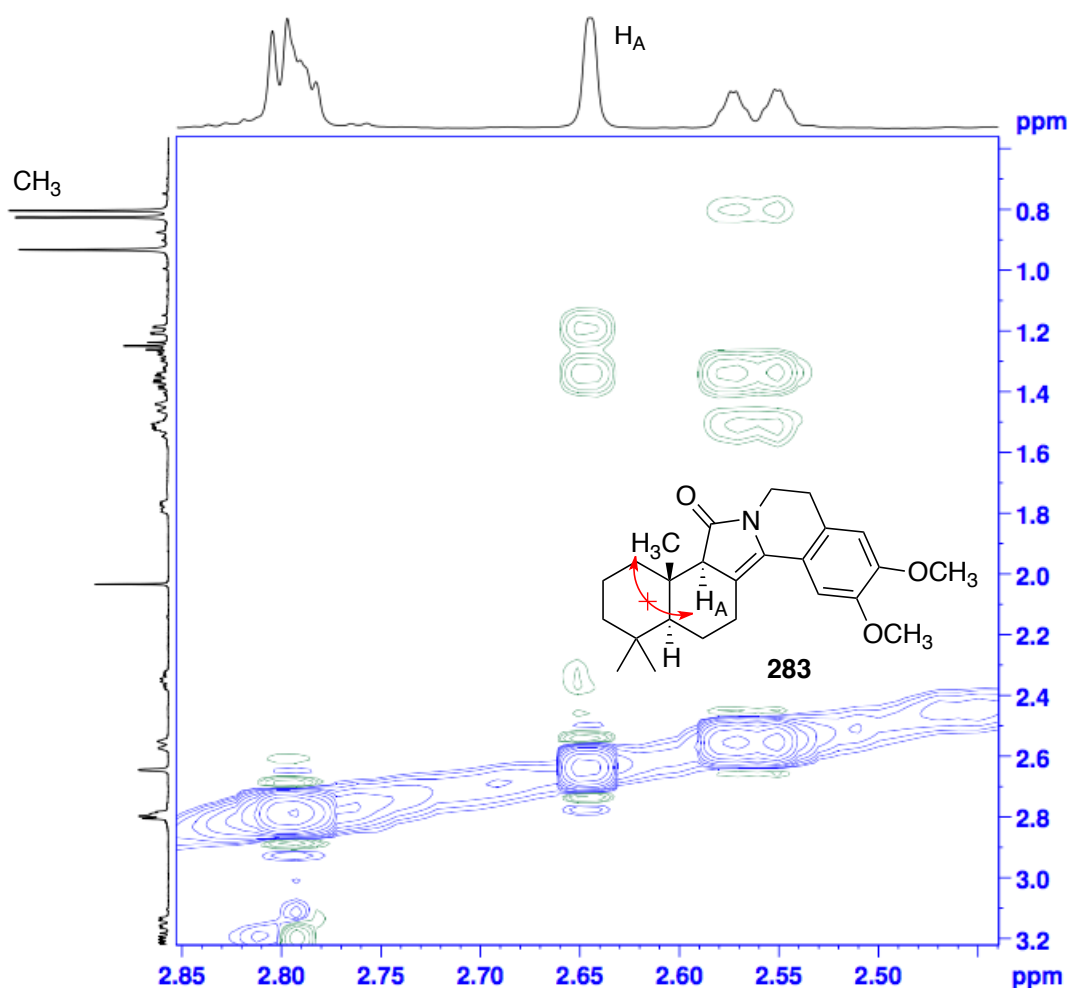
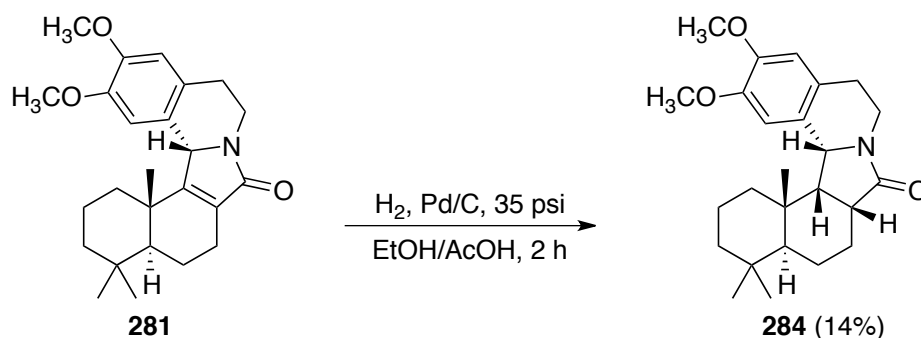


Figure 3.6: NOESY NMR spectrum of 4-pyrrolinone **283**

However, there were significant changes in the proportion of 4-pyrrolinone **283**, such that when TMSOTf was used it was the only product isolated other than lactam **281**. This was a pleasing result on the grounds that it greatly reduced the complexity of the mixtures obtained from the reaction, while still giving a good overall yield. It was proposed that this could result from adventitious water in the TMSOTf leading to formation of some triflic acid, that when added with the TMSOTf to the reaction promotes the isomerisation. This is supported by observations that an NMR sample of the mixed diastereomers **282a** and **282b** left in chloroform converted entirely to 4-pyrrolinone **283** within 6 h, presumably due to the presence of residual DCI.

Ideally, crystallisation of these compounds and assignment of their absolute stereochemical configurations would have been carried out. However, all four of the compounds **281–283** proved unstable, decomposing completely within a week even if stored at  $<0^{\circ}\text{C}$  under a nitrogen atmosphere. As such, they were taken and reduced immediately after purification and characterisation.

Hydrogenation was first carried out on a sample of lactam **281**. This was found to proceed smoothly when the reaction was carried out in the presence of acetic acid at 35 psi, furnishing the single product pyrrolidinone **284** in a modest yield of 14% (Scheme 3.13).



**Scheme 3.13:** Hydrogenation of **281**

Success of the hydrogenation reaction was supported by the appearance of new methine resonances in the  $^1\text{H}$  NMR spectrum, at 2.41 ppm, 2.68–2.72 ppm and 4.54 ppm that were identified through 2D NMR spectral analysis as the three lactam methine protons. Importantly, in the  $^{13}\text{C}$  NMR spectrum there were only six resonances between 109.9 ppm and 148.2 ppm,

indicating that while the dimethoxyphenyl moiety was still present, there was no longer an alkene in the molecule. The accurate mass of the compounds as determined by HRMS was also consistent with an increase of two mass units from pyrrolinone **281** to pyrrolidinone **284**.

The stereochemistry of pyrrolidinone **284** was assigned through analysis of the NOESY NMR spectrum (Figure 3.7). Correlations between the methyl group signal at 1.27 ppm, identified through the HSQC and HMBC spectra as the stereogenic centre methyl, and three of the four methine proton resonances at 2.41 ppm, 2.71 ppm and 4.54 ppm suggested that all three of these are likely to be on the same face of the molecule. This implied that that hydrogen was delivered on the face opposite the aromatic substituent, and thus that the steric bulk of this substituent played a deciding role in stereochemical outcomes of transformations to the molecule, over the angular methyl group.

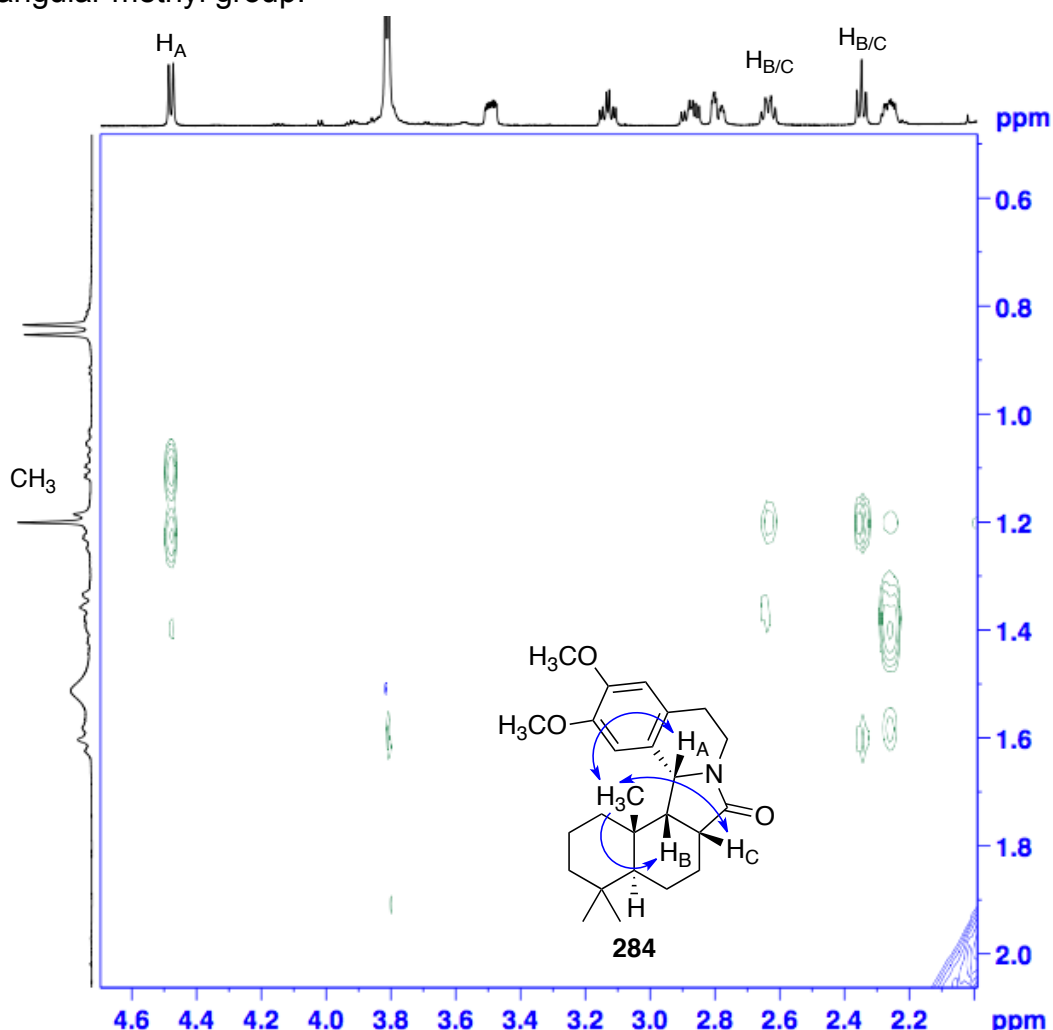
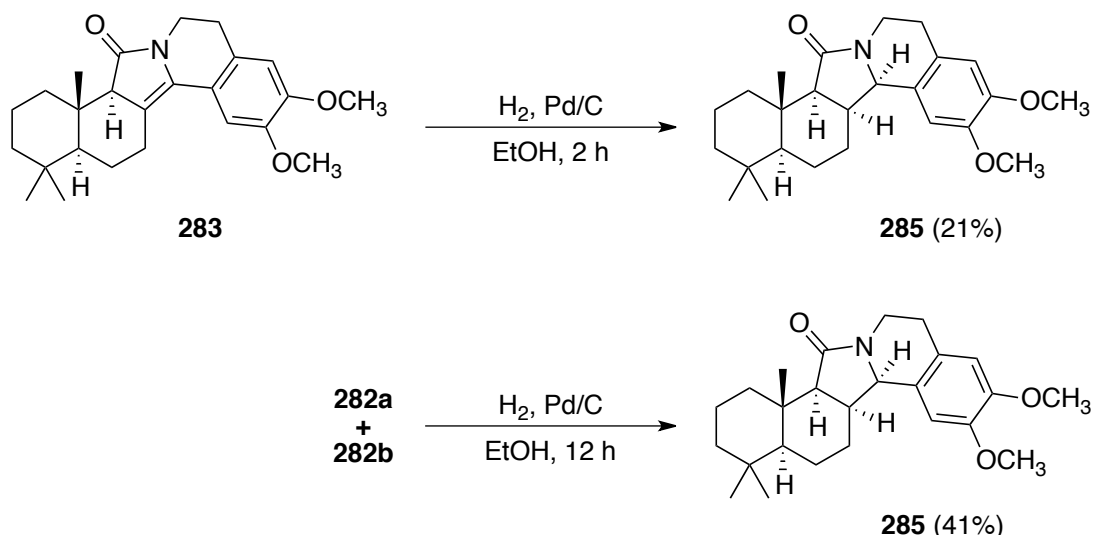


Figure 3.7: NOESY NMR spectrum of pyrrolidinone **284**

Hydrogenation of the mixture of diastereomeric lactams **282a** and **282b** was more demanding, requiring a much longer reaction time to be complete, although unlike for lactam **281** it would proceed in the absence of AcOH. In the end, a single product was obtained, identified as pyrrolidinone **285** (Scheme 3.14). Interestingly, hydrogenation of 4-pyrrolinone **283** proceeded much more readily even without the addition of acid to the reaction mixture, only taking 2 h, and gave the single product pyrrolidine **285** as well. This is consistent with the mixed diastereomers **282** spontaneously converting to the single diastereomer of 4-pyrrolinone **283** prior to hydrogenation. Given that there was no acid present for this hydrogenation, it seems possible that the two diastereomers isomerise in protic solvents as well, and that this process is more facile than hydrogenation of the alkene.



**Scheme 3.14:** Hydrogenation of the other isomers to give the single product **285**

The identity of pyrrolidinone **285** was, much like for compound **284**, established through the appearance of new methine resonances in the  $^1\text{H}$  NMR spectrum, at 2.54 ppm, 2.80 ppm and 4.68 ppm. It was also supported by the disappearance of the alkene resonances of pyrrolinones **282/283** in the  $^{13}\text{C}$  NMR spectrum. Likewise HRMS analysis showed an increase in molecular weight consistent with adding two hydrogen atoms. The stereochemistry of pyrrolidinone **285** was likewise established through analysis of the NOESY NMR spectrum. There were no correlations between the signal at 1.02 ppm (the angular methyl substituent) and the three resonances at 2.54 ppm, 4.68 ppm, and 2.80 ppm assigned to the three

methine protons in the lactam ring (Figure 3.8). This is consistent both with the conversion of 3-pyrrolinones **282a** and **282b** to 4-pyrrolinone **283**, and with hydrogenation favouring the face least hindered by the angular methyl group. In this case the aryl substituent would be approximately planar with the lactam ring prior to hydrogenation and thus play less of a role in hindering either face of the molecule.

Unfortunately, these compounds were also rather unstable, possibly explaining the rather low yields of products obtained. However, this study has demonstrated that the polygodial backbone can be used to rapidly access novel and interesting polycyclic chemical structures.

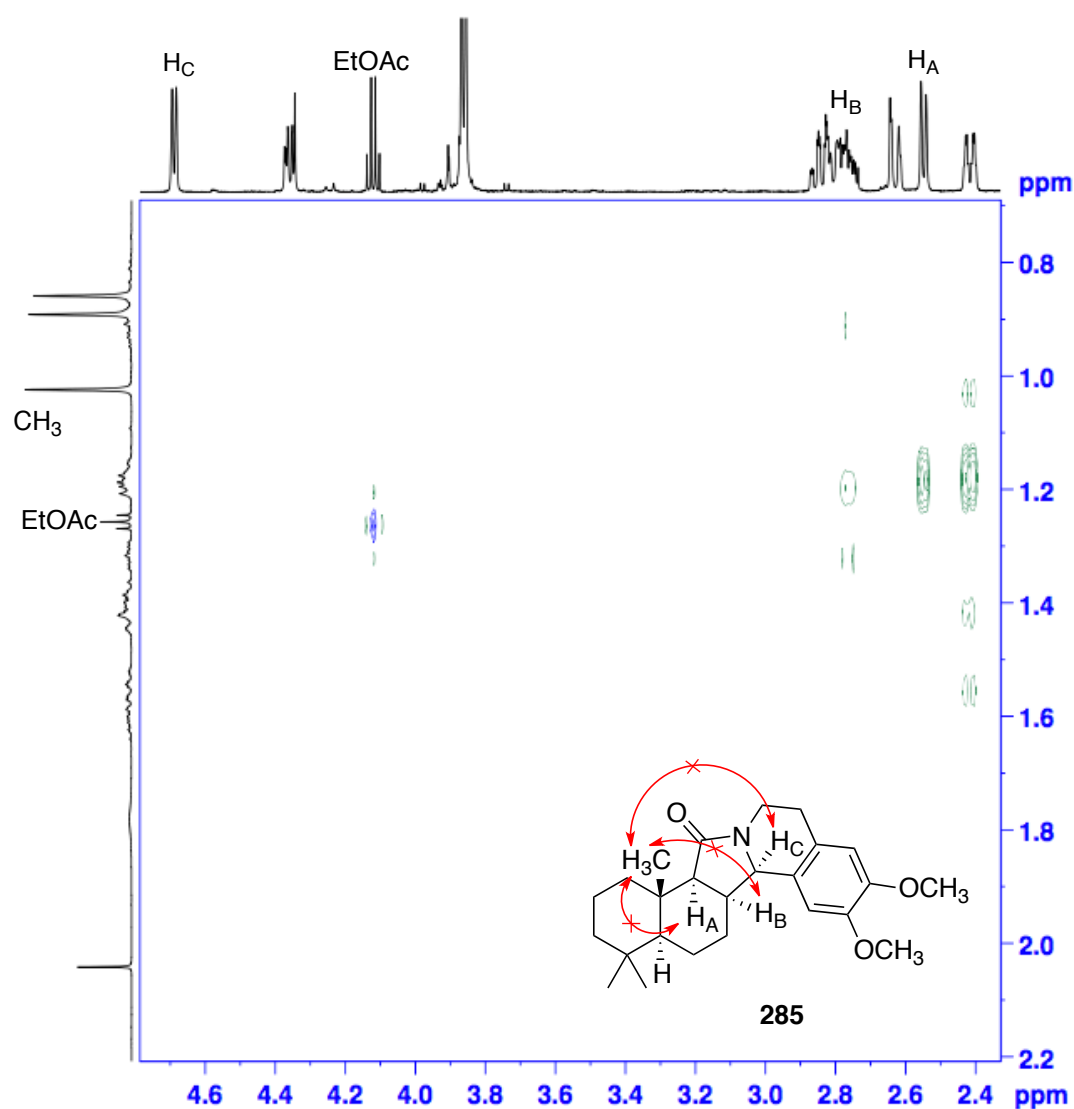
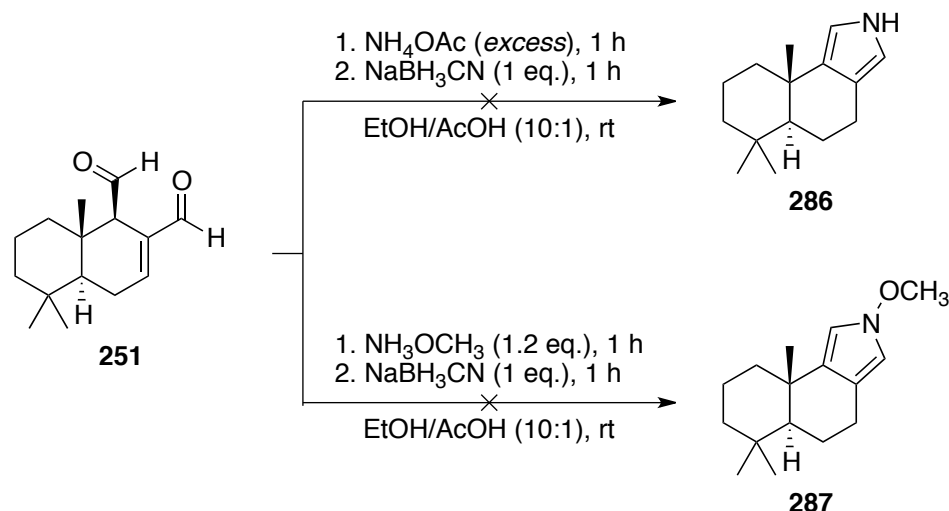


Figure 3.8: NOESY expansion of **285**

### 3.2.3 Other Attempted Applications

To reach *N*-H pyrrole/pyrrolidine species from polygodial, that could be used in chiral organocatalysis, a number of approaches were attempted. The first was to prepare the *N*-H pyrrole directly, using an ammonium salt as the nitrogen source (Scheme 3.15). However, use of ammonium acetate provided a complex mixture of products, even under conditions where large excesses of the salt were added, which were difficult to separate and where the majority of the starting material was lost to decomposition. It was also attempted to make the pyrrole using *N*-methoxyamine, to give a species that might be more readily converted to the *N*-H through hydrogenation (scheme 3.14).<sup>337,338</sup> However, similar decomposition of polygodial or any products was observed.

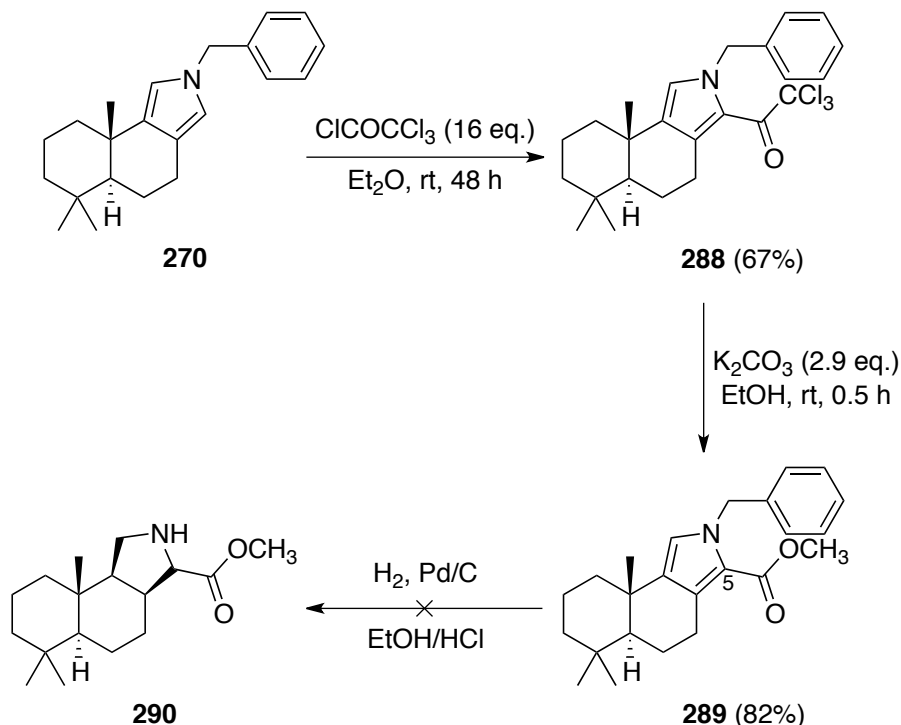


**Scheme 3.15:** Attempts to reach *N*-H pyrroles/pyrrolidines

Another approach was to investigate using the *N*-benzylpyrrole **270** as the starting material in the synthesis of proline analogues, and exploit the nucleophilic pyrrole to prepare a 2-carboxylic ester as a precursor for the proline analogue. Theoretically this species could then be reduced to both reduce the pyrrole to the pyrrolidine and cleave the benzyl protecting group. Thus, pyrrole **270** was taken and converted to the corresponding 2-trichloromethyl ketone derivative **288**, through stirring with an excess of trichloroacetyl chloride in diethyl ether for 48 h (Scheme 3.16).<sup>339</sup> The success of this reaction was supported through analysis of the  $^1\text{H}$  NMR of the single product obtained, which showed a single pyrrolic singlet peak at 6.85

ppm, indicative of only one of the pyrrole positions being substituted. Additionally, the NOESY spectrum showed a weak correlation between this signal and that of the angular methyl group at 1.20 ppm, providing further evidence that the substitution only occurred at C2 of the pyrrole, most distant of the angular methyl group which was predicted to be the least sterically hindered site.

Trichloromethyl ketone **288** was then converted to the corresponding methyl ester by treatment with base in MeOH to give pyrrole **289** in an 82% yield (Scheme 3.16). This was identified primarily through the appearance of a singlet peak integrating for 3 protons in the  $^1\text{H}$  NMR spectrum at 3.73 ppm, characteristic of the  $-\text{OCH}_3$ , and by mass spectrometry. It was proposed that this could be simply hydrogenated to remove the benzyl substituent and reduce the pyrrole to the corresponding pyrrolidine, thus furnishing an analogue of proline. However, hydrogenation at 35psi in EtOH/HCl for 3 h failed to show any reaction of the starting material to either reduce the pyrrole moiety or cleave the benzyl group (Scheme 3.16).

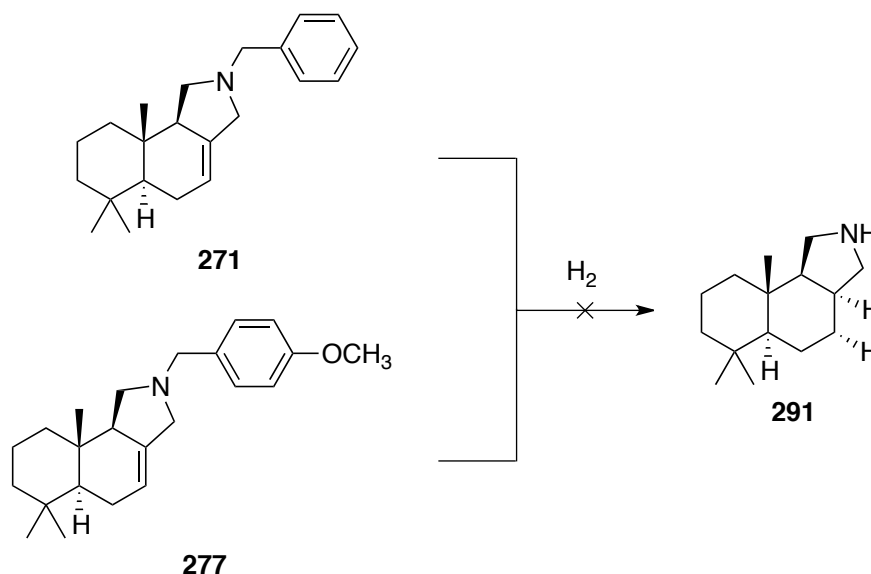


**Scheme 3.16:** Synthesis of 2-methylester pyrrole **289**

To circumvent this issue, a range of hydrogenation conditions were trialled on a number of the pyrrolidine products instead, namely the benzylpyrrolidine

**271** and the 4-methoxybenzylpyrrolidine **277** (Scheme 3.17). This was proposed as hydrogenation of pyrroles can be capricious and by starting with a pyrrolidine with an exocyclic alkene this problem could potentially be overcome.

Hydrogenation of pyrrolidine **271** under 1 atm of H<sub>2</sub> with Pd/C resulted in decomposition, which given the aforementioned instability of related compounds is perhaps unsurprising. Further attempts with HCl present led to similar results, where any likely products appeared to still include the benzyl group. Pd(OH)<sub>2</sub> was trialled as an alternative catalyst, and carrying out the reaction at higher pressures for shorter periods of time with both this or Pd/C. However these all led to decomposition or a complex mixture of products. Likewise for pyrrolidine **277**, it seemed problematic to remove the benzyl group without decomposition.

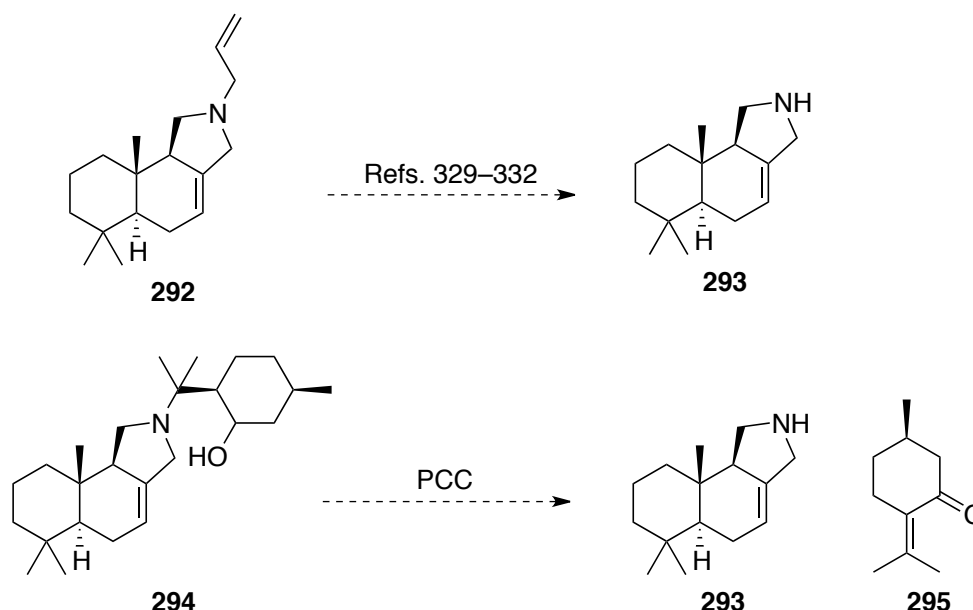


**Scheme 3.17:** Attempted global reduction of pyrrolidines

None of the approaches trialled, either in formation of the *N*-H pyrrole or by reduction of pyrroles or pyrrolidines, have thus far provided a straightforward route to the desired pyrrolidine species, giving at best complex mixtures of undesired products or decomposition. For future investigations, either more particular reduction conditions could be trialled, or else more specialised substrates that can have their *N*-substituents cleaved under different conditions. For example, a new pyrrolidine **292** could be prepared from allylamine (Scheme 3.18). There are many possible methods for cleaving *N*-



allyl groups, including de-allylation with a palladium catalyst and a barbituritic or thiobenzoic acid present to act as an allyl trapping reagent,<sup>340,341</sup> heating the substrate in the presence of Wilkinson's catalyst,<sup>342</sup> and treatment with hydrazine and a base at elevated temperatures.<sup>343</sup> Another more exotic method would require the use of particular amine starting materials, such as for the oxidative cleavage of a  $\gamma$ -hydroxy *N*-substituent in pyrrolidine **294**. This transformation has been previously demonstrated in work by Andrés and colleagues using (–)-8-aminomenthol derivatives and PCC.<sup>344</sup>



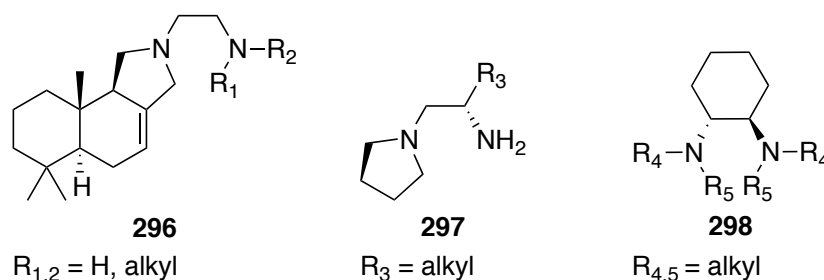
**Scheme 3.18:** Potential alternatives for reaching proline analogues

### 3.3 Conclusions

In conclusion, it is now clear that with well-chosen reaction conditions polygodial can be used as a starting point for the synthesis of a range of pyrroles and pyrrolidines. These in turn show promise as intermediates in the synthesis of complex organic scaffolds and novel analogues of biologically active natural products.

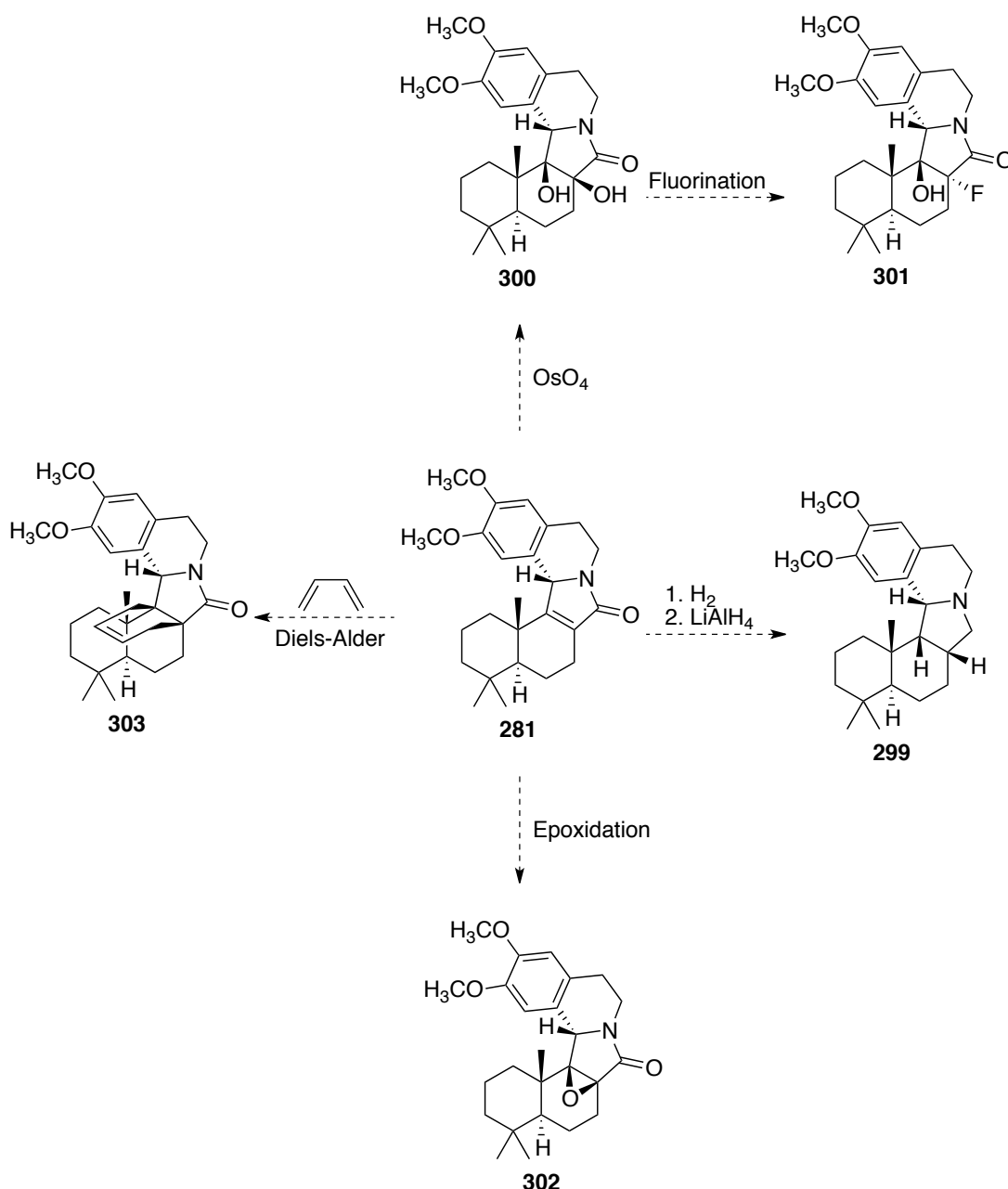
For future investigations, there are three main avenues to be explored: First, to widen the conditions and substrates to find a successful route to the desired proline analogues. This will involve either finding more specialised reduction conditions for the presently prepared starting pyrroles/pyrrolidines, or preparing new starting materials with *N*-substituents that are more amenable to cleavage by hydrogenation or some other chemical means.

One goal in this space beyond reaching the *N*-H pyrrolidine proline analogues is to look at forming pyrrolidines with beta amine *N*-substituents, to give diamine species such as **296** (figure 3.19). Diamines have wide range of uses in catalysis. Tertiary-primary diamines have been used extensively as catalysts for Aldol reactions and Michael additions (e.g. diamine **297**).<sup>345,346</sup> Tertiary-tertiary diamines, such as **298**, have been reported as catalysing stereoselective Knoevenagel reactions and alkyllithium additions.<sup>347,348</sup>



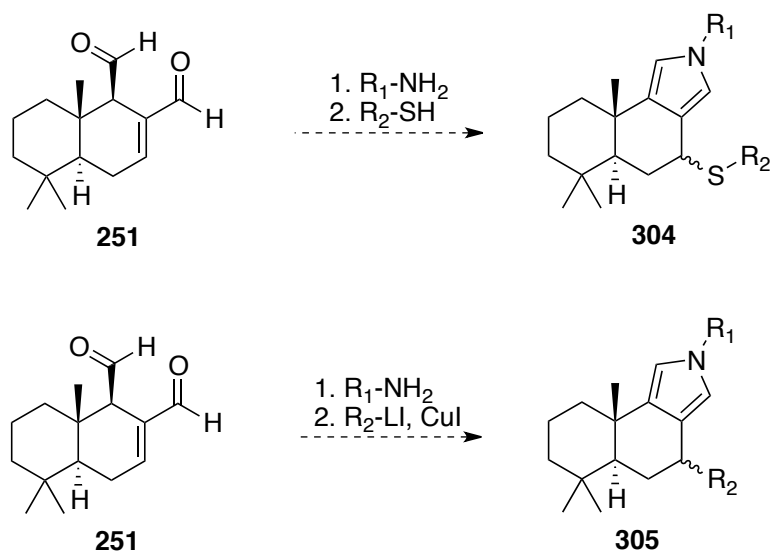
**Scheme 3.19:** Development of chiral diamines for organocatalysis

Secondly, the further derivatisation of the (+)-Crispin A analogues prepared in this work, to hopefully reach more stable species which might be screened for biological activity and compared to the natural product in their efficacy (Scheme 3.20, using pyrrolinone **281**). This would be pursued most simply through reduction of the amide functionality present in pyrrolidinones **284** and **285**. However, the functional lactams intermediates **281-283** could also be derivatised in a variety of ways, such as hydroxylation, to give dihydroxy compound **300**. This could even be further transformed to give fluorinated analogues, using some the methods discussed in Chapter 2. Epoxidation could also be carried out to give epoxide **302**. Another type of reaction that could rapidly give libraries of more complex polycyclic frameworks would be Diels–Alder reactions, to give species such as hexacyclic compound **303**. Studies of the stereoselectivity of such transformations would also be interesting to compare to the case where only hydrogen is added across the double bond.



**Scheme 3.20:** A range of potential transformations to lactam **281**

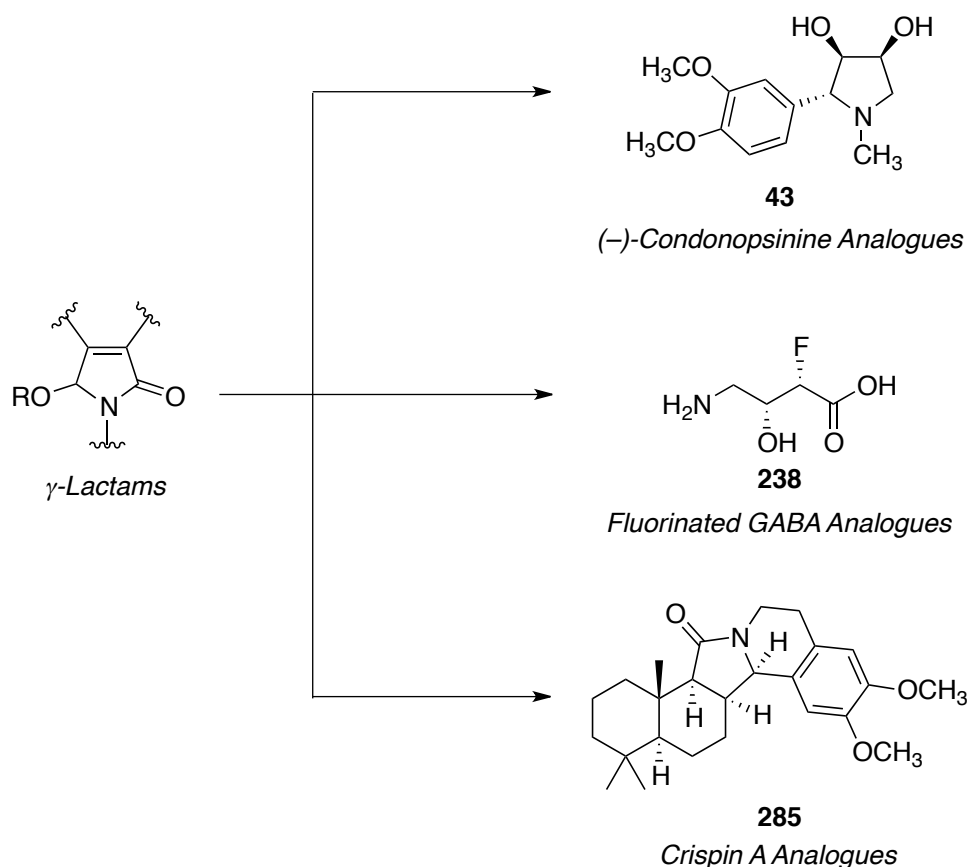
Thirdly, widening the scope of the pyrrole formation reaction by exploring a range of different nucleophiles other than reduction with  $\text{NaBH}_3\text{CN}$ , such as thiols or cuprate reagents (Scheme 3.21). Depending on the mechanism involved in the pyrrole formation (See section 3.2.2), this could lead to the introduction of interesting substituents at the position of the alkene. This would be useful synthetically for providing more substituted intermediates for further reaction, and also from a mechanistic standpoint for understanding more about how polygodial may react in biological systems.



**Scheme 3.21:** Potential use of alternative nucleophiles in pyrrole synthesis

## Chapter 4: Conclusions

The controlled oxidation of pyrroles is a powerful tool for accessing a variety of natural product analogues and other biologically active molecules. In this work two approaches to controlled pyrrole oxidation, using hypervalent iodine reagents and photooxidation, have been utilised to reach three key targets and thus establish the usefulness of these techniques (Scheme 4.1).



**Scheme 4.1:** Summary of this work

It was demonstrated that oxidation of simple *N*-substituted pyrroles could be used as a starting point to reach a library of racemic analogues of the natural product codonopsinine. In the pursuit of asymmetric syntheses of these analogues, it was shown that oxidation of pyrroles derived from chiral amino alcohols can be used to reach previously reported chiral bicyclic intermediates in a more step-efficient and mild fashion.

These oxidation-derived bicyclic intermediates were also used to form fluorinated derivatives of GABA, without the undesirable rearrangement

products observed when preparing these analogues from acyclic starting materials.

Finally, it was demonstrated that pyrrole oxidation methods could be applied to pyrroles formed from more complex chiral scaffolds, in this case the natural product polygodial. This approach was used to reach analogues of another biologically active natural product, (+)-crispin A.

These three streams of research are united in their use of controlled pyrrole oxidation as a key step, and represent the potential of this technique to be used to rapidly reach desirable natural product targets and access novel complex molecular scaffolds. Looking toward the future, these methods could be applied to many objectives, both in the expansion on the individual research areas as described in Chapters 1–3, and elsewhere. A variety of other biologically active pyrroline and pyrrolidine natural products could be pursued, such as Pramanicin (**306**, Figure 4.1), an antifungal and possible anticancer agent;<sup>349</sup> and Erysotrine (**307**), found in folk medicines.<sup>350,351</sup> For both of these and many others a single of bicyclic pyrrole-derived lactam could provide a convenient template for total synthesis or access to libraries of analogues.

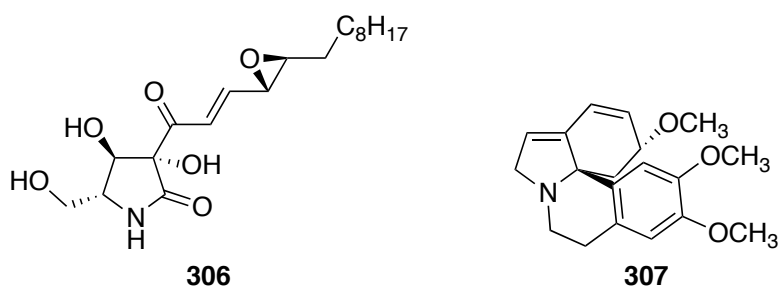


**Figure 4.1:** Potential future natural product targets.

## Chapter 5: Experimental

### 5.1 General Experimental

#### *Nuclear Magnetic Resonance Spectroscopy*

Proton ( $^1\text{H}$ ), carbon ( $^{13}\text{C}$ ) and fluorine ( $^{19}\text{F}$ ) nuclear magnetic resonance spectra were obtained either on a Bruker Avance III spectrometer operating at 400 MHz, 100 MHz and 400 MHz respectively, or on a Bruker spectrometer operating at 600 MHz, 150 MHz and 600 MHz respectively. Where necessary, resonances were assigned using two-dimensional COSY, HSQC and HMBC experiments, and coupling constants from complex or non-first-order spectra were determined by simulation/iteration sequences using the Daisy module of the Bruker TopSpin software. Samples were dissolved in deuterated chloroform ( $\text{CDCl}_3$ ) unless otherwise stated. Chemical shifts were recorded as  $\delta$  values in parts per million (ppm) and referenced to the solvent used.<sup>352</sup> Coupling constants were recorded as  $J$  values in Hz. The following abbreviations were used to describe  $^1\text{H}$ ,  $^{13}\text{C}$  and  $^{19}\text{F}$  splitting patterns: s = singlet, bs = broad singlet, d = doublet, t = triplet, q = quartet, sex = sextet, ad = apparent doublet, , at = apparent triplet, dd = doublet of doublets, ddd = doublet of doublets of doublets.

#### *Infrared Spectroscopy*

Infrared spectra were obtained on a Shimadzu FTIR 8400s spectrometer, using NaCl plates. Liquids and solids were recorded as thin films from either  $\text{CDCl}_3$  or  $\text{CH}_2\text{Cl}_2$ , unless otherwise stated, in  $\text{cm}^{-1}$

#### *Mass Spectrometry*

Mass spectrometry and high resolution mass spectrometry were performed on a Kratos Concept ISQ mass instrument using electron impact mass spectrometry, or by electrospray ionization by direct infusion into an LTQ-Orbitrap XL mass spectrometer using a syringe pump. Accurate mass was measured by “peak matching” at 10000 resolution against perfluorokerosene.

Analyses were performed by The Central Science Laboratory at the University of Tasmania. The molecular ion and mass fragments are quoted,

with relative intensities of the peaks referenced to the most intense taken as 100%.

### *Column Chromatography*

Flash column chromatography was performed using Merck flash grade silica (32-63  $\mu\text{m}$ ) according to the general method of Still *et al.*<sup>353</sup>

Automated flash chromatography was carried out using a Reveleris® X2 Flash Chromatography System using silica gel cartridges.

### *Thin Layer Chromatography (TLC)*

Merck silica gel 60 F254 aluminium backed sheets were used for analytical thin layer chromatography. TLC plates were visualised under a 254 nm UV lamp and by treatment with either a cerium molybdate dip (37.5 g phosphomolybdic acid, 7.5 g ceric sulfate, 37.5 mL sulfuric acid, 720 mL water) or a potassium permanganate dip (3 g  $\text{KMnO}_4$ , 20 g  $\text{K}_2\text{CO}_3$ , 5 mL 5 % aqueous NaOH, 300 mL water), followed by heating.

### *Solvents and Reagents*

All solvents and reagents were either purchased at high purity suitable for immediate use, or when necessary purified by standard laboratory procedures.<sup>354</sup>

### *Optical Rotations*

Optical Rotations were recorded using a Rudolph research analytical Autopol III automatic polarimeter. Unless otherwise stated, all optical rotations were carried out using chloroform as the solvent.

### *X-ray Crystallography*

Crystals suitable for X-ray diffraction were grown by recrystallization from hot MeOH for compounds **155a** and **155b**, and by slow evaporation from  $\text{CH}_2\text{Cl}_2$  or MeOH for all other compounds. Data were collected at  $-173^\circ\text{C}$  on crystals mounted on a Hampton Scientific cryoloop, at the MX1 or MX2 beamline of the Australian Synchrotron for compounds **163**, **173**, and **175**,<sup>355,356</sup> and on a



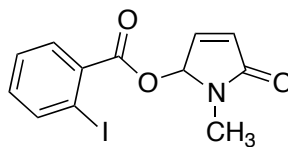
Bruker D8 Quest diffractometer with copper  $\text{ImS}$  microfocus source for compounds **155a**, **155b**, **232–234** and **246**. The structures were solved by direct methods with SHELXS-97,<sup>357</sup> refined using full-matrix least-squares routines against  $F^2$  with SHELXL-97, and visualised using X-SEED or OLEX2.<sup>358,359</sup> The following standard procedure was adopted for refinement and modelling of disorder: All non-hydrogen atoms were refined anisotropically. All hydrogen atoms were placed in calculated positions and refined using a riding model with fixed C–H distances of 0.95 Å ( $sp^2\text{CH}$ ), 0.99 Å ( $\text{CH}_2$ ), 0.98 Å ( $\text{CH}_3$ ). The thermal parameters of all hydrogen atoms were estimated as  $U_{\text{iso}}(\text{H}) = 1.2U_{\text{eq}}(\text{C})$  except for  $\text{CH}_3$ , where  $U_{\text{iso}}(\text{H}) = 1.5U_{\text{eq}}(\text{C})$ .

### *Photoreactions*

Photooxidation reactions were carried out in a photoreactor constructed from a 100 mL measuring cylinder tightly wrapped with a strip of green LEDs up to the 70 mL graduation. The green LEDs emitted with a  $\lambda_{\text{max}}$  of 515 nm, and an overall emission range measured to be approximately 450–600 nm. The strip of LEDs was 85 cm long and contained 102 individual LEDs, providing 4.1 W (0.024 W  $\text{cm}^{-2}$ ) of radiant flux to the photoreactor.

## 5.2 Chapter 1 Experimental Details

### (±)-5-(2-Iodobenzoyoxy)-1-methyl-3,4-dehydropyrrolidin-2-one (37)

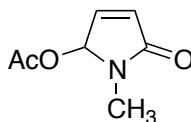


(±) 37

To a stirred solution of *N*-methylpyrrole (1.0076 g, 12.42 mmol) in CH<sub>2</sub>Cl<sub>2</sub> (40 mL) at 0 °C was added Dess–Martin periodinane (13.0867 g, 30.85 mmol, 2.48 eq.). The reaction was stirred for 2 h, at which point H<sub>2</sub>O (30 mL) was added, and the reaction quenched by addition of solid Na<sub>2</sub>S<sub>2</sub>O<sub>5</sub>. The aqueous and organic layers were separated, and the aqueous layer extracted with CH<sub>2</sub>Cl<sub>2</sub> (3 x 25 mL). The combined organic layers were washed with saturated NaHCO<sub>3</sub> (50 mL), dried over MgSO<sub>4</sub>, filtered, and the solvent removed under reduced pressure to give the product as a dark red oil (2.7724 g, 8.079 mmol, 65% yield). NMR spectra agreed with those reported by Howard *et al.*<sup>62</sup>

<sup>1</sup>H NMR δ (400 MHz): 3.03 (s, 3 H), 6.32 (d, *J* = 6.0 Hz, 1 H), 6.67 (apparent d, *J* = 1.4 Hz, 1 H), 7.10 (dd, *J* = 6.0 Hz, 1.7 Hz, 1 H), 7.20 (td, *J* = 7.7 Hz, 1.7 Hz, 1 H), 7.42 (td, *J* = 7.6 Hz, 1.1 Hz, 1 H), 7.82 (dd, *J* = 7.8 Hz, 1.7 Hz, 1 H), 8.03 (dd, *J* = 8.0 Hz, 1.0 Hz, 1 H)

### (±)-5-Acetoxy-1-methyl-3,4-dehydropyrrolidin-2-one (29)



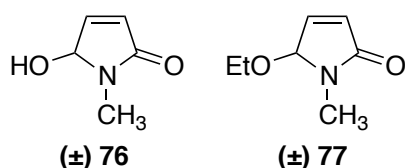
(±) 29

To a stirred solution of IBX (3.0229 g, 10.79 mmol, 2.5 eq.) in AcOH (10 mL) at room temperature was added *N*-methylpyrrole (0.3473 g, 4.28 mmol), and the reaction stirred for 20 h. H<sub>2</sub>O (25 mL) and CH<sub>2</sub>Cl<sub>2</sub> (25 mL) were added, excess Na<sub>2</sub>S<sub>2</sub>O<sub>5</sub> was added, and the solution made basic by addition of solid NaHCO<sub>3</sub>. The aqueous and organic layers were separated, and the aqueous layer extracted with CH<sub>2</sub>Cl<sub>2</sub> (4 x 25 mL). The combined organic layers were

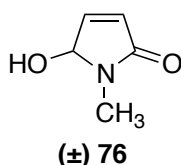
washed with  $\text{NaHCO}_3$  (25 mL), dried over  $\text{MgSO}_4$ , filtered, and the solvent removed under reduced pressure to give the product as a brown oil (0.6272 g, 4.04 mmol, 94% yield) that was used without further purification. NMR spectra matched those reported by Feringa *et al.*<sup>360</sup>

$^1\text{H}$  NMR  $\delta$  (400 MHz): 2.13 (s, 3 H), 2.91 (s, 3 H), 6.23 (d,  $J$  = 5.6 Hz, 1 H), 6.40 (s, 1 H), 6.93 (d,  $J$  = 5.6 Hz, 1 H)

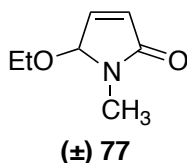
**( $\pm$ )-5-Hydroxy-1-methyl-3,4-dehydropyrrolidin-2-one (**76**) and ( $\pm$ )-5-Ethoxy-1-methyl-3,4-dehydropyrrolidin-2-one (**77**)**



Into the green LED photoreactor was added Rose bengal (0.0113 g), NaOAc (200  $\mu\text{L}$  saturated aqueous solution), EtOH (70 mL), followed by the addition of *N*-methylpyrrole (0.4780 g, 5.892 mmol). The resultant solution was then submerged in an ice/water bath and a stream of  $\text{O}_2$  bubbled through it before the light was turned on. The solution was irradiated for 2 h before the light was turned off and the solvent evaporated. The crude mixture was passed through a plug of silica gel with ethyl acetate to yield a 0.5:1 mixture of the 5-hydroxy-pyrrolin-2-one **76** and the 5-ethoxy-pyrrolin-2-one **77** as a red oil (0.3376 g, 2.569 mmol, 44% yield). NMR spectra agreed with those reported by Howard *et al.*<sup>80</sup>

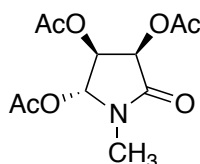


$^1\text{H}$  NMR  $\delta$  (400 MHz): 2.90 (s, 3 H), 5.27 (s, 1 H), 6.06 (d,  $J$  = 5.9 Hz, 1 H), 6.91 (dd,  $J$  = 5.9, 1.5 Hz, 1 H)



$^1\text{H}$  NMR  $\delta$  (400 MHz): 1.16 (t,  $J$  = 7.0 Hz, 3 H), 2.89 (s, 3 H), 3.29 (q,  $J$  = 7.0 Hz, 2 H), 5.27 (s, 1 H), 6.19 (dd,  $J$  = 6.0, 0.8 Hz, 1 H), 6.88 (dd,  $J$  = 6.0, 1.5 Hz, 1 H)

**( $\pm$ )-(2*R*,3*S*,4*R*)-1-Methyl-5-oxopyrrolidine-2,3,4-triyl triacetate (**39**)**



**( $\pm$ ) 39**

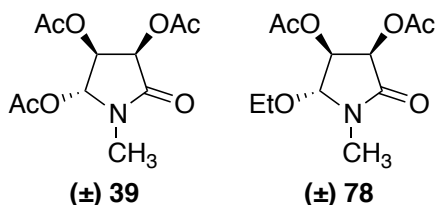
To a stirred solution of acetoxylactam **29** (0.7136 g, 4.599 mmol) in a 5:1 mixture of acetone and  $\text{H}_2\text{O}$  (18 mL), at 0 °C, was added *N*-methylmorpholine-*N*-oxide (3.00 mL of a 50% w/w solution in  $\text{H}_2\text{O}$ , 14.47 mmol, 3.1 eq.) and  $\text{OsO}_4$  (3.60 mL of a 0.0393 M solution in  $\text{H}_2\text{O}$ , 0.1415 mmol, 0.03 eq.). The resulting solution was stirred for 16 h, at which time acetonitrile was added and the solvent removed under reduced pressure. The crude product was then dissolved in pyridine (9 mL) and  $\text{Ac}_2\text{O}$  (9 mL) at 0 °C, and stirred for 16 h.  $\text{H}_2\text{O}$  (30 mL) and  $\text{CH}_2\text{Cl}_2$  (30 mL) were added, and the aqueous and organic layers separated. The aqueous layer was extracted with  $\text{CH}_2\text{Cl}_2$  (3 x 30 mL). The combined organic layers were washed with 2 M HCl (2 x 30 mL) and saturated  $\text{NaHCO}_3$  (2 x 30 mL), dried over  $\text{MgSO}_4$ , filtered, and the solvent removed under reduced pressure. The crude material was purified by elution through a plug of silica using EtOAc/hexanes (70:30) as eluent to give **39** as a yellow oil (0.8331 g, 3.049 mmol, 66% yield)

$^1\text{H}$  NMR  $\delta$  (400 MHz): 2.09 (s, 3 H), 2.11 (s, 3 H), 2.12 (s, 3 H), 2.94 (s, 3 H), 5.36 (d,  $J$  = 5.2 Hz, 1 H), 5.65 (d,  $J$  = 5.2 Hz, 1 H), 6.01 (s, 1 H)

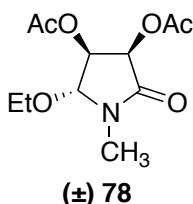
$^{13}\text{C}$  NMR  $\delta$  (100 MHz): 20.4, 20.5, 20.8, 29.0, 67.5, 70.2, 85.1, 169.3, 169.5, 169.6, 170.0

IR  $V_{\text{max}}$ : 1751 (C=O), 1734 (C=O)

HRMS: For  $\text{C}_{11}\text{H}_{15}\text{NO}_7+\text{H}$ , predicted 296.0741, found 296.0749

**(±)-(2*R*,3*S*,4*R*)-1-Methyl-5-oxopyrrolidine-2,3,4-triyl triacetate (39)****and (±)- (2*R*,3*S*,4*R*)-2-ethoxy-1-methyl-5-oxopyrrolidine-3,4-diyl diacetate (78)**

To a stirred solution of a 3:1 mixture of hydroxylactam **76** and ethoxylactam **77** (0.6257 g, 5.206 mmol) in a 5:1 mixture of acetone and H<sub>2</sub>O (12 mL), at 0 °C, was added *N*-methylmorpholine-*N*-oxide (3.20 mL of a 50% w/w solution in H<sub>2</sub>O, 15.43 mmol, 2.96 eq.) and OsO<sub>4</sub> (3.90 mL of a 0.0393 M solution in H<sub>2</sub>O, 0.155 mmol, 0.029 eq.). The resulting solution was stirred for 16 h, at which time acetonitrile was added and the solvent removed under reduced pressure. The crude product was then dissolved in pyridine (6 mL) and Ac<sub>2</sub>O (6 mL) at 0 °C, and stirred for 16 h. H<sub>2</sub>O (25 mL) and CH<sub>2</sub>Cl<sub>2</sub> (25 mL) were added, and the aqueous and organic layers separated. The aqueous layer was extracted with CH<sub>2</sub>Cl<sub>2</sub> (3 x 15 mL). The combined organic layers were washed with 2 M HCl (2 x 25 mL) and saturated NaHCO<sub>3</sub> (2 x 25 mL), dried over MgSO<sub>4</sub>, filtered, and the solvent removed under reduced pressure. The crude mixture was purified by elution through a plug of silica using EtOAc/hexanes (80:20) as eluent, to give a 1:2 mixture of ethoxylactam **78** and acetoxylactam **39** as yellow oil (0.9194 g, 3.423 mmol, 66% yield).

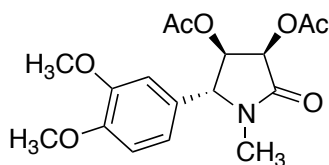


<sup>1</sup>H NMR δ (400 MHz): 1.23 (t, *J* = 7.0 Hz, 3 H), 2.06 (s, 3 H), 2.11 (s, 3 H), 2.93 (s, 3 H), 4.09 (q, *J* = 7.0 Hz, 2 H), 4.60 (s, 1 H), 5.29 (d, *J* = 5.4 Hz, 1 H), 5.54 (d, *J* = 5.4 Hz, 1 H)

### General Procedure for the Introduction of Aryl Groups to Acetoxy-protected Diol Intermediates

To a solution of either acetoxy **39** or a mixture of **39** and ethoxy **78**, in dry  $\text{CH}_2\text{Cl}_2$  at 0 °C under  $\text{N}_2$ , was added the arene (1.2 eq) and  $\text{BF}_3 \cdot \text{OEt}_2$  (1.5 eq) via syringe. The reaction was allowed to warm to room temperature and stirred for 16 h. It was then cooled on an ice bath and quenched with saturated  $\text{NaHCO}_3$ . The aqueous and organic layers were separated and the aqueous layer extracted three times with  $\text{CH}_2\text{Cl}_2$ . The combined organic layers were dried over  $\text{MgSO}_4$  or  $\text{Na}_2\text{SO}_4$ , and the solvent was removed under reduced pressure. Products were purified by flash column chromatography with a mixture of EtOAc and hexanes as eluent, or by washing through a plug of silica with a mixture of EtOAc and hexanes.

#### (±)-(2*R*,3*R*,4*R*)-2-(3,4-Dimethoxyphenyl)-1-methyl-5-oxopyrrolidine-3,4-diyl diacetate (**79**)



(±) **79**

Prepared from triacetoxy **39** (0.1132 g, 0.4143 mmol), with veratrole (0.065 mL, 0.5099 mmol, 1.23 eq.) and  $\text{BF}_3 \cdot \text{OEt}_2$  (77.5  $\mu\text{L}$ , 0.6076 mmol, 1.46 eq.) in dry  $\text{CH}_2\text{Cl}_2$  (5 mL). The crude material was purified by elution through a silica plug with EtOAc/hexanes (80:20) to give **79** as a clear oil (0.0463 g, 0.1318 mmol, 32% yield).

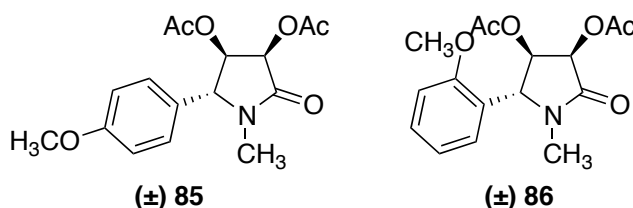
$^1\text{H}$  NMR  $\delta$  (400 MHz): 2.05 (s, 3 H), 2.06 (s, 3 H), 2.82 (s, 3 H), 3.80 (s, 3 H), 3.81 (s, 3 H), 4.46 (s, 1 H), 5.16 (d,  $J$  = 5.6 Hz, 1 H), 5.45 (d,  $J$  = 5.6 Hz, 1 H), 6.61 (dd,  $J$  = 8.0 Hz, 2.0 Hz, 1 H), 6.68 (d,  $J$  = 2.0 Hz, 1 H), 6.80 (d,  $J$  = 8.0 Hz, 1 H)

$^{13}\text{C}$  NMR  $\delta$  (100 MHz): 20.55, 20.90, 29.28, 56.17, 56.18, 67.81, 68.32, 73.62, 109.50, 111.79, 118.00, 127.39, 149.61, 150.10, 168.55, 169.83, 170.28

IR  $V_{\max}$ : 2936, 1750, 1716, 1606, 1594, 1518, 1464, 1374, 1241, 1141, 1064, 1026, 732

HRMS: For  $C_{17}H_{21}NO_7+Na$ , predicted 374.1210, found 374.1221

**(±)-(2*R*,3*R*,4*R*)-2-(4-Methoxyphenyl)-1-methyl-5-oxopyrrolidine-3,4-diyl diacetate (85) and (±)-(2*R*,3*R*,4*R*)-2-(2-methoxyphenyl)-1-methyl-5-oxopyrrolidine-3,4-diyl diacetate (86)**

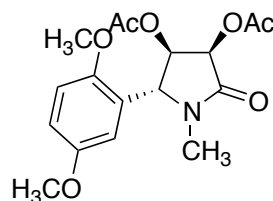


Prepared from a mixture of **39** and **78** (1:0.3, 0.2577 g, 0.9543 mmol), with anisole (0.125 mL, 1.150 mmol, 1.20 eq.) and  $BF_3 \cdot OEt_2$  (0.180 mL, 1.458 mmol, 1.52 eq.) in dry  $CH_2Cl_2$  (10 mL). The crude material was purified by elution through a silica plug with EtOAc/hexanes (80:20) to give an inseparable mixture of **85** and **86** (1:1.3, 0.1977g, 0.8332 mmol, 87% total yield).

$^1H$  NMR  $\delta$  (400 MHz): 2.04 (s, 3.3 H), 2.06 (s, 3 H), 2.07 (s, 4 H), 2.08 (s, 3 H), 2.81 (s, 3 H), 2.82 (s, 3.6 H), 4.48 (s, 1 H), 4.73 (s, 1.3 H), 5.17 (dd,  $J$  = 5.5, 6.7 Hz, 1 H), 5.33 (d,  $J$  = 5.6 Hz, 1.3 H), 5.49 (d,  $J$  = 5.6 Hz, 1 H), 5.51 (d,  $J$  = 5.5 Hz, 1.3 H), 6.85–6.93 (m, 6 H), 7.06 (d,  $J$  = 8.6 Hz, 2 H), 7.29 (ddd,  $J$  = 8.0, 7.0, 2.3 Hz, 1.3)

$^{13}C$  NMR  $\delta$  (100 MHz): 20.3 (2 C), 20.62, 20.68, 28.9, 29.0, 55.3, 55.4, 63.7, 67.3, 68.1, 68.5, 71.7, 73.3, 111.0, 114.8, 120.9, 122.6, 126.3, 126.7, 127.3, 130.1, 157.0, 159.9, 168.2, 168.8, 169.61, 169.67, 169.9, 171.0

**(±)-(2*R*,3*R*,4*R*)-2-(2,5-Dimethoxyphenyl)-1-methyl-5-oxopyrrolidine-3,4-diyl diacetate (80)**



**(±) 80**

Prepared from triacetoxyl **39** (0.0954 g, 0.3491 mmol), with 1,4-dimethoxybenzene (0.0603 g, 0.4379 mmol, 1.25 eq.) and  $\text{BF}_3 \cdot \text{OEt}_2$  (70.0  $\mu\text{L}$ , 0.5671 mmol, 1.62 eq.) in dry  $\text{CH}_2\text{Cl}_2$  (5 mL). The crude material was purified by elution through a silica plug with EtOAc/hexanes (80:20) to give **80** as a clear oil (0.0730 g, 0.2078 mmol, 60% yield).

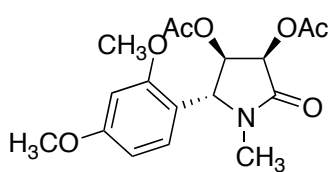
$^1\text{H}$  NMR  $\delta$  (400 MHz): 2.09 (s, 3H), 2.12 (s, 3 H), 2.88 (s, 3 H), 3.77 (s, 3 H), 3.81 (s, 3 H), 4.73 (s, 1 H), 5.38 (d,  $J = 5.6$  Hz, 1 H), 5.56 (d,  $J = 5.2$  Hz, 1 H), 6.51 (ad,  $J = 2.4$  Hz, 1 H), 6.81–6.87 (m, 2 H)

$^{13}\text{C}$  NMR  $\delta$  (100 MHz): 20.6, 20.9, 29.3, 56.0, 56.1, 64.0, 68.7, 72.0, 112.1, 113.5, 113.8, 124.1, 151.3, 154.1, 169.1, 169.8, 169.9

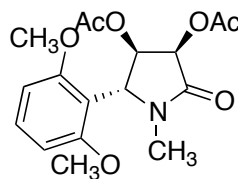
IR  $V_{\text{max}}$ : 2937, 1752, 1719, 1501, 1374, 1243, 1219, 1047

HRMS: For  $\text{C}_{17}\text{H}_{21}\text{NO}_7$ , predicted 351.13180, found 351.13225.

**(±)-(2*R*,3*R*,4*R*)-2-(2,4-Dimethoxyphenyl)-1-methyl-5-oxopyrrolidine-3,4-diyl diacetate (87) and (±)-(2*R*,3*R*,4*R*)-2-(2,6-dimethoxyphenyl)-1-methyl-5-oxopyrrolidine-3,4-diyl diacetate (88)**



**(±) 87**



**(±) 88**

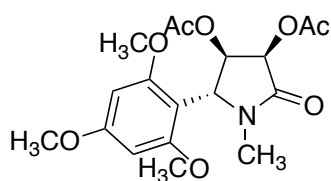


Prepared from a mixture of **39** and **78** (1:0.3, 0.5080 g, 1.881 mmol), with 1,3-dimethoxybenzene (0.300 mL, 2.291 mmol, 1.22 eq.) and  $\text{BF}_3\cdot\text{OEt}_2$  (0.350 mL, 2.835 mmol, 1.51 eq.) in dry  $\text{CH}_2\text{Cl}_2$  (10 mL). The crude material was purified by elution through a silica plug with EtOAc/hexanes (80:20) to give an inseparable 1:0.27 mixture of **87** and **88** (0.4385 g, 1.641 mmol, 87% total yield).

$^1\text{H}$  NMR  $\delta$  (400 MHz): 2.03 (s, 1 H), 2.04 (s, 3 H), 2.06 (s, 3 H), 2.08 (s, 3 H), 2.60 (s, 0.8 H), 2.79 (s, 3 H), 3.75 (s, 3.2 H), 3.76 (s, 4.4 H), 4.63 (s, 1 H), 5.14 (s, 0.27 H), 5.30 (d,  $J = 5.5$  Hz, 1 H), 5.39 (d,  $J = 6.8$  Hz, 0.27 H), 5.52 (d,  $J = 5.5$  Hz, 1 H), 5.71 (d,  $J = 6.8$  Hz, 0.27 H), 6.39–6.46 (m, 2 H), 6.52 (d,  $J = 8.4$  Hz, 0.57 H), 6.80 (d,  $J = 8.3$  Hz, 1 H), 7.22 (t,  $J = 8.4$  Hz, 0.27 H)

$^{13}\text{C}$  NMR  $\delta$  (100 MHz): 14.1, 20.3, 20.4, 20.5, 20.6, 20.9, 27.8, 28.8, 55.43, 55.49, 55.8, 59.1, 60.3, 63.7, 68.6, 69.5, 70.6, 71.7, 99.2, 104.0, 104.3, 110.9, 114.9, 127.4, 130.4, 158.1, 158.5, 161.4, 168.7, 169.5, 169.7

**(±)-(3*R*,4*R*,5*R*)-1-Methyl-2-oxo-5-(2,4,6-trimethoxyphenyl)pyrrolidine-3,4-diyl diacetate (**81**)**

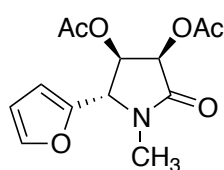


**(±) 81**

Prepared from a mixture of **39** and **78** (1:0.3, 0.2154 g, 0.7948 mmol), with 1,3,5-trimethoxybenzene (0.1604 g, 0.9537 mmol, 1.20 eq.) and  $\text{BF}_3\cdot\text{OEt}_2$  (0.150 mL, 1.215 mmol, 1.53 eq.) in dry  $\text{CH}_2\text{Cl}_2$  (5 mL). The crude material was purified by flash column chromatography with EtOAc/hexanes (90:10) and EtOAc as the eluents to give **81** as a clear oil (0.1597 g, 0.5371 mmol, 68% total yield).

$^1\text{H}$ NMR $\delta$ (400 MHz):	2.04 (s, 3 H), 2.09 (s, 3 H), 2.61 (s, 3 H), 3.76 (s, 3 H), 3.77 (s, 6 H), 5.05 (s, 1 h), 5.38 (d, $J$ = 6.7 Hz, 1 H), 5.72 (d, $J$ = 6.7 Hz, 1 H), 6.09 (s, 2 H)
$^{13}\text{C}$ NMR $\delta$ (100 MHz):	20.4, 20.6, 27.7, 55.3, 55.8, 59.1, 69.6, 70.9, 90.8, 103.5, 159.4, 161.8, 168.6, 169.80, 169.84
IR $V_{\text{max}}$ :	2944, 2243, 1755 (C=O), 1695 (C=O), 1608, 1592, 1470, 1436, 1423, 1373, 1245, 1207, 1154, 1124
HRMS:	For $\text{C}_{18}\text{H}_{24}\text{NO}_8+\text{H}$ , predicted 382.1496, found 382.1496

**( $\pm$ )-(2*S*,3*R*,4*R*)-2-(Furan-2-yl)-1-methyl-5-oxopyrrolidine-3,4-diyl diacetate (**82**)**



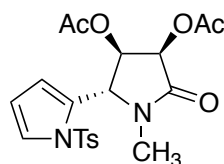
**( $\pm$ ) 82**

Prepared from **39** (0.0410 g, 0.150 mmol), furan (0.020 mL, 0.275 mmol, 1.8 eq.), and 0.028 mL (0.226 mmol, 1.5 eq.) of  $\text{BF}_3\cdot\text{OEt}_2$  in dry  $\text{CH}_2\text{Cl}_2$  (3 mL). The crude material was purified by flash column chromatography using EtOAc/hexanes (80:20) as eluent to give **82** as a clear semi-solid (0.0227 g, 0.0807 mmol, 54 % yield)

$^1\text{H}$ NMR $\delta$ (400 MHz):	2.09 (s, 3 H), 2.12 (s, 3 H), 2.82 (s, 3 H), 4.53 (s, 1 H), 5.48 (d, $J$ = 5.5 Hz, 1 H), 5.73 (d, $J$ = 5.5 Hz, 1 H), 6.32–6.38 (m, 2 H), 7.41 (ad, $J$ = 0.7 Hz, 1 H)
$^{13}\text{C}$ NMR $\delta$ (100 MHz):	20.5, 20.6, 28.7, 61.2, 68.7, 70.7, 109.6, 110.6, 143.9, 147.9, 168.0, 169.7, 169.8
IR $V_{\text{max}}$ :	2937, 1751 (C=O), 1716 (C=O), 1437, 1404, 1375, 1240, 1217

HRMS: For  $C_{13}H_{15}NO_6+Na$ , predicted 304.0792, found 304.0786

**(±)-(3*R*,4*R*,5*R*)-1-Methyl-2-oxo-5-(1-tosyl-1*H*-pyrrol-2-yl)pyrrolidine-3,4-diyl diacetate (**83**)**



**(±) 83**

Prepared from **39** (0.0725 g, 0.265 mmol), *N*-tosylpyrrole (0.0734 g, 0.331 mmol, 1.25 eq.), and  $BF_3 \cdot OEt_2$  (0.050 mL, 0.405 mmol, 1.5 eq.) in dry  $CH_2Cl_2$ , with exclusion from light. The resulting solution was stirred at room temperature for 16 h. The crude material was purified by flash column chromatography using EtOAc/hexanes (80:20) as eluent to give **83** as an off white solid (0.0753 g, 0.1733 mmol, 65 % yield).

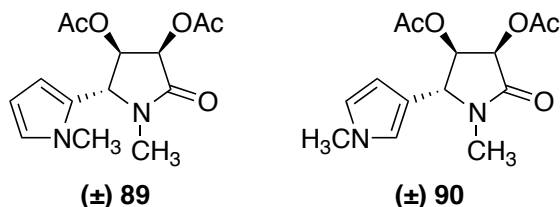
$^1H$  NMR  $\delta$  (400 MHz): 2.05 (s, 3 H), 2.11 (s, 3 H), 2.40 (s, 3H), 2.74 (s, 3 H), 5.04 (s, 1 H), 5.26 (d,  $J$  = 5.2 Hz, 1 H), 5.60 (d,  $J$  = 5.2 Hz, 1 H), 6.04 (s, 1 H), 6.27 (t,  $J$  = 3.4 Hz, 1 H), 7.28–7.35 (m, 3 H), 7.64 (d,  $J$  = 8.3 Hz, 2 H)

$^{13}C$  NMR  $\delta$  (100 MHz): 20.4, 20.5, 21.7, 29.1, 60.7, 67.7, 71.2, 112.1, 113.5, 124.7, 126.7, 128.4, 130.4, 135.8, 145.9, 168.3, 169.42, 169.45

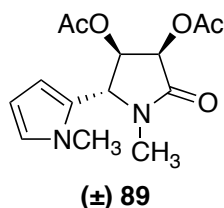
IR  $V_{max}$ : 2933, 2249, 1755 (C=O), 1716 (C=O), 1595, 1481, 1437, 1402, 1371, 1240, 1192

HRMS: For  $C_{20}H_{22}N_2O_7S+Na$ , predicted 457.1040, found 457.1030

(±)-(2*R*,3*R*,4*R*)-1-methyl-2-(1-Methyl-1*H*-pyrrol-2-yl)-5-oxopyrrolidine-3,4-diyl diacetate (**89**) and (±)-(2*R*,3*R*,4*R*)-1-methyl-2-(1-methyl-1*H*-pyrrol-3-yl)-5-oxopyrrolidine-3,4-diyl diacetate (**90**)



Prepared from a mixture of **39** and **78** (1:0.2, 0.3751 g, 1.384 mmol), with *N*-methylpyrrole (0.1368 g, 1.686 mmol, 1.22 eq.) and  $\text{BF}_3 \cdot \text{OEt}_2$  (0.260 mL, 1.215 mmol, 1.52 eq.) in dry  $\text{CH}_2\text{Cl}_2$  (10 mL). The crude mixture was purified by automated flash column chromatography, using a solvent gradient from  $\text{CH}_2\text{Cl}_2$  to  $\text{EtOAc}/\text{CH}_2\text{Cl}_2$  (60:40) to give **89** as a clear oil (0.1136g, 0.3860 mmol, 28% yield) and **90** as a clear oil (0.0909 g, 0.3089 mmol, 22% yield).

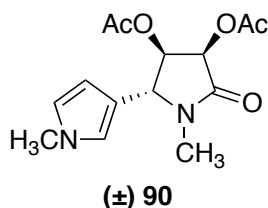


$^1\text{H}$  NMR  $\delta$  (400 MHz): 2.12 (s, 3 H), 2.13 (s, 3H), 2.92 (s, 3 H), 3.67 (s, 3 H), 4.58 (s, 1 H), 5.34 (d,  $J = 5.1$  Hz, 1 H), 5.56 (d,  $J = 5.1$  Hz, 1 H), 5.85 (d,  $J = 2.76$  Hz, 1 H), 6.07 (t,  $J = 3.1$  Hz, 1 H), 6.65 (s, 1 H)

$^{13}\text{C}$  NMR  $\delta$  (100 MHz): 20.4, 20.7, 29.2, 33.9, 61.0, 68.4, 71.3, 107.1, 107.7, 124.4, 125.3, 168.0, 169.0, 170.0

IR  $V_{\text{max}}$ : 2936, 1755 (C=O), 1713 (C=O), 1494, 1436, 1402, 1374, 1296, 1242, 1220, 1128, 1084, 1061

HRMS: For  $\text{C}_{14}\text{H}_{18}\text{N}_2\text{O}_5$ , predicted 294.12157, found 294.12232.  $m/z$  (EI+): 294 ( $\text{M}^+$ , 5), 234 (50), 192



(100), 175 (45), 163 (10), 134 (10), 123 (80), 106 (10), 94 (20)

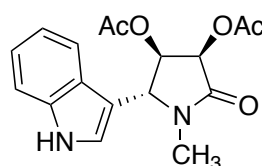
$^1\text{H}$  NMR  $\delta$  (400 MHz): 2.08 (s, 3 H), 2.11 (s, 3 H), 2.87 (s, 3 H), 3.61 (s, 3 H), 4.46 (s, 1 H), 5.29 (d,  $J$  = 5.3 Hz, 1 H), 5.61 (d,  $J$  = 5.3 Hz, 1 H), 5.96 (s, 1 H), 6.49 (s, 1 H), 6.57 (s, 1 H)

$^{13}\text{C}$  NMR  $\delta$  (100 MHz): 20.4, 20.7, 28.8, 36.3, 62.1, 68.7, 73.5, 106.6, 118.3, 119.5, 123.2, 167.8, 169.7, 170.0

IR  $V_{\text{max}}$ : 2936, 1750 (C=O), 1713 (C=O), 1558, 1510, 1481, 1438, 1403, 1373, 1301, 1242, 1221, 1168, 1128, 1081, 1060

HRMS: For  $\text{C}_{14}\text{H}_{18}\text{N}_2\text{O}_5$ , predicted 294.12157, found 294.12100.  $m/z$  (EI+): 294 ( $M^+$ , 1), 268 (1), 234 (80), 192 (100), 175 (80), 163 (5), 136 (5), 123 (100), 106 (5)

**( $\pm$ )-(2*R*,3*R*,4*R*)-2-(1*H*-Indol-3-yl)-1-methyl-5-oxopyrrolidine-3,4-diyl diacetate (**84**)**



**( $\pm$ ) 84**

Prepared from a mixture of **39** and **78** (1:0.3, 0.0981 g, 0.3607 mmol), with indole (0.0524 g, 0.4473 mmol, 1.24 eq.) and  $\text{BF}_3 \cdot \text{OEt}_2$  (0.070 mL, 0.5672 mmol, 1.57 eq.) in dry  $\text{CH}_2\text{Cl}_2$  (4 mL). The crude material was purified by flash column chromatography using EtOAc/hexanes (90:10) as eluent to give **84** as a white solid (0.0824 g, 0.2494 mmol, 69% yield).

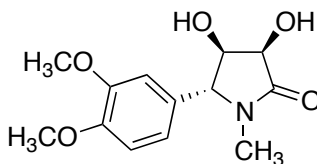
$^1\text{H}$  NMR  $\delta$  (400 MHz): 2.10 (s, 3 H), 2.16 (s, 3 H), 2.96 (s, 3 H), 4.93 (s, 1 H), 5.46 (dd,  $J$  = 5.3, 1.0 Hz, 1 H), 5.66 (d,  $J$  = 5.2 Hz, 1 H), 6.99 (d,  $J$  = 2.4 Hz, 1 H), 7.16 (td,  $J$  = 7.5, 0.7 Hz, 1 H), 7.24 (td,  $J$  = 7.5, 0.8 Hz, 1 H),

	7.41 (d, $J$ = 8.1 Hz, 1 H) 7.65 (d, $J$ = 7.9 Hz, 1 H), 8.81 (bs, 1 H)
$^{13}\text{C}$ NMR $\delta$ (100 MHz):	20.5, 20.9, 29.3, 61.5, 69.0, 72.6, 110.1, 111.8, 118.6, 120.5, 122.0, 123.0, 125.3, 137.0, 168.4, 169.8, 170.2
IR $V_{\text{max}}$ :	3311, 2931, 1751 (C=O), 1705 (C=O), 1460, 1435, 1404, 1371, 1242, 1085, 1062
HRMS:	For $\text{C}_{17}\text{H}_{18}\text{N}_2\text{O}_5$ , predicted 330.12157, found 330.12116. $m/z$ (EI+): 330 ( $M^+$ , 10), 270 (50), 228 (100), 211 (60), 159 (70), 130 (25), 60 (10)
MP:	184.5–185 °C

### General Procedure for Deacetoxylation of Diols With Base

To a solution of the diacetoxylactam in MeOH (5 mL) was added  $\text{K}_2\text{CO}_3$  (2–10 eq). This was stirred at room temperature for 30 minutes, at which point sufficient  $\text{CH}_2\text{Cl}_2$  was added to make the reaction mixture a 20% v/v solution of MeOH in dichloromethane. This was then filtered through a small plug of silica, which was washed with further MeOH/ $\text{CH}_2\text{Cl}_2$  (20:80) and the solvent evaporated. When necessary, further purification was carried out by flash column chromatography.

### (±)-(3*R*,4*R*,5*R*)-5-(3,4-Dimethoxyphenyl)-3,4-dihydroxy-1-methylpyrrolidin-2-one (**45**)

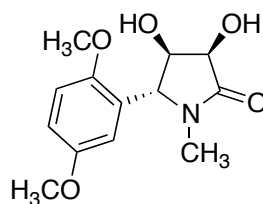


(±) **45**

Prepared from **79** (0.0644 g, 0.18 mmol) and  $\text{K}_2\text{CO}_3$  (0.0511 g, 0.370 mmol, 2.0 eq.). Product **45** was isolated as a clear oil (0.0322 g, 0.1204 mmol, 66 % yield).

$^1\text{H}$ NMR $\delta$ (400 MHz):	2.79 (s, 3 H), 3.84 (s, 3 H), 3.85 (s, 3 H), 4.16 (s, 1 H), 4.46 (s, 1 H), 4.81 (s, b, 1 H), 6.61 (d, $J$ = 8.0 Hz, 1 H), 6.68 (s, 1 H), 6.83 (d, $J$ = 8.4 Hz, 1 H)
$^{13}\text{C}$ NMR $\delta$ (100 MHz):	29.4, 56.2, 69.5, 70.38, 73.3, 109.5, 111.8, 118.2, 128.6, 149.3, 150.0, 173.4
IR $V_{\text{max}}$ :	3356 (OH), 2934, 1681 (C=O), 1518, 1464, 1419, 1400, 1256, 1239, 1139, 1079, 1024
HRMS:	For $\text{C}_{13}\text{H}_{17}\text{NO}_5$ , predicted 267.11067, found 267.11111. $m/z$ (EI+): 267 ( $M^+$ , 100), 249 (5), 220 (5), 192 (5), 180 (45), 164 (15), 151 (50), 133 (5)

**( $\pm$ )-(3*R*,4*R*,5*R*)-5-(2,5-Dimethoxyphenyl)-3,4-dihydroxy-1-methylpyrrolidin-2-one (**50**)**



**( $\pm$ ) 50**

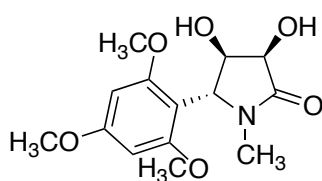
Prepared from **80** (0.0157 g, 0.0446 mmol) in MeOH (3 mL) with  $\text{K}_2\text{CO}_3$  (0.0803 g, 0.581 mmol, 13 eq.). The solution in 20% MeOH in  $\text{CH}_2\text{Cl}_2$  was filtered through a pad of celite, and the solvent removed. The crude material was purified by by flash column chromatography, with EtOAc/MeOH (90:10) as eluent, to give **50** as a clear oil (0.0048 g, 0.0179mmol, 40 % yield)

$^1\text{H}$ NMR $\delta$ (400 MHz):	2.81 (s, 3 H), 3.73 (s, 3 H), 3.84 (s, 3 H), 4.06 (d, $J$ = 5.1 Hz, 1 H), 4.25 (d, $J$ = 5.1 Hz, 1 H), 4.70 (s, 1 H), 6.42 (d, $J$ = 2.8 Hz, 1 H), 6.88 (dd, $J$ = 8.8, 2.8 Hz, 1 H), 6.99 (d, $J$ = 8.9 Hz, 1 H)
$^{13}\text{C}$ NMR $\delta$ (100 MHz):	29.4, 56.1, 56.4, 67.7, 71.1, 73.5, 113.3, 113.6, 114.2, 126.5, 152.8, 155.4, 175.9

IR  $V_{\max}$ : 3313 (OH), 2931, 1689 (C=O), 1496, 1280, 1219, 1155, 1078, 1047, 1024

HRMS: For  $C_{13}H_{17}NO_5$ , predicted 267.11067, found 267.11020.  $m/z$  (EI+): 267 ( $M^+$ , 100), 249 (5), 206 (10), 190 (10), 180 (45), 164 (20), 151 (45), 121 (15)

**(±)-(3*R*,4*R*,5*R*)-5-(2,4,6-Trimethoxyphenyl)-3,4-dihydroxy-1-methylpyrrolidin-2-one (56)**



**(±) 56**

Prepared from **81** (0.1027g, 0.2693 mmol) and  $K_2CO_3$  (0.0801g, 0.5795 mmol, 2.15 eq.). Product **56** isolated as a clear oil (0.0628 g, 0.2112 mmol, 78% yield).

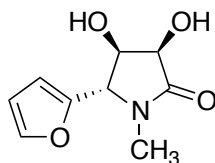
$^1H$  NMR  $\delta$  (400 MHz): 2.57 (s, 3 H), 3.72 (s, 6 H), 3.76 (s, 3 H), 3.92 (bs, 1 H), 4.21 (d,  $J$  = 6.5 Hz, 1 H), 4.63 (d,  $J$  = 6.5 Hz, 1 H), 5.05 (s, 1 H), 6.07 (s, 2 H), 6.11 (bs, 1 H)

$^{13}C$  NMR  $\delta$  (100 MHz): 27.8, 55.3, 55.7, 62.4, 70.1, 70.3, 90.6, 104.6, 159.5, 161.4, 174.1

IR  $V_{\max}$ : 3330 (OH), 2941, 2245, 1674 (C=O), 1608, 1495, 1467, 1418, 1335, 1226, 1205, 1153, 1124

HRMS: For  $C_{14}H_{19}NO_6$ , predicted 297.12124, found 297.12196.  $m/z$  (EI+): 297 ( $M^+$ , 50), 279 (20), 220 (15), 210 (60), 194 (20), 181 (100), 168 (15), 151 (10), 121 (15)



**(±)-(3*R*,4*R*,5*S*)-5-(Furan-2-yl)-3,4-dihydroxy-1-methylpyrrolidin-2-one (62)****(±) 62**

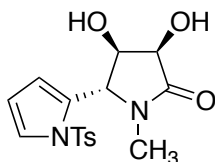
Prepared from **82** (0.0144 g, 0.0511 mmol) and K<sub>2</sub>CO<sub>3</sub> (0.0881 g, 0.6374 mmol, 12 eq.). The crude material was purified by flash column chromatography with EtOAc/hexanes (10:90) as eluent to give the product **62** as a clear oil (0.0034 g, 0.0172 mmol, 34 % yield)

<sup>1</sup>H NMR δ (400 MHz): 2.76 (s, 3 H), 4.26 (dd, *J* = 5.2, 1.2 Hz, 1 H), 4.47 (d, *J* = 5.2 hz, 1 H), 4.49 (d, *J* = 1.2 Hz, 1 H), 6.41 (ad, *J* = 1.3 hz, 2 H), 7.51 (at, *J* = 1.3 hz, 1 H)

<sup>13</sup>C NMR δ (100 MHz): 28.7, 65.0, 71.5, 72.1, 110.0, 111.5, 144.6, 151.2, 174.9

IR V<sub>max</sub>: 3259 (OH), 1689 (C=O), 1485, 1402, 1311, 1247, 1143, 1076, 1012

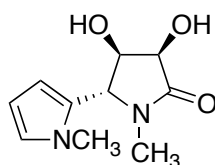
HRMS: For C<sub>9</sub>H<sub>11</sub>NO<sub>4</sub>, predicted 197.06881, found 197.06875. *m/z* (EI+): 197 (M+, 85), 180 (10), 168 (10), 150 (5), 122 (5), 110 (100), 100 (25), 94 (15), 81 (75), 66 (10), 60 (20), 53 (10)

**(±)-(3*R*,4*R*,5*R*)-3,4-Dihydroxy-1-methyl-5-(1-tosyl-1*H*-pyrrol-2-yl)pyrrolidin-2-one (58)****(±) 65**

Prepared from **83** (0.0888g, 0.2044 mmol) and K<sub>2</sub>CO<sub>3</sub> (0.0577g, 0.4175 mmol, 2.0 eq.). The crude material was purified by flash column chromatography using EtOAc/hexanes (80:20) and EtOAc/MeOH (90:10) as eluents to give the product **58** as a clear oil (0.0256 g, 0.0730 mmol, 36% yield)

$^1\text{H}$ NMR $\delta$ (400 MHz, MeOD):	2.42 (s, 3 H), 2.59 (s, 3 H), 4.04 (d, $J$ = 4.9 Hz, 1 H), 4.28 (d, $J$ = 4.9 Hz, 1 H), 4.90 (s, 1 H), 5.97–5.99 (m, 1 H), 6.31 (t, $J$ = 3.4 Hz, 1 H), 7.41–7.48 (m, 3 H), 7.81 (d, $J$ = 8.4 Hz, 2 H)
$^{13}\text{C}$ NMR $\delta$ (100 MHz):	21.5, 29.2, 65.0, 70.6, 72.9, 112.9, 113.9, 125.5, 128.0, 131.0, 131.4, 137.2, 147.3, 175.2
IR $V_{\text{max}}$ :	3335 (OH), 2490, 1689 (C=O), 1595, 1485, 1448, 1402, 1369, 1240, 1192, 1174, 1128, 1080
HRMS:	For $\text{C}_{16}\text{H}_{18}\text{N}_2\text{O}_5\text{S}$ , predicted 350.09364, found 350.09459. $m/z$ (EI+): 350 ( $\text{M}^+$ , 15), 263 (20), 195 (100), 177 (40), 155 (20), 120 (15), 109 (40), 91 (80)

**( $\pm$ )-(3*R*,4*R*,5*R*)-3,4-Dihydroxy-1-methyl-5-(1-methyl-1*H*-pyrrol-2-yl)pyrrolidin-2-one (60)**



**( $\pm$ ) 60**

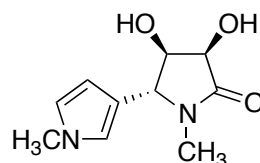
Prepared from **89** (0.0350 g, 0.1189 mmol) and  $\text{K}_2\text{CO}_3$  (0.0296 g, 0.2141 mmol, 1.80 eq.). Product isolated as a clear oil (0.0186 g, 0.0885 mmol, 74% yield).

$^1\text{H}$ NMR $\delta$ (400 MHz):	2.88 (s, 3 H), 3.66 (s, 3 H), 4.15 (bs, 1 H), 4.20 (d, $J$ = 4.9 Hz, 1 H), 4.50 (d, $J$ = 4.7 Hz, 1 H), 4.59 (s, 1 H), 5.32 (bs, 1 H), 5.76 (s, 1 H), 6.04 (s, 1 H), 6.62 (s, 1 H)
$^{13}\text{C}$ NMR $\delta$ (100 MHz):	29.5, 34.0, 63.6, 69.6, 71.4, 106.2, 107.5, 123.7, 127.1, 173.7

IR  $V_{\max}$ : 3336 (OH), 1683 (C=O), 1496, 1448, 1399, 1298, 1247, 1147, 1078

HRMS: For  $C_{10}H_{14}N_2O_3+Na$ , predicted 233.0897, found 233.0905

**(±)-(3*R*,4*R*,5*R*)-3,4-dihydroxy-1-methyl-5-(1-methyl-1*H*-pyrrol-3-yl)pyrrolidin-2-one (92)**



**(±) 92**

Prepared from **90** (0.0296 g, 0.1006 mmol) and  $K_2CO_3$  (0.0346 g, 0.2503 mmol, 2.49 eq.). Product isolated as a clear oil (0.0156 g, 0.0742 mmol, 74% yield).

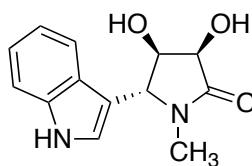
$^1H$  NMR  $\delta$  (400 MHz): 2.82 (s, 3 H), 3.61 (s, 3 H), 4.21 (d,  $J$  = 4.4 Hz, 1 H), 4.42 (s, 1 H), 4.57 (s, 1 H), 5.90 (s, 1 H), 6.46 (s, 1 H), 6.55 (s, 1 H)

$^{13}C$  NMR  $\delta$  (100 MHz): 28.9, 36.3, 64.6, 70.0, 73.4, 106.7, 119.6, 119.7, 123.0, 173.1

IR  $V_{\max}$ : 3341 (OH), 1679 (C=O), 1555, 1509, 1401, 1299, 1247, 1146, 1075

HRMS: For  $C_{10}H_{14}N_2O_3+Na$ , predicted 233.0897, found 233.0905

**(±)-(3*R*,4*R*,5*R*)-3,4-dihydroxy-5-(1*H*-indol-3-yl)-1-methylpyrrolidin-2-one (64)**



**(±) 64**

Prepared from **84** (0.0376g, 0.1138 mmol) and K<sub>2</sub>CO<sub>3</sub> (0.0322g, 0.2329 mmol). Product isolated as a yellow oil (0.0185 g, 0.07512 mmol, 66 % yield).

<sup>1</sup>H NMR δ (400 MHz, CD<sub>3</sub>OD): 2.84 (s, 3 H), 4.25 (dd, *J* = 5.17, 1.93 Hz, 1 H), 4.40 (d, *J* = 5.2 Hz, 1 H), 4.79 (d, *J* = 1.6 Hz, 1 H), 7.05 (t/dd, *J* = 7.3 Hz, 1 H), 7.11 (s, 1 H), 7.15 (t/dd, 7.3 Hz, 1 H), 7.39 (d, *J* = 8.2 Hz, 1 H), 7.47 (d, *J* = 7.9 Hz, 1 H)

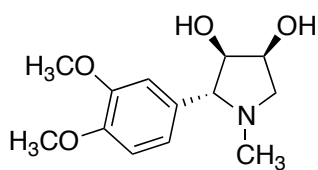
<sup>13</sup>C NMR δ (100 MHz, CD<sub>3</sub>OD): 29.0, 65.4, 71.6, 73.8, 111.6, 112.8, 118.9, 120.5, 123.0, 123.7, 126.9, 138.7, 175.0

IR V<sub>max</sub>: 3308 (OH), 2436, 1678 (C=O), 1483, 1454, 1402, 1334, 1234, 1147, 1076

HRMS: For C<sub>13</sub>H<sub>14</sub>N<sub>2</sub>O<sub>3</sub>, predicted 246.10044, found 246.10053. *m/z* (EI+): 246 (M+, 100), 230 (15), 212 (100), 178 (100), 157 (80), 149 (60), 130 (80), 123 (60), 104 (60), 97 (35), 91 (40), 81 (40)

### General Procedure For Reduction of Amides With LiAlH<sub>4</sub>

To a solution of the diacetoxylactam in anhydrous THF (3 mL) under N<sub>2</sub> was added LiAlH<sub>4</sub> (5 eq.). The reaction was heated at reflux for 4 hours, before being allowed to cool to room temperature, and quenched by addition of EtOAc and H<sub>2</sub>O. The mixture was filtered through celite, the organic and aqueous layers were separated, and the aqueous layer extracted with EtOAc. Combined organic extracts were dried over MgSO<sub>4</sub> and solvent removed under reduced pressure to yield the target diols. When necessary, Purification was carried out by flash column chromatography.

**(±)-(2*R*,3*R*,4*S*)-2-(3,4-Dimethoxyphenyl)-1-methylpyrrolidine-3,4-diol (43)****(±) 43**

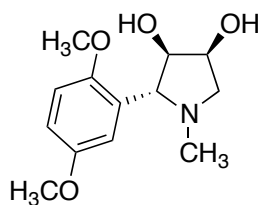
Prepared from lactam **79** (0.0552 g, 0.1571 mmol,) and LiAlH<sub>4</sub> (0.0333 g, 0.8774 mmol, 5.58 mmol). Product isolated as a white amorphous solid (0.0164 g, 0.0647 mmol, 41% yield).

<sup>1</sup>H NMR δ (400 MHz): 2.14 (s, 3 H), 2.37 (dd, *J* = 8.0 Hz, 4.0 Hz, 1 H), 2.68 (bs, 2 H), 3.06 (d, *J* = 8.0 Hz, 1 H), 3.60 (dd, *J* = 12.0 Hz, 8.0 Hz, 1 H), 3.82-3.92 (m, 7 H), 4.27 (q, *J* = 5.0 Hz, 1 H), 6.82-6.92 (m, 3 H)

<sup>13</sup>C NMR δ (100 MHz): 40.6, 56.2, 56.3, 63.3, 68.7, 75.7, 78.7, 110.4, 111.5, 120.6, 132.6, 149.0, 149.7

IR V<sub>max</sub>: 3347, 2936, 1593, 1517 1464, 1419, 1263, 1231, 1139, 1025

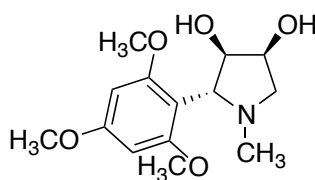
HRMS: For C<sub>13</sub>H<sub>19</sub>NO<sub>4</sub>, predicted 253.13141, found 253.13143. *m/z* (EI<sup>+</sup>): 253 (M<sup>+</sup>, 15), 217 (100), 202 (50), 192 (60), 178 (90), 164 (30), 151 (45), 133 (15), 108 (10), 91 (10), 83 (20), 77 (15), 65 (10), 44 (25)

**(±)-(2*R*,3*R*,4*S*)-2-(2,5-Dimethoxyphenyl)-1-methylpyrrolidine-3,4-diol (44)****(±) 44**

Prepared from lactam **80** (0.0809 g, 0.2302 mmol,) and LiAlH<sub>4</sub> (0.0465 g, 1.225 mmol, 5.32 mmol). Product isolated as a white amorphous solid (0.0404 g, 0.1595 mmol, 69% yield).

$^1\text{H}$ NMR $\delta$ (400 MHz):	2.23 (s, 3 H), 2.49 (dd, $J$ = 9.9, 5.9 Hz, 1 H), 3.19 (bs, 2 H), 3.53 (dd, $J$ = 9.9, 6.0 Hz, 1 H), 3.69 (d, $J$ = 6.3 Hz, 1 H), 3.76 (s, 3 H), 3.80 (s, 3 H), 3.84 (t, $J$ = 6.3 Hz, 1 H), 4.17 (q, $J$ = 6.0 Hz, 1 H), 6.74 (dd, $J$ = 8.9, 3.1 Hz, 1 H), 6.83 (d, $J$ = 8.9 Hz, 1 H), 7.03 (d, $J$ = 3.1 Hz, 1 H)
$^{13}\text{C}$ NMR $\delta$ (100 MHz):	41.3, 55.9, 56.5, 62.7, 69.2, 69.8, 79.1, 112.0, 112.6, 113.1, 130.2, 151.9, 154.7
IR $V_{\text{max}}$ :	3403, 2940, 2834, 2785, 1495, 1464, 1275, 1217, 1177, 1159, 1045
HRMS:	For $\text{C}_{13}\text{H}_{19}\text{NO}_4$ , predicted 253.13141, found 253.13160. $m/z$ (EI+): 253 ( $\text{M}^+$ , 30), 235 (10), 217 (15), 202 (10), 192 (100), 178 (30), 162 (40), 150 (25), 121 (20), 83 (25), 44 (15)

**( $\pm$ )-(2*R*,3*R*,4*S*)-1-Methyl-2-(2,4,6-trimethoxyphenyl)pyrrolidine-3,4-diol**  
**(55)**



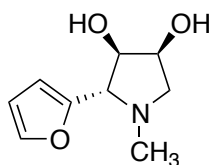
**( $\pm$ ) 55**

prepared from lactam **81** (0.1021 g, 0.2677 mmol,) and  $\text{LiAlH}_4$  (0.0510 g, 1.344 mmol, 5.02 mmol). Product isolated as an amorphous white solid (0.0503 g, 0.1775 mmol, 66% yield).

$^1\text{H}$ NMR $\delta$ (400 MHz, in MeOD):	2.22 (s, 3 H), 2.45 (t, $J$ = 8.9 Hz, 1 H), 3.24 (dd, $J$ = 9.1, 5.9 Hz, 1 H), 3.79 (s, 6 H), 3.80 (s, 3 H), 4.01 (d, $J$ = 4.1 Hz, 1 H), 4.33 (dd, $J$ = 14.4, 6.0 Hz, 1 H), 4.42 (t, $J$ = 5.2 Hz, 1 H), 6.20 (s, 2 H)
---	--

$^{13}\text{C}$ NMR $\delta$ (100 MHz):	42.0, 55.7, 56.0 (broad, more than one methoxy signal), 61.8, 69.6, 70.8, 75.4, 91.8, 161.2, 162.8
IR $V_{\text{max}}$ :	3469 (OH), 1607, 1591, 1461, 1416, 1331, 1224, 1204, 1153, 1118
HRMS:	For $\text{C}_{14}\text{H}_{21}\text{NO}_5$ , predicted 283.14197, found 283.14212. $m/z$ (EI+): 283 ( $M^+$ , 20), 266 (95), 247 (10), 223 (30), 210 (25), 192 (40), 179 (100), 164 (5), 136 (10), 118 (100)

**( $\pm$ )-(2*S*,3*R*,4*S*)-2-(Furan-2-yl)-1-methylpyrrolidine-3,4-diol (**61**)**



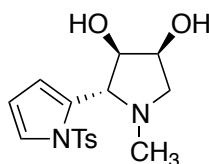
**( $\pm$ ) 61**

Prepared from lactam **82** (0.0631 g, 0.2243 mmol) and  $\text{LiAlH}_4$  (0.0457 g, 1.204 mmol, 5.37 eq.). The crude material was purified by flash column chromatography using EtOAc as eluent to give the product **61** as a clear oil (0.0115g, 0.0627 mmol, 28% yield).

$^1\text{H}$ NMR $\delta$ (400 MHz):	2.22 (s, 3 H), 2.41 (dd, $J$ = 10.3, 4.9 Hz, 1 H), 2.93 (bs, 2 H), 3.33 (d, $J$ = 6.7 Hz, 1 H), 3.51 (dd, $J$ = 10.2, 6.2 Hz, 1 H), 4.21 (t, $J$ = 6.6 Hz, 1 H), 4.29 (dd, $J$ = 11.6, 5.8 Hz, 1 H), 6.32 (d, $J$ = 10.5 Hz, 2 H), 7.40 (s, 1 H)
$^{13}\text{C}$ NMR $\delta$ (100 MHz):	40.4, 62.4, 68.8, 68.9, 75.1, 109.0, 110.3, 142.8, 152.5
IR $V_{\text{max}}$ :	3335 (OH), 2945, 2847, 2791, 1599, 1508, 1450, 1402, 1348, 1327, 1236, 1215, 1151, 1105, 1080, 1043, 1010

HRMS: For  $C_9H_{13}NO_3$ , predicted 183.08954, found 183.08957.  $m/z$  (EI+): 183 ( $M^+$ , 30), 166 (5), 147 (5), 123 (100), 108 (60), 94 (10), 87 (40), 82 (20), 73 (5)

**(±)-(2*R*,3*R*,4*S*)-1-Methyl-2-(1-tosyl-1*H*-pyrrol-2-yl)pyrrolidine-3,4-diol (57)**



**(±) 57**

Prepared from lactam **83** (0.0918 g, 0.2113 mmol) and  $LiAlH_4$  (0.0402 g, 1.059 mmol, 5.01 eq). The crude material was purified by flash column chromatography using EtOAc/MeOH (90:10) as the eluent, to give **57** as a clear oil (0.0320 g, 0.0951 mmol, 45 % yield)

$^1H$  NMR  $\delta$  (400 MHz): 1.90 (s, 3 H), 2.37-2.42 (m, 4 H), 2.91 (sb, 2 H), 3.32 (dd,  $J = 9.1, 6.0$  Hz, 1 H), 3.58 (d,  $J = 4.2$  Hz, 1 H), 3.94 (dd,  $J = 5.9, 4.5$  Hz, 1 H), 4.16 (dd,  $J = 13.3, 6.3$  Hz, 1 H), 6.27 (t,  $J = 3.3$  Hz, 1 H), 6.30-6.33 (m, 1 H), 7.28 (d,  $J = 8.1$  Hz, 1 H)

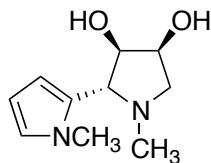
$^{13}C$  NMR  $\delta$  (100 MHz): 21.7, 40.6, 60.9, 69.3, 69.8, 77.9, 112.1, 123.5, 126.8, 130.0, 135.1, 136.4, 145.3

IR  $V_{max}$ : 3396 (OH), 2941, 1597, 1363, 1190, 1174, 1149, 1120, 1091, 1057

HRMS: For  $C_{16}H_{20}N_2O_4S$ , predicted 336.11438, found 336.11402.  $m/z$  (EI+): 336 ( $M^+$ , 10), 301 (5), 276 (30), 263 (20), 212 (30), 197 (20), 181 (80), 155 (20), 121 (100), 108 (30), 91 (60)



**(±)-(2R,3R,4S)-1-Methyl-2-(1-methyl-1H-pyrrol-2-yl)pyrrolidine-3,4-diol**  
**(59)**



**(±) 59**

Prepared from lactam **89** (0.0344g, 0.1169 mmol) and LiAlH<sub>4</sub> (0.0221 g, 0.5823 mmol, 4.98 eq.). The crude material was purified by flash column chromatography using 95:5 MeOH/NH<sub>3</sub> in CH<sub>2</sub>Cl<sub>2</sub> (15:85) as eluent to give **59** as a pale yellow oil (0.0143 g, 0.0728 mmol, 62% yield).

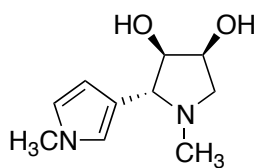
<sup>1</sup>H NMR δ (600 MHz): 2.20 (s, 3 H), 2.61 (dd, *J* = 10.7, 4.6 Hz, 1 H), 3.37–3.51 (m, 3 H), 3.62 (s, *J* = 7.2 Hz, 1 H), 3.65 (s, 3 H), 4.11 (at, *J* = 6.7 Hz, 1 H), 4.28 (dd, *J* = 11.0, 5.88 Hz, 1 H), 6.09–6.11 (m, 1 H), 6.12–6.15 (m, 1 H), 6.58–6.61 (m, 1 H)

<sup>13</sup>C NMR δ (150 MHz): 34.4, 39.9, 62.0, 67.2, 68.6, 76.7, 107.4, 108.5, 123.6, 128.9

IR V<sub>max</sub>: 3319, 2938, 1733, 1574, 1489, 1450, 1409, 1301, 1240, 1165, 1090

HRMS: For C<sub>10</sub>H<sub>16</sub>N<sub>2</sub>O<sub>2</sub>, predicted 196.12118, found 196.121527. *m/z* (EI+): 196 (M<sup>+</sup>, 50), 160 (35), 145 (10), 135 (75), 121 (90), 106 (30), 94 (80), 80 (50), 72 (15)

**(±)-(2R,3R,4S)-1-Methyl-2-(1-methyl-1H-pyrrol-3-yl)pyrrolidine-3,4-diol**  
**(93)**



**(±) 93**

Prepared from lactam **90** (0.0464 g, 0.158 mmol) and LiAlH<sub>4</sub> (0.0304 g, 0.801 mmol, 5.0 eq.). The crude material was purified by flash column chromatography using 95:5 MeOH/NH<sub>3</sub> in CH<sub>2</sub>Cl<sub>2</sub> (20:80) as eluent to give **93** as a pale brown oil (0.0091 g, 0.0463 mmol, 29% yield).

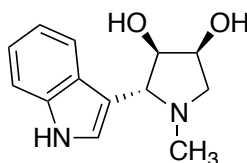
<sup>1</sup>H NMR δ (400 MHz): 2.22 (s, 3 H), 2.35 (dd, *J* = 10.5, 4.8 Hz, 1 H), 2.77 (bs, 2 H), 3.09 (d, *J* = 7.8 Hz, 1 H), 3.59 (dd, *J* = 10.5, 6.5 Hz, 1 H), 3.62 (s, 3 H), 3.96 (at, *J* = 7.2 Hz, 1 H), 4.23–4.30 (m, 1 H), 6.07–6.13 (m, 1 H), 6.55–6.59 (m, 1 H), 6.59–6.63 (m, 1 H)

<sup>13</sup>C NMR δ (100 MHz): 36.2, 40.3, 62.7, 63.2, 68.1, 69.1, 107.2, 120.9, 121.8, 122.4

IR V<sub>max</sub>: 3291, 2941, 2780, 1507, 1448, 1419, 1309, 1166, 1103, 1096

HRMS: For C<sub>10</sub>H<sub>16</sub>N<sub>2</sub>O<sub>2</sub>, predicted 196.12118, found 196.12150. *m/z* (EI+): 196 (M<sup>+</sup>, 45), 179 (10), 160 (15), 136 (80), 121 (60), 106 (15), 94 (60), 87 (50), 82 (35)

**(±)-(2*R*,3*R*,4*S*)-2-(1*H*-Indol-3-yl)-1-methylpyrrolidine-3,4-diol (**63**)**



**(±) 63**

Prepared from lactam **84** (0.0603 g, 0.182 mmol) and LiAlH<sub>4</sub> (0.0346 g, 0.911 mmol, 5.0 eq.). The crude material was purified by flash column chromatography using 95:5 MeOH/NH<sub>3</sub> in CH<sub>2</sub>Cl<sub>2</sub> (30:70) as eluent to give **63** as a pale orange oil (0.0211 g, 0.0908 mmol, 50% yield).

<sup>1</sup>H NMR δ (600 MHz, MeOD): 2.29 (s, 3 H), 2.50 (dd, *J* = 10.5, 5.3 Hz, 1 H), 3.57 (dd, *J* = 10.5, 6.2 Hz, 1 H), 3.65 (d, *J* = 7.7 Hz, 1 H), 4.25 (at, *J* = 7 Hz, 1 H), 4.30 (dd, *J* = 11.9, 5.9 Hz, 1 H), 7.01

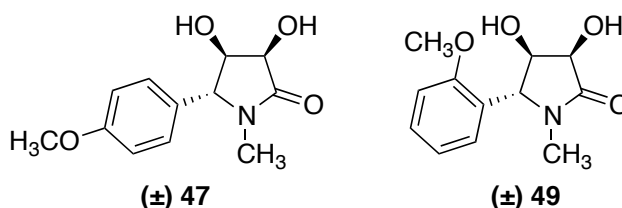
(at,  $J = 7.2$  Hz, 1 H), 7.10 (at, 7.2 Hz, 1 H),  
7.28 (s, 1 H), 7.36 (d,  $J = 8.1$  Hz, 1 H) 7.68  
(d,  $J = 7.9$  Hz, 1 H)

$^{13}\text{C}$  NMR  $\delta$  (150 MHz): 41.3, 63.4, 69.5, 77.3, 112.4, 119.9 (2 C),  
122.6, 124.8, 138.4

IR  $V_{\text{max}}$ : 3404 (OH), 3289, 2943, 2839, 2786, 1456,  
1338, 1228, 1195, 1162, 1096

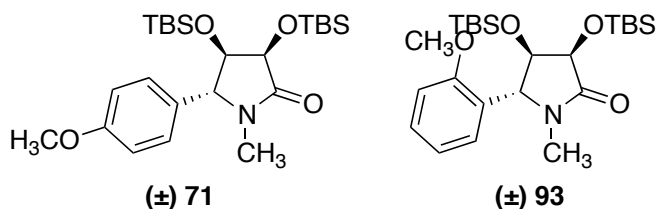
HRMS: For  $\text{C}_{13}\text{H}_{16}\text{N}_2\text{O}_2$ , predicted 232.12118,  
found 232.12172.  $m/z$  (EI+): 232 ( $\text{M}^+$ , 30),  
196 (15), 172 (70), 157 (35), 144 (10), 130  
(40), 117 (25), 102 (10), 87 (40)

**( $\pm$ )-(3*R*,4*R*,5*R*)-3,4-Dihydroxy-5-(4-methoxyphenyl)-1-methylpyrrolidin-2-one (47) and ( $\pm$ )-(3*R*,4*R*,5*R*)-3,4-dihydroxy-5-(2-methoxyphenyl)-1-methylpyrrolidin-2-one 5 (49)**

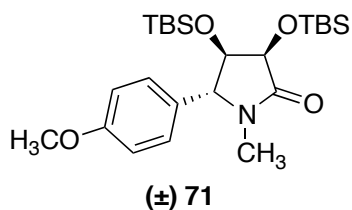


To a solution of **85** and **86** (0.1013 g of a 2:1 mixture, 0.3152 mmol) in MeOH (5 mL), was added  $\text{K}_2\text{CO}_3$  (0.0900 g, 0.6512 mmol, 2.07 eq). This was stirred at room temperature for 30 minutes, at which point  $\text{CH}_2\text{Cl}_2$  (20 mL) was added and the solution filtered through a small plug of silica, which was washed with further MeOH/ $\text{CH}_2\text{Cl}_2$  (20:80) and the solvent evaporated. This gave a mixture of **47** and **49** as clear oil (0.0453 g of a 2:1 mixture, 0.1909 mmol, 61% yield)

**(±)-(3*R*,4*R*,5*R*)-3,4-bis((*tert*-Butyldimethylsilyl)oxy)-5-(4-methoxyphenyl)-1-methylpyrrolidin-2-one (71) and (±)-(3*R*,4*R*,5*R*)-3,4-bis((*tert*-butyldimethylsilyl)oxy)-5-(2-methoxyphenyl)-1-methylpyrrolidin-2-one (93)**



To a stirred solution of **47** and **49** (1 : 1.5, 0.1752 g, 0.7384 mmol) in anhydrous DMF (10 mL), under an N<sub>2</sub> atmosphere, was added TBDMSCl (0.4065 g, 2.697 mmol, 3.65 eq.) and imidazole (0.3632 g, 5.335 mmol, 7.22 eq.) were added, and the mixture stirred at room temperature for 24 h. At this time water (10 mL) was added, and the solution extracted with toluene (3 x 10 mL). The combined organic extracts were dried over MgSO<sub>4</sub>, filtered, and the solvent removed under reduced pressure to give the crude product. The crude mixture was purified by automated flash column chromatography, with a solvent gradient of 0–20% EtOAc/hexanes to give **93** as a clear oil (0.1062 g, 0.2280 mmol, 31% yield) and **71** as a white semisolid (0.0585 g, 0.1256 mmol, 17% yield)

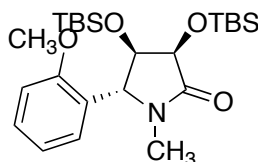


<sup>1</sup>H NMR δ (400 MHz): −0.09 (s, 3 H), 0.00 (s, 3 H), 0.12 (s, 3 H), 0.18 (s, 3 H), 0.85 (s, 9 H), 0.91 (s, 9 H), 2.72 (s, 3 H), 3.80 (s, 3 H), 3.95 (dd, *J* = 3.7 Hz, 1 H), 4.23 (d, *J* = 4.6 Hz, 1 H), 4.31 (d, *J* = 2.7 Hz, 1 H), 6.91 (d, *J* = 8.6 Hz, 2 H), 7.04 (d, *J* = 8.6 Hz, 2 H)

<sup>13</sup>C NMR δ (100 MHz): −5.0, −4.6, −4.3, −4.2, 18.2, 18.6, 25.8, 26.0, 28.6, 55.4, 70.0, 71.5, 114.5, 127.9, 128.9, 159.6, 172.6

IR  $V_{\max}$ : 2953, 2929, 2894, 2856, 1713 (C=O), 1612, 1514, 1472, 1464, 1250, 1173, 1116, 1102

HRMS: For  $C_{24}H_{43}NO_4Si_2+H$ , predicted 466.2803, found 466.2818



(±) **93**

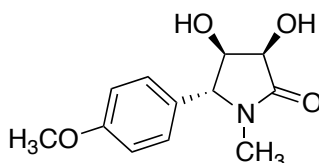
$^1H$  NMR  $\delta$  (400 MHz): 0.07 (s, 3 H), 0.10 (s, 6 H), 0.17 (s, 3 H), 0.902 (s, 9 H), 0.909 (s, 9H), 2.82 (s, 3 H), 3.86 (s, 3 H), 4.10 (d,  $J$  = 4.2 Hz, 1 H), 4.22 (d,  $J$  = 4.1 Hz, 1 H), 4.62 (s, 1 H), 6.83 (d,  $J$  = 7.2 Hz, 1 H), 6.91–6.97 (m, 2 H), 7.30 (t,  $J$  = 7.6 Hz, 1 H)

$^{13}C$  NMR  $\delta$  (100 MHz): -4.9, -4.6, -4.3, -4.1, 18.2, 18.6, 25.8, 26.1, 29.3, 55.0, 66.0, 71.8, 110.7, 120.8, 124.4, 125.5, 129.1, 157.2, 173.2

IR  $V_{\max}$ : 2957, 2929, 2894, 2885, 2856, 1721 (C=O), 1716, 1713, 1601, 1589, 1491, 1471, 1462, 1247, 1177

HRMS: For  $C_{24}H_{43}NO_4Si_2+H$ , predicted 466.2803, found 466.2818

**(±)-(3*R*,4*R*,5*R*)-3,4-Dihydroxy-5-(4-methoxyphenyl)-1-methylpyrrolidin-2-one (47)**



(±) **47**

To a stirred solution of **71** (0.0146 g, 0.0313 mmol), in dry THF (3 mL) at 0 °C, was added TBAF (0.080 mL of a 1 M solution in THF, 0.080 mmol, 2.55 eq.). The solution was allowed to warm to room temperature and stirred for 2.5 h, at which time saturated  $NH_4Cl$  (2 mL) was added. The aqueous and organic layers were separated, and the aqueous layer extracted with EtOAc

(3 x 5 mL). The combined organic layers were dried over  $\text{MgSO}_4$ , filtered, and the solvent removed under reduced pressure. The crude material was purified by flash column chromatography using EtOAc/MeOH (85:15) as eluent, to give product **47** as a clear oil (0.0049 g, 0.0206 mmol, 66% yield)

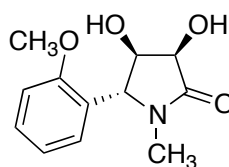
$^1\text{H}$  NMR  $\delta$  (600 MHz): 2.84 (s, 3 H), 3.81 (s, 3 H), 4.17 (d,  $J$  = 2.5 Hz, 1 H), 4.49 (s, 1 H), 4.52 (bs, 1 H), 6.91 (d,  $J$  = 8.6 Hz, 2 H), 7.06 (d,  $J$  = 8.6 Hz, 1 H)

$^{13}\text{C}$  NMR  $\delta$  (150 MHz): 29.2, 55.5, 69.4, 70.2, 73.2, 114.8, 127.5, 128.1, 159.8, 173.5

IR  $V_{\text{max}}$ : 3364 (OH), 1687 (C=O), 1611, 1514, 1398, 1248, 1177, 1150, 1078, 1030

HRMS: For  $\text{C}_{12}\text{H}_{15}\text{NO}_4$ , predicted 237.10011, found 237.09980.

**( $\pm$ )-(3*R*,4*R*,5*R*)-3,4-Dihydroxy-5-(2-methoxyphenyl)-1-methylpyrrolidin-2-one (**49**)**



**( $\pm$ ) 49**

To a stirred solution of **93** (0.0228 g, 0.0489 mmol), in dry THF (3 mL) at 0 °C, was added TBAF (0.120 mL of a 1 M solution in THF, 0.120 mmol, 2.45 eq.). The solution was allowed to warm to room temperature and stirred for 2.5 h, at which time saturated  $\text{NH}_4\text{Cl}$  (2 mL) was added. The aqueous and organic layers were separated, and the aqueous layer extracted with EtOAc (3 x 5 mL). The combined organic layers were dried over  $\text{MgSO}_4$ , filtered, and the solvent removed under reduced pressure. The crude material was purified by flash column chromatography using EtOAc:MeOH (85:15) as eluent, to give product **49** as a clear oil (0.0103 g, 0.0434 mmol, 89% yield).

$^1\text{H}$  NMR  $\delta$  (600 MHz): 2.86 (s, 3 H), 3.89 (s, 3 H), 4.19 (d,  $J$  = 4.6 Hz, 1 H), 4.41 (bs, 1 H), 4.83 (s, 1 H), 6.87 (d,  $J$  = 7.3

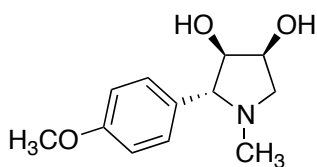
Hz, 1 H), 6.91–6.97 (m, 2 H), 7.31 (at,  $J = 7.6$  Hz, 1 H)

$^{13}\text{C}$  NMR  $\delta$  (150 MHz): 29.4, 55.6, 65.9, 69.7, 71.9, 111.0, 120.8, 124.0, 125.8, 129.6, 157.2, 174.1

IR  $V_{\text{max}}$ : 3389 (OH), 1687 (C=O), 1601, 1588, 1491, 1455, 1438, 1401, 1244, 1077, 1024

HRMS: For  $\text{C}_{12}\text{H}_{15}\text{NO}_4$ , predicted 237.10011, found 237.09980.

**(±)-(2*R*,3*R*,4*S*)-2-(4-Methoxyphenyl)-1-methylpyrrolidine-3,4-diol (**46**)**



**(±) 46**

To a solution of the lactam **71** (0.0176 g, 0.0378 mmol) in anhydrous THF (3 mL) under  $\text{N}_2$  was added  $\text{LiAlH}_4$  (0.0089 g, 0.234 mmol, 6.2 eq.). The reaction was heated at reflux for 4 hours, before being allowed to cool to room temperature. The reaction was quenched by addition of  $\text{H}_2\text{O}$  (0.5 mL) and 1 M NaOH (0.5 mL). The mixture was filtered through celite, and the solvent removed under reduced pressure. The crude material was purified by flash column chromatography using 95:5 MeOH/ $\text{NH}_3$  in  $\text{CH}_2\text{Cl}_2$  (30:70) as eluent to give **46** as a colourless oil (0.0059 g, 0.0264 mmol, 70% yield).

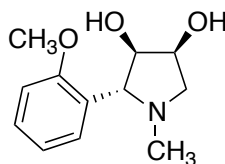
$^1\text{H}$  NMR  $\delta$  (600 MHz, MeOD): 2.13 (s, 3 H), 2.35 (dd,  $J = 10.3, 5.4$  Hz, 1 H), 3.07 (d,  $J = 7.6$  Hz, 1 H), 3.53 (dd,  $J = 10.3, 6.4$  Hz, 1 H), 3.78 (s, 3 H), 3.83 (at,  $J = 7.2$  Hz, 1 H), 4.19 (dd,  $J = 12.1, 6.4$  Hz, 1 H), 6.90 (d,  $J = 8.7$  Hz, 2 H), 7.26 (d,  $J = 8.7$  Hz, 2 H)

$^{13}\text{C}$  NMR  $\delta$  (150 MHz, MeOD): 40.8, 55.7, 63.8, 69.4, 76.5, 79.3, 114.9, 130.2, 133.1, 160.8

IR  $V_{\text{max}}$ : 3291, 1576, 1419, 1346, 1247, 1022

HRMS: For  $C_{12}H_{17}NO_3+H$ , predicted 224.1281, found 224.1289

**(±)-(2*R*,3*R*,4*S*)-2-(2-Methoxyphenyl)-1-methylpyrrolidine-3,4-diol (48)**



**(±) 48**

To a solution of the lactam **93** (0.00269 g, 0.0577 mmol) in anhydrous THF (3 mL) under  $N_2$  was added  $LiAlH_4$  (0.0175 g, 0.461 mmol, 8 eq.). The reaction was heated at reflux for 4 hours, before being allowed to cool to room temperature. The reaction was quenched by addition of  $H_2O$  (0.5 mL) and 1 M NaOH (0.5 mL). The mixture was filtered through celite, and the solvent removed under reduced pressure. The crude material was purified by flash column chromatography using 95:5 MeOH/ $NH_3$  in  $CH_2Cl_2$  (20:80) as eluent to give **48** as a colourless oil (0.0065 g, 0.0291 mmol, 50% yield).

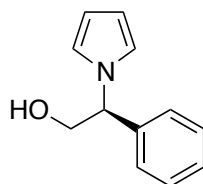
$^1H$  NMR  $\delta$  (600 MHz, MeOD): 2.36 (s, 3 H), 2.62–2.73 (m, 1 H), 3.56 (dd,  $J = 9.0, 5.2$  Hz, 1 H), 3.86 (s, 3 H), 3.93 (d,  $J = 4.8$  Hz, 1 H), 4.15–4.21 (m, 1 H), 4.23–4.27 (m, 1 H), 6.98 (t,

$^{13}C$  NMR  $\delta$  (150 MHz, MeOD): 41.9, 56.0, 62.5, 70.3, 71.7, 77.6, 112.2, 121.9, 126.8, 130.4, 130.6, 159.7

IR  $V_{max}$ : 3355 (OH), 3247, 1495, 1454, 1242, 1155, 1108, 1047, 1022

HRMS: For  $C_{12}H_{17}NO_3+H$ , predicted 224.1281, found 224.1288

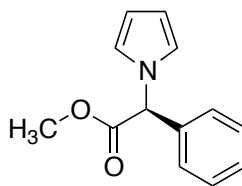


**(S)-2-Phenyl-2-(1H-pyrrol-1-yl)ethan-1-ol (156)****156**

2,5-Dimethoxytetrahydrofuran (16.0 mL, 123.5 mmol) in water (120 mL) under an atmosphere of N<sub>2</sub> was heated at reflux and stirred for 2.5 h. The solution was allowed to cool to room temperature before dichloromethane (180 mL), sodium acetate (12.1845 g, 148.5 mmol, 1.20 eq.), acetic acid (8.5 mL, 148.5 mmol, 1.20 eq.) and (S)-(+)-2-phenylglycinol (20.3714 g, 148.5, 1.20 eq. mmol) were added. The resulting solution was stirred with exclusion from light for 66 h. Solid Na<sub>2</sub>CO<sub>3</sub> was added until the solution was alkaline, before the aqueous and organic layers were separated and the aqueous layer extracted with dichloromethane (3 x 50 mL). The combined organic layers were dried over MgSO<sub>4</sub>, and passed through a silica plug, washed with EtOAc/hexanes (20:80). The solvent was removed under reduced pressure to yield **156** as a yellow semi-solid (22.6300 g, 120.9 mmol, 98% yield). NMR spectra agreed with those reported by Katritzky *et al* and Jefford *et al.*<sup>282,361</sup>

<sup>1</sup>H NMR  $\delta$  (400 MHz): 1.70 (bs, 1 H), 4.16–4.28 (m, 2H), 5.27 (dd,  $J$  = 8.1, 5.1 Hz, 1 H), 6.24 (as, 2 H), 6.82 (as, 2 H), 7.12–7.20 (m, 2 H), 7.27–7.38 (m, 3 H)

<sup>13</sup>C NMR  $\delta$  (100 MHz): 65.1, 65.4, 109.0, 120.1, 126.8, 128.3, 129.0, 138.6

**Methyl (S)-2-phenyl-2-(1H-pyrrol-1-yl)acetate (154)****154**

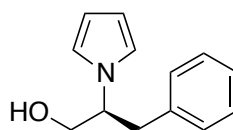
2,5-Dimethoxytetrahydrofuran (2.70 mL, 20.84 mmol) in water (30 mL) under an atmosphere of N<sub>2</sub> was heated at reflux and stirred for 2.5 h. The solution was allowed to cool to room temperature before CH<sub>2</sub>Cl<sub>2</sub> (45 mL) and sodium acetate (4.0759 g, 49.68 mmol, 2.38 eq), and (S)-(+)-2-phenylglycine methyl ester hydrochloride (4.9960 g, 24.77 mmol, 1.19 eq.) were added. The reaction mixture was stirred with exclusion from light for 18 h. 2 M Na<sub>2</sub>CO<sub>3</sub> (75 mL) was added to make the solution alkaline, before the aqueous and organic layers were separated and the aqueous layer extracted with dichloromethane (3 x 45 mL). The combined organic layers were dried over MgSO<sub>4</sub>, and passed through a silica plug, washed with EtOAc/hexanes (20:80). The solvent was removed under reduced pressure to yield **154** as a yellow oil (4.4019 g, 20.45 mmol, 98% yield). Data agreed with that reported by Demir *et al.*<sup>362</sup>

<sup>1</sup>H NMR δ (400 MHz): 3.82 (s, 3 H), 5.88 (s, 1 H), 6.20–6.23 (m, 2 H), 6.75–6.78 (m, 2 H), 7.27–7.34 (m, 2 H), 7.35–7.44 (m, 3 H)

<sup>13</sup>C NMR δ (100 MHz): 52.9, 65.5, 108.9, 121.0, 127.8, 129.0, 129.1, 135.4, 170.1

IR V<sub>max</sub>: 2953, 1751 (C=O), 1487, 1454, 1435, 1278, 1201, 1168, 1091, 1006

### (S)-3-Phenyl-2-(1H-pyrrol-1-yl)propan-1-ol (**157**)



**157**

2,5-Dimethoxytetrahydrofuran (3.60 mL, 27.78 mmol) in water (30 mL) under an atmosphere of N<sub>2</sub> was heated at reflux and stirred for 2 h. The solution was allowed to cool to room temperature before dichloromethane (45 mL), sodium acetate (2.7358 g, 33.35 mmol, 1.20 eq), acetic acid (1.90 mL, 33.19 mmol, 1.20 eq.) and L-Phenylalaninol (5.0550 g, 33.43 mmol, 1.20 eq.) were added. The reaction mixture was stirred with exclusion from light for 18 h. before the aqueous and organic layers were separated and the aqueous

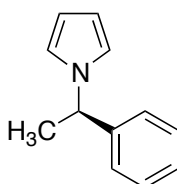
layer extracted with dichloromethane (3 x 45 mL). The combined organic layers were dried over  $\text{MgSO}_4$ , and passed through a silica plug, washed with EtOAc/hexanes (20:80). The solvent was removed under reduced pressure to yield **157** as an off white semi-solid (5.2063 g, 25.86 mmol, 93% yield). Data agreed with that reported by Tokumaru *et al.*<sup>363</sup>

$^1\text{H}$  NMR  $\delta$  (400 MHz): 1.99 (bs, 1 H), 3.02–3.12 (m, 2 H), 3.78 (d,  $J$  = 6.0 Hz, 2 H), 4.14–4.24 (m, 1 H), 6.19 (at,  $J$  = 2.1 Hz, 2 H), 6.71 (at,  $J$  = 2.1 Hz, 2 H), 7.04–7.10 (m, 2 H), 7.21–7.32 (m, 3 H)

$^{13}\text{C}$  NMR  $\delta$  (100 MHz): 38.7, 63.6, 65.5, 108.6, 119.3, 126.8, 128.7, 129.0, 137.7

IR  $V_{\text{max}}$ : 3470 (OH), 2943, 1489, 1454, 1273, 1091, 1064, 1031

#### (*R*)-1-(1-Phenylethyl)-1*H*-pyrrole (**158**)



**158**

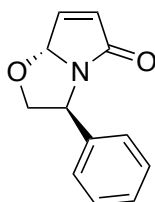
2,5-Dimethoxytetrahydrofuran (0.180 mL, 1.389 mmol) in water (5 mL) under an atmosphere of  $\text{N}_2$  was heated at reflux and stirred for 2 h. The solution was allowed to cool to room temperature before *R*-Phenylethylamine (0.210 mL, 1.649 mmol, 1.19 eq.) were added. The reaction mixture was stirred with exclusion from light for 18 h, before the aqueous layer was extracted with dichloromethane (3 x 5 mL). The combined organic layers were dried over  $\text{MgSO}_4$ , and passed through a silica plug, washed with EtOAc/hexanes (20:80). The solvent was removed under reduced pressure to yield **158** as an orange oil (0.0953 g, 0.557 mmol, 40% yield).  $^1\text{H}$  and  $^{13}\text{C}$  NMR spectra were in agreement with those reported by Gourlay *et al.*<sup>131</sup>

$^1\text{H}$  NMR  $\delta$  (400 MHz): 1.85 (d,  $J$  = 7.0 Hz, 3 H), 5.30 (q,  $J$  = 7.0 Hz, 1 H), 6.20–6.23 (m, 2 H), 6.76–6.80 (m, 2 H), 7.09–7.13 (m, 2 H), 7.23–7.36 (m, 3 H)

$^{13}\text{C}$  NMR  $\delta$  (100 MHz): 22.2, 58.1, 108.1, 119.5, 125.9, 127.5, 128.7, 143.6

**Procedures For the Preparation of (3*S*,7*aR*)-3-phenyl-2,3-dihydropyrrolo[2,1-*b*]oxazol-5(7*aH*)-one (118)**

**Using Dess–Martin Periodinane**



**118**

To a solution of pyrrole **156** (0.3316 g, 1.771 mmol) in dichloromethane (10 mL) was added  $\text{Boc}_2\text{O}$  (0.4661 g, 2.135 mmol, 1.2 eq.) and DMAP (0.0254 g, 0.2079 mmol, 0.12 eq.), and the mixture stirred for 1.5 h. Water (10 mL) was added, and the aqueous and organic layers separated. The aqueous layer was extracted with dichloromethane (3 x 10 mL), the combined organic layers dried over  $\text{MgSO}_4$ , filtered and the solvent removed under reduced pressure. The crude product was taken up in dichloromethane (15 mL) and cooled to 0 °C, before addition of Dess–Martin periodinane (1.9716 g, 4.648 mmol, 2.62 eq.) and 2 drops of  $\text{H}_2\text{O}$ , and stirring for a further 1.5 h.  $\text{H}_2\text{O}$  (15 mL) was added, followed by solid  $\text{Na}_2\text{S}_2\text{O}_5$  until the solids dissolved to give a transparent red-brown organic layer. The organic and aqueous layers were separated, and the aqueous layer extracted with dichloromethane (3 x 15 mL). The combined organic layers were then washed with saturated  $\text{NaHCO}_3$  (2 x 15 mL), dried over  $\text{MgSO}_4$ , filtered, and the solvent removed under reduced pressure. This crude product was likewise taken up in dichloromethane (15 mL) and cooled to 0 °C. TFA (1.5 mL) was added, and the solution was stirred for 16 h. The reaction was quenched by addition of saturated  $\text{NaHCO}_3$  (20 mL). The aqueous and organic layers were separated, and the aqueous layer extracted with dichloromethane (3 x 15 mL). The combined organic extracts were dried over  $\text{MgSO}_4$ , filtered, and the solvent removed under reduced pressure. The crude material was purified first by elution through a short plug of silica with EtOAc/hexanes (50:50), then on by automated flash column chromatography with a solvent gradient of 10–

50% EtOAc/hexanes, to give **118** as a crystalline pale orange solid (0.1948 g, 0.9681 mmol, 55% yield). Experimental data agreed with those reported in the literature.<sup>102</sup>

<sup>1</sup>H NMR  $\delta$  (400 MHz): 4.10 (dd,  $J$  = 8.7, 7.3 Hz, 1 H), 4.75 (at,  $J$  = 8.7, 1 H), 4.98 (at,  $J$  = 7.3 Hz, 1 H), 5.67 (s, 1 H), 6.24 (d,  $J$  = 5.9 Hz, 1 H), 7.21 (dd,  $J$  = 5.9, 1.4 Hz, 1 H), 7.27–7.40 (m, 5 H)

<sup>13</sup>C NMR  $\delta$  (100 MHz): 58.1, 78.4, 94.1, 126.2, 127.9, 129.0, 131.6, 139.5, 145.8, 176.8

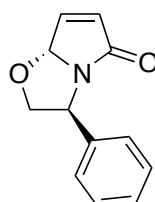
IR  $V_{\max}$ : 2872, 1712 (C=O), 1383, 1240, 1165, 1082

HRMS For C<sub>12</sub>H<sub>11</sub>NO<sub>2</sub>, predicted 201.07898, found 201.07938.  $m/z$  (EI+): 201 (M<sup>+</sup>, 20), 171 (100), 143 (60), 115 (15), 104 (10), 87 (20), 82 (10)

$[\alpha]_D^{20}$  +104 ° ( $c$  = 0.0361 in acetone)

MP: 72.5–73.0 °C

### Using IBX

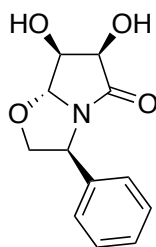


**118**

To a solution of pyrrole **156** (1.1057 g, 5.905 mmol) in dichloromethane (25 mL) was added Boc<sub>2</sub>O (1.5652 g, 7.171 mmol, 1.2 eq.) and DMAP (0.0721 g, 0.590 mmol, 0.10 eq.), and the solution stirred for 2.5 h. Water (25 mL) was added, and the aqueous and organic layers separated. The aqueous layer was extracted with dichloromethane (3 x 25 mL), the combined organic layers dried over MgSO<sub>4</sub>, filtered and the solvent removed under reduced pressure. The crude product was taken up in AcOH (15 mL). IBX (4.1463 g, 14.80 mmol, 2.5 eq.) was added, and the reaction stirred at room temperature for 16 h. Water (50 mL) and CH<sub>2</sub>Cl<sub>2</sub> (50 mL) were added,

excess solid  $\text{Na}_2\text{S}_2\text{O}_5$  was added, and the solution made basic by addition of solid  $\text{NaHCO}_3$ . The aqueous and organic layers were separated, and the aqueous layer extracted with  $\text{CH}_2\text{Cl}_2$  (4 x 25 mL). The combined organic layers were dried over  $\text{MgSO}_4$ , and the solvent removed under reduced pressure to give a brown oil. This crude product was likewise taken up in dichloromethane (25 mL) and cooled to 0 °C. FA (2.5 mL) was added, and the solution was stirred for 16 h. The reaction was quenched by addition of saturated  $\text{NaHCO}_3$  (25 mL). The aqueous and organic layers were separated, and the aqueous layer extracted with dichloromethane (3 x 25 mL). The combined organic extracts were dried over  $\text{MgSO}_4$ , filtered, and the solvent removed under reduced pressure. The crude product was purified first by elution through a short plug of silica with EtOAc/hexanes (50:50), then by automated flash column chromatography with a solvent gradient of 10–50% EtOAc/hexanes, to give **118** as a crystalline pale orange solid (0.5302 g, 2.634 mmol, 45% yield).

**(3*S*,6*R*,7*S*,7*aR*)-6,7-Dihydroxy-3-phenyltetrahydropyrrolo[2,1-*b*]oxazol-5(6*H*)-one (162)**



**162**

To a stirred solution of lactam **118** (0.5906 g, 2.935 mmol) in a 5:1 mixture of acetone and  $\text{H}_2\text{O}$  (12 mL), at 0 °C, was added *N*-methylmorpholine-*N*-oxide (1.85 mL of a 50% w/w solution in  $\text{H}_2\text{O}$ , 8.922 mmol, 3.04 eq.) and  $\text{OsO}_4$  (2.3 mL of a 0.0393 M solution in  $\text{H}_2\text{O}$ , 0.09039 mmol, 0.030 eq.). The resulting solution was stirred for 16 h, at which time acetonitrile was added and the solvent removed under reduced pressure. The crude product was adsorbed on silica and purified by washing through a silica plug with EtOAc/MeOH (90:10) as eluent to give **162** as a white solid (0.5789 g, 2.463 mmol, 84 % yield)

$^1\text{H}$  NMR  $\delta$  (400 MHz, DMSO): 3.77 (dd,  $J$  = 8.7, 6.7 Hz, 1 H), 3.92–3.96 (m, 1 H), 4.07 (t,  $J$  = 5.9 Hz, 1 H), 4.52 (dd,  $J$  = 8.6, 7.2 Hz, 1 H), 4.91 (t,  $J$  = 6.8 Hz, 1 H), 5.19 (d,  $J$  = 3.6 Hz, 1 H), 5.51 (d,  $J$  = 7.0 Hz, 1 OH), 5.95 (d,  $J$  = 5.7 Hz, 1 OH), 7.27–7.32 (m, 3 H), 7.35–7.39 (m, 2 H)

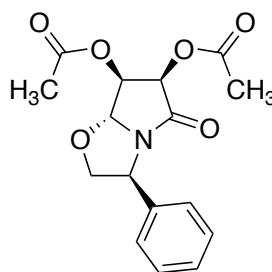
$^{13}\text{C}$  NMR  $\delta$  (100 MHz, DMSO): 56.4, 72.2, 74.6, 74.9, 97.2, 126.0, 127.4, 128.5, 139.5, 174.8

IR  $V_{\text{max}}$ : 3345 (OH), 3149, 1694 (C=O), 1314, 1267, 1126, 1079

HRMS: For  $\text{C}_{12}\text{H}_{13}\text{N}_1\text{O}_4+\text{Na}$ , predicted 258.0737, found 258.0729

$[\alpha]_{\text{D}}^{20}$  (DMSO) +153.3  $^{\circ}$  ( $c$  = 0.3)

**(3*S*,6*R*,7*S*,7*aR*)-5-Oxo-3-phenylhexahydropyrrolo[2,1-*b*]oxazole-6,7-diyl diacetate (163)**

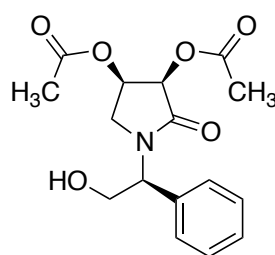


**163**

To diol **162** (0.0998 g, 0.4242 mmol) was added in  $\text{Ac}_2\text{O}$  (2 mL) and pyridine (2 mL), at 0  $^{\circ}\text{C}$ , and the resulting solution allowed to warm to room temperature and stirred for 16 h.  $\text{H}_2\text{O}$  (10 mL) and  $\text{CH}_2\text{Cl}_2$  (10 mL) were added, and the aqueous and organic layers separated. The aqueous layer was extracted with  $\text{CH}_2\text{Cl}_2$  (3 x 10 mL). The combined organic layers were dried over  $\text{MgSO}_4$ , filtered, and the solvent removed under reduced pressure. The crude material was purified by flash column chromatography with EtOAc/hexanes (50:50) as eluent to give the title compound **163** as a crystalline pale yellow solid (0.1165 g, 0.3650 mmol, 86% yield)

$^1\text{H}$ NMR $\delta$ (400 MHz):	2.09 (s, 3 H), 2.14 (s, 3 H), 3.96 (dd, $J$ = 8.9, 6.5 Hz, 1 H), 4.57 (dd, $J$ = 8.9, 7.4 Hz, 1 H), 5.13 (at, $J$ = 6.9 Hz, 1 H), 5.28 (dd, $J$ = 6.8, 2.9 Hz, 1 H), 5.33 (d, $J$ = 2.9 Hz, 1 H), 5.56 (d, $J$ = 6.8 Hz, 1 H), 7.25–7.40 (m, 5 H)
$^{13}\text{C}$ NMR $\delta$ (100 MHz):	20.30, 20.34, 57.7, 69.9, 72.7, 75.4, 94.6, 125.8, 128.1, 129.0, 138.1, 169.1, 170.4
IR $V_{\text{max}}$ :	2922, 1755 (C=O), 1733 (C=O), 1418, 1371, 1240, 1212, 1068
HRMS:	For $\text{C}_{16}\text{H}_{17}\text{NO}_6$ , predicted 319.10559, found 315.10622. $m/z$ (EI+): 319 ( $M^+$ , 2), 317 (10), 302 (40), 289 (10), 260 (80), 217 (20), 190 (50), 160 (30), 148 (100), 132 (15), 120 (70), 104 (50), 87 (60)
$[\alpha]_{\text{D}}^{20}$	+146.67 $^\circ$ ( $c$ = 0.60)
MP:	109.5–110.5 $^\circ\text{C}$

**(3*R*,4*R*)-1-((*S*)-2-Hydroxy-1-phenylethyl)-2-oxopyrrolidine-3,4-diyl diacetate (172)**



**172**

*Note: this was the best observed and an irreproducible result, with yields ranging from 0% up to 40%*

To a stirred solution of **163** (0.1061 g, 0.3322 mmol) in dry dichloromethane (6 mL), under an atmosphere of  $\text{N}_2$ , cooled on a dry ice/acetone bath to  $-78^\circ\text{C}$ , was added triethylsilane (0.325 mL, 2.035 mmol, 6.1 eq.) and  $\text{TiCl}_4$  (0.190 mL, 1.733 mmol, 5.2 eq.). The reaction was allowed to warm to room



temperature and stirred for 20 h, before being quenched by addition of saturated  $\text{NH}_4\text{Cl}$  (10 mL).  $\text{H}_2\text{O}$  (20 mL) and  $\text{CH}_2\text{Cl}_2$  (10 mL) were added, and the aqueous and organic layers separated. The aqueous layer was extracted with  $\text{CH}_2\text{Cl}_2$  (3 x 10 mL), the organic fractions were combined, dried over  $\text{MgSO}_4$ , filtered, and the solvent removed under reduced pressure. The crude material was purified by flash column chromatography using EtOAc as eluent to give **172** as a pale yellow solid (0.0421 g, 0.1310 mmol, 39% yield)

$^1\text{H}$  NMR  $\delta$  (400 MHz): 1.99 (s, 3 H), 2.14 (s, 3 H), 3.17 (d,  $J$  = 11.8 Hz, 1 H), 3.33 (bs, 1 H), 3.69 (dd,  $J$  = 11.8, 4.0 Hz, 1 H), 4.01 (dd,  $J$  = 11.8, 9.2 Hz, 1 H), 4.10 (dd,  $J$  = 12.0, 4.4 Hz, 1 H), 5.21 (dd,  $J$  = 9.0, 4.4 Hz, 1 H), 5.50 (t,  $J$  = 4.5 Hz, 1 H), 5.66 (d,  $J$  = 5.4 Hz, 1 H), 7.21–7.37 (m, 5 H)

$^{13}\text{C}$  NMR  $\delta$  (100 MHz): 20.5, 20.7, 47.4, 58.4, 61.9, 67.8, 70.3, 127.3, 128.3, 129.0, 135.8, 169.5, 169.9, 170.1

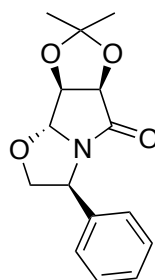
IR  $\nu_{\text{max}}$ : 3379 (OH), 2956, 1747 (C=O), 1688 (C=O), 1373, 1246

HRMS: For  $\text{C}_{16}\text{H}_{19}\text{NO}_6 + \text{H}$ , predicted 322.1285, found 322.1276

$[\alpha]_{\text{D}}^{20}$  +45.58  $^\circ$  ( $c$  = 0.68)

MP: 120.2–121  $^\circ\text{C}$

**(3a*S*,3b*R*,6*S*,8a*R*)-2,2-Dimethyl-6-phenyltetrahydro-[1,3]dioxolo[4',5':3,4]pyrrolo[2,1-*b*]oxazol-8(3b*H*)-one (164)**



**164**

To a stirred solution of diol **162** (0.1347 g, 0.5726 mmol) in acetone (10 mL) under an atmosphere of N<sub>2</sub> was added 2,2-dimethoxypropane (0.360 mL, 2.93 mmol, 5 eq.) via syringe and catalytic amberlyst resin, and the reaction stirred at room temperature for 16 h. The reaction mixture was then filtered on cotton wool and the solvent removed under reduced pressure. The crude material was purified by flash column chromatography with EtOAc/hexanes (50:50) as the eluent, giving acetal **164** as a white semi-solid (0.1126 g, 0.4090 mmol, 71 % yield)

<sup>1</sup>H NMR  $\delta$  (600 MHz): 1.42 (s, 3 H), 1.56 (s, 3 H), 3.85 (s, 3 H), 3.85 (dd,  $J$  = 8.7, 7.0 Hz, 1 H), 4.55 (at,  $J$  = 8.2 Hz, 1 H), 4.74 (d,  $J$  = 6.8 Hz, 1 H), 4.78 (d,  $J$  = 6.8 Hz, 1 H), 5.11 (s, 1 H), 5.12 (at,  $J$  = 7.1 Hz, 1 H), 7.22–7.25 (m, 2 H), 7.28–7.32 (m, 1 H), 7.34–7.38 (m, 2 H)

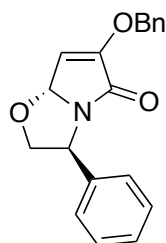
<sup>13</sup>C NMR  $\delta$  (150 MHz): 25.5, 26.7, 58.3, 74.5, 77.6, 79.8, 96.4, 114.6, 125.9, 128.0, 129.1, 139.0, 175.3

IR  $V_{\max}$ : 1727 (C=O), 1399, 1383, 1376, 1210, 1087, 1055, 1035

HRMS: For C<sub>15</sub>H<sub>17</sub>NO<sub>4</sub>+Na, predicted 298.1050, found 298.1062.

$[\alpha]_D^{20}$  +84.68 ° (c = 0.55)

**(3*S*,7*aR*)-6-(Benzyloxy)-3-phenyl-2,3-dihydropyrrolo[2,1-*b*]oxazol-5(7*aH*)-one (173)**



**173**

To a solution of diol **162** (0.1375 g, 0.5845 mmol), in dry DMF (6 mL) was added NaH (0.0762 g of 60% in mineral oil, 1.905 mmol, 3.25 eq.) and benzyl bromide (0.140 mL, 1.177 mmol, 2.01 eq.), and the solution stirred for

3 h. The reaction was quenched with H<sub>2</sub>O (10 mL), and extracted with toluene (3 x 10 mL). The combined organic layers were dried over MgSO<sub>4</sub>, filtered, and the solvent removed under reduced pressure. The crude material was purified by flash column chromatography with EtOAc/hexanes (40:60) as the eluent to give **173** as a crystalline white solid (0.1474 g, 0.4799 mmol, 82% yield).

<sup>1</sup>H NMR δ (400 MHz): 4.02 (dd, *J* = 9.0, 7.7 Hz, 1 H), 4.78 (dd, *J* = 9.0, 7.5 Hz, 1 H), 4.96 (t, *J* = 7.5 Hz, 1 H), 5.03 (dd, *J* = 16.7, 12 Hz, 2 H), 5.56 (d, *J* = 2.2 Hz, 1 H), 5.88 (d, *J* = 2.2 Hz, 1 H), 7.26–7.45 (m, 10 H)

<sup>13</sup>C NMR δ (100 MHz): 57.9, 72.7, 77.8, 90.2, 108.2, 126.1, 127.80, 127.82, 128.6, 128.7, 128.9, 134.9, 139.2, 153.8, 170.8

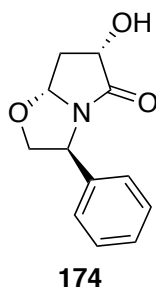
IR V<sub>max</sub>: 2873, 1728 (C=O), 1637, 1455, 1396, 1309, 1231, 1217, 1203

HRMS: For C<sub>19</sub>H<sub>17</sub>NO<sub>3</sub>, predicted 307.12084, found 307.12170. *m/z* (EI+): 307 (M<sup>+</sup>, 10), 277 (85), 216 (18), 186 (50), 158 (80), 146 (30), 128 (40), 104 (50), 91 (100), 77 (30), 65 (20)

[α]<sub>D</sub><sup>20</sup> +146.1 ° (*c* = 0.95)

MP: 108.4–109.5 °C

**(3*S*,6*S*,7*aR*)-6-Hydroxy-3-phenyltetrahydropyrrolo[2,1-*b*]oxazol-5(6*H*)-one (174)**



To a solution of **173** (0.1608 g, 0.5231 mmol) in EtOH (10 mL) was added Pd/C (~0.1 g of a 10% w/w mixture), and the reaction stirred under a balloon of H<sub>2</sub> (1 atm) for 20 h. The reaction mixture was filtered through a plug of celite, and the solvent removed under reduced pressure. The crude product was purified by flash column chromatography to give **174** as a white semi-solid (0.0633 g, 0.2887 mmol, 55% yield).

<sup>1</sup>H NMR  $\delta$  (400 MHz): 2.05 (ddd,  $J$  = 13.2, 9.5, 4.7 Hz, 1 H), 2.96–3.05 (m, 1 H), 3.88 (dd,  $J$  = 8.8, 7.7 Hz, 1 H), 4.62 (dd,  $J$  = 8.8, 7.7 Hz, 1 H), 4.73 (t,  $J$  = 9.0 Hz, 1 H), 5.11 (t,  $J$  = 7.4 Hz, 1 H), 5.24 (t,  $J$  = 5.2 Hz, 1 H), 7.21–7.39 (m, 5 H)

<sup>13</sup>C NMR  $\delta$  (100 MHz): 37.1, 57.3, 71.7, 75.0, 88.8, 126.1, 128.1, 129.1, 138.8, 177.4

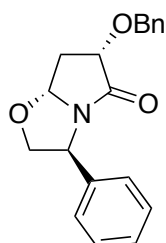
IR  $V_{\max}$ : 3335 (OH), 1695 (C=O), 1633, 1456, 1298, 1091, 997

HRMS: For C<sub>12</sub>H<sub>13</sub>NO<sub>3</sub>+Na, predicted 242.0788, found 242.0795

$[\alpha]_D^{20}$  +140.6 ° ( $c$  = 0.34)

MP: 136–137 °C

**(3*S*,6*S*,7*aR*)-6-(Benzyloxy)-3-phenyltetrahydropyrrolo[2,1-*b*]oxazol-5(6*H*)-one (175)**



**175**

To a solution of **174** (0.0269 g, 0.1228 mmol) in dry DMF (4 mL) was added NaH (0.0080 g of a 60% dispersion in mineral oil, 0.2000 mmol, 1.63 eq.) and benzyl bromide (0.015 mL, 0.1261 mmol, 1.03 eq.), and the solution

stirred for 3 h. The reaction was quenched with H<sub>2</sub>O (5 mL), and extracted with toluene (3 x 10 mL). The combined organic layers were dried over Na<sub>2</sub>SO<sub>4</sub>, filtered, and the solvent removed under reduced pressure. The crude material was purified by flash column chromatography with EtOAc/hexanes (30:70) as the eluent to give **175** as a clear crystalline solid (0.0255 g, 0.08247 mmol, 67% yield).

<sup>1</sup>H NMR δ (600 MHz): 2.08 (ddd, *J* = 13.5, 9.2, 4.5 Hz, 1 H), 2.86 (ddd, *J* = 13.5, 8.2, 5.6 Hz, 1 H), 3.86 (dd, *J* = 8.7, 7.4 Hz, 1 H), 4.49 (at, *J* = 8.9 Hz, 1 H), 4.58 (dd, *J* = 8.6, 7.7 Hz, 1 H), 4.76 (d, *J* = 11.9 Hz, 1 H), 5.01 (d, *J* = 11.9 Hz, 1 H), 5.12–5.17 (m, 2 H), 7.20–7.41 (m, 10 H)

<sup>13</sup>C NMR δ (150 MHz): 35.4, 57.2, 72.5, 74.7, 76.8, 88.4, 126.1, 127.9, 128.0, 128.2, 128.6, 129.0, 137.6, 139.1, 175.5

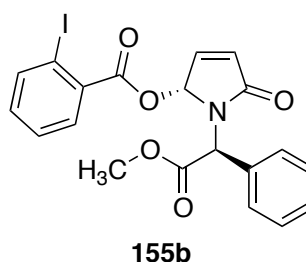
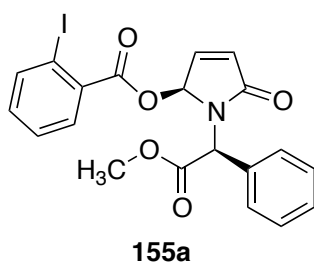
IR V<sub>max</sub>: 1695 (C=O), 1495, 1455, 1412, 1328, 1289, 1169, 1127, 1072, 1024

HRMS: For C<sub>19</sub>H<sub>19</sub>NO<sub>3</sub>+Na, predicted 332.1257, found 332.1255

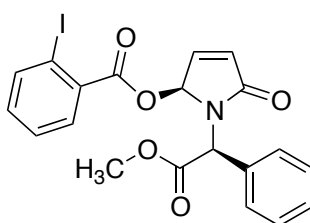
[α]<sub>D</sub><sup>20</sup> +41.4 ° (c = 0.27)

MP: 91.0–91.5 °C

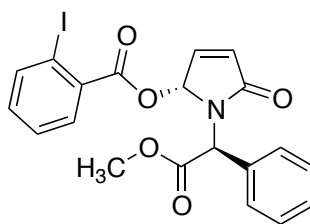
**(S)-1-((S)-2-Methoxy-2-oxo-1-phenylethyl)-5-oxo-2,5-dihydro-1H-pyrrol-2-yl 2-iodobenzoate (155a) and (R)-1-((S)-2-methoxy-2-oxo-1-phenylethyl)-5-oxo-2,5-dihydro-1H-pyrrol-2-yl 2-iodobenzoate (155b)**



To a solution of pyrrole **154** (1.1720 g, 5.444 mmol) in dichloromethane (35 mL) at 0 °C was added Dess–Martin periodinane (5.8989 g, 13.908 mmol, 2.55 eq.), and the reaction stirred for 6 h. Water (35 mL) was added, and the reaction quenched by addition of Na<sub>2</sub>S<sub>2</sub>O<sub>5</sub>. The aqueous and organic layers were separated, and the aqueous layer extracted with dichloromethane (3 x 20 mL). The combined organic layers were dried over MgSO<sub>4</sub>, filtered, and the solvent removed under reduced pressure. The crude mixture was purified by automated flash column chromatography with a solvent gradient from 15–40% EtOAc/hexanes, to give **155a** as a clear crystalline solid (0.7057 g, 1.479 mmol, 27%) and **155b** as an orange crystalline solid (0.6356 g, 1.332 mmol, 24%).

**155a**

<sup>1</sup> H NMR δ (400 MHz):	3.76 (s, 3 H), 5.94 (s, 1 H), 6.35 (d, <i>J</i> = 6.0 Hz, 1 H), 6.83 (dd, <i>J</i> = 7.7, 1.6 Hz, 1 H), 7.02–7.23 (m, 7 H), 7.27–7.33 (m, 2 H), 7.89 (d, <i>J</i> = 7.8 Hz, 1 H)
<sup>13</sup> C NMR δ (100 MHz):	52.8, 57.9, 83.7, 94.6, 127.4, 128.7 (2 C), 129.0, 129.1, 131.5, 132.0, 133.2, 133.3, 141.6, 144.3, 164.1, 170.6, 171.1
IR V <sub>max</sub> :	1716 (C=O), 1579, 1390, 1249, 1219, 1197, 1101, 1004
HRMS:	For C <sub>20</sub> H <sub>16</sub> INO <sub>5</sub> +Na, predicted 499.9965, found 499.9984.
[α] <sub>D</sub> <sup>20</sup>	+217.9 ° ( <i>c</i> = 6.3)
MP:	82–84 °C

**155b**

$^1\text{H}$  NMR  $\delta$  (400 MHz): 3.73 (s, 3 H), 5.81 (s, 1 H), 6.31 (d,  $J$  = 6.0 Hz, 1 H), 6.43 (ad,  $J$  = 1.3 Hz, 1 H), 7.10 (dd,  $J$  = 6.0, 1.6 Hz, 1 H), 7.18 (td,  $J$  = 7.7, 1.3 Hz, 1 H), 7.27–7.34 (m, 5 H), 7.38–7.43 (m, 1 H), 7.83 (dd,  $J$  = 7.8, 1.2 Hz, 1 H), 8.02 (d,  $J$  = 8 Hz, 1 H)

$^{13}\text{C}$  NMR  $\delta$  (100 MHz): 52.8, 58.9, 83.5, 94.8, 128.2, 129.0, 129.10, 129.13, 129.16, 131.7, 132.7, 133.5, 133.6, 141.9, 143.3, 164.8, 169.7, 170.2

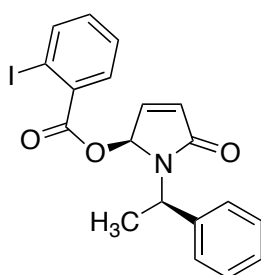
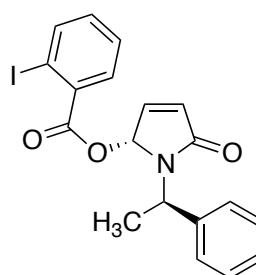
IR  $V_{\text{max}}$ : 1716 (C=O), 1579, 1390, 1249, 1219, 1197, 1101, 1004

HRMS: For  $\text{C}_{20}\text{H}_{16}\text{INO}_5 + \text{Na}$ , predicted 499.9965, found 499.9984.

$[\alpha]_{\text{D}}^{20}$   $-30.9^\circ$  ( $c$  = 6.3)

MP: 92–94  $^\circ\text{C}$

**(S)-5-Oxo-1-((R)-1-phenylethyl)-2,5-dihydro-1H-pyrrol-2-yl 2-iodobenzoate (176a) and (R)-5-oxo-1-((R)-1-phenylethyl)-2,5-dihydro-1H-pyrrol-2-yl 2-iodobenzoate (176b)**

**176a****176b**

To a solution of pyrrole **158** (0.0953 g, 0.556 mmol) in dichloromethane (10 mL) at 0  $^\circ\text{C}$  was added Dess–Martin periodinane (0.6368 g, 1.501 mmol,

2.70 eq.), and the reaction stirred for 45 min. H<sub>2</sub>O (10 mL) was added, and the reaction quenched by addition of Na<sub>2</sub>S<sub>2</sub>O<sub>5</sub>. The aqueous and organic layers were separated, and the aqueous layer extracted with dichloromethane (3 x 5 mL). The combined organic layers were washed with saturated Na<sub>2</sub>SO<sub>4</sub> (10 mL), dried over MgSO<sub>4</sub>, filtered, and the solvent removed under reduced pressure. The crude mixture was purified by flash column chromatography with EtOAc/hexanes (40:60) as the eluent, to give an inseparable mixture of **176a** and **176b** as an orange oil (0.1133 g, 0.2615 mmol, 47% yield)

<sup>1</sup>H NMR δ (600 MHz): 1.66 (d, *J* = 7.3 Hz, 2.6 H), 1.69 (d, *J* = 7.3 Hz, 3 H), 5.44 (p, *J* = 6.9 Hz, 1.8 H), 6.26 (d, *J* = 5.9 Hz, 0.8 H), 6.31 (d, *J* = 5.9 Hz, 1 H), 6.42 (d, *J* = 1.5 Hz, 0.8 H), 6.81 (dd, *J* = 7.7, 1.7 Hz, 1 H), 6.90 (d, *J* = 1.5 Hz, 1 H), 7.01–7.08 (m, 3.8 H), 7.09–7.13 (m, 1 H), 7.15–7.19 (m, 2.8 H), 7.24–7.36 (m, 7 H), 7.40 (at, *J* = 7.6 Hz, 1 h), 7.73 (dd, *J* = 7.8, 1.5 hz, 0.8 H), 7.90 (dd, *J* = 7.7, 0.8 Hz, 1 H), 8.01 (dd, *J* = 7.9, 0.4 Hz, 0.8 H)

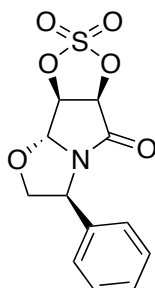
<sup>13</sup>C NMR δ (150 MHz): 17.0, 18.4, 49.1, 50.6, 82.1, 84.0, 94.5, 94.6, 127.10, 127.16, 127.2, 127.6, 128.0, 128.1, 128.4, 128.9, 129.6, 129.7, 131.0, 131.6, 132.1, 133.2, 133.3, 133.4, 139.8, 140.9, 141.5, 141.8, 142.2, 142.4, 164.5, 165.0, 170.12, 170.14



### 5.3 Chapter 2 Experimental Details

(3a*S*,3b*R*,6*S*,8a*R*)-6-Phenyltetrahydro-

[1,3,2]dioxathio[4',5':3,4]pyrrolo[2,1-*b*]oxazol-8(3b*H*)-one 2,2-dioxide  
(**232**)



**232**

To a stirred solution of diol **162** (0.2631 g, 1.118 mmol) in dry CH<sub>2</sub>Cl<sub>2</sub> (10 mL), under N<sub>2</sub> at 0 °C, was added pyridine (0.280 mL, 3.462 mmol, 3.1 eq.) and SOCl<sub>2</sub> (0.170 mL, 2.329 mmol, 2.1 eq.) *via* syringe. After stirring for 30 minutes, the reaction was quenched by addition of a saturated solution of CuSO<sub>4</sub> (10 mL). The aqueous and organic layers were separated, and the aqueous layer extracted with CH<sub>2</sub>Cl<sub>2</sub> (3 x 10 mL). The combined organic layers were dried over MgSO<sub>4</sub>, filtered, and the solvent removed under reduced pressure. The crude residue was dissolved in a 50:50 solution of CH<sub>2</sub>Cl<sub>2</sub> and CH<sub>3</sub>CN (15 mL) under an N<sub>2</sub> atmosphere, cooled to 0 °C and stirred. NaIO<sub>4</sub> (0.4961 g, 2.319 mmol, 2.0 eq.) and RuCl<sub>3</sub>·xH<sub>2</sub>O (0.007 g) were added and the reaction stirred for 5 minutes, at which point Et<sub>2</sub>O (20 mL) and H<sub>2</sub>O (15 mL) were added. The aqueous and organic layers were separated, and the organic layer washed with saturated NaHCO<sub>3</sub> (2 x 10 mL), dried over MgSO<sub>4</sub>, filtered, and the solvent removed under reduced pressure. The crude material was purified by flash column chromatography using EtOAc/hexanes (45:55) as the eluent to give the product **232** as a white crystalline solid (0.1681 g, 0.565 mmol, 51% yield)

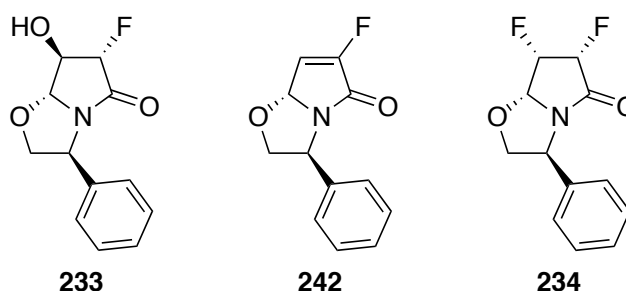
<sup>1</sup>H NMR δ (600 MHz):

3.97 (dd, *J* = 8.8, 6.8 Hz, 1 H), 4.63 (dd, *J* = 8.8, 7.8 Hz, 1 H), 5.19–5.23 (m, 1 H), 5.29 (d, *J* = 7.5 Hz, 1 H), 5.38 (d, *J* = 7.5 Hz, 1 H), 5.47 (s, 1 H), 7.22–7.26 (m, 2 H), 7.32–7.36 (m, 1 H), 7.38–7.42 (m, 2 H)

$^{13}\text{C}$ NMR $\delta$ (150 MHz):	58.4, 75.1, 77.1, 80.1, 94.2, 125.6, 128.6, 129.4, 137.3, 167.4
IR $V_{\text{max}}$ :	1732, 1408, 1209, 1021, 839
HRMS:	For $\text{C}_{12}\text{H}_{11}\text{NO}_6\text{S}$ , predicted 297.02939, found 297.02939.
$[\alpha]_{\text{D}}^{20}$	+155.8 $^{\circ}$ ( $c = 0.33$ $\text{CH}_2\text{Cl}_2$ )
MP	142.5–143.0 $^{\circ}\text{C}$

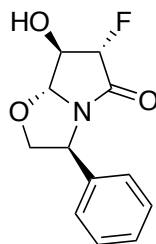
(3*S*,6*S*,7*R*,7*aR*)-6-Fluoro-7-hydroxy-3-phenyltetrahydropyrrolo[2,1-*b*]oxazol-5(6*H*)-one (233), (3*S*,7*aR*)-6-fluoro-3-phenyl-2,3-dihydropyrrolo[2,1-*b*]oxazol-5(7*aH*)-one (242), and (3*S*,6*R*,7*S*,7*aR*)-6,7-difluoro-3-phenyltetrahydropyrrolo[2,1-*b*]oxazol-5(6*H*)-one (234)

#### Fluorination With Deoxofluor<sup>®</sup>

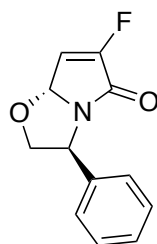


To a stirred solution of diol **162** (0.5047 g, 2.1469 mmol) in dry  $\text{CH}_2\text{Cl}_2$  (20 mL) under an atmosphere of  $\text{N}_2$ , at 0  $^{\circ}\text{C}$ , was added Deoxofluor<sup>®</sup> (2.00 mL of a 50 wt% solution in THF, 4.7007 mmol, 2.19 eq.) *via* syringe. The reaction was allowed to warm to room temperature and stirred for 18 h, at which time it was cooled on an ice bath quenched by slow addition of saturated  $\text{NaHCO}_3$  (20 mL). The aqueous and organic layers were separated, and the aqueous layer extracted with  $\text{CH}_2\text{Cl}_2$  (2 x 20 mL). The combined organic extracts were dried over  $\text{Na}_2\text{SO}_4$ , and the solvent removed under reduced pressure. The crude mixture was purified by automated flash column chromatography using a solvent gradient from 0–50% EtOAc/hexanes, to give the fluoroalkene **242** (0.0095 g, 0.0433 mmol, 2% yield) as a pale yellow oil, difluoro compound **234** (0.0340 g, 0.1421 mmol, 7% yield) as a white crystalline solid, and

fluorohydrin **233** (0.2774 g, 1.169 mmol, 54% yield) as a white crystalline solid.

**233**

$^1\text{H}$ NMR $\delta$ (400 MHz):	3.92 (dd, $J$ = 8.8, 6.9 Hz, 1 H), 4.49 (ddd, $J$ = 20.8, 7.3, 3.3 Hz, 1 H), 4.51–4.56 (m, 1 H), 5.14 (at, $J$ = 3.3 Hz, 1 H), 5.19 (at, $J$ = 6.9 Hz, 1 H), 5.35 (dd, $J$ = 52.2, 7.3 Hz, 7.20–7.41 (m, 5 H)
$^{13}\text{C}$ NMR $\delta$ (100 MHz):	57.3, 74.3, 78.7 (d, $J_{\text{C-F}}$ = 20.0 Hz), 93.1 (d, $J_{\text{C-F}}$ = 9.4 Hz), 95.2 (d, $J_{\text{C-F}}$ = 196.9 Hz), 125.9, 128.2, 129.0, 137.8, 168.8 (d, $J_{\text{C-F}}$ = 24.1 Hz)
$^{19}\text{F}$ NMR $\delta$ (375 MHz, MeOD):	–198.3 (ddd, $J$ = 52.1, 20.7, 3.6, 1 F)
IR $V_{\text{max}}$ :	3407 (OH), 1733 (C=O), 1668, 1404, 1362, 1264, 1213, 1096, 1028
HRMS:	For $\text{C}_{12}\text{H}_{12}\text{FNO}_3$ , predicted 237.08012, found 237.07943. $m/z$ (EI+): 237 ( $\text{M}^+$ , 1), 219 (10), 189 (50), 171 (20), 161 (30), 147 (20), 130 (25), 117 (75), 104 (100), 90 (40), 77 (25)
$[\alpha]_{\text{D}}^{20}$	+140.95 $^\circ$ ( $c$ = 0.42)
MP:	138–139 $^\circ\text{C}$

**242**

$^1\text{H}$  NMR  $\delta$  (600 MHz, MeOD): 3.99 (dd,  $J$  = 8.3, 7.2 Hz, 1 H), 4.83–4.89 (m, 2 H), 5.71 (dd,  $J$  = 6.0, 2.0 Hz, 1 H), 6.75 (dd,  $J$  = 2.0, 1.0 Hz, 1 H), 7.30 (sx,  $J$  = 4.2 Hz, 1 H), 7.37 (d,  $J$  = 4.3 Hz, 4 H)

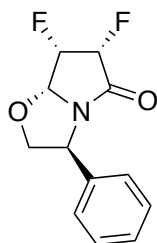
$^{13}\text{C}$  NMR  $\delta$  (150 MHz, MeOD): 59.6, 79.2, 89.9 (d,  $J_{\text{C-F}}$  = 10.6 Hz), 119.0 (d,  $J_{\text{C-F}}$  = 6.0 Hz), 127.2, 128.8, 129.8, 156.3 (d,  $J_{\text{C-F}}$  = 286 Hz), 169.5 (d,  $J_{\text{C-F}}$  = 30.9 Hz)

$^{19}\text{F}$  NMR  $\delta$  (600 MHz, MeOD): -134.48 (d,  $J$  = 6.0 Hz, 1 F)

IR  $V_{\text{max}}$ : 1736 (C=O), 1733, 1665, 1495, 1451, 1397, 1307, 1218, 1156, 1084

HRMS: For  $\text{C}_{12}\text{H}_{10}\text{FNO}_2$ , predicted 219.06956, found 219.06956.  $m/z$  (EI+): 219 ( $\text{M}^+$ , 20), 189 (100), 161 (50), 133 (25), 103 (25), 91 (10), 77 (20), 51 (10)

$[\alpha]_{\text{D}}^{20}$  +126.67  $^\circ$  ( $c$  = 0.72)

**234**

$^1\text{H}$  NMR  $\delta$  (400 MHz): 4.25 (ddd,  $J$  = 8.4, 3.0, 1.2 Hz, 1 H), 4.32 (dd,  $J$  = 8.4, 6.0 Hz, 1 H), 5.34 (ddd,  $J$  = 47.8, 25.2, 3.0 Hz, 1 H), 5.37 (dd,  $J$  = 14.1, 2.7 Hz, 1 H), 5.38 (dd,  $J$  = 6.0, 3.0 Hz, 1 H), 5.43 (ddd,  $J$  = 55.7, 3.0,

2.7 Hz, 1 H), 7.25–7.29 (m, 2 H), 7.30–7.34 (m, 1 H), 7.35–7.39 (m, 2 H)

$^{13}\text{C}$  NMR  $\delta$  (100 MHz): 57.5, 74.6, 87.1 (dd,  $J_{\text{C-F}} = 17.1, 4.8$  Hz), 87.6 (dd,  $J_{\text{C-F}} = 209.5, 16.9$  Hz), 89.2 (dd,  $J_{\text{C-F}} = 197.9, 13.5$  Hz), 126.1, 128.4, 129.1, 138.0, 168.6 (d,  $J_{\text{C-F}} = 24.3$  Hz)

$^{19}\text{F}$  NMR  $\delta$  (600 MHz): -215.89 (dd,  $J = 47.8, 5.6$  Hz, 1 F), -221.79 (dddd,  $J = 55.7, 25.2, 14.1, 5.6$  Hz, 1 F)

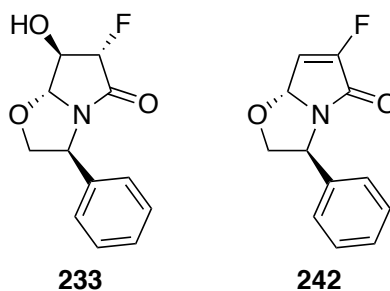
IR  $V_{\text{max}}$ : 1738 (C=O), 1709, 1457, 1423, 1346, 1297, 1155, 1111

HRMS: For  $\text{C}_{12}\text{H}_{11}\text{F}_2\text{NO}_2$ , predicted 239.07579, found 239.07573.  $m/z$  (EI+): 239 ( $\text{M}^+$ , 7), 219 (15), 209 (45), 189 (100), 161 (55), 133 (25), 117 (40), 104 (10), 91 (20), 77 (10)

$[\alpha]_{\text{D}}^{20}$  +125.8  $^\circ$  ( $c = 0.345$ )

MP: 139–140  $^\circ\text{C}$

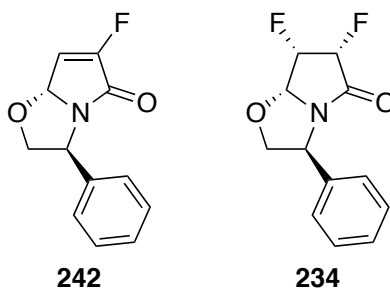
### Fluorination With DAST



To a stirred solution of diol **162** (0.1105 g, 0.4697 mmol) in dry  $\text{CH}_2\text{Cl}_2$  (7 mL) under  $\text{N}_2$  was added DAST (0.100 mL, 0.7568 mmol, 1.61 eq.). The mixture was heated to 35  $^\circ\text{C}$  and stirred at that temperature for 18 h. The reaction was quenched by addition of saturated  $\text{NaHCO}_3$  (5 mL), and the aqueous and organic layers separated. The aqueous layer was extracted with  $\text{CH}_2\text{Cl}_2$  (3 x 5 mL), the combined organic layers dried over  $\text{MgSO}_4$ , and the solvent removed under reduced pressure. The crude mixture was adsorbed on silica

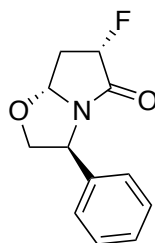
and purified by flash column chromatography using EtOAc (30:70), EtOAc/hexanes (60:40), and EtOAc/MeOH (90:10) as the eluents to give fluorohydrin **233** (0.0468 g, 0.1972 mmol, 42% yield), fluoroalkene **241** (0.0027 g, 0.0123 mmol, 3% yield), traces of difluoro compound **234**, and unreacted diol **162** (0.0094 g, 0.0399 mmol, 8%).

#### Fluorination With Greater Excess of Deoxofluor<sup>®</sup>



To a stirred solution of diol **162** (0.0934 g, 0.3970 mmol), in dry CH<sub>2</sub>Cl<sub>2</sub> (10 mL), under an atmosphere of N<sub>2</sub>, was added deoxofluor (0.8501 mL of a 50 wt% solution in THF, 1.9978 mmol, 5.03 eq.) *via* syringe. The reaction was heated at reflux and stirred for 18 h, at which time an additional portion of Deoxofluor (0.450 mL, 1.057 mmol, 2.66 eq) was added and the reaction stirred at reflux for 6 h. It was then cooled on an ice bath quenched by slow addition of saturated NaHCO<sub>3</sub> (15 mL). The aqueous and organic layers were separated, and the aqueous layer extracted with CH<sub>2</sub>Cl<sub>2</sub> (2 x 10 mL). The combined organic extracts were dried over MgSO<sub>4</sub>, and the solvent removed under reduced pressure. The crude mixture was purified by flash column chromatography using EtOAc/hexanes (30:70) as eluent, to give the fluoroalkene **242** (0.0196 g, 0.0894 mmol, 22% yield) as a pale yellow oil, difluoro compound **234** (0.0211 g, 0.0882 mmol, 22% yield) as a white crystalline solid, and trace amounts of fluorohydrin **233**.

**(3*S*,6*S*,7*aR*)-6-Fluoro-3-phenyltetrahydropyrrolo[2,1-*b*]oxazol-5(6*H*)-one (244)**



**244**

To a stirred solution of fluoroalkene **242** (0.0232 g, 0.1058 mmol) in EtOH (3 mL) was added Pd/C (~0.1 g of a 10% w/w mixture) and the mixture stirred under a balloon of H<sub>2</sub> for 16 h, before being filtered through a small plug of celite and the solvent removed under reduced pressure. The crude material was adsorbed onto silica and purified by flash column chromatography, using EtOAc/hexanes (40:60) as the eluent to give the compound **244** as a clear oil (0.0120 g, 0.0542 mmol, 51 % yield)

<sup>1</sup>H NMR δ (600 MHz): 2.28 (dddd, *J* = 26.6, 13.9, 8.2, 4.0 Hz, 1 H), 3.06–3.13 (m, 1 H), 3.90 (dd, *J* = 8.8, 7.5 Hz, 1 H), 4.63 (dd, *J* = 8.8, 7.7 Hz, 1 H), 5.17–5.21 (m, 2 H), 5.41 (dt, *J* = 52.3, 8.4 Hz, 1 H), 7.22–7.32 (m, 3 H), 7.33–7.37 (m, 2 H)

<sup>13</sup>C NMR δ (150 MHz): 35.0 (d, *J*<sub>C-F</sub> = 19.7 Hz, 1 C), 57.5, 74.8, 87.9 (d, *J*<sub>C-F</sub> = 5.4 Hz, 1 C), 89.2 (d, *J*<sub>C-F</sub> = 190.9 Hz, 1 C), 126.0, 128.1, 129.1, 138.5, 171.9 (d, *J*<sub>C-F</sub> = 22.9 Hz, 1 C)

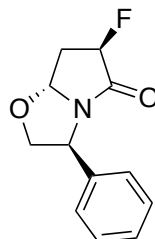
<sup>19</sup>F NMR δ (600 MHz): –187.97 (ddt, *J* = 52, 26, 5 Hz)

IR V<sub>max</sub>: 1727, 1495, 1447, 1414, 1332, 1293, 1167, 1089, 1044, 1018, 996

HRMS: For C<sub>12</sub>H<sub>12</sub>FNO<sub>2</sub>, predicted 221.08521, found 221.08559. *m/z* (EI+): 221 (M<sup>+</sup>, 10), 191 (75), 163 (60), 146 (25), 128 (55), 117 (100), 104 (30), 87 (70), 70 (10)

$[\alpha]_D^{20}$  +100.9 ° (c = 0.61)

**(3*S*,6*R*,7*aR*)-6-Fluoro-3-phenyltetrahydropyrrolo[2,1-*b*]oxazol-5(6*H*)-one (245)**



**245**

To a solution of alcohol **174** (0.0211 g, 0.0962 mmol), in dry CH<sub>2</sub>Cl<sub>2</sub> (5 mL), under an atmosphere of N<sub>2</sub>, was added DAST (0.020 mL, 0.1513 mmol, 1.57 eq.) *via* syringe. The mixture was heated to 35 °C, and stirred for 16 h. The reaction was quenched with saturated NaHCO<sub>3</sub> (3 mL), and the organic and aqueous layers separated. The aqueous layer was extracted with CH<sub>2</sub>Cl<sub>2</sub> (2 x 5 mL) and EtOAc (1 x 5 mL), and the combined organic extracts dried over MgSO<sub>4</sub> and the solvent removed under reduced pressure. The crude mixture was purified by flash column chromatography using EtOAc/hexanes (50:50) and EtOAc as the eluents, to give the compound **245** as a white solid (0.0113 g, 0.0511 mmol, 53 % yield) and unreacted starting material **174** (0.0028 g, 0.0127 mmol, 13%).

<sup>1</sup>H NMR δ (600 MHz): 2.40 (dddd, *J* = 31.0, 15.6, 7.0, 3.1 Hz, 1 H), 2.68 (dddd, *J* = 25.3, 15.6, 5.7, 1.6 Hz, 1 H), 3.92 (dd, *J* = 8.8, 7.6 Hz, 1 H), 4.65 (at, *J* = 8.3 Hz, 1 H), 5.06 (at, *J* = 7.3 Hz, 1 H), 5.17 (ddd, *J* = 51.6, 7.0, 1.4 Hz, 1 H), 5.46 (dd, *J* = 5.6, 3.1 Hz, 1 H), 7.24–7.28 (m, 2 H), 7.28–7.32 (m, 1 H), 7.34–7.39 (m, 2 H)

<sup>13</sup>C NMR δ (150 MHz): 34.4 (d, *J*<sub>C-F</sub> = 23.4 Hz, 1 C), 57.6, 76.0, 91.2 (d, *J*<sub>C-F</sub> = 0.7 Hz, 1 C), 92.0 (d, *J*<sub>C-F</sub> = 184.6 Hz, 1 C), 125.9, 128.1, 129.1, 138.4, 172.0 (d, *J*<sub>C-F</sub> = 16.6 Hz, 1 C)

<sup>19</sup>F NMR δ (600 MHz): –181.81 (ddd, *J* = 51.6, 31, 25 Hz)

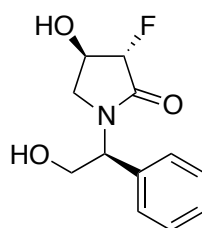


IR  $V_{\max}$ : 1717, 1429, 1412, 1295, 1167, 1091, 1083

HRMS: For  $C_{12}H_{12}FNO_2+Na$ , predicted 244.0744, found 244.0755

$[\alpha]_D^{20}$  +170.26 ° ( $c = 0.56$ )

**(3*S*,4*R*)-3-fluoro-4-hydroxy-1-((*S*)-2-hydroxy-1-phenylethyl)pyrrolidin-2-one (246)**



**246**

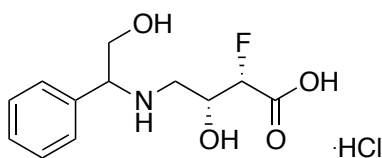
To a stirred solution of fluorohydrin **233** (0.1909 g, 0.8047 mmol) in dry  $CH_2Cl_2$  (8 mL) at 0 °C, was added triethylsilane (0.525 mL, 3.286 mmol, 4.1 eq.) and  $BF_3 \cdot OEt_2$  (0.400 mL, 3.241 mmol, 4.0 eq.) *via* syringe. The reaction was stirred for 18 h, before being quenched with saturated  $NaHCO_3$  (8 mL). The aqueous and organic layers were separated, and the aqueous layer extracted with EtOAc (3 x 5 mL). The combined organic extracts were dried over  $MgSO_4$ , filtered, and the solvent removed under reduced pressure. The crude material was purified by flash column chromatography using EtOAc/hexanes (50:50) and EtOAc as the eluents, to give the compound **246** as a crystalline white solid (0.1291 g, 0.5396 mmol, 67 % yield).

$^1H$  NMR  $\delta$  (400 MHz, MeOD): 2.94 (ddd,  $J = 9.7, 6.8, 1.1$  Hz, 1 H), 3.79 (dd,  $J = 9.8, 7.9$  Hz, 1 H), 3.94 (dd,  $J = 11.8, 5.2$  Hz, 1 H), 4.08 (dd,  $J = 11.8, 9.3$  Hz, 1 H), 4.48 (m (likely dddd), 1 H), 4.94 (dd,  $J = 52.6, 6.5$  Hz, 1 H), 5.21 (dd,  $J = 9.3, 5.2$  Hz, 1 H), 7.28–7.39 (m, 5 H)

$^{13}C$  NMR  $\delta$  (100 MHz, MeOD): 47.9 (d,  $J_{C-F} = 8.5$  Hz), 58.7, 61.1, 71.4 (d,  $J_{C-F} = 21.3$  Hz), 95.9 (d,  $J_{C-F} = 189.5$  Hz), 128.7, 129.2, 129.8, 137.5, 170.5 (d,  $J_{C-F} = 21.6$  Hz)

$^{19}\text{F}$ NMR $\delta$ (400 MHz, MeOD):	-200.63 (dd, $J$ = 52.5, 21.1 Hz, 1 F)
IR $V_{\text{max}}$ :	3340 (OH), 1690 (C=O), 1488, 1452, 1355, 1260, 1176, 1127, 1079, 1046
HRMS:	For $\text{C}_{12}\text{H}_{14}\text{FNO}_3 + \text{Na}$ , predicted 262.0850, found 262.0857
$[\alpha]_{\text{D}}^{20}$ (acetone)	+30.18 $^{\circ}$ ( $c$ = 0.34)
MP:	130.6–131 $^{\circ}\text{C}$

**(2*S*,3*R*)-2-fluoro-3-hydroxy-4-((2-hydroxy-1-phenylethyl)amino)butanoic acid hydrochloride (**249**)**



**249**

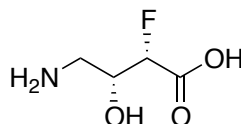
Ring-opened fluorohydrin **246** (0.0805 g, 0.3364 mmol) was dissolved in 6 M HCl (5mL) and the solution heated at reflux and stirred for 16 h. The solvent was removed under reduced pressure to yield the hydrochloride salt **249** (0.0966 g, 0.3288 mmol, 98% yield) as a white amorphous solid.

$^1\text{H}$ NMR $\delta$ (600MHz, $\text{D}_2\text{O}$ ):	3.08 (dd, $J$ = 12.8, 10.8 Hz, 1 H), 3.31 (dd, $J$ = 13.0, 2.5 Hz, 1 H), 4.01 (dd, $J$ = 12.3, 5.2 Hz, 1 H), 4.06 (dd, $J$ = 12.3, 7.8 Hz, 1 H), 4.46–4.55 (m, 2 H), 5.01 (d, $J$ = 47.7 Hz, 1 H), 7.47–7.57 (m, 5 H)
$^{13}\text{C}$ NMR $\delta$ (150 MHz, $\text{D}_2\text{O}$ ):	47.3 (d, $J_{\text{C-F}}$ = 5.3 HZ, 1 C), 61.4, 63.6, 66.7 (d, $J_{\text{C-F}}$ = 19.9 Hz, 1 C), 90.5 (d, $J_{\text{C-F}}$ = 188.0 Hz, 1 C), 128.2, 129.5, 130.1, 131.1, 173.3 (d, $J_{\text{C-F}}$ = 21.8 Hz, 1 C)
$^{19}\text{F}$ NMR $\delta$ (600 MHz, $\text{D}_2\text{O}$ ):	-206.45 (dd, $J_{\text{H-F}}$ = 47.3, 26.1 Hz, 1 F)
IR $V_{\text{max}}$ :	3322, 2942, 1738, 1592, 1455, 1423, 1225, 1133, 1071

HRMS: For  $C_{12}H_{17}FNO_4$ , predicted 258.1136, found 258.1133

$[\alpha]_D^{20}$  (MeOH) +26.22 ° (c = 2.55)

**(2S,3R)-4-amino-2-fluoro-3-hydroxybutanoic acid (238)**



**238**

A mixture of hydrochloride salt **249** (0.0184 g, 0.0626 mmol) and Pd/C (~0.030 g of 10% w/w mixture) in a solution of 95:5 EtOH/AcOH (10 mL), was reacted under a balloon of  $H_2$  for 18 h. The reaction mixture was then filtered on celite, and the solvent removed under reduced pressure to give the crude product **238** (0.0187 g).

$^1H$  NMR  $\delta$  (600MHz,  $D_2O$ ): 3.24 (dd,  $J$  = 13.2, 9.6 Hz, 1 H), 3.36 (dd,  $J$  = 13.2, 2.9 Hz, 1 H), 4.37–4.45 (m, 1 H), 5.04 (dd,  $J$  = 48.5, 1.7 Hz, 1 H)

$^{13}C$  NMR  $\delta$  (150 MHz,  $D_2O$ ): 41.3 (d,  $J_{C-F}$  = 5.4 Hz, 1 C), 67.4 (d,  $J_{C-F}$  = 19.6 Hz, 1 C), 90.5 (d,  $J_{C-F}$  = 188.0 Hz, 1 C), 172.6 (d,  $J_{C-F}$  = 22.2 Hz, 1 C)

$^{19}F$  NMR  $\delta$  (600 MHz,  $D_2O$ ): -199.39 (dd,  $J_{H-F}$  = 47.6, 24.1 Hz, 1 F)

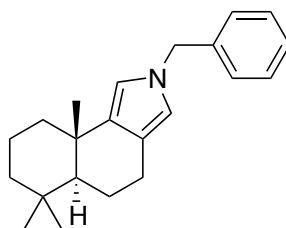
HRMS: For  $C_4H_9FNO_3$ , predicted 138.0516, found 138.0559

## 5.4 Chapter 3 Experimental Details

### General Method For the Synthesis of Pyrroles From Polygodial

Polygodial (1 eq.) was dissolved in 5 mL of EtOH and 0.5 mL AcOH, under an atmosphere of N<sub>2</sub>. Light was excluded, the primary amine (1.2 eq.) was added, and the solution allowed to stir for 0.5 h. NaBH<sub>3</sub>CN (1.0 eq) was then added, and the reaction allowed to stir for a further 0.5 h. H<sub>2</sub>O (5 mL) and CH<sub>2</sub>Cl<sub>2</sub> (5 mL) were added, and the solution made alkaline by addition of solid Na<sub>2</sub>CO<sub>3</sub>. The aqueous and organic layers were separated and the aqueous layer extracted with CH<sub>2</sub>Cl<sub>2</sub> (3 x 5 mL). The combined organic layers were dried over MgSO<sub>4</sub>, filtered, and the solvent removed under reduced pressure. Compounds were purified by adsorption on silica and elution through a silica plug, with EtOAc/hexanes (20:80) as the eluent.

#### (5a*S*,9a*S*)-2-Benzyl-6,6,9a-trimethyl-4,5,5a,6,7,8,9,9a-octahydro-2*H*-benzo[*e*]isoindole (270)



**270**

Prepared from polygodial (0.0513 g, 0.220 mmol), benzylamine (0.030 mL, 0.27 mmol, 1.2 eq.) and NaBH<sub>3</sub>CN (0.0142g, 0.220 mmol, 1.0 eq.). Product isolated as a clear oil (0.0506 g, 0.164 mmol, 75 % yield).

<sup>1</sup>H NMR δ (400 MHz): 0.98 (s, 3 H), 1.01 (s, 3 H), 1.29 (s, 3 H), 1.34 (dd, *J* = 13.8, 4.2 Hz, 1 H), 1.43 (dd, *J* = 12, 1.8 Hz, 1 H), 1.47–1.62 (m, 3 H), 1.67–1.84 (m, 2 H), 1.84–1.91 (m, 1 H), 1.97–2.05 (m, 1 H), 2.56–2.68 (m, 1 H), 2.82 (d, *J* = 15.6, 6.2 Hz, 1 H), 5.00 (s, 2 H), 6.31–6.35 (m, 1 H), 6.37 (d, *J* = 2.2 Hz, 1 H), 7.16–7.21 (m, 2 H), 7.29–7.41 (m, 3 H)

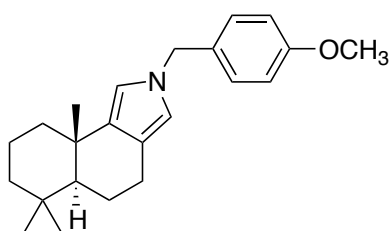
$^{13}\text{C}$  NMR  $\delta$  (100 MHz): 19.4, 19.9, 21.6, 23.0, 25.8, 33.2, 33.7, 34.7, 40.0, 42.3, 52.2, 53.4, 113.6, 115.9, 118.0, 127.3, 127.5, 128.6, 136.3, 138.7

IR  $V_{\text{max}}$ : 2922, 1521, 1494, 1454, 1440, 1394, 1373, 1352, 1317, 1215, 1139

HRMS: For  $\text{C}_{22}\text{H}_{29}\text{N}$ , predicted 307.23000, found 307.22913.  $m/z$  (EI+): 307 ( $M^+$ , 10), 292 (45), 236 (5), 118 (55), 87 (100), 70 (10)

$[\alpha]_{\text{D}}^{20}$  +19.8  $^{\circ}$  ( $c$  = 0.0456)

**(5a*S*,9a*S*)-2-(4-Methoxybenzyl)-6,6,9a-trimethyl-4,5,5a,6,7,8,9,9a-octahydro-2*H*-benzo[*e*]isoindole (272)**



**272**

Prepared from polygodial (0.0527 g, 0.2249 mmol), 4-methoxybenzylamine (0.0375 mL, 0.2869 mmol, 1.27 eq.) and  $\text{NaBH}_3\text{CN}$  (0.0148 g, 0.2355 mmol, 1.05 eq.). Product isolated as a clear oil (0.0743 g, 0.2201 mmol, 98% yield).

$^1\text{H}$  NMR  $\delta$  (400 MHz): 0.95 (s, 3 H), 0.98 (s, 3 H), 1.26 (s, 3 H), 1.28–1.34 (m, 1 H), 1.40 (dd,  $J$  = 11.9, 1.5 Hz, 1 H), 1.44–1.59 (m, 3 H), 1.63–1.78 (m, 2 H), 1.81–1.89 (m, 1 H), 1.94–2.02 (m, 1 H), 2.54–2.66 (m, 1 H), 2.79 (dd,  $J$  = 15.7, 6.2 Hz, 1 H), 3.83 (s, 3 H), 4.91 (s, 2 H), 6.30 (s, 1 H), 6.33 (d,  $J$  = 2.1 Hz, 1 H), 6.89 (d,  $J$  = 8.6 Hz, 2 H), 7.13 (d,  $J$  = 8.6 Hz, 2 H)

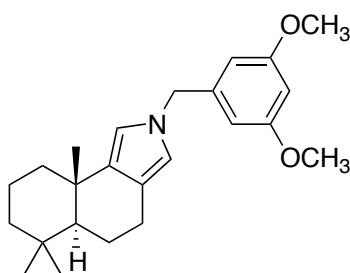
$^{13}\text{C}$  NMR  $\delta$  (100 MHz): 19.4, 19.8, 21.6, 23.0, 25.8, 33.2, 33.6, 34.7, 39.9, 42.2, 52.2, 52.8, 55.3, 113.3, 114.0, 115.7, 117.8, 128.7, 130.5, 136.2, 159.0

IR  $V_{\max}$ : 2922, 1612, 1586, 1513, 1458, 1440, 1387, 1302, 1290, 1174, 1139, 1035

HRMS: For  $C_{23}H_{31}NO+H$ , predicted 338.2478, found 338.2475

$[\alpha]_D^{20}$ : +31.87 ° ( $c = 3.10$ )

**(5a*S*,9a*S*)-2-(3,5-Dimethoxybenzyl)-6,6,9a-trimethyl-4,5,5a,6,7,8,9,9a-octahydro-2*H*-benzo[*e*]isoindole (273)**



**273**

Prepared from Polygodial (0.0552 g, 0.2356 mmol), 3,5-dimethoxybenzylamine (0.0581 g, 0.3474 mmol, 1.47 eq.) and  $NaBH_3CN$  (0.0185 g, 0.2943 mmol, 1.25 eq.). Product isolated as a clear oil (0.0713 g, 0.1940 mmol, 82 % yield).

$^1H$  NMR  $\delta$  (400 MHz): 0.94 (s, 3 H), 0.97 (s, 3 H), 1.24 (s, 3 H), 1.26–1.33 (m, 1 H), 1.38 (dd,  $J = 11.9, 1.6$  Hz, 1 H), 1.43–1.57 (m, 3 H), 1.63–1.76 (m, 2 H), 1.80–1.86 (m, 1 H), 1.94–2.01 (m, 1 H), 2.52–2.63 (m, 1 H), 2.77 (dd,  $J = 15.6, 6.1$  Hz, 1 H), 3.77 (s, 6 H), 4.90 (s, 2 H), 6.27–6.30 (m, 3 H), 6.32–6.34 (m, 1 H), 6.37–6.40 (m, 1 H)

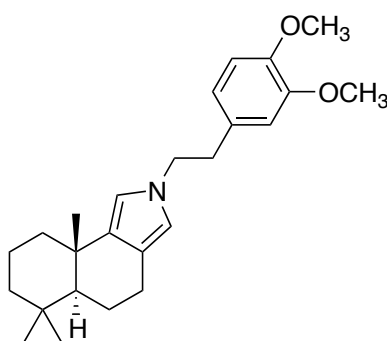
$^{13}C$  NMR  $\delta$  (100 MHz): 19.4, 19.9, 21.6, 23.0, 25.8, 33.2, 33.7, 34.7, 40.0, 42.3, 52.2, 53.4, 55.3, 99.3, 105.2, 113.7, 116.1, 118.0, 136.4, 141.2, 161.1

IR  $V_{\max}$ : 2937, 1610, 1597, 1471, 1460, 1429, 1388, 1346, 1317, 1205, 1157, 1138, 1068

HRMS: For  $C_{24}H_{33}NO_2+H$ , predicted 368.2584, found 368.2582

$[\alpha]_D^{20}$ : +34.35 ° (c = 2.12)

**(5a*S*,9a*S*)-2-(3,4-Dimethoxyphenethyl)-6,6,9a-trimethyl-4,5,5a,6,7,8,9,9a-octahydro-2*H*-benzo[*e*]isoindole (263)**



**263**

Prepared from polygodial (0.2002 g, 0.8543 mmol), 3,4-dimethoxyphenethylamine (0.200 mL, 1.203 mmol, 1.40 eq.) and  $NaBH_3CN$  (0.0574 g, 0.9134 mmol, 1.07 eq.). Product isolated as a clear oil (0.2854 g, 0.7480 mmol, 87 % yield).

$^1H$  NMR  $\delta$  (400 MHz): 0.90 (s, 3 H), 0.93 (s, 3 H), 1.19 (s, 3 H), 1.23–1.35 (m, 2 H), 1.37–1.56 (m, 3 H), 1.58–1.84 (m, 3 H), 1.88–1.97 (m, 1 H), 2.47–2.60 (m, 1 H), 2.73 (dd,  $J$  = 15.6, 6.1 Hz, 1 H), 2.94 (t,  $J$  = 7.4 Hz, 2 H), 3.80 (s, 3 H), 3.86 (s, 3 H), 3.94 (t,  $J$  = 7.3, 2 H), 6.21 (s, 1 H), 6.22 (s, 1 H), 6.44 (s, 1 H), 6.66 (d,  $J$  = 6.9 Hz, 1 H), 6.78 (d,  $J$  = 8.12 Hz, 1 H)

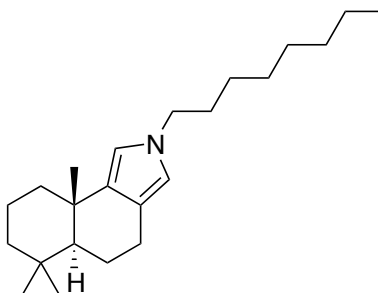
$^{13}C$  NMR  $\delta$  (100 MHz): 19.4, 19.9, 21.6, 23.0, 25.8, 33.2, 33.7, 34.7, 38.0, 40.0, 42.3, 51.5, 52.4, 55.8, 56.0, 111.3, 112.1, 112.8, 115.5, 117.4, 120.6, 131.6, 136.0, 147.7, 148.9

IR  $V_{max}$ : 2935, 1516, 1452, 1263, 1236, 1135, 1031

HRMS: For  $C_{25}H_{35}NO_2+Na$ , predicted 404.2560, found 404.2558

$[\alpha]_{\text{D}}^{20}$  : +27.4 ° (c = 3.15)

**(5a*S*,9a*S*)-6,6,9a-Trimethyl-2-octyl-4,5,5a,6,7,8,9,9a-octahydro-2*H*-benzo[*e*]isoindole (274)**



**274**

Prepared from polygodial (0.0489 g, 0.2086 mmol), octylamine (0.0425 mL, 0.2572 mmol, 1.23 eq.) and NaBH<sub>3</sub>CN (0.0150 g, 0.2387 mmol, 1.14 eq.). Product isolated as a clear oil (0.0532 g, 0.1614 mmol, 77 % yield).

<sup>1</sup>H NMR δ (400 MHz): 0.88–0.92 (m, 3 H), 0.93 (s, 3 H), 0.95 (s, 3 H), 1.23 (s, 3 H), 1.26–1.35 (m, 8 H), 1.36–1.41 (m, 1 H), 1.42–1.57 (m, 4 H), 1.61–1.86 (m, 5 H), 1.94–2.02 (m, 1 H), 2.52–2.64 (m, 1 H), 2.77 (dd, *J* = 15.6, 6.0 Hz, 1 H), 3.75 (t, *J* = 7.3 Hz, 2 H), 6.26 (s, 1 H), 6.28 (s, 1 H)

<sup>13</sup>C NMR δ (100 MHz): 14.2, 19.5, 19.9, 21.6, 22.7, 23.1, 25.8, 27.0, 29.30, 29.33, 31.7, 31.9, 33.2, 33.7, 34.7, 40.0, 42.3, 49.7, 52.3, 112.9, 115.2, 117.2, 135.6

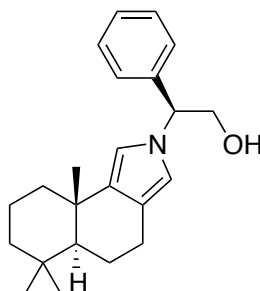
IR *V*<sub>max</sub>: 2924, 2853, 1526, 1457, 1441, 1387, 1372, 1354, 1213, 1149, 1140

HRMS: For C<sub>23</sub>H<sub>39</sub>N, predicted 329.30825, found 329.30752. *m/z* (EI<sup>+</sup>): 329 (M<sup>+</sup>,20), 314 (100), 286 (5), 244 (10), 231 (5), 190 (5), 148 (10), 118 (35)

$[\alpha]_{\text{D}}^{20}$  : +22.93 ° (c = 4.1)



**(S)-2-Phenyl-2-((5a*S*,9a*S*)-6,6,9a-trimethyl-4,5,5a,6,7,8,9,9a-octahydro-2*H*-benzo[*e*]isoindol-2-yl)ethan-1-ol (275)**



**275**

Prepared from polygodial (0.0426 g, 0.1818 mmol), *S*-(+)-2-phenylglycinol (0.0319 g, 0.2325 mmol, 1.28 eq.) and NaBH<sub>3</sub>CN (0.0123g, 0.1957 mmol, 1.08 eq.). Product isolated as a clear oil (0.0354 g, 0.1049 mmol, 58 % yield).

<sup>1</sup>H NMR  $\delta$  (400 MHz): 0.91 (s, 3 H), 0.95 (s, 3 H), 1.20 (s, 3 H), 1.24–1.31 (m, 1 H), 1.33–1.38 (m, 1 H), 1.40–1.55 (m, 3 H), 1.60–1.85 (m, 3 H), 1.92–2.00 (m, 1 H), 2.49–2.61 (m, 1 H), 2.76 (dd, *J* = 15.8, 6.0 Hz, 1 H), 4.06–4.20 (m, 2 H), 5.12 (dd, *J* = 8.2, 5.2 Hz, 1 H), 6.39 (s, 1 H), 6.43 (d, *J* = 1.7 Hz, 1 H), 7.14 (d, *J* = 7.2 Hz, 2 H), 7.26–7.37 (m, 3 H)

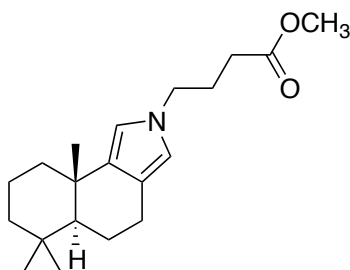
<sup>13</sup>C NMR  $\delta$  (100 MHz): 19.4, 19.8, 21.6, 23.1, 25.8, 33.2, 33.7, 34.8, 40.0, 42.2, 52.1, 65.0, 65.4, 112.4, 114.5, 118.3, 126.8, 127.9, 128.8, 136.6, 139.1

IR  $V_{\max}$ : 3362 (OH), 2924, 1662, 1452, 1386, 1373, 1211, 1139, 1066, 1037

HRMS: For C<sub>23</sub>H<sub>31</sub>NO+Na, predicted 360.2298, found 360.2292

$[\alpha]_D^{20}$ : +29.4 ° (*c* = 1.43)

**Methyl 4-((5a*S*,9a*S*)-6,6,9a-trimethyl-4,5,5a,6,7,8,9,9a-octahydro-2*H*-benzo[*e*]isoindol-2-yl)butanoate (276)**



**276**

NaOAc (0.0360 g, 0.4388 mmol, 1.55 eq.) and  $\gamma$ -aminobutyric acid methyl ester hydrochloride (0.0324 g, 0.2109 mmol, 1.20 eq.) were added to a magnetically stirred solution of polygodial (0.0412 g, 0.1758 mmol) in EtOH/AcOH (6 mL of 10:1 solution) maintained under N<sub>2</sub> (the reaction flask was covered in foil to exclude light). After 0.5 h, NaBH<sub>3</sub>CN (0.0171 g, 0.2721 mmol, 1.55 eq.) was added. After 0.5 h, H<sub>2</sub>O (5 mL) and CH<sub>2</sub>Cl<sub>2</sub> (5 mL) were added followed by solid Na<sub>2</sub>CO<sub>3</sub> until the solution was made alkaline. The aqueous and organic layers were then separated and the aqueous layer extracted with CH<sub>2</sub>Cl<sub>2</sub> (3 x 5 mL). The combined organic layers were dried over MgSO<sub>4</sub>, filtered, and concentrated under reduced pressure. The crude material was purified by flash column chromatography using EtOAc/hexanes (12: 88) as the eluent to give pyrrole **276** as a clear, colourless oil (0.0166 g, 0.0523 mmol, 30% yield)

<sup>1</sup>H NMR  $\delta$  (400 MHz): 0.89 (s, 3 H), 0.92 (s, 3 H), 1.19 (s, 3 H), 1.22–1.29 (m, 1 H), 1.30–1.36 (m, 1 H), 1.38–1.54 (m, 3 H), 1.58–1.73 (m, 2 H), 1.74–1.83 (m, 1 H), 1.90–1.97 (m, 1 H), 1.98–2.09 (m, 2 H), 2.28 (t,  $J$  = 7.2 Hz, 2 H), 2.47–2.59 (m, 1 H), 2.73 (dd,  $J$  = 15.7, 6.2 Hz, 1 H), 3.67 (s, 3 H), 3.80 (t,  $J$  = 6.9 Hz, 2 H), 6.22 (s, 1 H), 6.24 (s, 1 H)

<sup>13</sup>C NMR  $\delta$  (150 MHz): 19.4, 19.9, 21.6, 23.0, 25.8, 26.8, 31.1, 33.2, 33.7, 34.7, 40.0, 42.3, 48.6, 51.7, 52.2, 113.0, 115.4, 117.7, 136.1, 173.5

IR  $V_{\max}$ : 2922, 1739, 1653, 1459, 1437, 1363, 1208, 1149, 1141

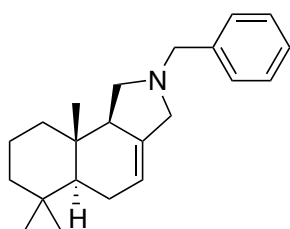
HRMS: For  $C_{20}H_{31}NO_2$ , predicted 317.23548, found 317.23591.  $m/z$  (EI+): 317 ( $M^+$ , 20), 302 (100), 274 (5), 246 (10), 171 (20), 143 (15), 101 (10)

$[\alpha]_D^{20}$ : +15.62° ( $c = 0.32$ )

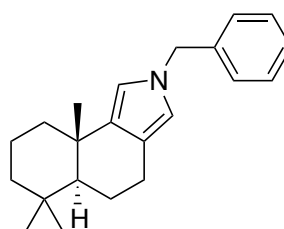
### General Method For the Synthesis of Pyrrolidines From Polygodial

Polygodial (1 eq.) was dissolved in EtOH (7 mL) and AcOH (0.7 mL), under an atmosphere of  $N_2$ .  $NaBH_3CN$  (5 eq.) was added, and the flask covered to exclude light. A solution of the amine (1.2 eq.) in EtOH (5 mL) was then added slowly *via* pressure equalising dropping funnel, and the reaction allowed to stir for 1 h.  $H_2O$  (10 mL) and  $CH_2Cl_2$  (10 mL) were added and the solution made alkaline by addition of solid  $Na_2CO_3$ , before the organic and aqueous layers were separated and the aqueous layer extracted with  $CH_2Cl_2$  (3 x 5 mL). The combined organic layers were dried over  $MgSO_4$ , filtered, and the solvent removed under reduced pressure. The crude mixture was purified by flash column chromatography using EtOAc/hexanes as eluent.

**(5a*S*,9a*S*)-2-Benzyl-6,6,9a-trimethyl-4,5,5a,6,7,8,9,9a-octahydro-2*H*-benzo[*e*]isoindole (270) and (5a*S*,9a*S*,9b*R*)-2-benzyl-6,6,9a-trimethyl-2,3,5,5a,6,7,8,9,9a,9b-decahydro-1*H*-benzo[*e*]isoindole (271)**

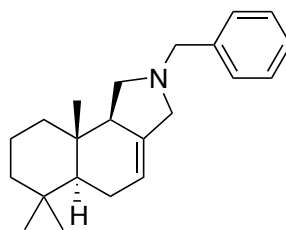


**271**



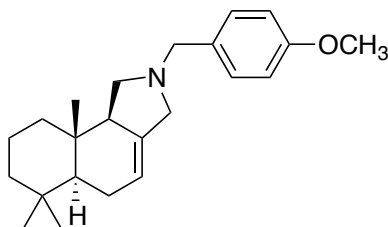
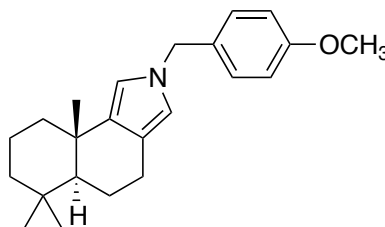
**270**

Using polygodial (0.0989 g, 0.4220 mmol), benzylamine (0.055 mL, 0.5035 mmol, 1.19 eq.) and  $NaBH_3CN$  (0.1350 g, 2.148 mmol, 5.09 eq.). The crude mixture was purified by flash column chromatography using EtOAc/hexanes (20:80) as eluent to give **271** as a clear oil (0.0656 g, 0.2119 mmol, 50% yield) and **270** as a clear oil (0.0089 g, 0.0289 mmol, 7% yield).

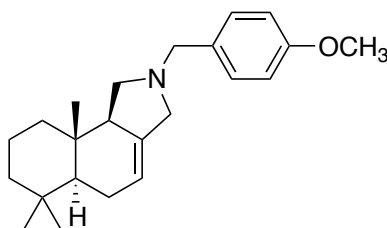
**271**

$^1\text{H}$ NMR $\delta$ (400 MHz):	0.77 (s, 3 H), 0.85 (s, 3 H), 0.89 (s, 3 H), 1.04–1.25 (m, 2 H), 1.27 (dd, $J$ = 11.8, 5.3 Hz, 1 H), 1.34–1.47 (m, 2 H), 1.48–1.61 (m, 2 H), 1.80–1.93 (m, 1 H), 2.06–2.15 (m, 1 H), 2.18 (t, $J$ = 9.1 Hz, 1 H), 2.34–2.44 (m, 1 H), 2.79 (t, $J$ = 8.1 Hz, 1 H), 2.82–2.89 (m, 1 H), 3.40–3.48 (m, 1 H), 3.55 (d, $J$ = 12.8 Hz, 1 H), 3.71 (d, $J$ = 12.8 Hz, 1 H), 5.39 (s, 1 H), 7.20–7.36 (m, 5 H)
$^{13}\text{C}$ NMR $\delta$ (100 MHz):	13.8, 18.8, 21.6, 24.2, 33.0, 33.4, 34.1, 40.4, 42.6, 50.2, 54.1, 55.2, 58.1, 61.0, 115.9, 127.0, 128.1, 128.3, 128.9, 138.6
IR $V_{\text{max}}$ :	2921, 1494, 1471, 1453, 1441, 1387, 1365, 1350, 1142, 1072, 1028
HRMS:	For $\text{C}_{22}\text{H}_{31}\text{N}$ , predicted 309.24565, found 309.24533. $m/z$ (EI+): 309 ( $M^+$ , 50), 308 (55), 290 (20), 266 (10), 236 (10), 222 (25), 200 (30), 184 (20), 170 (30), 157 (10), 131 (10), 105 (50), 91 (100)
$[\alpha]_{\text{D}}^{20}$ :	+15.88 $^{\circ}$ ( $c$ = 2.595)

**(5a*S*,9a*S*)-2-(4-Methoxybenzyl)-6,6,9a-trimethyl-4,5,5a,6,7,8,9,9a-octahydro-2*H*-benzo[*e*]isoindole (272) and (5a*S*,9a*S*,9b*R*)-2-(4-methoxybenzyl)-6,6,9a-trimethyl-2,3,5,5a,6,7,8,9,9a,9b-decahydro-1*H*-benzo[*e*]isoindole (277)**

**277****272**

Using polygodial (0.1005 g, 0.4288 mmol), 4-methoxybenzylamine (0.070 mL, 0.5357 mmol, 1.25 eq.) and NaBH<sub>3</sub>CN (0.1350 g, 2.148 mmol, 5.01 eq.). The crude mixture was purified by flash column chromatography using EtOAc/hexanes (20:80) as eluent to give **277** as a clear oil (0.0615 g, 0.1811 mmol, 42% yield) and **272** as a clear oil (0.0100 g, 0.0296 mmol, 7% yield).

**277**

<sup>1</sup>H NMR δ (400 MHz): 0.77 (s, 3 H), 0.86 (s, 3 H), 0.90 (s, 3 H), 1.06–1.23 (m, 2 H), 1.24–1.31 (m, 1 H), 1.35–1.46 (m, 2 H), 1.49–1.59 (m, 2 H), 1.80–1.92 (m, 1 H), 2.16–2.18 (m, 2 H), 2.33–2.42 (m, 1 H), 2.76 (t, *J* = 8.0 Hz, 1 H), 2.79–2.86 (m, 1 H), 3.37–3.44 (m, 1 H), 3.48 (d, *J* = 12.6 Hz, 1 H), 3.63 (d, *J* = 12.6 Hz, 1 H), 3.79 (s, 3 H), 5.38 (s, 1 H), 6.84 (d, *J* = 8.5 Hz, 2 H), 7.24 (d, *J* = 8.5 Hz, 2 H)

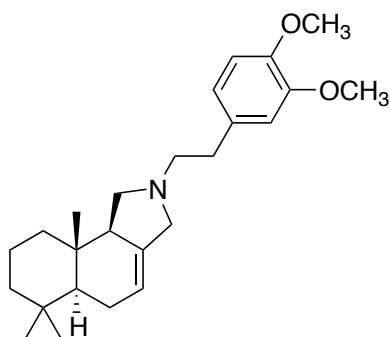
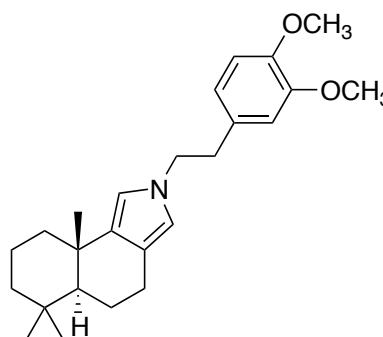
<sup>13</sup>C NMR δ (100 MHz): 13.8, 18.8, 21.6, 24.2, 33.0, 33.3, 34.1, 40.4, 42.6, 50.2, 54.0, 55.2, 55.3, 58.0, 60.4, 113.7, 115.7, 129.9, 131.4, 138.7, 158.7

IR V<sub>max</sub>: 2921, 1612, 1585, 1512, 1464, 1441, 1387, 1365, 1349, 1301, 1247, 1171, 1038

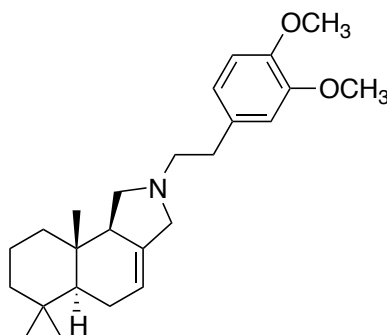
HRMS: For  $C_{23}H_{33}NO$ , predicted 339.25621, found 339.25602.  $m/z$  (EI+): 339 ( $M^+$ , 45), 322 (10), 296 (5), 218 (25), 202 (10), 148 (10), 121 (100), 109 (25), 77 (15)

$[\alpha]_D^{20}$  25.51 ° ( $c = 1.21$ )

**(5a*S*,9a*S*)-2-(3,4-Dimethoxyphenethyl)-6,6,9a-trimethyl-4,5,5a,6,7,8,9,9a-octahydro-2*H*-benzo[*e*]isoindole (263)** and **(5a*S*,9a*S*,9b*R*)-2-(3,4-dimethoxyphenethyl)-6,6,9a-trimethyl-2,3,5,5a,6,7,8,9,9a,9b-decahydro-1*H*-benzo[*e*]isoindole (278)**

**278****263**

Using polygodial (0.1063 g, 0.4536 mmol), 3,4-dimethoxyphenethylamine (0.0925 mL, 0.5568 mmol, 1.22 eq.) and  $NaBH_3CN$  (0.1590 g, 2.530 mmol, 5.58 eq.). The crude mixture was purified by flash column chromatography using EtOAc/hexanes (50:50), and EtOAc as eluents to give **278** as a white amorphous solid (0.0903 g, 0.2354 mmol, 52% yield) and **263** as a clear oil (0.0231 g, 0.0605 mmol, 13% yield).

**278**

$^1H$  NMR  $\delta$  (600 MHz): 0.77 (s, 3 H), 0.86 (s, 3 H), 0.90 (s, 3 H), 1.11-1.24 (m, 2 H), 1.28 (dd,  $J = 11.8, 5.3$  Hz, 1 H), 1.38-1.45 (m, 2 H), 1.52-1.61 (m, 2 H), 1.83-1.91

(m, 1 H), 2.08–2.15 (m, 1 H), 2.22 (t,  $J = 9.1$  Hz, 1 H), 2.36–2.42 (m, 1 H), 2.55–2.63 (m, 1 H), 2.72–2.79 (m, 3 H), 2.83–2.89 (m, 2 H), 3.54 (d,  $J = 13.1$  Hz, 1 H), 3.84 (s, 3 H), 3.85 (s, 3 H), 5.42 (s, 1 H), 6.71–6.75 (m, 2 H), 6.76–6.79 (m, 1 H)

$^{13}\text{C}$  NMR  $\delta$  (150 MHz): 13.8, 18.8, 21.6, 24.2, 33.0, 33.3, 34.1, 35.2, 40.4, 42.6, 50.1, 54.3, 55.1, 55.9, 56.0, 58.2, 59.1, 111.3, 112.1, 115.9, 120.5, 133.2, 138.3, 147.4, 148.9

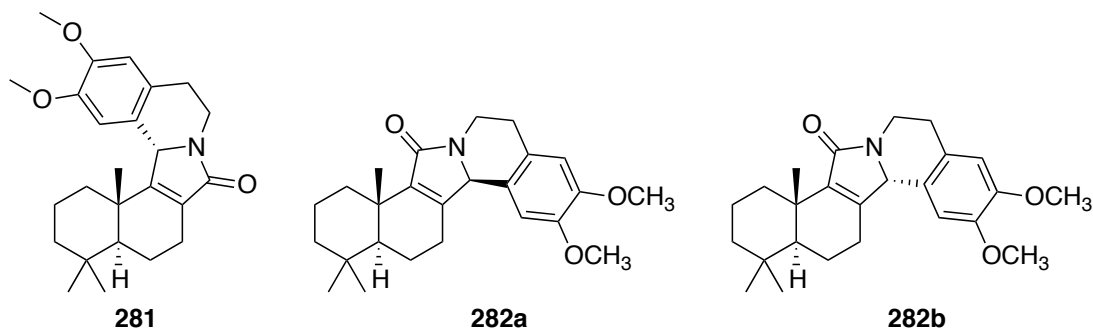
IR  $V_{\text{max}}$ : 2927, 2332, 2171, 1592, 1517, 1464, 1441, 1261, 1238, 1158, 1141, 1119, 1028

HRMS: For  $\text{C}_{25}\text{H}_{37}\text{NO}_2 + \text{H}$ , predicted 384.2897, found 384.2895

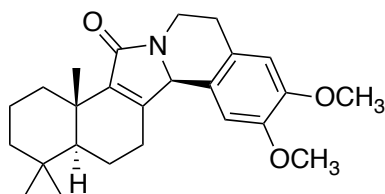
$[\alpha]_{\text{D}}^{20}$ : +18.22  $^{\circ}$  ( $c = 2.52$ )

### Synthesis of Crispin A Analogues

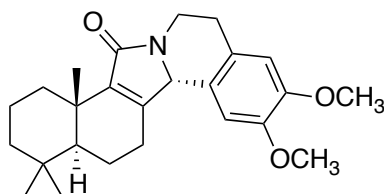
**(10a*S*,14a*S*,14c*S*)-2,3-Dimethoxy-11,11,14a-trimethyl-5,9,10,10a,11,12,13,14,14a,14c-decahydrobenzo[6,7]isoindolo[1,2-*a*]isoquinolin-8(6*H*)-one (281), (8b*S*,12a*S*,14b*R*)-2,3-dimethoxy-8b,12,12-trimethyl-5,8b,9,10,11,12,12a,13,14,14b-decahydrobenzo[4,5]isoindolo[1,2-*a*]isoquinolin-8(6*H*)-one (282a) and (8b*S*,12a*S*,14b*S*)-2,3-dimethoxy-8b,12,12-trimethyl-5,8b,9,10,11,12,12a,13,14,14b-decahydrobenzo[4,5]isoindolo[1,2-*a*]isoquinolin-8(6*H*)-one (282b)**



To a stirred solution of pyrrole **263** (0.2854 g, 0.7480 mmol) in CH<sub>2</sub>Cl<sub>2</sub> (15 mL) at 0 °C was added Dess–Martin periodinane (0.8267 g, 1.949 mmol, 2.60 eq.) in a single portion, and the reaction mixture stirred for 50 minutes, until TLC analysis indicated complete consumption of starting material. The reaction was quenched by addition of H<sub>2</sub>O (15 mL) and Na<sub>2</sub>S<sub>2</sub>O<sub>5</sub>. The aqueous and organic layers were separated, and the aqueous layer extracted with CH<sub>2</sub>Cl<sub>2</sub> (3 x 10 mL). The combined organic extracts were washed with saturated NaHCO<sub>3</sub> (2 x 15 mL), dried over MgSO<sub>4</sub>, and the solvent removed under reduced pressure. The crude residue was dissolved in dry CH<sub>2</sub>Cl<sub>2</sub> (10 mL), under N<sub>2</sub>, and stirred at 0 °C. BF<sub>3</sub>·OEt<sub>2</sub> (0.140 mL, 1.134 mmol, 1.52 eq.) was added *via* syringe, and the reaction stirred and allowed to warm slowly to room temperature for 1 h. The reaction was quenched with saturated NaHCO<sub>3</sub> (10 mL), the aqueous and organic layers separated, and the aqueous layer extracted with CH<sub>2</sub>Cl<sub>2</sub> (3 x 10 mL). The combined organic layers were dried over MgSO<sub>4</sub>, and the solvent removed under reduced pressure. The crude mixture was purified by flash column chromatography, using EtOAc/hexanes (50:50) and EtOAc/hexanes (70:30) as the eluent, to give **282a** and **282b** as a pale yellow oil (0.1852 g, 0.4682 mmol, 63 % yield; inseparable mixture of diastereomers) and compound **281** as a pale yellow oil (0.0666 g, 0.1683 mmol, 22% yield).

**282a**

<sup>1</sup>H NMR δ (600 MHz, acetone-*d*<sub>6</sub>):

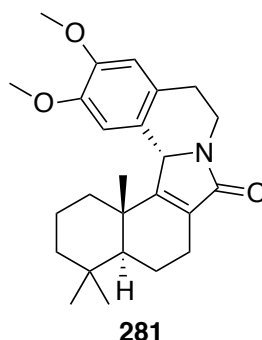
**282b**

0.87 (s, 1.8 H), 0.89 (s, 6 H), 0.94 (s, 1.8 H), 0.99–1.05 (m, 1 H), 1.06 (s, 1.8 H), 1.11–1.25 (m, 8 H), 1.39–1.51 (m, 4.3 H), 1.53–1.61 (m, 1 H), 1.63–1.73 (m, 1.6 H), 1.88–1.94 (m, 1.6 H), 2.50–2.67 (m, 4 H), 2.73–2.81 (m, 3 H), 2.89–2.95 (m, 0.6 H), 2.98 (ddd, *J* = 12.7, 12.0, 3.8 Hz, 1 H), 3.77 (s, 3 H), 3.78 (s, 1.8 H),



3.81 (s, 3 H), 3.83 (s, 1.8 H), 4.26–  
4.32 (m, 1.6 H), 4.99 (s, 1.6 H),  
6.750 (s, 1 H), 6.759 (s, 0.6 H), 6.92  
(s, 0.6 H), 6.94 (s, 1 H)

$^{13}\text{C}$  NMR  $\delta$  (150 MHz, acetone- $d_6$ ): 19.23, 19.27, 19.3, 19.5, 20.2, 20.5,  
21.7, 21.8, 26.3, 27.7, 30.0, 30.1,  
33.72, 33.74, 33.77, 35.6, 36.00,  
36.08, 36.6, 38.5, 38.9, 42.5, 42.7,  
52.8, 53.1, 56.0, 56.1, 56.33, 56.36,  
61.9, 62.0, 110.8, 111.62, 113.62,  
113.61, 126.0, 126.5, 127.4, 128.0,  
141.3, 141.5, 148.9, 149.0, 149.2,  
149.3, 153.0, 153.2, 171.2, 171.8



$^1\text{H}$  NMR  $\delta$  (600 MHz): 0.89 (s, 3 H), 0.93 (s, 3 H), 1.12 (dd,  $J$  = 12.2, 1.1  
Hz, 1 H), 1.16 (s, 3 H), 1.23–1.30 (m, 1 H), 1.42–  
1.52 (m, 2 H), 1.59 (td,  $J$  = 13.0, 3.4 Hz, 1 H),  
1.64–1.70 (m, 1 H), 1.79–1.88 (m, 2 H), 2.16–  
2.25 (m, 1 H), 2.36–2.45 (m, 2 H), 2.48–2.53 (m,  
1 H), 2.84–2.92 (m, 1 H), 2.95 (td,  $J$  = 12.1, 3.0  
Hz, 1 H), 3.84 (s, 3 H), 3.87 (s, 3 H), 4.42 (ddd,  $J$   
= 12.6, 5.0, 1.8 Hz, 1 H), 5.28 (s, 1 H), 6.60 (s, 1  
H), 7.15 (s, 1 H)

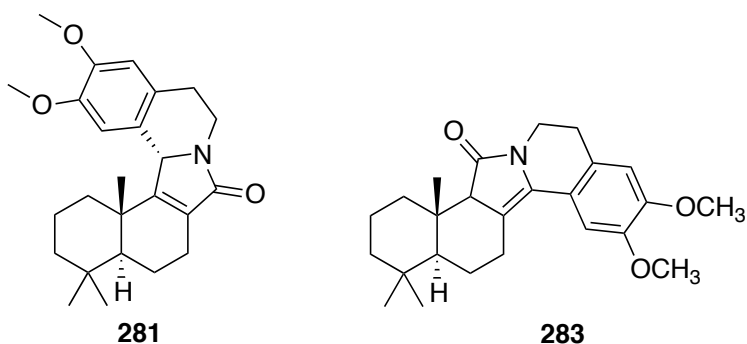
$^{13}\text{C}$  NMR  $\delta$  (150 MHz): 17.8, 18.9, 20.1, 21.8, 22.7, 30.6, 33.6, 33.7,  
37.7, 39.0, 39.1, 41.7, 54.3, 55.9, 56.2, 61.8,  
112.3, 112.7, 126.0, 128.8, 132.0, 146.8, 147.8,  
163.2, 172.8

IR  $V_{\max}$ : 2932, 1682 (C=O), 1516, 1464, 1283, 1271, 1224

HRMS: For  $C_{25}H_{33}NO_3$ , predicted 395.24604, found 395.24552.  $m/z$  (EI+): 395 ( $M^+$ , 30), 393 (40), 378 (95), 308 (10), 257 (100), 164 (80), 149 (10), 118 (60)

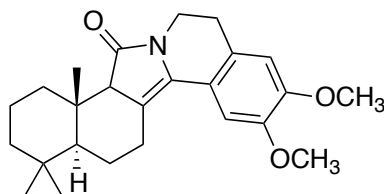
$[\alpha]_D^{20}$   $-55.38^\circ$  ( $c = 0.910$ )

**(10a*S*,14a*S*,14c*S*)-2,3-Dimethoxy-11,11,14a-trimethyl-5,9,10,10a,11,12,13,14,14a,14c-decahydrobenzo[6,7]isoindolo[1,2-*a*]isoquinolin-8(6*H*)-one (281) and (8b*S*,12a*S*)-2,3-dimethoxy-8b,12,12-trimethyl-5,8a,8b,9,10,11,12,12a,13,14-decahydrobenzo[4,5]isoindolo[1,2-*a*]isoquinolin-8(6*H*)-one (283)**



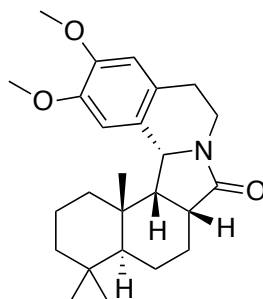
To a stirred solution of pyrrole **263** (0.0400 g, 0.1040 mmol) in  $CH_2Cl_2$  (5 mL) at  $0^\circ C$  was added Dess–Martin periodinane (0.1110 g, 0.2617 mmol, 2.51 eq.) in a single portion, and the reaction mixture stirred for 1 hour, until TLC analysis indicated complete consumption of starting material. The reaction was quenched by addition of  $H_2O$  (5 mL) and  $Na_2S_2O_5$ . The aqueous and organic layers were separated, and the aqueous layer extracted with  $CH_2Cl_2$  (3 x 5 mL). The combined organic extracts were washed with saturated  $NaHCO_3$  (2 x 5 mL), dried over  $MgSO_4$ , and the solvent removed under reduced pressure. The crude residue was dissolved in dry  $CH_2Cl_2$  (5 mL), under  $N_2$ , and stirred at  $0^\circ C$ . TMSOTf (0.030 mL, 0.165 mmol, 1.58 eq.) was added *via* syringe, and the reaction allowed to warm to room temperature and stirred for 18 h. The reaction was quenched with saturated  $NaHCO_3$  (5 mL), the aqueous and organic layers separated, and the aqueous layer extracted with  $CH_2Cl_2$  (3 x 5 mL). The combined organic layers were dried

over  $\text{MgSO}_4$ , and the solvent removed under reduced pressure. The crude mixture was purified by flash column chromatography, using EtOAc/hexanes (70:30) as the eluent, to give **281** as a pale yellow oil (0.0060 g, 0.015 mmol, 15% yield) and **283** as a pale yellow oil (0.0200 g, 0.051 mmol, 49 % yield).

**283**

$^1\text{H}$ NMR $\delta$ (600 MHz):	0.80 (s, 3 H), 0.82 (s, 3 H), 0.93 (s, 3 H), 1.19 (dd, $J = 12.5, 2.3$ Hz, 1 H), 1.28 (dd, $J = 12.6, 5.0$ Hz, 1 H), 1.31–1.41 (m, 2 H), 1.42–1.47 (m, 1 H), 1.48–1.53 (m, 2 H), 1.75–1.80 (m, 1 H), 2.31–2.38 (m, 1 H), 2.53–2.58 (m, 1 H), 2.64 (ad, $J = 0.5$ Hz, 1 H), 2.77–2.82 (m, 2 H), 3.12–3.17 (m, 1 H), 3.17–3.23 (m, 1 H), 3.895 (s, 3 H), 3.898 (s, 3 H), 4.02 (dt, $J = 12.4, 4.4$ Hz, 1 H), 6.72 (s, 1 H), 7.10 (s, 1 H)
$^{13}\text{C}$ NMR $\delta$ (150 MHz):	14.4, 18.6, 21.9, 22.9, 25.8, 29.9, 33.6, 33.9, 37.1, 39.2, 40.2, 42.3, 53.4, 56.1, 56.2, 62.1, 109.6, 111.5, 113.5, 120.8, 128.5, 129.1, 147.9, 148.7, 175.6
IR $V_{\text{max}}$ :	2945, 1687 (C=O), 1511, 1464, 1390, 1367, 1285, 1269, 1243, 1224, 1211, 1169, 1116
HRMS:	For $\text{C}_{25}\text{H}_{33}\text{NO}_3$ , predicted 395.24604, found 395.24519. $m/z$ (EI+): 395 ( $\text{M}^+$ , 25), 380 (10), 308 (10), 258 (50), 207 (95), 178 (40), 164 (100), 150 (50), 135 (40), 121 (25), 95 (15)
$[\alpha]_{\text{D}}^{20}$	+21.54 $^\circ$ (c = 0.13)

**(8a*R*,10a*S*,14a*S*,14b*R*,14c*R*)-2,3-Dimethoxy-11,11,14a-trimethyl-5,8a,9,10,10a,11,12,13,14,14a,14b,14c-dodecahydrobenzo[6,7]isoindolo[1,2-*a*]isoquinolin-8(6*H*)-one (284)**



**284**

A mixture of **281** (0.0378 g, 0.0956 mmol) and Pd/C (~0.1 g of a 10% w/w mixture) in a solution of 95/5 EtOH/AcOH (15.75 mL), was reacted under H<sub>2</sub> in a Parr shaker hydrogenator (35 psi) for 2 h. The reaction mixture was then filtered on celite, and the solvent removed under reduced pressure. The crude material was purified by flash column chromatography using EtOAc as eluent, to give the product **284** as a pale yellow oil (0.0054 g, 0.014 mmol, 14% yield)

<sup>1</sup>H NMR δ (600 MHz): 0.90 (s, 3 H), 0.92 (s, 3 H) 1.08–1.14 (m, 1 H), 1.14–1.19 (m, 1 H), 1.23–1.33 (m, 1 H), 1.27 (s, 3 H), 1.36–1.51 (m, 4 H), 1.55–1.70 (m, 3 H), 2.30–2.36 (m, 1 H), 2.41 (t, *J* = 8.2 Hz, 1 H), 2.68–2.74 (m, 1 H), 2.83–2.88 (m, 1 H), 2.90–2.98 (m, 1 H), 3.19 (td, *J* = 11.9, 5.0 Hz, 1 H), 3.53–3.59 (m, 1 H), 3.87 (s, 3 H), 3.88 (s, 3 H), 4.54 (d, *J* = 8.0 Hz, 1 H), 6.75 (s, 1 H), 6.92 (s, 1 H)

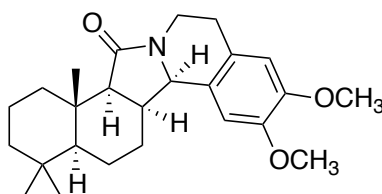
<sup>13</sup>C NMR δ (150 MHz): 18.7, 19.9, 22.2, 24.0, 28.4, 29.7, 33.51, 33.53, 35.9, 39.5, 40.5, 41.4, 41.6, 47.8, 50.5, 56.0, 56.2, 56.5, 109.9, 111.1, 130.4, 131.7, 147.1, 148.2, 176.8

IR V<sub>max</sub>: 2935, 1678 (C=O), 1513, 1463, 1453, 1438, 1329, 1286, 1246, 1212, 1102

HRMS: For  $C_{25}H_{35}NO_3$ , predicted 397.26169, found 397.26191.  $m/z$  (EI+): 397 ( $M^+$ , 70), 382 (20), 258 (20), 191 (100), 176 (20), 123 (10), 81 (10)

$[\alpha]_D^{20}$  +17.04 ° ( $c = 0.270$ )

**(8a*S*,8b*S*,12a*S*,14a*S*,14b*R*)-2,3-Dimethoxy-8b,12,12-trimethyl-5,8a,8b,9,10,11,12,12a,13,14,14a,14b-dodecahydrobenzo[4,5]isoindolo[1,2-*a*]isoquinolin-8(6*H*)-one (285)**



**285**

A mixture of **282a** and **282b** (0.1768 g, 0.4469 mmol) and Pd/C (~0.1 g of a 10% w/w mixture) in EtOH (15 mL), was reacted under  $H_2$  on a Parr shaker hydrogenator (35 psi) for 12 h. The reaction mixture was then filtered on celite, and the solvent removed under reduced pressure. The crude material was purified by flash column chromatography using EtOAc/hexanes (70:30) as eluent, to give the product **285** as a pale yellow oil (0.0734 g, 0.1846 mmol, 41% yield)

$^1H$  NMR  $\delta$  (600 MHz): 0.85 (s, 3 H), 0.89 (s, 3 H), 0.89 (s, 3 H), 0.89–0.95 (m, 1 H), 1.02 (s, 3 H), 1.14–1.21 (m, 3 H), 1.31 (ddd,  $J = 13.7, 9.3, 4.4$  Hz, 1 H), 1.35–1.46 (m, 3 H), 1.50–1.64 (2 H), 2.38–2.44 (m, 1 H), 2.54 (d,  $J = 8.5$  Hz, 1 H), 2.60–2.64 (m, 1 H), 2.73–2.87 (m, 3 H), 3.85 (s, 3 H), 3.86 (s, 3 H), 4.33–4.38 (m, 1 H), 4.68 (d,  $J = 7.0$  Hz, 1 H), 6.48 (s, 1 H), 6.59 (s, 1 H)

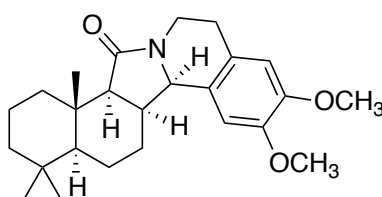
$^{13}C$  NMR  $\delta$  (150 MHz): 17.8, 18.8, 18.9, 19.1, 22.0, 29.1, 33.2, 33.6, 35.3, 35.8, 37.0, 42.6, 44.8, 47.1, 55.9, 56.3, 57.98, 57.99, 109.4, 111.9, 125.9, 127.3, 147.8, 147.9, 173.3

IR  $V_{\max}$ : 2926, 1680, 1518, 1464, 1430, 1358, 1316, 1255, 1231, 1121

HRMS: For  $C_{25}H_{35}NO_3+Na$ , predicted 420.2509, found 420.2511

$[\alpha]_D^{20}$  +62.42 ° ( $c = 0.165$ )

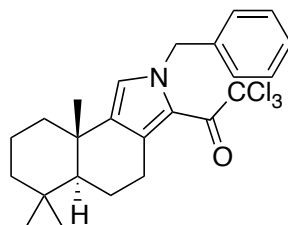
**(8a*S*,8b*S*,12a*S*,14a*S*,14b*R*)-2,3-Dimethoxy-8b,12,12-trimethyl-5,8a,8b,9,10,11,12,12a,13,14,14a,14b-dodecahydrobenzo[4,5]isoindolo[1,2-*a*]isoquinolin-8(6*H*)-one (285)**



**285**

A mixture of **283** (0.1768 g, 0.4469 mmol) and Pd/C (~0.1 g of a 10% w/w mixture) in EtOH (15 mL), with a spatula full of 10% Pd/C was reacted under  $H_2$  on a Parr shaker hydrogenator (35 psi) for 2 h. The reaction mixture was then filtered on celite, and the solvent removed under reduced pressure. The crude material was purified by flash column chromatography using EtOAc/hexanes (70:30) as eluent, to give the product **285** as a pale yellow oil (0.040 g, 0.1006 mmol, 21% yield)

**1-((5a*S*,9a*S*)-2-Benzyl-6,6,9a-trimethyl-4,5,5a,6,7,8,9,9a-octahydro-2*H*-benzo[*e*]isoindol-3-yl)-2,2,2-trichloroethan-1-one (288)**



**288**

To a stirred solution of benzylpyrrole **270** (0.1460 g, 0.4748 mmol) in  $Et_2O$  (8 mL) was added trichloroacetyl chloride (0.320 mL, 2.867 mmol, 6 eq.), and the mixture stirred for 24 h. At this time a further 0.320 mL of trichloroacetyl chloride was added and the reaction stirred for a further 24 h.  $H_2O$  (8 mL)

was added, and solid  $K_2CO_3$  until the solution was alkaline. The aqueous and organic layers were separated, and the aqueous layer extracted with dichloromethane (3 x 8 mL). The combined organic extracts were dried over  $MgSO_4$ , filtered, and the solvent removed under reduced pressure. The crude material was purified by elution through a plug of silica with EtOAc/hexanes (10:90) as eluent, to give the title compound as a yellow oil (0.1435 g, 0.3169 mmol, 67% yield).

$^1H$  NMR  $\delta$  (400 MHz): 0.91 (s, 3 H), 0.95 (s, 3 H), 1.20 (s, 3 H), 1.23–1.33 (m, 2 H), 1.37–1.59 (m, 3 H), 1.59–1.79 (m, 2 H), 1.85–1.93 (m, 1 H), 1.93–2.00 (m, 1 H), 2.84 (ddd,  $J$  = 17.6, 11.3, 7.0 Hz, 1 H), 3.29 (ddd,  $J$  = 17.6, 5.9, 1.1 Hz, 1 H), 6.85 (s, 1 H), 7.01 (d,  $J$  = 6.9 Hz, 2 H), 7.20–7.31 (m, 3 H)

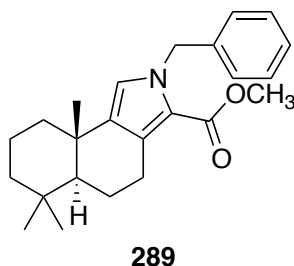
$^{13}C$  NMR  $\delta$  (100 MHz): 19.2, 19.6, 21.5, 27.6, 33.0, 33.4, 34.6, 39.6, 41.9, 51.0, 53.8, 96.5, 121.3, 126.8, 127.5, 128.3, 128.6, 129.6, 136.8, 138.1, 175.4

IR  $V_{max}$ : 2926, 1654, 1651, 1456, 1383, 1330, 1209, 1157

HRMS: For  $C_{24}H_{28}Cl_3NO$ , predicted 451.12365, found 451.12305.  $m/z$  (EI+): 451 ( $M^+$ , 20), 438 (40), 403 (65), 388 (70), 366 (60), 334 (100), 298 (50), 228 (70), 172 (50), 131 (60), 91 (85), 69 (85), 55 (60)

$[\alpha]_D^{20}$  -0.116  $^\circ$  ( $c$  = 1.17)

**Methyl (5a*S*,9a*S*)-2-benzyl-6,6,9a-trimethyl-4,5,5a,6,7,8,9,9a-octahydro-2*H*-benzo[*e*]isoindole-3-carboxylate (289)**



To a stirred solution of chloromethylketone **288** (0.0407 g, 0.0899 mmol) in MeOH (5 mL), was added solid K<sub>2</sub>CO<sub>3</sub> (0.0361 g, 0.2612 mmol, 2.9 eq.), and stirred for 30 minutes, until TLC analysis indicated consumption of the starting material. The solvent was removed under reduced pressure, and the crude residue purified by elution through a plug of silica with EtOAc/hexanes (10:90) as eluent to give the title compound as an orange oil (0.0268 g, 0.0733 mmol, 82% yield)

<sup>1</sup>H NMR δ (400 MHz): 0.91 (s, 3 H), 0.95 (s, 3 H), 1.19 (s, 3 H), 1.21–1.33 (m, 2 H), 1.34–1.44 (m, 1 H), 1.45–1.56 (m, 2 H), 1.59–1.77 (m, 2 H), 1.83–1.91 (m, 1 H), 1.92–1.99 (m, 1 H), 2.70 (ddd, *J* = 18.0, 11.8, 7.4 Hz, 1 H), 3.06 (dd, *J* = 18.0, 5.8 Hz, 1 H), 3.73 (s, 3 H), 5.48 (s, 2 H), 6.59 (s, 1 H), 7.05–7.10 (m, 2 H), 7.20–7.32 (m, 3 H)

<sup>13</sup>C NMR δ (100 MHz): 19.2, 19.4, 21.5, 25.3, 25.6, 33.1, 33.5, 34.3, 39.7, 42.2, 50.6, 51.5, 52.4, 116.9, 122.7, 126.8, 127.2, 128.6, 129.0, 136.1, 139.1, 162.3

IR V<sub>max</sub>: 2943, 1693, 1456, 1438, 1396, 1388, 1282, 1205, 1163, 1120, 1095, 1072

HRMS: For C<sub>24</sub>H<sub>31</sub>NO<sub>2</sub>, predicted 365.23548, found 365.23580. *m/z* (EI<sup>+</sup>): 365 (M<sup>+</sup>, 60), 350 (100), 322 (10), 292 (30), 228 (10), 118 (40), 87 (100), 69 (15)

[α]<sub>D</sub><sup>20</sup> +16.39 ° (c=0.80)



## Chapter 6: References

- (1) Matkhalikova, S. F.; Malikov, V. M.; Yunusov, S. Y. *Chem. Nat. Comp.* **1969**, 5, 24–25.
- (2) Matkhalikova, S. F.; Malikov, V. M.; Yunusov, S. Y. *Chem. Nat. Comp.* **1969**, 5, 530.
- (3) Ishida, S.; Okasaka, M.; Ramos, F.; Kashiwada, Y.; Takaishi, Y.; Kodzhimatov, O. K.; Ashurmetov, O. *J. Nat. Med.* **2008**, 62 (2), 236–238.
- (4) Matkhalikova, S. F.; Malikov, V. M.; Yunusov, S. Y. *Chem. Nat. Comp.* **1969**, 5, 528–529.
- (5) Matkhalikova, S. F.; Malikov, V. M.; Yugudaev, M. R. *Chem. Nat. Comp.* **1971**, 7, 207–208.
- (6) Matkhalikova, S. F.; Malikov, V. M.; Yugudaev, M. R. *Chem. Nat. Comp.* **1974**, 8, 488–490.
- (7) Iida, H.; Yamazaki, N.; Kibayashi, C. *Tetrahedron Lett.* **1985**.
- (8) Iida, H.; Yamazaki, N.; Kibayashi, C.; Nagase, H. *Tetrahedron Lett.* **1986**.
- (9) Kibayashi, C.; Yamazaki, N.; Iida, H. *J. Org. Chem.* **1987**, 52 (10), 1956–1962.
- (10) Tashkhodzhaev, B.; Aripova, S. F.; Turgunov, K. K.; Abdilalimov, O. *Chem. Nat. Comp.* **2004**, 40 (6), 618–619.
- (11) Matkhalikova, S. F.; Malikov, V. M.; Yugudaev, M. R.; Yunusov, S. Y. *Farmakol. Alkaloidov. Serdech. Glikoyidov* **1971**, 210.
- (12) Padró, M.; Castillo, J. A.; Gómez, L.; Joglar, J.; Clapés, P.; de Bolós, C. *Glycoconj. J.* **2010**, 27, 277–285.
- (13) Kotland, A.; Accadbled, F.; Robeyns, K.; Behr, J.-B. *J. Org. Chem.* **2011**, 76 (10), 4094–4098.
- (14) Toyau, A.; Tamura, O.; Takagi, H. *Synlett* **2002**, No. 1, 35–38.
- (15) Dharuman, S.; Palanivel, A. K.; Vankar, Y. D. *Org. Biomol. Chem.* **2014**, 12 (27), 4983.
- (16) Chandrasekhar, S.; Saritha, B.; Jagadeshwar, V.; Prakash, S. J. *Tetrahedron: Asymmetry* **2006**, 17, 1380–1386.
- (17) Reddy, J. S.; Rao, B. V. *J. Org. Chem.* **2007**, 72 (6), 2224–2227.
- (18) Davies, S. G.; Lee, J. A.; Roberts, P. M.; Thomson, J. E.; West, C. J. *Tetrahedron* **2012**, 68 (22), 4302–4319.
- (19) Severino, E. A.; Correia, C. R. D. *Org. Lett.* **2000**, 2 (20), 3039–3042.
- (20) Goti, A.; Cicchi, S.; Mannucci, V.; Cardona, F.; Guarna, F.; Merino, P.; Tejero, T. *Org. Lett.* **2003**, 5 (22), 4235–4238.
- (21) Uraguchi, D.; Nakamura, S.; Ooi, T. *Angew. Chem. Int. Ed.* **2010**, 49 (41), 7562–7565.
- (22) Donohoe, T. J.; Pullin, R. D. C. *Chem. Commun.* **2012**, 48 (98), 11924.
- (23) Ding, Q.; Zhou, X.; Fan, R. *Org. Biomol. Chem.* **2014**, 12 (27), 4807.
- (24) Zhuo, C.-X.; Zheng, C.; You, S.-L. *Acc. Chem. Res.* **2014**, 47 (8), 2558–2573.
- (25) Donohoe, T. J.; Thomas, R. E. *Chem. Record.* **2007**, 7 (3), 180–190.
- (26) Wang, D.-S.; Chen, Q.-A.; Lu, S.-M.; Zhou, Y.-G. *Chem. Rev.* **2012**,

- 112 (4), 2557–2590.
- (27) Donohoe, T. J.; Sintim, H. O.; Hollinshead, J. *J. Org. Chem.* **2005**, *70* (18), 7297–7304.
- (28) Donohoe, T. J.; Sintim, H. O. *Org. Lett.* **2004**, *6* (12), 2003–2006.
- (29) You, H. T.; Grosse, A. C.; Howard, J. K.; Hyland, C. J. T.; Just, J.; Molesworth, P. P.; Smith, J. A. *Org. Biomol. Chem.* **2011**, *9* (10), 3948.
- (30) MacDiarmid, A. G. *Synth. Met.* **1997**, *84*, 27–34.
- (31) Howard, J. K.; Rihak, K. J.; Bissember, A. C.; Smith, J. A. *Chem. Asian J.* **2015**, *11* (2), 155–167.
- (32) Angeli, A.; Lutri, C. *Gazz. Chim. Ital.* **1920**, *50*, 128–139.
- (33) Pieroni, A.; Moggi, A. *Gazz. Chim. Ital.* **1923**, *53*, 120–135.
- (34) Bocchi, V.; Chierici, L.; Gardini, G. P. *Tetrahedron* **1970**, *26*, 4073–4082.
- (35) Gardini, G. P.; Bocchi, V. *Gazz. Chim. Ital.* **1972**, *102*, 91–101.
- (36) Pichon-Santander, C.; Scott, I. A. *Tetrahedron Lett.* **2000**, *41*, 2825–2829.
- (37) Coffin, A. R.; Roussel, M. A.; Tserlin, E.; Pelkey, E. T. *J. Org. Chem.* **2006**, *71* (17), 6678–6681.
- (38) Greger, J. G.; Yoon-Miller, S. J. P.; Bechtold, N. R.; Flewelling, S. A.; MacDonald, J. P.; Downey, C. R.; Cohen, E. A.; Pelkey, E. T. *J. Org. Chem.* **2011**, *76* (20), 8203–8214.
- (39) Aiura, M.; Kanaoka, Y. *Chem. Pharm. Bull.* **1975**, *23* (11), 2835–2841.
- (40) Bonnett, R.; Cornell, P.; McDonagh, A. F. *J. Chem. Soc., Perkin Trans. 1* **1976**, No. 7, 794.
- (41) Inomata, K.; Sakata, R.; Iwamoto, R.; Fujinami, S.; Ukaji, Y. *Heterocycles* **2010**, *82* (2), 1157–1162.
- (42) Iwamoto, R.; Ukaji, Y.; Inomata, K. *Chem. Lett.* **2010**, *39* (3), 176–177.
- (43) Takahashi, K.; Iwamoto, R.; Sakata, R.; Soeta, T.; Inomata, K. *Heterocycles* **2012**, *86* (2), 1031–1038.
- (44) Awruch, J.; Frydman, B. *Tetrahedron Lett.* **1973**, *14* (28), 2611–2614.
- (45) Battersby, A. R.; Dutton, C. J.; Fookes, C. J. R. *J. Chem. Soc., Perkin Trans. 1* **1988**, No. 6, 1569–1576.
- (46) Diaz, A. F.; Martinez, A.; Kanazawa, K. K.; Salmón, M. J. *Electroanal. Chem.* **1981**, *130*, 181–187.
- (47) Tabba, H. D.; Smith, K. M. *J. Org. Chem.* **1984**, *49*, 1870–1875.
- (48) Tedjar, F.; Ymmel, S.; Janda, M.; Duchek, P.; Holý, P.; Stibor, I. *Collect. Czech. Chem. Commun.* **1989**, *54*, 1299–1305.
- (49) Tajima, T.; Nakajima, A.; Fuchigami, T. *J. Org. Chem.* **2006**, *71* (4), 1436–1441.
- (50) Bonnett, R.; Dimsdale, M. J.; Stephenson, G. F. *J. Chem. Soc., Perkin Trans. 1* **1987**, 439.
- (51) Yamamoto, M.; Izukawa, H.; Saiki, M.; Yamada, K. *J. Chem. Soc., Chem. Commun.* **1988**, No. 8, 560.
- (52) Inomata, K.; Jayasundera, K. P.; Kinoshita, H. *Bull. Chem. Soc. Jpn.* **2000**, *73*, 497–505.
- (53) Inomata, K.; Kinoshita, H.; Hammam, M. A. S. *Chem. Lett.* **2005**, 34

- (6), 800–801.
- (54) Nishiyama, K.; Kamiya, A.; Hammam, M. A. S.; Kinoshita, H.; Fujinami, S.; Ukaji, Y.; Inomata, K. *Bull. Chem. Soc. Jpn.* **2010**, *83* (11), 1309–1322.
- (55) Liermann, J. C.; Opatz, T. *J. Org. Chem.* **2008**, *73* (12), 4526–4531.
- (56) Riplinger, C.; Kao, J. P. Y.; Rosen, G. M.; Kathirvelu, V.; Eaton, G. R.; Eaton, S. S.; Kutateladze, A.; Neese, F. *J. Am. Chem. Soc.* **2009**, *131* (29), 10092–10106.
- (57) Kao, J. P. Y.; Muralidharan, S.; Zavalij, P. Y.; Fletcher, S.; Xue, F.; Rosen, G. M. *Tetrahedron Lett.* **2014**, *55*, 3111–3113.
- (58) Kancharla, P.; Lu, W.; Salem, S. M.; Kelly, J. X.; Reynolds, K. A. *J. Org. Chem.* **2014**, *79* (23), 11674–11689.
- (59) Wang, X.; Gallardo-Donaire, J.; Martin, R. *Angew. Chem. Int. Ed.* **2014**, *53* (41), 11084–11087.
- (60) Alp, C.; Ekin, D.; Gültekin, M. S.; Sentürk, M.; Sahin, E.; Küfrevioğlu, O. I. *Bioorganic Med. Chem.* **2010**, *18*, 4468–4474.
- (61) Lubriks, D.; Sokolovs, I.; Suna, E. *Org. Lett.* **2011**, *13* (16), 4324–4327.
- (62) Howard, J. K.; Hyland, C. J. T.; Just, J.; Smith, J. A. *Org. Lett.* **2013**, *15* (7), 1714–1717.
- (63) Schreiber, S. L.; Meyer, S. D. *J. Org. Chem.* **1994**, *59*, 7549–7552.
- (64) Zhdankin, V. V. *J. Org. Chem.* **2011**, *76* (5), 1185–1197.
- (65) Frigerio, M.; Santagostino, M.; Sputore, S. *J. Org. Chem.* **1999**, *64* (12), 4537–4538.
- (66) Howard, J. K. New Methods for the Synthesis of Nitrogen Containing, Biologically Relevant Small Molecules, PhD Thesis, University of Tasmania: Hobart, 2015, pp 1–219.
- (67) Lightner, D. A. *Photochem. Photobiol.* **1974**, *19*, 457–459.
- (68) Frimer, A. A. *Chem. Rev.* **1979**, *79* (5), 359–387.
- (69) Ogilby, P. R. *Chem. Soc. Rev.* **2010**, *39* (8), 3181.
- (70) George, M. V.; Bhat, V. *Chem. Rev.* **1979**, *79* (5), 447–478.
- (71) Lightner, D. A.; Bisacchi, G. S.; Norris, R. D. *J. Am. Chem. Soc.* **1976**, *98*, 802–807.
- (72) Alberti, M. N.; Vougioukalakis, G. C.; Orfanopoulos, M. *J. Org. Chem.* **2009**, *74* (19), 7274–7282.
- (73) Boger, D. L.; Baldino, C. M. *J. Org. Chem.* **1991**, *56*, 6942–6944.
- (74) Boger, D. L.; Baldino, C. M. *J. Am. Chem. Soc.* **1993**, *115*, 11418–11425.
- (75) Demir, A. S.; Aydogan, F.; Akhmedov, I. M. *Tetrahedron: Asymmetry* **2002**, *13*, 601–605.
- (76) Kijewska, K.; Blanchard, G. J.; Szlachetko, J.; Stolarski, J.; Kisiel, A.; Michalska, A.; Maksymiuk, K.; Pisarek, M.; Majewski, P.; Krysiński, P.; Mazur, M. *Chem. Eur. J.* **2011**, *18* (1), 310–320.
- (77) Rodríguez, I.; González-Velasco, J. *J. Chem. Soc., Chem. Commun.* **1990**, *32* (5), 387–388.
- (78) Lightner, D. A.; Pak, C.-S. *J. Org. Chem.* **1975**, *40*, 2724–2728.
- (79) Chang, C.-C.; Yang, Y.-T.; Yang, J.-C.; Wu, H.-D.; Tsai, T. *Dyes Pigm.* **2008**, *79* (2), 170–175.
- (80) Howard, J. K.; Rihak, K. J.; Hyland, C. J. T.; Bissember, A. C.; Smith, J. A. *Org. Biomol. Chem.* **2016**, *14* (37), 8873–8880.

- (81) Carney, J.; Hammer, R.; Hulce, M.; Lomas, C.; Miyashiro, D. *Synthesis* **2012**, 44 (16), 2560–2566.
- (82) Rihak, K. J. Pyrrole as a Molecular Template, University of Tasmania, 2013.
- (83) Van Rheen, V.; Kelly, R. C.; Cha, D. Y. *Tetrahedron Lett.* **1976**, 23, 1973–1976.
- (84) Schröder, M. *Chem. Rev.* **1980**, 80, 187–213.
- (85) D'Oca, M. G. M.; Moraes, L. A. B.; Pilli, R. A.; Eberlin, M. N. *J. Org. Chem.* **2001**, 66 (11), 3854–3864.
- (86) Karplus, M. *J. Am. Chem. Soc.* **1963**, 85 (18), 2870–2871.
- (87) Martínez-Montero, S.; Fernández, S.; Sanghvi, Y. S.; Theodorakis, E. A.; Detorio, M. A.; Mcbrayer, T. R.; Whitaker, T.; Schinazi, R. F.; Gotor, V.; Ferrero, M. *Bioorganic Med. Chem.* **2012**, 20 (23), 6885–6893.
- (88) Reist, E. J.; Fisher, L. V.; Goodman, L. *J. Org. Chem.* **1967**, 32, 2541–2514.
- (89) Flores, R.; Alibés, R.; Figueredo, M.; Font, J. *Tetrahedron* **2009**, 65 (34), 6912–6917.
- (90) Hwang, Y. C.; Chu, M.; Fowler, F. W. *J. Org. Chem.* **1985**, 50, 3885–3890.
- (91) Amat, M.; Llor, N. R.; Hidalgo, J.; Escolano, C.; Bosch, J. *J. Org. Chem.* **2003**, 68 (5), 1919–1928.
- (92) Xiao, K.-J.; Luo, J.-M.; Ye, K.-Y.; Wang, Y.; Huang, P.-Q. *Angew. Chem. Int. Ed.* **2010**, 49 (17), 3037–3040.
- (93) Xiao, K.-J.; Wang, Y.; Ye, K.-Y.; Huang, P.-Q. *Chem. Eur. J.* **2010**, 16 (43), 12792–12796.
- (94) Gourlay, B. S. New synthetic approaches to indolizidine and pyrrolidine alkaloids, PhD Thesis, University of Tasmania, 2016, pp 1–232.
- (95) Pin, F.; Comesse, S.; Garrigues, B.; Marchalín, Š.; Daich, A. *J. Org. Chem.* **2007**, 72 (4), 1181–1191.
- (96) Du-a-man, S.; Soorukram, D.; Kuhakarn, C.; Tuchinda, P.; Reutrakul, V.; Pohmakotr, M. *Eur. J. Org. Chem.* **2014**, 2014 (8), 1708–1715.
- (97) de Vries, E. F. J.; Brussee, J.; van der Gen, A. *J. Org. Chem.* **1994**, 59 (23), 7133–7137.
- (98) Corey, E. J.; Venkateswarlu, A. *J. Am. Chem. Soc.* **1972**, 94 (17), 6190–6191.
- (99) Dias, L. C.; Polo, E. C. *J. Org. Chem.* **2017**, 82 (8), 4072–4112.
- (100) Blake, K. W.; Gillies, I.; Denney, R. C. *J. Chem. Soc., Perkin Trans. 1* **1981**, 700–702.
- (101) Murphy, P. J.; Lee, S. E. *J. Chem. Soc., Perkin Trans. 1* **1999**, No. 21, 3049–3066.
- (102) Meyers, A. I.; Lefker, B. A.; Sowin, T. J.; Westrum, L. J. *J. Org. Chem.* **1989**, 54, 4243–4246.
- (103) Meyers, A. I.; Snyder, L. *J. Org. Chem.* **1993**, 58, 36–42.
- (104) Degnan, A. P.; Meyers, A. I. *J. Am. Chem. Soc.* **1999**, 121 (12), 2762–2769.
- (105) Waterson, A. G.; Meyers, A. I. *J. Org. Chem.* **2000**, 65 (21), 7240–7243.

- (106) Hughes, R. C.; Dvorak, C. A.; Meyers, A. I. *J. Org. Chem.* **2001**, *66* (16), 5545–5551.
- (107) Meyers, A. I.; Andres, C. J.; Resek, J. E.; McLaughlin, M. A.; Woodall, C. C.; Lee, P. H. *J. Org. Chem.* **1996**, *61*, 2586–2587.
- (108) Aydogan, F.; Demir, A. S. *Tetrahedron: Asymmetry* **2004**, *15* (2), 259–265.
- (109) Catak, S.; Celik, H.; Demir, A. S.; Aviyente, V. *J. Phys. Chem. A* **2007**, *111* (26), 5855–5863.
- (110) Maki, Y.; Sako, M.; Kurahashi, N.; Hirota, K. *J. Chem. Soc., Chem. Commun.* **1988**, No. 2, 110–111.
- (111) Anaya, J.; Fernández-Mateos, A.; Grande, M.; Martiáñez, J.; Ruano, G.; Rubio-González, M. R. *Tetrahedron* **2003**, *59*, 241–248.
- (112) Dekeukeleire, S.; D’hooghe, M.; De Kimpe, N. *J. Org. Chem.* **2009**, *74* (4), 1644–1649.
- (113) Tähtinen, P.; Sillanpää, R.; Stájer, G.; Szabó, A. E.; Pihlaja, K. *J. Chem. Soc., Perkin Trans. 2* **1999**, No. 10, 2011–2021.
- (114) Desai, R. C. *J. Org. Chem.* **2001**, *66* (14), 4939–4940.
- (115) Amat, M.; Ponzo, V.; Llor, N.; Bassas, O.; Escolanao, C.; Bosch, J. *ARKIVOC* **2003**, 69–81.
- (116) Allin, S. M.; Thomas, C. I.; Allard, J. E.; Duncton, M.; Elsegood, M. R. J.; Edgar, M. *Tetrahedron Lett.* **2003**, *44* (11), 2335–2337.
- (117) Clive, D. L. J.; Wang, J. *Tetrahedron Lett.* **2003**, *44* (42), 7731–7733.
- (118) Ndungu, J. M.; Gu, X.; Gross, D. E.; Cain, J. P.; Carducci, M. D.; Hruby, V. J. *Tetrahedron Lett.* **2004**, *45* (21), 4139–4142.
- (119) Malaquin, S.; Jida, M.; Courtin, J.; Laconde, G.; Willand, N.; Deprez, B.; Deprez-Poulain, R. *Tetrahedron Lett.* **2013**, *54* (6), 562–567.
- (120) Pereira, N. A. L.; Monteiro, Â.; Machado, M.; Gut, J.; Molins, E.; Perry, M. J.; Dourado, J.; Moreira, R.; Rosenthal, P. J.; Prudêncio, M.; Santos, M. M. M. *ChemMedChem* **2015**, *10* (12), 2080–2089.
- (121) Scott, W. L.; Martynow, J. G.; Huffman, J. C.; O'Donnell, M. J. *J. Am. Chem. Soc.* **2007**, *129* (22), 7077–7088.
- (122) Allin, S. M.; James, S. L.; Martin, W. P.; Smith, T. A. D. *Tetrahedron Lett.* **2001**, *42*, 3943–3946.
- (123) Bahajaj, A. A.; Vernon, J. M.; Wilson, G. D. *Tetrahedron* **2004**, *60* (5), 1247–1253.
- (124) Jiang, L.-J.; Lan, H.-Q.; Zheng, J.-F.; Ye, J.-L.; Huang, P.-Q. *Synlett* **2009**, 2009 (02), 0297–0301.
- (125) Indukuri, K.; Unnava, R.; Deka, M. J.; Saikia, A. K. *J. Org. Chem.* **2013**, *78* (21), 10629–10641.
- (126) Maity, A. K.; Roy, S. *Adv. Synth. Catal.* **2014**, *356* (11–12), 2627–2642.
- (127) Belvisi, L.; Gennari, C.; Poli, G.; Scolastico, C.; Salom, B.; Vassallo, M. *Tetrahedron* **1992**, *48*, 3945–3960.
- (128) Kanizsai, I.; Szakonyi, Z.; Sillanpää, R.; D’hooghe, M.; Kimpe, N. D.; Fülöp, F. *Tetrahedron: Asymmetry* **2006**, *17* (20), 2857–2863.
- (129) Le Goff, R.; Martel, A.; Sanselme, M.; Lawson, A. M.; Daïch, A.; Comesse, S. *Chem. Eur. J.* **2014**, *21* (7), 2966–2979.
- (130) Kobayashi, T.; Takeuchi, K.; Miwa, J.; Tsuchikawa, H.; Katsumura, S. *Chem. Commun.* **2009**, 39 (23), 3363.

- (131) Smith, J. A.; Gourlay, B. S.; Molesworth, P. P.; Ryan, J. H. *Tetrahedron Lett.* **2006**, *47*, 799–801.
- (132) Corey, E. J.; Ensley, H. E. *J. Am. Chem. Soc.* **1975**, *97*, 6908–6909.
- (133) Wuts, P. G. M.; Greene, T. W. *Greene's Protective Groups in Organic Synthesis, Fourth Edition*; John Wiley and Sons: Hoboken, 2007.
- (134) Beattie, J. K.; McErlean, C. S. P.; Phippen, C. B. W. *Chem. Eur. J.* **2010**, *16* (30), 8972–8974.
- (135) Norcott, P.; Spielman, C.; McErlean, C. S. P. *Green Chem.* **2012**, *14* (3), 605.
- (136) Batey, R. A.; MacKay, D. B.; Santhakumar, V. *J. Am. Chem. Soc.* **1999**, *121* (21), 5075–5076.
- (137) Morgan, I. R.; Yazici, A.; Pyne, S. G. *Tetrahedron* **2008**, *64* (7), 1409–1419.
- (138) Pyne, S. G.; Au, C. W. G.; Davis, A. S.; Morgan, I. R.; Ritthiwigrom, T.; Yazici, A. *Pure & Appl. Chem.* **2008**, *80* (4), 751–762.
- (139) Moriyama, K.; Nakamura, Y.; Togo, H. *Org. Lett.* **2014**, *16* (14), 3812–3815.
- (140) Chan, K. K. J.; O'Hagan, D. *The Rare Fluorinated Natural Products and Biotechnological Prospects for Fluorine Enzymology*, 1st ed.; Elsevier Inc., 2012; Vol. 516, pp 219–235.
- (141) Ma, L.; Bartholome, A.; Tong, M. H.; Qin, Z.; Yu, Y.; Shepherd, T.; Kyeremeh, K.; Deng, H.; O'Hagan, D. *Chem. Sci.* **2015**, *6*, 1414–1419.
- (142) Xu, X.-H.; Yao, G.-M.; Li, Y.-M.; Lu, J.-H.; Lin, C.-J.; Wang, X.; Kong, C.-H. *J. Nat. Prod.* **2003**, *66* (2), 285–288.
- (143) Deng, H.; O'Hagan, D.; Schaffrath, C. *Nat. Prod. Rep.* **2004**, *21* (6), 773.
- (144) Jaivel, N.; Uvarani, C.; Rajesh, R.; Velmurugan, D.; Marimuthu, P. *J. Nat. Prod.* **2014**, *77* (1), 2–8.
- (145) Aldemir, H.; Kohlhepp, S. V.; Gulder, T.; Gulder, T. A. M. *J. Nat. Prod.* **2014**, *77* (11), 2331–2334.
- (146) Müller, K.; Faeh, C.; Diederich, F. *Science* **2007**, *317*, 1881–1886.
- (147) O'Hagan, D. *J. Fluorine Chem.* **2010**, *131* (11), 1071–1081.
- (148) Hagmann, W. K. *J. Med. Chem.* **2008**, *51* (15), 4359–4369.
- (149) Isanbor, C.; O'Hagan, D. *J. Fluorine Chem.* **2006**, *127* (3), 303–319.
- (150) Bégué, J.-P.; Bonnet-Delpon, D. *Chimie Bioorganique et Médicinale du Fluor*; CNRS Ed.: Paris, 2005.
- (151) Wong, D. T.; Horng, J. S.; Bymaster, F. P.; Hauser, K. L.; Molloy, B. B. *Life Sci.* **1974**, *15*, 471–479.
- (152) Wong, D. T.; Bymaster, F. P.; Engleman, E. A. *Life Sci.* **1995**, *57* (5), 411–441.
- (153) Bocan, T. M. A.; Mazur, M. J.; Mueller, S. B.; Brown, E. Q.; Sliskovic, D. R.; O'Brien, P. M.; Creswell, M. W.; Lee, H.; Uhlendorf, P. D.; Roth, B. D.; Newton, R. S. *Atherosclerosis* **1994**, *111*, 127–142.
- (154) O'Hagan, D. *Chem. Soc. Rev.* **2008**, *37* (2), 308–319.
- (155) Pauling, L. *The Nature of the Chemical Bond and the Structure of Molecules and Crystals: An Introduction to Modern Structural Chemistry*; Cornell University Press: Ithaca, NY, 1939.

- (156) Bondi, A. *J. Phys. Chem.* **1964**, 68 (3), 441–451.
- (157) Patani, G. A.; LaVoie, E. J. *Chem. Rev.* **1996**, 96, 3147–3176.
- (158) Dunitz, J. D.; Schweizer, W. B. *Chem. Eur. J.* **2006**, 12 (26), 6804–6815.
- (159) Zanda, M. *New J. Chem.* **2004**, 28 (12), 1401.
- (160) Molteni, M.; Pesenti, C.; Sani, M.; Volonterio, A.; Zanda, M. J. *Fluorine Chem.* **2004**, 125 (11), 1735–1743.
- (161) Paulini, R.; Müller, K.; Diederich, F. *Angew. Chem. Int. Ed.* **2005**, 44 (12), 1788–1805.
- (162) Schlosser, M.; Michel, D. *Tetrahedron* **1996**, 52, 99–108.
- (163) Abraham, R. J.; Schonholzer, P.; Thomas, W. A. *Tetrahedron* **1986**, 42, 2101–2110.
- (164) Zhao, K.; Lim, D. S.; Funaki, T.; Welch, J. T. *Bioorganic Med. Chem.* **2003**, 11, 207–215.
- (165) Couve-Bonnaire, S.; Cahard, D.; Pannecoucke, X. *Org. Biomol. Chem.* **2007**, 5 (8), 1151.
- (166) Kool, E. T.; Sintim, H. O. *Chem. Commun.* **2006**, 59 (35), 3665–3675.
- (167) Mikami, K.; Itoh, Y.; Yamanaka, M. *Chem. Rev.* **2004**, 104 (1), 1–16.
- (168) Wolf, C.; König, W. A.; Roussel, C. *Liebigs Ann.* **1995**, 781–786.
- (169) Leroux, F. *ChemBioChem* **2004**, 5 (5), 644–649.
- (170) Doan, K. M. M. *J. Pharmacol. Exp. Ther.* **2002**, 303 (3), 1029–1037.
- (171) Böhm, H.-J.; Banner, D.; Bendels, S.; Kansy, M.; Kuhn, B.; Müller, K.; Obst-Sander, U.; Stahl, M. *ChemBioChem* **2004**, 5 (5), 637–643.
- (172) Morgenthaler, M.; Schweizer, E.; Hoffmann-Röder, A.; Benini, F.; Martin, R. E.; Jaeschke, G.; Wagner, B.; Fischer, H.; Bendels, S.; Zimmerli, D.; Schneider, J.; Diederich, F.; Kansy, M.; Müller, K. *ChemMedChem* **2007**, 2 (8), 1100–1115.
- (173) van Niel, M. B.; Collins, I.; Beer, M. S.; Broughton, H. B.; Cheng, S. K. F.; Goodacre, S. C.; Heald, A.; Locker, K. L.; MacLeod, A. M.; Morrison, D.; Moyes, C. R.; O'Connor, D.; Pike, A.; Rowley, M.; Russell, M. G. N.; Sohal, B.; Stanton, J. A.; Thomas, S.; Verrier, H.; Watt, A. P.; Castro, J. L. *J. Med. Chem.* **1999**, 42 (12), 2087–2104.
- (174) Rowley, M.; Hallett, D. J.; Goodacre, S.; Moyes, C.; Crawforth, J.; Sparey, T. J.; Patel, S.; Marwood, R.; Patel, S.; Thomas, S.; Hitzel, L.; O'Connor, D.; Szeto, N.; Castro, J. L.; Hutson, P. H.; MacLeod, A. M. *J. Med. Chem.* **2001**, 44 (10), 1603–1614.
- (175) Schweizer, E.; Hoffmann-Röder, A.; Schärer, K.; Olsen, J. A.; Fäh, C.; Seiler, P.; Obst-Sander, U.; Wagner, B.; Kansy, M.; Diederich, F. *ChemMedChem* **2006**, 1 (6), 611–621.
- (176) Avdeef, A. *Curr. Top. Med. Chem.* **2001**, 1, 277–351.
- (177) Dunitz, J. D.; Taylor, R. *Chem. Eur. J.* **1997**, 3, 89–98.
- (178) DiMagno, S. G.; Sun, H. *Curr. Top. Med. Chem.* **2006**, 6, 1473–1482.
- (179) Olsen, J. A.; Banner, D. W.; Seiler, P.; Obst-Sander, U.; D'Arcy, A.; Stihle, M.; Müller, K.; Diederich, F. *Angew. Chem. Int. Ed.* **2003**, 42 (22), 2507–2511.
- (180) Hof, F.; Scofield, D. M.; Schweizer, W. B.; Diederich, F. *Angew. Chem. Int. Ed.* **2004**, 43 (38), 5056–5059.

- (181) Banks, J. W.; Batsanov, A. S.; Howard, J. A. K.; O'Hagan, D.; Rzepa, H. S.; Martin-Santamaria, S. *J. Chem. Soc., Perkin Trans. 2* **1999**, No. 11, 2409–2411.
- (182) van der Veken, B. J.; Truyen, S.; Herrebout, W. A.; Watkins, G. J. *Mol. Struct.* **1993**, 293, 55–58.
- (183) Abraham, R. J.; Jones, A. D.; Warne, M. A.; Rittner, R.; Tormena, C. F. *J. Chem. Soc., Perkin Trans. 2* **1996**, No. 4, 533.
- (184) Phan, H. V.; Durig, J. R. *THEOCHEM* **1990**, 209, 330–347.
- (185) Wu, D.; Tian, A.; Sun, H. *J. Phys. Chem. A* **1998**, 102 (48), 9901–9905.
- (186) Hunter, L.; Slawin, A. M. Z.; Kirsch, P.; O'Hagan, D. *Angew. Chem. Int. Ed.* **2007**, 46 (41), 7887–7890.
- (187) Hernández-Trujillo, J.; Vela, A. *J. Phys. Chem.* **1996**, 100, 6524–6530.
- (188) Matsushima, A.; Fujita, T.; Nose, T.; Shimonhigashi, Y. *J. Biochem.* **2000**, 128, 225–232.
- (189) Kim, C.-Y.; Chandra, P. P.; Jain, A.; Christianson, D. W. *J. Am. Chem. Soc.* **2001**, 123 (39), 9620–9627.
- (190) Sun, A.; Lankin, D. C.; Hardcastle, K.; Snyder, J. P. *Chem. Eur. J.* **2005**, 11 (5), 1579–1591.
- (191) Briggs, C. R. S.; Allen, M. J.; O'Hagan, D.; Tozer, D. J.; Slawin, A. M. Z.; Goeta, A. S. E.; Howard, J. A. K. *Org. Biomol. Chem.* **2004**, 2 (5), 732.
- (192) Gooseman, N. E. J.; O'Hagan, D.; Peach, M. J. G.; Slawin, A. M. Z.; Tozer, D. J.; Young, R. J. *Angew. Chem. Int. Ed.* **2007**, 46 (31), 5904–5908.
- (193) Wolfe, S. *Acc. Chem. Res.* **1972**, 5, 102–111.
- (194) Brunck, T. K.; Weinhold, F. *J. Am. Chem. Soc.* **1979**, 101, 1700–1709.
- (195) Rablen, P.; Hoffmann, R.; Hrovat, D.; Thatcher Borden, W. J. *Chem. Soc., Perkin Trans. 2* **1999**, 5 (8), 1719–1726.
- (196) Goodman, L.; Gu, H.; Pophristic, V. *J. Phys. Chem. A* **2005**, 109 (6), 1223–1229.
- (197) Wiberg, K. B.; Murcko, M. A.; Laidig, K. E.; MacDougall, P. J. *J. Phys. Chem.* **1990**, 94, 6956–6959.
- (198) Wiberg, K. B. *Acc. Chem. Res.* **1997**, 29, 229–234.
- (199) Juaristi, E.; Cuevas, G. *Tetrahedron* **1992**, 48, 5019–5087.
- (200) Tozer, D. J. *Chem. Phys. Lett.* **1999**, 308, 160–164.
- (201) O'Hagan, D.; Bilton, C.; Howard, J. A. K.; Knight, L.; Tozer, D. J. *J. Chem. Soc., Perkin Trans. 2* **2000**, No. 4, 605–607.
- (202) Briggs, C. R. S.; O'Hagan, D.; Rzepa, H. S.; Slawin, A. M. Z. *J. Fluorine Chem.* **2004**, 125 (1), 19–25.
- (203) Trapp, M. L.; Watts, J. K.; Weinberg, N.; Pinto, B. M. *Can. J. Chem.* **2006**, 84 (4), 692–701.
- (204) Padgett, C. L.; Slesinger, P. A. *Receptor Coupling to G-proteins and Ion Channels*; Adv. Pharmacol., 2010; Vol. 58, pp 123–147.
- (205) Chebib, M.; Johnston, G. A. R. *J. Med. Chem.* **2000**, 43 (8), 1427–1447.
- (206) Mody, I.; Pearce, R. A. *Trends Neurosci.* **2004**, 27 (9), 569–575.
- (207) Johnston, G. A. R. *Curr. Pharm. Des.* **2005**, 11, 1867–1885.



- (208) Farrant, M.; Kaila, K. *Prog. Brain. Res.* **2007**, *160*, 59–87.
- (209) Bettler, B. *Physiol. Rev.* **2004**, *84* (3), 835–867.
- (210) Emson, P. C. *Prog. Brain. Res.* **2007**, *160*, 43–57.
- (211) Rudolph, U.; Knoflach, F. *Nat. Rev. Drug Discov.* **2011**, *10*, 685–697.
- (212) Yee, B. K.; Keist, R.; Boehmer, von, L.; Studer, R.; Benke, D.; Hagenbuch, N.; Dong, Y.; Malenka, R. C.; Fritschy, J. M.; Bluethmann, H.; Feldon, J.; Möhler, H.; Rudolph, U. *Proc. Natl. Acad. Sci. USA* **2005**, *102* (47), 17154–17159.
- (213) Trudell, J. R.; Bertaccini, E.; MacIver, M. B. *Anesth. Analg.* **2012**, *115* (2), 270–273.
- (214) Benke, D. *Biochem. Pharmacol.* **2013**, *86* (11), 1525–1530.
- (215) Brejc, K.; van Dijk, W. J.; Klaassen, R. V.; Schuurmans, M.; van der Oost, J.; Smit, A. B.; Sixma, T. K. *Nature* **2001**, *411*, 269–276.
- (216) Hilf, R. J. C.; Dutzler, R. *Nature* **2008**, *452* (7185), 375–379.
- (217) Hilf, R. J. C.; Dutzler, R. *Nature* **2008**, *457* (7225), 115–119.
- (218) Bocquet, N.; Nury, H.; Baaden, M.; Le Poupon, C.; Changeux, J.-P.; Delarue, M.; Corringer, P.-J. *Nature* **2008**, *457* (7225), 111–114.
- (219) Geng, Y.; Bush, M.; Mosyak, L.; Wang, F.; Fan, Q. R. *Nature* **2013**, *504* (7479), 254–259.
- (220) Crittenden, D. L.; Chebib, M.; Jordan, M. J. T. *THEOCHEM* **2005**, *755* (1-3), 81–89.
- (221) O'Hagan, D. *Future Med. Chem.* **2011**, *3* (2), 189–195.
- (222) Winkler, M.; O'Hagan, D. *Mol. Med. Med. Chem.* **2012**, *6*, 299–331.
- (223) Hunter, L.; Jolliffe, K. A.; Jordan, M. J. T.; Jensen, P.; Macquart, R. B. *Chem. Eur. J.* **2011**, *17* (8), 2340–2343.
- (224) Hunter, L. *Beilstein J. Org. Chem.* **2010**, *6*.
- (225) Yamamoto, I.; Jordan, M. J. T.; Gavande, N.; Doddareddy, M. R.; Chebib, M.; Hunter, L. *Chem. Commun.* **2012**, *48* (6), 829–831.
- (226) Absalom, N.; Yamamoto, I.; O'Hagan, D.; Hunter, L.; Chebib, M. *Aust. J. Chem.* **2015**, *68* (1), 23–30.
- (227) Deniau, G.; Slawin, A. M. Z.; Lebl, T.; Chorki, F.; Issberner, J. P.; van Mourik, T.; Heygate, J. M.; Lambert, J. J.; Etherington, L.-A.; Sillar, K. T.; O'Hagan, D. *ChemBioChem* **2007**, *8* (18), 2265–2274.
- (228) Champagne, P. A.; Desroches, J.; Hamel, J.-D.; Vandamme, M.; Paquin, J.-F. *Chem. Rev.* **2015**, *115* (17), 9073–9174.
- (229) Barluenga, J.; González, J. M.; Campos, P. J.; Arsenio, G. *Angew. Chem. Int. Ed.* **1985**, *24*, 319–320.
- (230) Tsushimi, T.; Kawada, K.; Tsuji, T. *Tetrahedron Lett.* **1982**, *23*, 1165–1168.
- (231) Frohn, H. J.; Giesen, M. *J. Fluorine Chem.* **1998**, *89*, 59–63.
- (232) Sun, H.; DiMagno, S. G. *J. Am. Chem. Soc.* **2005**, *127* (7), 2050–2051.
- (233) Sun, H.; DiMagno, S. G. *Chem. Commun.* **2007**, *312* (5), 528–529.
- (234) Kim, D. W.; Jeong, H.-J.; Lim, S. T.; Sohn, M.-H. *Angew. Chem. Int. Ed.* **2008**, *47* (44), 8404–8406.
- (235) Okoromoba, O. E.; Han, J.; Hammond, G. B.; Xu, B. *J. Am. Chem. Soc.* **2014**, *136* (41), 14381–14384.
- (236) Hara, S.; Monoi, M.; Umemura, R.; Fuse, C. *Tetrahedron* **2012**, *68* (49), 10145–10150.

- (237) Shishimi, T.; Hara, S. *J. Fluorine Chem.* **2014**, *168*, 55–76.
- (238) Taylor, S. D.; Kotoris, C. C.; Hum, G. *Tetrahedron* **1999**, *55*, 12431–12477.
- (239) Kiselyov, A. S. *Chem. Soc. Rev.* **2005**, *34* (12), 1031.
- (240) Differding, E.; Ofner, H. *Synlett* **1991**, 187–189.
- (241) Nyffeler, P. T.; Durón, S. G.; Burkart, M. D.; Vincent, S. P.; Wong, C.-H. *Angew. Chem. Int. Ed.* **2004**, *44* (2), 192–212.
- (242) Singh, R. P.; Shreeve, J. M. *Acc. Chem. Res.* **2004**, *37* (1), 31–44.
- (243) Stavber, S.; Zupan, M.; Poss, A. J.; Shia, G. A. *Tetrahedron Lett.* **1995**, *36* (37), 6769–6772.
- (244) Poss, A. J.; Shia, G. A. *Tetrahedron Lett.* **1999**, *40*, 2673–2676.
- (245) Yasui, H.; Yamamoto, T.; Ishimaru, T.; Fukuzumi, T.; Tokunaga, E.; Akikazu, K.; Shiro, M.; Shibata, N. *J. Fluorine Chem.* **2011**, *132* (3), 222–225.
- (246) Zhu, C.-L.; Maeno, M.; Zhang, F.-G.; Shigehiro, T.; Kagawa, T.; Kawada, K.; Shibata, N.; Ma, J.-A.; Cahard, D. *Eur. J. Org. Chem.* **2013**, *2013* (29), 6501–6505.
- (247) Wolstenhulme, J. R.; Rosenqvist, J.; Lozano, O.; Ilupeju, J.; Wurz, N.; Engle, K. M.; Pidgeon, G. W.; Moore, P. R.; Sandford, G.; Gouverneur, V. *Angew. Chem. Int. Ed.* **2013**, *52* (37), 9796–9800.
- (248) Wang, F.; Li, J.; Hu, Q.; Yang, X.; Wu, X.-Y.; He, H. *Eur. J. Org. Chem.* **2014**, *2014* (17), 3607–3613.
- (249) Geary, G. C.; Hope, E. G.; Singh, K.; Stuart, A. M. *Chem. Commun.* **2013**, *49* (81), 9263.
- (250) Sibi, M. P.; Landais, Y. *Angew. Chem. Int. Ed.* **2013**, *52* (13), 3570–3572.
- (251) Grakauskas, V. *J. Org. Chem.* **1969**, *34* (8), 2446–2450.
- (252) Rozen, S. *Acc. Chem. Res.* **1988**, *21* (8), 307–312.
- (253) Patrick, T. B.; Khazaeli, S.; Nadji, S.; Hering-Smith, K.; Reif, D. J. *Org. Chem.* **1993**, *58* (3), 705–708.
- (254) Rueda-Becerril, M.; Chatalova-Sazepin, C.; Leung, J. C. T.; Okbinoglu, T.; Kennepohl, P.; Paquin, J.-F.; Sammis, G. M. *J. Am. Chem. Soc.* **2012**, *134* (9), 4026–4029.
- (255) Yin, F.; Wang, Z.; Li, Z.; Li, C. *J. Am. Chem. Soc.* **2012**, *134* (25), 10401–10404.
- (256) Leung, J. C. T.; Chatalova-Sazepin, C.; West, J. G.; Rueda-Becerril, M.; Paquin, J.-F.; Sammis, G. M. *Angew. Chem. Int. Ed.* **2012**, *51* (43), 10804–10807.
- (257) Yamada, S.; Gavryushin, A.; Knochel, P. *Angew. Chem. Int. Ed.* **2010**, *49* (12), 2215–2218.
- (258) Döbele, M.; Vanderheiden, S.; Jung, N.; Bräse, S. *Angew. Chem. Int. Ed.* **2010**, *49* (34), 5986–5988.
- (259) Middleton, W. J. *J. Org. Chem.* **1975**, *40* (5), 574–578.
- (260) Lal, G. S.; Pez, G. P.; Pesaresi, R. J.; Prozonic, F. M. *Chem. Commun.* **1999**, No. 2, 215–216.
- (261) Lal, G. S.; Pez, G. P.; Pesaresi, R. J.; Prozonic, F. M.; Cheng, H. J. *Org. Chem.* **1999**, *64*, 7048–7054.
- (262) Beaulieu, F.; Beauregard, L.-P.; Courchesne, G.; Couturier, M.; LaFlamme, F.; L'Heureux, A. *Org. Lett.* **2009**, *11* (21), 5050–5053.
- (263) L'Heureux, A.; Beaulieu, F.; Bennett, C.; Bill, D. R.; Clayton, S.;

- LaFlamme, F.; Mirmehrabi, M.; Tadayon, S.; Tovell, D.; Couturier, M. *J. Org. Chem.* **2010**, *75* (10), 3401–3411.
- (264) Mahé, O.; L'Heureux, A.; Couturier, M.; Bennett, C.; Clayton, S.; Tovell, D.; Beaulieu, F.; Paquin, J.-F. *J. Fluorine Chem.* **2013**, *153*, 57–60.
- (265) Nielsen, M. K.; Ugaz, C. R.; Li, W.; Doyle, A. G. *J. Am. Chem. Soc.* **2015**, *137* (30), 9571–9574.
- (266) Umemoto, T.; Singh, R. P.; Xu, Y.; Saito, N. *J. Am. Chem. Soc.* **2010**, *132* (51), 18199–18205.
- (267) Singh, R. P. *J. Fluorine Chem.* **2012**, *140*, 15–25.
- (268) Tang, P.; Wang, W.; Ritter, T. *J. Am. Chem. Soc.* **2011**, *133* (30), 11482–11484.
- (269) Fujimoto, T.; Becker, F.; Ritter, T. *Org. Process Res. Dev.* **2014**, *18* (8), 1041–1044.
- (270) Sladojevich, F.; Arlow, S. I.; Tang, P.; Ritter, T. *J. Am. Chem. Soc.* **2013**, *135* (7), 2470–2473.
- (271) Hunter, L.; O'Hagan, D.; Slawin, A. M. Z. *J. Am. Chem. Soc.* **2006**, *128* (51), 16422–16423.
- (272) Brunet, V. A.; Slawin, A. M. Z.; O'Hagan, D. *Beilstein J. Org. Chem.* **2009**, *5*.
- (273) Schöler, M.; O'Hagan, D.; Slawin, A. M. Z. *Chem. Commun.* **2005**, *32* (34), 4324.
- (274) Siddiqui, S.; Narkhede, U.; Lahoti, R.; Srinivasan, K. *Synlett* **2006**, *2006* (11), 1771–1773.
- (275) Gao, Y.; Sharpless, K. B. *J. Am. Chem. Soc.* **1988**, *110* (22), 7538–7539.
- (276) Bio, M.; Waters, M.; Javadi, G.; Song, Z.; Zhang, F.; Thomas, D. *Synthesis* **2008**, *2008* (6), 891–896.
- (277) Bresciani, S.; O'Hagan, D. *Tetrahedron Lett.* **2010**, *51* (44), 5795–5797.
- (278) Carlsen, P. H. J.; Katsuki, T.; Martin, V. S.; Sharpless, K. B. *J. Org. Chem.* **1981**, *46* (19), 3936–3938.
- (279) Nilewski, C.; Geisser, R. W.; Carreira, E. M. *Nature* **2009**, *457* (7229), 573–576.
- (280) Hamatani, T.; Matsubara, S.; Matsuda, H.; Schlosser, M. *Tetrahedron* **1988**, *44*, 2875–2881.
- (281) Katritzky, A. R.; Cui, X.-L.; Yang, B.; Steel, P. J. *Tetrahedron Lett.* **1998**, *39*, 1697–1700.
- (282) Katritzky, A. R.; Cui, X.-L.; Yang, B.; Steel, P. J. *J. Org. Chem.* **1999**, *64* (6), 1979–1985.
- (283) Burgess, L. E.; Meyers, A. I. *J. Org. Chem.* **1992**, *57* (6), 1656–1662.
- (284) Kim, G.; Lee, E.-J. *Tetrahedron: Asymmetry* **2001**, *12*, 2073–2076.
- (285) Clark, J. S.; Hodgson, P. B.; Goldsmith, M. D.; Street, L. J. *J. Chem. Soc., Perkin Trans. 1* **2001**, No. 24, 3312–3324.
- (286) Aue, W. P.; Karhan, J.; Ernst, R. R. *J. Chem. Phys.* **1976**, *64* (10), 4226–4227.
- (287) Singh, A.; Roth, G. P. *Org. Lett.* **2011**, *13* (8), 2118–2121.
- (288) Barker, T. J.; Boger, D. L. *J. Am. Chem. Soc.* **2012**, *134* (33), 13588–13591.

- (289) Shigehisa, H.; Nishi, E.; Fujisawa, M.; Hiroya, K. *Org. Lett.* **2013**, *15* (20), 5158–5161.
- (290) Read, C.; Menary, R. *J. Essent. Oil. Res.* **2001**, *13* (5), 348–350.
- (291) Mecchi, M. C.; Lago, J. H. G. *Nat. Prod. Res.* **2013**, *27* (20), 1927–1929.
- (292) Asakawa, Y.; Ludwiczuk, A.; Harinantenaina, L.; Toyota, M.; Nishiki, M.; Bardon, A.; Nii, K. *Nat. Prod. Commun.* **2012**, *7*, 685–692.
- (293) Kubo, I. *J. Nat. Prod.* **1988**, *51* (1), 22–29.
- (294) Butler, M. S.; Capon, R. J. *Aust. J. Chem.* **1993**, *46*, 1255–1267.
- (295) Prota, N.; Bouwmeester, H. J.; Jongsma, M. A. *Pest. Manag. Sci.* **2013**, *70* (4), 682–688.
- (296) Just, J.; Deans, B. J.; Olivier, W. J.; Paull, B.; Bissember, A. C.; Smith, J. A. *Org. Lett.* **2015**, *17* (10), 2428–2430.
- (297) Just, J.; Jordan, T. B.; Paull, B.; Bissember, A. C.; Smith, J. A. *Org. Biomol. Chem.* **2015**, *13*, 11200–11207.
- (298) Faulkner, J. D.; Hochlowski, J. E.; Walker, R. P.; Ireland, C. J. *Org. Chem.* **1982**, *47*, 88–91.
- (299) Gulavita, N. K.; Gunasekera, S. P.; Pomponi, S. A. *J. Nat. Prod.* **1992**, *55* (4), 506–508.
- (300) Valderrama, J. A.; Benites, J.; Cortés, M.; Pessoa-Mahana, D.; Prina, E.; Fournet, A. *Tetrahedron* **2002**, *58*, 881–886.
- (301) Newman, D. J.; Cragg, G. M. *J. Nat. Prod.* **2016**, *79* (3), 629–661.
- (302) Cahill, P. L.; Kuhajek, J. M. *Biofouling* **2014**, *30* (9), 1035–1043.
- (303) Caprioli, V.; Cimino, G.; Colle, R.; Gavagnin, M.; Sodano, G.; Spinella, A. *J. Nat. Prod.* **1987**, *50*, 146–151.
- (304) Asakawa, Y.; Dawson, G. W.; Griffiths, D. C.; Lallemant, J. Y.; Ley, S. V.; Mori, K.; Mudd, A.; Pezechk-Leclaire, M.; Pickett, J. A.; Watanabe, H.; Woodcock, C. M.; Zhong-Ning, Z. *J. Chem. Ecol.* **1988**, *14* (10), 1845–1855.
- (305) Kubo, I.; Fujita, K.; Lee, S. H.; Ha, T. J. *Phytother. Res.* **2005**, *19*, 1013–1017.
- (306) Claudino, V. D.; da Silva, K. C.; Filho, V. C.; Yunes, R. A.; Monache, F. D.; Giménez, A.; Salamanca, E.; Gutierrez-Yapu, D.; Malheiros, A. *Mem. Inst. Oswaldo Cruz* **2013**, *108*, 140–144.
- (307) Corrêa, D. S.; Tempone, A. G.; Reimão, J. Q.; Taniwaki, N. N.; Romoff, P.; Fávero, O. A.; Sartorelli, P.; Mecchi, M. C.; Lago, J. H. G. *Parasitol Res* **2011**, *109* (1), 231–236.
- (308) McCallion, R. F.; Cole, A. L. J.; Walker, J. R. L.; Blunt, J. W.; Munro, M. H. G. *Planta Med.* **1982**, *44*, 134–138.
- (309) Lee, S. H.; Lee, J. R.; Lunde, C. S.; Kubo, I. *Planta Med.* **1999**, *65*, 204–208.
- (310) Kubo, I.; Fujita, K.; Lee, S. H. *J. Agric. Food Chem.* **2001**, *49* (3), 1607–1611.
- (311) da Cunha, F. M.; Fröde, T. S.; Mendes, G. L.; Malheiros, A.; Filho, V. C.; Yunes, R. A.; Calixto, J. B. *Life Sci.* **2001**, *70*, 159–169.
- (312) Sterner, O.; Szallasi, A. *Trends Pharmacol. Sci.* **1999**, *20*, 459–465.
- (313) Andre, E.; Ferreira, J.; Malheiros, A.; Yunes, R. A.; Calixto, J. B. *Neuropharmacology* **2004**, *46* (4), 590–597.
- (314) Andre, E.; Campi, B.; Trevisani, M.; Ferreira, J.; Malheiros, A.; Yunes, R. A.; Calixto, J. B.; Geppetti, P. *Biochem. Pharmacol.* **2006**,

- 71 (8), 1248–1254.
- (315) Monica, Della, C.; De Petrocellis, L.; Di Marzo, V.; Landi, R.; Izzo, I.; Spinella, A. *Bioorganic Med. Chem. Lett.* **2007**, 17 (23), 6444–6447.
- (316) Iwasaki, Y.; Tanabe, M.; Kayama, Y.; Abe, M.; Kashio, M.; Koizumi, K.; Okumura, Y.; Morimitsu, Y.; Tominaga, M.; Ozawa, Y.; Watanabe, T. *Life Sci.* **2009**, 85 (1–2), 60–69.
- (317) D’Acunto, M.; Monica, Della, C.; Izzo, I.; De Petrocellis, L.; Di Marzo, V.; Spinella, A. *Tetrahedron* **2010**, 66 (52), 9785–9789.
- (318) Cimino, G.; Spinella, A.; Sodano, G. *Tetrahedron Lett.* **1984**, 25, 4151–4152.
- (319) D’Ischia, M.; Prota, G.; Sodano, G. *Tetrahedron Lett.* **1982**, 23 (32), 3295–3298.
- (320) Cimino, G.; Sodano, G.; Spinella, A. *Tetrahedron* **1987**, 43 (22), 5401–5410.
- (321) Dasari, R.; De Carvalho, A.; Medellin, D. C.; Middleton, K. N.; Hague, F.; Volmar, M. N. M.; Frolova, L. V.; Rossato, M. F.; La Chapa, De, J. J.; Dybdal-Hargreaves, N. F.; Pillai, A.; Mathieu, V.; Rogelj, S.; Gonzales, C. B.; Calixto, J. B.; Evidente, A.; Gautier, M.; Munirathinam, G.; Glass, R.; Burth, P.; Pelly, S. C.; van Otterlo, W. A. L.; Kiss, R.; Kornienko, A. *ChemMedChem* **2015**, 10 (12), 2014–2026.
- (322) Dasari, R.; De Carvalho, A.; Medellin, D. C.; Middleton, K. N.; Hague, F.; Volmar, M. N. M.; Frolova, L. V.; Rossato, M. F.; La Chapa, De, J. J.; Dybdal-Hargreaves, N. F.; Pillai, A.; Kálin, R. E.; Mathieu, V.; Rogelj, S.; Gonzales, C. B.; Calixto, J. B.; Evidente, A.; Gautier, M.; Munirathinam, G.; Glass, R.; Burth, P.; Pelly, S. C.; van Otterlo, W. A. L.; Kiss, R.; Kornienko, A. *Eur. J. Med. Chem.* **2015**, 103 (C), 226–237.
- (323) Gourlay, B. S.; Ryan, J. H.; Smith, J. A. *Beilstein J. Org. Chem.* **2008**, 4 (1), 3.
- (324) Zhao, Y.; Zhang, Q.; Tu, G.; Cheng, T. *Tetrahedron* **2002**, 58, 6795–6798.
- (325) Hajos, Z. G.; Parrish, D. R. *J. Org. Chem.* **1974**, 39 (12), 1615–1621.
- (326) List, B.; Lerner, R. A.; Barbas, C. F. *J. Am. Chem. Soc.* **2000**, 122 (10), 2395–2396.
- (327) List, B.; Pojarliev, P.; Castello, C. *Org. Lett.* **2001**, 3 (4), 573–575.
- (328) Bahmanyar, S.; Houk, K. N.; Martin, H. J.; List, B. *J. Am. Chem. Soc.* **2003**, 125 (9), 2475–2479.
- (329) Sakthivel, K.; Notz, W.; Bui, T.; Barbas, C. F. *J. Am. Chem. Soc.* **2001**, 123 (22), 5260–5267.
- (330) List, B. *J. Am. Chem. Soc.* **2000**, 122 (38), 9336–9337.
- (331) List, B.; Pojarliev, P.; Biller, W. T.; Martin, H. J. *J. Am. Chem. Soc.* **2002**, 124 (5), 827–833.
- (332) Córdova, A.; Notz, W.; Zhong, G.; Betancort, J. M.; Barbas, C. F. *J. Am. Chem. Soc.* **2002**, 124 (9), 1842–1843.
- (333) Córdova, A.; Watanabe, S.-I.; Tanaka, F.; Notz, W.; Barbas, C. F. *J. Am. Chem. Soc.* **2002**, 124 (9), 1866–1867.
- (334) Barbas, C. F.; Córdova, A. *Tetrahedron Lett.* **2002**, 43, 7749–7752.
- (335) Ahrendt, K. A.; Borths, C. J.; MacMillan, D. W. C. *J. Am. Chem.*

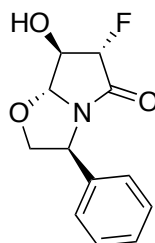
- Soc. **2000**, 122 (17), 4243–4244.
- (336) Jen, W. S.; Wiener, J. J. M.; MacMillan, D. W. C. *J. Am. Chem. Soc.* **2000**, 122 (40), 9874–9875.
- (337) Pan, D.; Wei, Y.; Shi, M. *Org. Lett.* **2016**, 18, 3930–3933.
- (338) Loy, N. S. Y.; Choi, S.; Kim, S.; Park, C.-M. *Chem. Commun.* **2016**, 52, 7336–7339.
- (339) Baird, E. E.; Dervan, P. B. *J. Am. Chem. Soc.* **1996**, 118 (26), 6141–6146.
- (340) Garro-Helion, F.; Merzouk, A.; Guibe, F. *J. Org. Chem.* **1993**, 58 (22), 6109–6113.
- (341) Lemaire-Audoire, S.; Savignac, M.; Genêt, J. P. *Tetrahedron Lett.* **1995**, 36, 1267–1270.
- (342) Kemppainen, E. K.; Sahoo, G.; Valkonen, A.; Pihko, P. M. *Org. Lett.* **2012**, 14 (4), 1086–1089.
- (343) Chiou, W.-H.; Chen, G.-T.; Kao, C.-L.; Gao, Y.-K. *Org. Biomol. Chem.* **2012**, 10 (13), 2518.
- (344) Andrés, C.; Duque-Soladana, J. P.; Pedrosa, R. *J. Org. Chem.* **1999**, 64 (12), 4273–4281.
- (345) Li, J.; Luo, S.; Cheng, J.-P. *J. Org. Chem.* **2009**, 74 (4), 1747–1750.
- (346) Kumar, A.; Chimni, S. S. *Beilstein J. Org. Chem.* **2014**, 10, 929–935.
- (347) Gu, X.; Tang, Y.; Zhang, X.; Luo, Z.; Lu, H. *New J. Chem.* **2016**, 40, 6580–6583.
- (348) Kizirian, J.-C.; Cabello, N.; Pinchard, L.; Caille, J.-C.; Alexakis, A. *Tetrahedron* **2005**, 61 (37), 8939–8946.
- (349) Tan, S. W. B.; Chai, C. L. L.; Moloney, M. G.; Thompson, A. L. *J. Org. Chem.* **2015**, 80 (5), 2661–2675.
- (350) Mondon, A.; Nestler, H. J. *Angew. Chem. Int. Ed.* **1964**, 3, 588.
- (351) Sarragiotto, M. H.; Filho, H. L.; Marsaioli, A. J. *Can. J. Chem.* **1981**, 59, 2771–2775.
- (352) Fulmer, G. R.; Miller, A. J. M.; Sherden, N. H.; Gottlieb, H. E.; Nudelman, A.; Stoltz, B. M.; Bercaw, J. E.; Goldberg, K. I. *Organometallics* **2010**, 29 (9), 2176–2179.
- (353) Still, W. C.; Kahn, M.; Mitra, A. *J. Org. Chem.* **1978**, 43, 2923–2925.
- (354) Armarego, W. L. F.; Chai, C. L. L. *Purification of Laboratory Chemicals, Sixth Edition*; Butterworth-Heinemann: Oxford, United Kingdom, 2009.
- (355) Cowieson, N. P.; Aragao, D.; Clift, M.; Ericsson, D. J.; Gee, C.; Harrop, S. J.; Mudie, N.; Panjikar, S.; Price, J. R.; Riboldi-Tunnicliffe, A.; Williamson, R.; T, C.-D. *J. Synchrotron. Radiat.* **2015**, 22, 187.
- (356) Kuhn, P.; McPhillips, T. M.; McPhillips, S. E.; Chiu, H. J.; Cohen, A. E.; Deacon, A. M.; Ellis, P. J.; Garman, E.; A, G.; Sauter, N. K. *J. Synchrotron. Radiat.* **2002**, 179, 401.
- (357) Sheldrick, G. M. *SHELX97. Programs for Crystal Structure Analysis. Universität Göttingen, Germany* **1998**.
- (358) Barbour, L. J. *J. Supramol. Chem.* **2001**, 1, 189.
- (359) Dolomanov, O. V.; Bourhis, L. J.; Gildea, R. J.; Howard, J. A. K.; Puschmann, H. *J. Appl. Cryst.* **2009**, 42, 339.
- (360) Cuiper, A. D.; Kouwijzer, M. L. C. E.; Grootenhuis, P. D. J.; Kellogg,

- R. M.; Feringa, B. L. *J. Org. Chem.* **1999**, *64* (26), 9529–9537.
- (361) Jefford, C. W.; de Villedon de Naide, F.; Sienkiewicz, K. *Tetrahedron: Asymmetry* **1996**, *7* (4), 1069–1076.
- (362) Demir, A. S.; Subasi, N. T.; Sahin, E. *Tetrahedron: Asymmetry* **2006**, *17* (18), 2625–2631.
- (363) Tokumaru, E.; Tengeiji, A.; Nakahara, T.; Shiina, I. *Chem. Lett.* **2015**, *44* (12), 1768–1770.

## Appendices

### Appendix 1: $^1\text{H}$ NMR Spectral Simulation Parameters

(3*S*,6*S*,7*R*,7*aR*)-6-Fluoro-7-hydroxy-3-phenyltetrahydropyrrolo[2,1-*b*]oxazol-5(6*H*)-one (233)



233

Frequency View

Fragment Options

Fragment Title: Fragment No. 1 – No Title

Statistical weight: 1.0000

Lower limit: 0.0000 Upper limit: 2.0000

Symmetry: C1

Reduce number of lines by

Lower limit for transitions: -2502.63 [ppm]

Upper limit for transitions: 2502.63 [ppm]

Minimum intensity: 0.0010

Add/Del	Spin #	Chemical shift [ppm]	Spins in group	Iterate	Lower limit [ppm]	Upper limit [ppm]	ISO Value	PSE	Spin Value	Disable	Group Index	Annotation
X	1	5.3773	1	<input type="checkbox"/>	5.3510	5.4010	1	H	1 / 2	<input type="checkbox"/>		
X	2	-198.00	1	<input type="checkbox"/>	-198.03	-197.97	19	F	1 / 2	<input type="checkbox"/>		
X	3	4.5149	1	<input type="checkbox"/>	4.4900	4.5400	1	H	1 / 2	<input type="checkbox"/>		
X	4	5.1655	1	<input type="checkbox"/>	5.1410	5.1910	1	H	1 / 2	<input type="checkbox"/>		
X	5	4.5596	1	<input type="checkbox"/>	4.5350	4.5850	1	H	1 / 2	<input type="checkbox"/>		
X	6	3.9487	1	<input type="checkbox"/>	3.9240	3.9740	1	H	1 / 2	<input type="checkbox"/>		
X	7	5.2194	1	<input type="checkbox"/>	5.1950	5.2450	1	H	1 / 2	<input type="checkbox"/>		
+												

Seq. Sim. >>>

PPM HZ

Scalar Couplings

Options for Coupling [1, 2] – Iteration, Sequence Simulation, Group

Group Index: ☐

Lower limit: 4.9000 Start Value: 51.7000 Upper limit: 53.7000

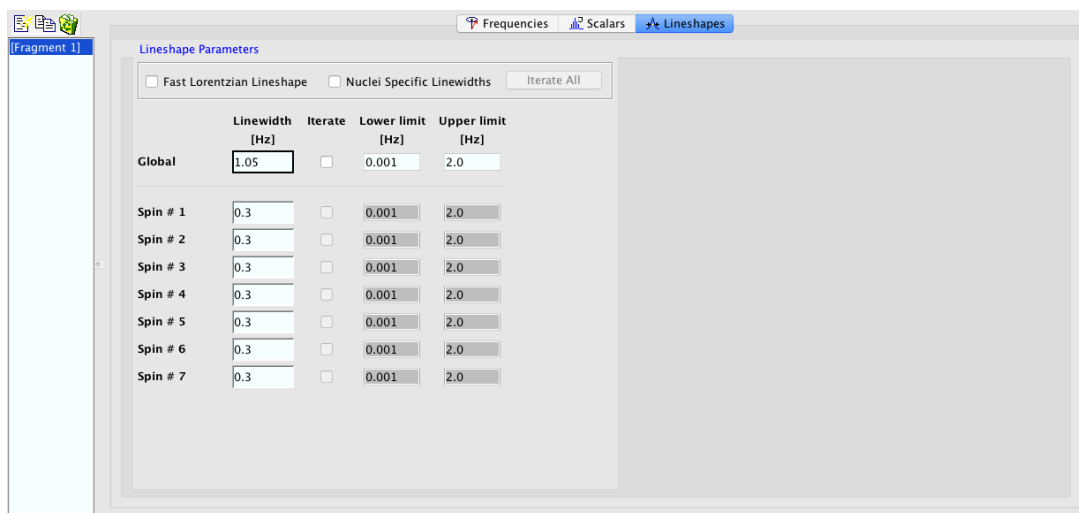
No. of steps: 1 Step width: 1.0000

Iterate: ☐ All

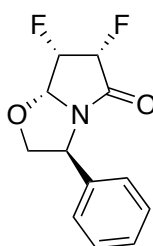
Seq. Simulate: ☒ All

1	2	3	4	5	6	7					
1:2	51.7000 (-)	1:3	7.3000 (-)	1:4	0.0000 (-)	1:5	0.0000 (-)	1:6	0.0000 (-)	1:7	0.0000 (-)
2		2:3	20.4000 (-)	2:4	2.7000 (-)	2:5	0.0000 (-)	2:6	0.0000 (-)	2:7	0.0000 (-)
3			3:4	3.4000 (-)	3:5	0.0000 (-)	3:6	0.0000 (-)	3:7	0.0000 (-)	
4				4:5	0.0000 (-)	4:6	0.0000 (-)	4:7	0.0000 (-)		
5					5:6	9.0000 (-)	5:7	7.4000 (-)			
6						6:7	6.9000 (-)				





**(3*S*,6*R*,7*S*,7*aR*)-6,7-difluoro-3-phenyltetrahydropyrrolo[2,1-*b*]oxazol-5(6*H*)-one (234)**



**234**

Frequency View

Fragment Options

Fragment Title: Fragment No. 1 - No Title

Statistical weight: 1.0000 ☐ Iterate

Symmetry: C1

Lower limit: 0.0000 Upper limit: 2.0000

Reduce number of lines by

Lower limit for transitions: -1666.47 [ppm]

Upper limit for transitions: 1666.47 [ppm]

Minimum intensity: 0.0010

Add/Del	Spin #	Chemical shift [ppm]	Spins in group	Iterate All	Lower limit [ppm]	Upper limit [ppm]	ISO Value	PSE	Spin Value	Disable	Group Index	Annotation
<input checked="" type="checkbox"/>	1	-190.00	1	<input type="checkbox"/>	-190.02	-189.98	19	F	1 / 2	<input type="checkbox"/> 1		
<input checked="" type="checkbox"/>	2	5.3425	1	<input type="checkbox"/>	5.3258	5.3592	1	H	1 / 2	<input type="checkbox"/> 2		
<input checked="" type="checkbox"/>	3	-200.00	1	<input type="checkbox"/>	-200.02	-199.98	19	F	1 / 2	<input type="checkbox"/> 3		
<input checked="" type="checkbox"/>	4	5.4300	1	<input type="checkbox"/>	5.4133	5.4467	1	H	1 / 2	<input type="checkbox"/> 4		
<input checked="" type="checkbox"/>	5	5.3790	1	<input type="checkbox"/>	5.3623	5.3957	1	H	1 / 2	<input type="checkbox"/> 5		
<input checked="" type="checkbox"/>	6	4.3250	1	<input type="checkbox"/>	4.3083	4.3417	1	H	1 / 2	<input type="checkbox"/> 6		
<input checked="" type="checkbox"/>	7	4.2505	1	<input type="checkbox"/>	4.2338	4.2672	1	H	1 / 2	<input type="checkbox"/> 7		
<input checked="" type="checkbox"/>	8	5.3860	1	<input type="checkbox"/>	5.3693	5.4027	1	H	1 / 2	<input type="checkbox"/> 8		
<input type="button" value="+"/>												

Seq. Sim. >>>

☒ PPM ☐ HZ

Scalar Couplings

Options for Coupling [1, 2] - Iteration, Sequence Simulation, Group

☐ Group Index

Lower limit: 45.8000 Start Value: 47.8000 Upper limit: 49.8000 ☐ Iterate

No. of steps: 1 Step width: 1.0000 ☐ Seq. Simulate

	2	3	4	5	6	7	8
1	1:2 47.8000 (-)	1:3 5.5000 (-)	1:4 0.0000 (-)	1:5 0.0000 (-)	1:6 0.0000 (-)	1:7 1.2000 (-)	1:8 0.0000 (-)
2		2:3 25.2000 (-)	2:4 3.0000 (-)	2:5 0.0000 (-)	2:6 0.0000 (-)	2:7 0.0000 (-)	2:8 0.0000 (-)
3			3:4 55.7000 (-)	3:5 14.1000 (-)	3:6 0.0000 (-)	3:7 0.0000 (-)	3:8 0.0000 (-)
4				4:5 2.7000 (-)	4:6 0.0000 (-)	4:7 0.0000 (-)	4:8 0.0000 (-)
5					5:6 0.0000 (-)	5:7 0.0000 (-)	5:8 0.0000 (-)
6						6:7 8.4000 (-)	6:8 6.0000 (-)
7							7:8 3.0000 (-)

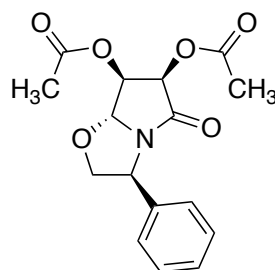
Lineshape Parameters

☐ Fast Lorentzian Lineshape ☐ Nuclei Specific Linewidths

	Linewidth [Hz]	Iterate	Lower limit [Hz]	Upper limit [Hz]
Global	1.5	<input type="checkbox"/>	0.001	2.0
Spin # 1	0.3	<input type="checkbox"/>	0.001	2.0
Spin # 2	0.3	<input type="checkbox"/>	0.001	2.0
Spin # 3	0.3	<input type="checkbox"/>	0.001	2.0
Spin # 4	0.3	<input type="checkbox"/>	0.001	2.0
Spin # 5	0.3	<input type="checkbox"/>	0.001	2.0
Spin # 6	0.3	<input type="checkbox"/>	0.001	2.0
Spin # 7	0.3	<input type="checkbox"/>	0.001	2.0
Spin # 8	0.3	<input type="checkbox"/>	0.001	2.0

**Appendix 2: X-ray Crystallography Data**

**(3*S*,6*R*,7*S*,7*aR*)-5-Oxo-3-phenylhexahydropyrrolo[2,1-*b*]oxazole-6,7-diyl diacetate (163)**

**163**

Bond precision:	C–C = 0.0022 Å	Wavelength=0.71090	
Cell:	<i>a</i> =6.6080(5)	<i>b</i> =9.1090(4)	<i>c</i> =12.9440(5)
	$\alpha$ =90	$\beta$ =104.234(3)	$\gamma$ =90
Temperature:	100 K		
	Calculated	Reported	
Volume	755.21(7)	755.21(7)	
Space group	P 21	P 21	
Hall group	P 2yb	P 2yb	
Moiety formula	C <sub>16</sub> H <sub>17</sub> N O <sub>6</sub>	?	
Sum formula	C <sub>16</sub> H <sub>17</sub> NO <sub>6</sub>	C <sub>16</sub> H <sub>17</sub> NO <sub>6</sub>	
Mr	319.31		
D <sub>x</sub> , gcm <sup>−3</sup>	1.404	1.404	
Z	2	2	
$\mu$ (mm <sup>−1</sup> )	0.107	0.108	
F <sub>000</sub>	336.0	336.0	
F <sub>000</sub> '	336.2		
<i>h</i> , <i>k</i> , <i>l</i> <sub>max</sub>	8,11,17	8,11,17	
N <sub>ref</sub>	3591[1908]	3458	
T <sub>min</sub> ,T <sub>max</sub>	0.984,0.984		
T <sub>min</sub> '	0.984		

Correction method = not given

Data completeness = 1.81/0.96

Theta(max) = 27.887

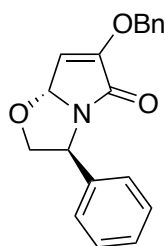
R (reflections) = 0.0293 (3440)

wR<sub>2</sub>(reflections) = 0.0757 (3458)

S = 1.121

N<sub>par</sub> = 210

**(3*S*,7*aR*)-6-(Benzyloxy)-3-phenyl-2,3-dihydropyrrolo[2,1-*b*]oxazol-5(7*aH*)-one (173)**



173

Bond precision:	C–C = 0.0025 Å	Wavelength=0.71080	
Cell:	<i>a</i> =17.784(4)	<i>b</i> =6.291(1)	<i>c</i> =13.938(3)
	$\alpha$ =90	$\beta$ =92.090(4)	$\gamma$ =90
Temperature:	100 K		
	Calculated	Reported	
Volume	1558.3(5)	1558.3(5)	
Space group	C 2	C 2	
Hall group	C 2y	C 2y	
Moiety formula	C <sub>19</sub> H <sub>17</sub> N O <sub>3</sub>	?	
Sum formula	C <sub>19</sub> H <sub>17</sub> N O <sub>3</sub>	C <sub>19</sub> H <sub>17</sub> N O <sub>3</sub>	
Mr	307.34		
Dx, gcm <sup>−3</sup>	1.310	1.310	
Z	4	4	
$\mu$ (mm <sup>−1</sup> )	0.088	0.089	
F <sub>000</sub>	648.0	648.0	
F <sub>000</sub> '	648.30		
<i>h</i> , <i>k</i> , <i>l</i> <sub>max</sub>	23,8,18	23,8,18	
N <sub>ref</sub>	3753[2045]	3564	
T <sub>min</sub> ,T <sub>max</sub>	0.995,0.996		
T <sub>min</sub> '	0.915		

Correction method = not given

Data completeness = 1.74/0.95

Theta(max) = 27.914

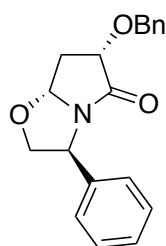
R (reflections) = 0.0322 (3523)

wR<sub>2</sub>(reflections) = 0.0832 (3564)

S = 1.101

N<sub>par</sub> = 208

**(3*S*,6*S*,7*aR*)-6-(Benzyloxy)-3-phenyltetrahydropyrrolo[2,1-*b*]oxazol-5(6*H*)-one (175)**



175

Bond precision:	C–C = 0.0024 Å	Wavelength=0.71080	
Cell:	<i>a</i> =6.6790(17)	<i>b</i> =9.0560(13)	<i>c</i> =13.292(3)
	$\alpha$ =90	$\beta$ =104.16(3)	$\gamma$ =90
Temperature:	100 K		
	Calculated	Reported	
Volume	779.5(3)	779.6(3)	
Space group	P 21	P 21	
Hall group	P 2yb	P 2yb	
Moiety formula	C <sub>19</sub> H <sub>19</sub> N O <sub>3</sub>	?	
Sum formula	C <sub>19</sub> H <sub>19</sub> N O <sub>3</sub>	C <sub>19</sub> H <sub>19</sub> N O <sub>3</sub>	
Mr	309.35		
D <sub>x</sub> , gcm <sup>−3</sup>	1.318	1.318	
Z	2	2	
$\mu$ (mm <sup>−1</sup> )	0.088	0.089	
F <sub>000</sub>	328.0	328.0	
F <sub>000</sub> '	328.15		
<i>h</i> , <i>k</i> , <i>l</i> <sub>max</sub>	9,12,18	9,12,18	
N <sub>ref</sub>	4577[2422]	4018	
T <sub>min</sub> ,T <sub>max</sub>	0.999,0.999		
T <sub>min</sub> '	0.998		

Correction method = not given

Data completeness = 1.66/0.88

Theta(max) = 30.028

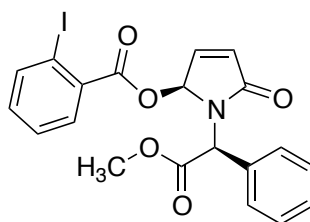
R (reflections) = 0.0418 (3932)

wR<sub>2</sub>(reflections) = 0.1096 (4018)

S = 1.051

N<sub>par</sub> = 208

**(S)-1-((S)-2-Methoxy-2-oxo-1-phenylethyl)-5-oxo-2,5-dihydro-1H-pyrrol-2-yl 2-iodobenzoate (155a)**



155a

Bond precision:	C–C = 0.0058 Å	Wavelength=1.54178	
Cell:	$a=9.2928(12)$	$b=12.7228(11)$	$c=16.320(4)$
	$\alpha=90$	$\beta=90$	$\gamma=90$
Temperature:	125 K		
	Calculated	Reported	
Volume	1929.5(6)	1929.5(6)	
Space group	P 21 21 21	P 21 21 21	
Hall group	P 2ac 2ab	P 2ac 2ab	
Moiety formula	C <sub>20</sub> H <sub>16</sub> I N O <sub>5</sub>	C <sub>20</sub> H <sub>16</sub> I N O <sub>5</sub>	
Sum formula	C <sub>20</sub> H <sub>16</sub> I N O <sub>5</sub>	C <sub>20</sub> H <sub>16</sub> I N O <sub>5</sub>	
Mr	477.24	477.26	
Dx, gcm <sup>-3</sup>	1.643	1.643	
Z	4	4	
$\mu$ (mm <sup>-1</sup> )	13.309	13.312	
F <sub>000</sub>	944.0	946.3	
F <sub>000</sub> '	945.59		
h,k,lmax	11,15,19	10,17,19	
Nref	3413[1961]	3251	
Tmin,Tmax	0.078,0.394	0.340,0.753	
Tmin'	0.010		

Correction method = # Reported T Limits: Tmin=0.340 Tmax=0.753

AbsCorr = MULTI-SCAN

Data completeness = 1.66/0.95

Theta(max) = 66.700

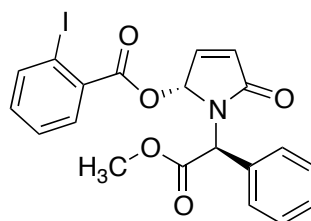
R (reflections) = 0.0296 (3205)

wR2(reflections) = 0.0750 (3251)

S = 1.042

Npar = 245

**(*R*)-1-((*S*)-2-methoxy-2-oxo-1-phenylethyl)-5-oxo-2,5-dihydro-1*H*-pyrrol-2-yl 2-iodobenzoate (155b)**



155b

Bond precision:	C–C = 0.0043 Å	Wavelength=1.54178	
Cell:	<i>a</i> =8.2367(2)	<i>b</i> =8.2369(2)	<i>c</i> =27.4363(7)
	$\alpha$ =90	$\beta$ =90	$\gamma$ =90
Temperature:	125 K		
	Calculated	Reported	
Volume	1861.41(8)	1861.41(8)	
Space group	P 21 21 21	P 21 21 21	
Hall group	P 2ac 2ab	P 2ac 2ab	
Moiety formula	C <sub>20</sub> H <sub>16</sub> I N O <sub>5</sub>	C <sub>20</sub> H <sub>16</sub> I N O <sub>5</sub>	
Sum formula	C <sub>20</sub> H <sub>16</sub> I N O <sub>5</sub>	C <sub>20</sub> H <sub>16</sub> I N O <sub>5</sub>	
Mr	477.24	477.26	
Dx, gcm <sup>−3</sup>	1.703	1.703	
Z	4	4	
$\mu$ (mm <sup>−1</sup> )	13.796	13.799	
F <sub>000</sub>	944.0	946.3	
F <sub>000</sub> '	945.59		
<i>h</i> , <i>k</i> , <i>l</i> <sub>max</sub>	9,9,32	9,9,32	
N <sub>ref</sub>	3273[1909]	3266	
T <sub>min</sub> ,T <sub>max</sub>	0.158,0.063	0.109,0.7287	
T <sub>min</sub> '	0.025		

Correction method = # Reported T Limits: T<sub>min</sub>=0.109 T<sub>max</sub>=0.287

AbsCorr = ANALYTICAL

Data completeness = 1.71/1.00

Theta(max) = 66.650

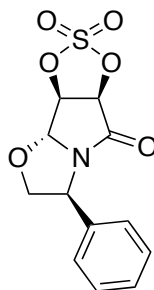
R (reflections) = 0.0205 (3222)

wR<sub>2</sub>(reflections) = 0.0517 (3266)

S = 1.043

N<sub>par</sub> = 245

**(3a*S*,3b*R*,6*S*,8a*R*)-6-Phenyltetrahydro-  
[1,3,2]dioxathiol[4',5':3,4]pyrrolo[2,1-*b*]oxazol-8(3b*H*)-one 2,2-dioxide**  
**(232)**

**232**

Bond precision:	C–C = 0.0031 Å	Wavelength=1.54178	
Cell:	<i>a</i> =6.4543(2)	<i>b</i> =10.6214(3)	<i>c</i> =17.9169(5)
	$\alpha$ =90	$\beta$ =90	$\gamma$ =90
Temperature:	100 K		
	Calculated	Reported	
Volume	1228.27(6)	1228.27(6)	
Space group	P 21 21 21	P 21 21 21	
Hall group	P 2ac 2ab	P 2ac 2ab	
Moiety formula	C12 H11 N O6 S	C12 H11 N O6 S	
Sum formula	C12 H11 N O6 S	C12 H11 N O6 S	
Mr	297.28		
Dx, gcm <sup>−3</sup>	1.608	1.607	
Z	4	4	
$\mu$ (mm <sup>−1</sup> )	2.623	2.623	
F000	616.0	619.6	
F000'	619.44		
<i>h</i> , <i>k</i> , <i>l</i> <sub>max</sub>	7,12,21	7,12,21	
Nref	2167[1281]	2162	
T <sub>min</sub> ,T <sub>max</sub>	0.766,0.854	0.675,0.753	
T <sub>min</sub> '	0.660		

Correction method = # Reported T Limits: T<sub>min</sub>=0.675 T<sub>max</sub>=0.753

AbsCorr = MULTI-SCAN

Data completeness = 1.69/1.00

Theta(max) = 66.440

R (reflections) = 0.0253 (2054)

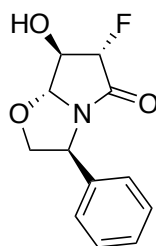
wR2(reflections) = 0.0625 (2162)

S = 1.053

Npar = 181



**(3*S*,6*S*,7*R*,7*aR*)-6-Fluoro-7-hydroxy-3-phenyltetrahydropyrrolo[2,1-*b*]oxazol-5(6*H*)-one (233)**



233

Bond precision:	C–C = 0.0022 Å	Wavelength=1.54178	
Cell:	<i>a</i> =6.5579(2)	<i>b</i> =21.3008(6)	<i>c</i> =7.6892(2)
	$\alpha$ =90	$\beta$ =90.2866(9)	$\gamma$ =90
Temperature:	100 K		
	Calculated	Reported	
Volume	1074.37(5)	1074.37(5)	
Space group	P 21	P 21	
Hall group	P 2yb	P 2yb	
Moiety formula	C <sub>12</sub> H <sub>12</sub> F N O <sub>3</sub>	C <sub>12</sub> H <sub>12</sub> F N O <sub>3</sub>	
Sum formula	C <sub>12</sub> H <sub>12</sub> F N O <sub>3</sub>	C <sub>12</sub> H <sub>12</sub> F N O <sub>3</sub>	
Mr	237.23		
D <sub>x</sub> , gcm <sup>−3</sup>	1.467	1.467	
Z	4	4	
$\mu$ (mm <sup>−1</sup> )	0.994	0.994	
F <sub>000</sub>	496.0	497.9	
F <sub>000</sub> '	497.80		
<i>h</i> , <i>k</i> , <i>l</i> <sub>max</sub>	7,25,9	7,25,9	
N <sub>ref</sub>	3788[1950]	3726	
T <sub>min</sub> ,T <sub>max</sub>	0.788,0.820	0.687,0.753	
T <sub>min</sub> '	0.672		

Correction method = # Reported T Limits: T<sub>min</sub>=0.687 T<sub>max</sub>=0.753

AbsCorr = MULTI-SCAN

Data completeness = 1.91/0.98

Theta(max) = 66.680

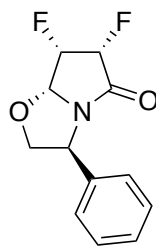
R (reflections) = 0.0296 (3668)

wR<sub>2</sub>(reflections) = 0.0767 (3726)

S = 1.055

N<sub>par</sub> = 309

**(3*S*,6*R*,7*S*,7*aR*)-6,7-Difluoro-3-phenyltetrahydropyrrolo[2,1-*b*]oxazol-5(6*H*)-one (234)**

**234**

Bond precision:	C–C = 0.0030 Å	Wavelength=1.54178	
Cell:	<i>a</i> =8.7855(3)	<i>b</i> =6.1749(2)	<i>c</i> =10.2618(4)
	$\alpha$ =90	$\beta$ =105.699(2)	$\gamma$ =90
Temperature:	100 K		
	Calculated	Reported	
Volume	535.93(3)	535.93(3)	
Space group	P 21	P 1 21 1	
Hall group	P 2yb	P 2yb	
Moiety formula	C <sub>12</sub> H <sub>11</sub> F <sub>2</sub> N O <sub>2</sub>	C <sub>12</sub> H <sub>11</sub> F <sub>2</sub> N O <sub>2</sub>	
Sum formula	C <sub>12</sub> H <sub>11</sub> F <sub>2</sub> N O <sub>2</sub>	C <sub>12</sub> H <sub>11</sub> F <sub>2</sub> N O <sub>2</sub>	
Mr	239.22		
Dx, gcm <sup>−3</sup>	1.482	1.482	
Z	2	2	
$\mu$ (mm <sup>−1</sup> )	1.068	1.068	
F <sub>000</sub>	248.0	249.0	
F <sub>000</sub> '	248.95		
h,k,l <sub>max</sub>	10,7,12	10,7,12	
N <sub>ref</sub>	1902[1048]	1856	
T <sub>min</sub> ,T <sub>max</sub>	0.825,0.852	0.541,0.753	
T <sub>min</sub> '	0.344		

Correction method = # Reported T Limits: T<sub>min</sub>=0.541 T<sub>max</sub>=0.753

AbsCorr = MULTI-SCAN

Data completeness = 1.77/0.98

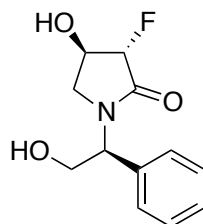
Theta(max) = 66.670

R (reflections) = 0.0321 (1739)

wR<sub>2</sub>(reflections) = 0.0770 (1856)

S = 1.071

N<sub>par</sub> = 154

**(3*S*,4*R*)-3-fluoro-4-hydroxy-1-((*S*)-2-hydroxy-1-phenylethyl)pyrrolidin-2-one (246)****246**

Bond precision:	C–C = 0.0019 Å	Wavelength=1.54178	
Cell:	<i>a</i> =9.2406(2)	<i>b</i> =14.4797(4)	<i>c</i> =16.1907(4)
	$\alpha$ =90	$\beta$ =90	$\gamma$ =90
Temperature:	100 K		
	Calculated	Reported	
Volume	2166.33(9)	2166.33(9)	
Space group	P 21 21 21	P 21 21 21	
Hall group	P 2ac 2ab	P 2ac 2ab	
Moiety formula	C <sub>12</sub> H <sub>14</sub> F N O <sub>3</sub>	C <sub>12</sub> H <sub>14</sub> F N O <sub>3</sub>	
Sum formula	C <sub>12</sub> H <sub>14</sub> F N O <sub>3</sub>	C <sub>12</sub> H <sub>14</sub> F N O <sub>3</sub>	
Mr	239.24		
Dx, gcm <sup>−3</sup>	1.467	1.467	
Z	8	8	
$\mu$ (mm <sup>−1</sup> )	0.986	0.986	
F <sub>000</sub>	1008.0	1011.8	
F <sub>000</sub> '	1011.61		
h,k,l <sub>max</sub>	11,17,19	10,17,19	
N <sub>ref</sub>	3815[2183]	3795	
T <sub>min</sub> ,T <sub>max</sub>	0.782,0.821	0.690,0.753	
T <sub>min</sub> '	0.782		

Correction method = # Reported T Limits: T<sub>min</sub>=0.690 T<sub>max</sub>=0.753

AbsCorr = MULTI-SCAN

Data completeness = 1.74/0.99

Theta(max) = 66.620

R (reflections) = 0.0255 (3730)

wR<sub>2</sub>(reflections) = 0.0655 (3795)

S = 1.079

N<sub>par</sub> = 311